OPTICAL SENSORS FOR THE IN VIVO ASSESSMENT OF FLAP PERFUSION IN PLASTIC SURGERY

By

TINA ZAMAN

A thesis submitted for the degree of Doctor of Philosophy

Biomedical Engineering Research Group,
School of Engineering and Mathematical Sciences,
City University London,
Northampton Square, London, EC1V 0HB

September 2013

Table of Contents

List of Figures

List of Tables

Acknowledgements

I would like to express my gratitude to my supervisor Professor Panayiotis Kyriacou for his continuous support, expert guidance, patience and encouragement throughout my research.

I am grateful to Professor Sandip Pal of Mid Essex Hospital for his support in this project as well as his assistance in recruiting patients for my clinical trials. I would also like to acknowledge Dr Justin Phillips for his advice and assistance during my studies.

A special thanks to Professor Richard Langford of Barts Health NHS Trust for his suggestions to expand the scope of this study. I would also like to extend my gratitude to Dr Alla Belhaj for his assistance on recruiting patients.

I would like to acknowledge the support of the nurses and clinicians at the Mid Essex Hospital and Barts Health NHS Trust, especially Miss Hasu Patel for her support in permitting the recruitment of her patients at the Barts. Thanks to the patients who generously consented for participation and allowed me to stay with them during the first 24 hours following their major surgery.

I would like to acknowledge Engineering and Physical Sciences Research Council for their financial support and also Worshipful Company of Scientific Instrument Makers, City University Future fund, Graduate School Conference Fund and IPEM for their additional contributions.

Thanks to my friends and colleagues in the Biomedical Engineering Research Group for all their advice and hours spent at the Coffee Club. And a special thanks to my friend Dr Sara Farrell for her constant support.

Above all I would like to thank my family, my parents and sisters for your love, support and encouragement. I am indebted to my parents for all the sacrifices they made to make my education possible.

List of Abbreviations

AC-Alternating Current

DAQ-Data Acquisition

DC-Direct Current

DIEP-Deep Inferior Epigastric Perforator

Hb- Haemoglobin

HbO_2-Oxyhaemoglobin

LDF-Laser Doppler Flowmetry

LD-Latissimus Dorsi

LED-Light Emitting Diode

NIRS-Near Infrared Spectroscopy

PCB-Printed Circuit Board

P_{CO2}- Carbon dioxide partial pressure

P_{O2}- Oxygen partial pressure

PPG-Photoplethysmography

SaO_2- Arterial oxygen saturation as measured using CO-Oximeter

SIEA-Superficial Inferior Epigastric Artery

SpO_2-Arterial oxygen saturation as measured using Pulse Oximeter

StO_2-Tissue Oxygen Saturation

TRAM-Transverse Rectus Abdominis Myocutaneous

UV-Ultraviolet

VI-Virtual Instrument

VRAM-Vertical Rectus Abdominis Myocutaneous

Abstract

Following mastectomy for breast cancer a wide variety of surgical techniques are currently available for post mastectomy breast reconstruction where autologous tissue is used to construct a natural looking breast. One of the most common types of reconstructive surgeries use Deep Inferior Epigastric Perforator (DIEP) free flap where skin and adipose tissue along with their blood supplies are transferred from the lower abdomen to the chest. The success of free flap reconstructive surgery depends strongly on the maintenance of adequate perfusion in the flap. Early diagnosis of ischaemia and surgical exploration to restore blood flow can often salvage the flap and may prevent graft failure. Even though many techniques have been used, there is still a need to develop a non-invasive, easy to use, reproducible and inexpensive monitoring device to assess flap perfusion. In an attempt to overcome the limitations of the current flap perfusion monitoring techniques a prototype reflectance three wavelength photoplethysmographic (PPG) sensor was developed. The PPG sensor consisted of two infrared (940 nm), two green (520 nm) and two red (660 nm) LEDs and a photodiode. A PPG processing system was also constructed in order to drive the optical components on the sensor and to detect and pre-process the PPG signals. A Virtual Instrument (VI) was also implemented in LabVIEW in order to display, analyse and archive the PPG signals with the capability of real-time estimation of arterial oxygen saturation (SpO_2) values. The system was evaluated in a pilot study on fifteen patients undergoing breast reconstructive surgery using (DIEP) flaps. Good quality red, infrared and green PPG signals were obtained pre-operatively from the donor site (abdomen), intra-operatively (capturing reperfusion of flap following anastomosis) and post-operatively at regular intervals for up to 12 hours post surgery. SpO_2 values were also estimated which were found to be in broad agreement with SpO_2 values recorded from the commercial pulse oximeter attached to the patients' finger. The flap PPGs were compared with PPGs and SpO_2s acquired from the finger of a small number of patients using a custom made reflectance finger PPG probe, optically and electrically, identical as the flap probe. The finger PPGs were found to be much larger than the flap PPGs which confirms the hypothesis of inadequate perfusion in the flap during and after the operative period. Furthermore the custom made PPG processing system and flap sensor were used successfully on a series of case studies to evaluate the versatility of the system in monitoring PPG signals and estimating blood oxygen saturation in other flaps. These included monitoring two patients undergoing Latissimus Dorsi (pedicle) flap reconstructive surgery and a head and neck free flap surgery where a Vertical Rectus Abdominis Myocutaneous (VRAM) flap was used following total petrosectomy. Also, two patients undergoing reconstructive surgery of the oesophagus using jejunum free flaps were also recruited into the study. For this study a purpose build oesophageal PPG sensor was developed. These case studies demonstrated the ability to use the developed PPG sensors to acquire PPG signals and estimate SpO_2s in a variety of flaps. The results have confirmed that the custom made PPG system and sensor has the potential to be used as an alternative technique for monitoring perfusion in various types of flaps at all operative periods.

Chapter 1

Introduction

Following mastectomy for breast cancer a wide variety of surgical techniques are currently available for post mastectomy breast reconstruction. One of the most common techniques used is Deep Inferior Epigastric Perforator (DIEP) free flap, which has proven to be a major advancement in transferring lower abdominal tissue for autologous breast reconstruction. The DIEP flap has the least donor-site morbidity and will cause less postoperative pain than some of the other breast reconstructive methods [1-2]. However, it has fewer perforating vessels, thus resulting in reduced blood supply to and from the DIEP flap, so fat necrosis and partial flap loss are more common [1]. Postoperative ischaemia due to arterial occlusion, or more commonly, venous occlusion, is the most common cause of failure in microvascular free flaps [2]. Therefore, the success of such procedures depends strongly on the maintenance of adequate perfusion in the flap. Early diagnosis of ischaemia and surgical exploration to restore blood flow can often salvage the flap and may prevent graft failure. Therefore, a continuous method for monitoring perfusion of the flap would assist in early detection of inadequate blood supply. Several techniques and monitoring devices have been used for assessing tissue perfusion postoperatively however limitations such as being heavy operator dependant, time consuming, intermittent and expensive prevent their routine application for monitoring perfusion in free flaps. Therefore, to date there is no widely accepted and readily available intra-operative or postoperative technique to reliably assess the viability of free flaps.

Research Hypothesis:

The hypothesis underlying this project is that the optical technique of photoplethysmography (PPG) may have the capability of continuously and non-invasively monitor the perfusion of free flaps pre, intra and post-operatively by

detecting any changes in volume of arterial blood pulsating through the DIEP flap and estimating the oxygen saturation level of that blood.

Aims and Objectives:

The main aims and objectives of this study are:

- Design and development of a DIEP flap three wavelength PPG sensor,
- Design and development of a PPG processing system,
- Use of a software required to display, store and analyze PPG signals,
- Preliminary clinical trials investigating the feasibility of using this technology in monitoring viability of flaps in patients undergoing DIEP flap reconstructive surgery in the pre, intra and post operative period.

The details of the design and development of this system will be the subject of the following chapters as well as the *in vitro* and *in vivo* evaluation of the developed system.

Brief descriptions of the topics covered in this thesis are presented below.

Chapter 2 covers the basic physiology of the respiratory system and the cardiovascular system with details explaining the mechanism of respiration, transport of oxygen and gas exchange and the role of haemoglobin and the effects of inadequate tissue perfusion.

Chapter 3 describes the different types of flap used in breast reconstructive surgery which is the main focus of this project, in specific free flaps. Also the procedure used for microvascular anastomosis as well as complications arising from flap reconstructive surgery are explained.

Chapter 4 presents the literature review on the current monitoring techniques and technologies and their use in monitoring free flap perfusion. Their disadvantages and shortcomings are also described which has led to the development of the current monitoring technique.

Chapter 5 reviews the history and explains the principles of photoplethysmography, the theory on the relationship of interaction of light with tissue and the utilization of PPG for estimating blood arterial oxygen saturation values in pulse oximetry.

Chapter 6 describes the choice of optical components, mechanical construction and the in vitro evaluation of the reflectance three wavelength flap photoplethysmography sensor and the reflectance finger PPG sensor.

Chapter 7 covers the development of the two channel flap and finger PPG processing system where details of the schematic design, choice of components and the construction of the circuit are described as well as results from the evaluation of the system.

Chapter 8 presents the software implemented in LabVIEW which is used to acquire, display, store and filter the obtained PPG signals. This chapter also describes the details of the algorithms used for estimating SpO_2 values.

Chapter 9 describes in detail the protocol and results of the clinical trials on fifteen patients undergoing breast reconstruction using DIEP free flap pre, intra and post-operatively. The results of investigation monitoring finger and free flap on five patients are also presented in this chapter.

Chapter 10 details unique and isolated case studies which were performed on head and neck flaps such as jejunum free flap and free flaps used following petrosectomy and pedicle flap such as latissimus dorsi flap used in breast reconstruction.

Chapter 11 presents the conclusions as well as suggestions for future work.

Chapter 2

Oxygen Transport and Respiration

2.1 Introduction

Oxygen is vital to the survival of organs and tissues in the human body; it is used by most cells to breakdown nutrients, an activity that is necessary to supply energy to the cells and the body [3].

When a person breathes in (inspiration), oxygen is carried into the lungs where it then diffuses down its concentration gradient into the blood in the capillaries. The blood carries the oxygen to the cells via its large (arteries) and small (capillaries) vessels. The bound oxygen can be taken up by cells and used as a source of energy. The product of cell activity i.e. carbon dioxide diffuses into the blood similar to oxygen and is transported to the lungs where it leaves the body when the person breaths out (expiration) [3].

Inadequate oxygen supply i.e. hypoxia however short-term can result in multiple organ failure and ultimately death [3]. It is therefore not uncommon to witness that the first parameter measured and corrected in an unwell patient is their oxygen levels. There are several methods to do this but the most common, easy to use and non-invasive technique is to use a pulse oximeter by the patient's bed side. This is due to the fact that this can often show the first signs of any underlying problems. Some conditions of the lungs, heart or blood flow and blood volume will be represented by the reading given by the pulse oximeter. For example if the saturation level is below the level that is normal for that person, or below 90%, investigations and corrective treatments will be needed to determine the cause and treat this as necessary [4].

This thesis discusses the use of a developed system based on pulse oximetry to monitor arterial oxygen saturation levels in newly transplanted tissue. Therefore before continuing, it is essential to understand normal oxygen transport and the process of body's oxygen transport where a simple explanation is as follows; oxygen is

diffused into blood via the lungs, blood is then circulated by a system of arteries, veins, and capillaries where the oxygen is diffused to tissue. The tissue also diffuses carbon dioxide to blood in the capillaries, which transports back to the lungs, where the carbon dioxide is diffused to the lungs for expiration. This chapter describes this process in detail including pathologies that can occur due to poor perfusion.

2.2 Respiration

Oxygen delivery to cells requires the use of the respiratory system as well as the circulatory system. Respiration is the involuntary rhythmic process of moving air in and out of the lungs [4].

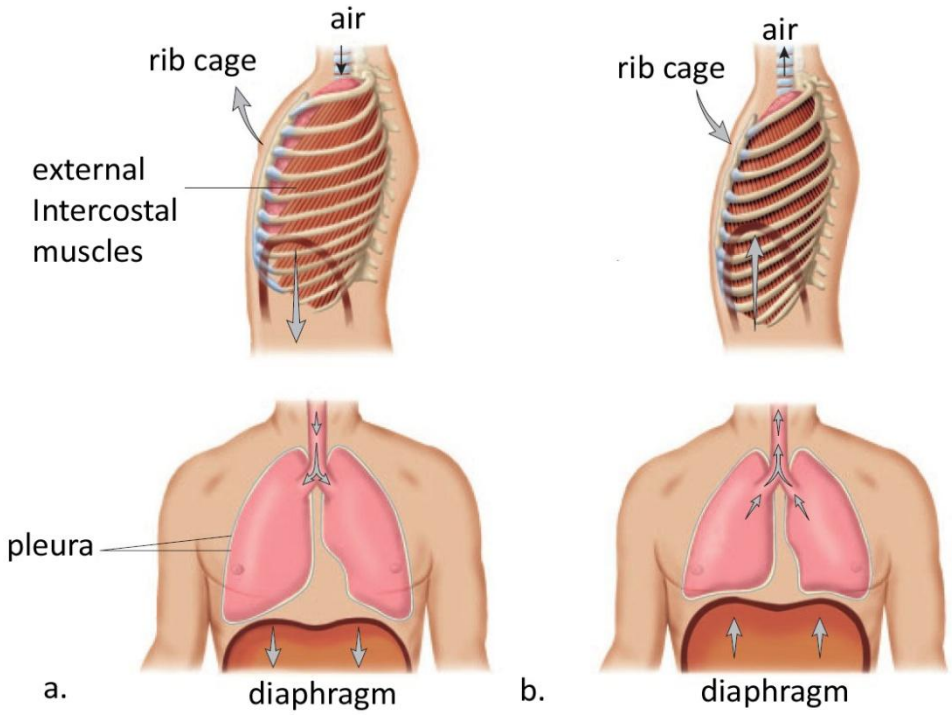

Figure 2.1: Ventilation a. Inspiration b. Expiration [5].

For respiration to be successful there is a precise order of coordinated events which are governed by the respiratory centre in the brain. The brain sends involuntary (motor) signals to the muscles such as the intercostal, pectoralis and the diaphragm to contract in a coordinated manner to expand the lungs on inspiration as seen in Figure 2.1(a). This action causes the intra-pleural pressure i.e. the pressure between the lungs and the chest wall to drop producing a sub-atmospheric pressure within the lungs which draws the air into the lungs [6].

On breathing out (i.e. expiration) the brain sends inhibitory signals to the same muscles causing them to relax which in turn causes the rib cage to contract. This result in higher pressures in the lungs hence the air moves out of the lungs as seen Figure 2.1(b).

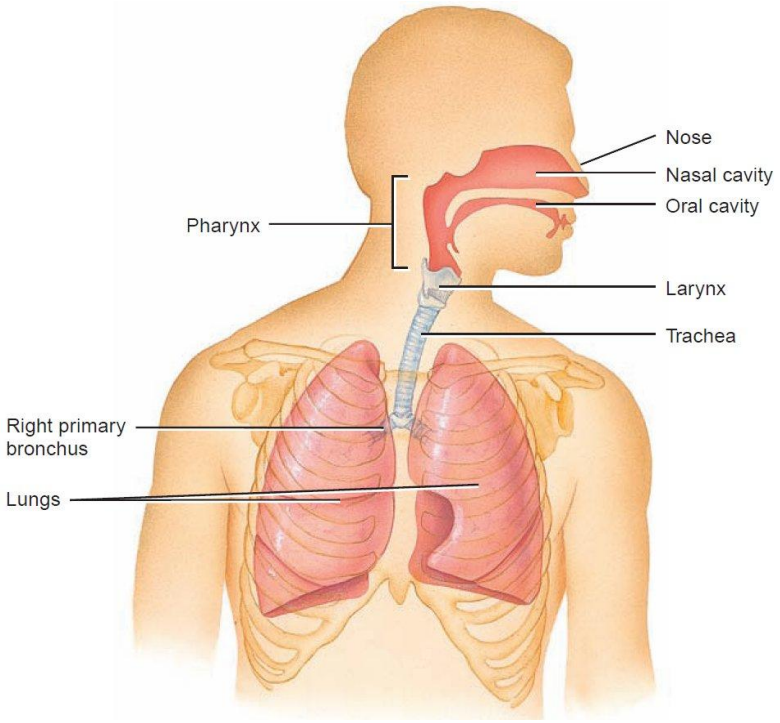

Figure 2.2: Overview of the respiratory organs [6].

The respiratory system as shown in Figure 2.2 starts at the nose and its cavity where air enters, as it then moves along the airways the air which is breathed in is cleansed, warmed, and moistened. Heat is given off by the blood vessels which are close to the surface of the lining of the airways, this helps warm the air breathed in, also as the surface of these passages are wet air is also moistened [6]. The air is then moved to the pharynx (the throat) located posterior to the oral cavity and connects the nasal cavity to the larynx. The larynx houses the vocal cords as well as providing an air passageway between the pharynx and the trachea, this assists in preventing food from entering the trachea while swallowing. The trachea is the main passage to the lungs and is approximately 10 cm long. The trachea is mainly made of cartilage and contains cilia; the main function of these organelles is to continuously sweep upwards towards the pharynx in order to prevent collection of dust and other materials. At its lower end,

the trachea divides in an inverted Y into the two main bronchi leading to the right and left lungs [3]. Each bronchus divides into small airways known as bronchioles as evident in Figure 2.3.

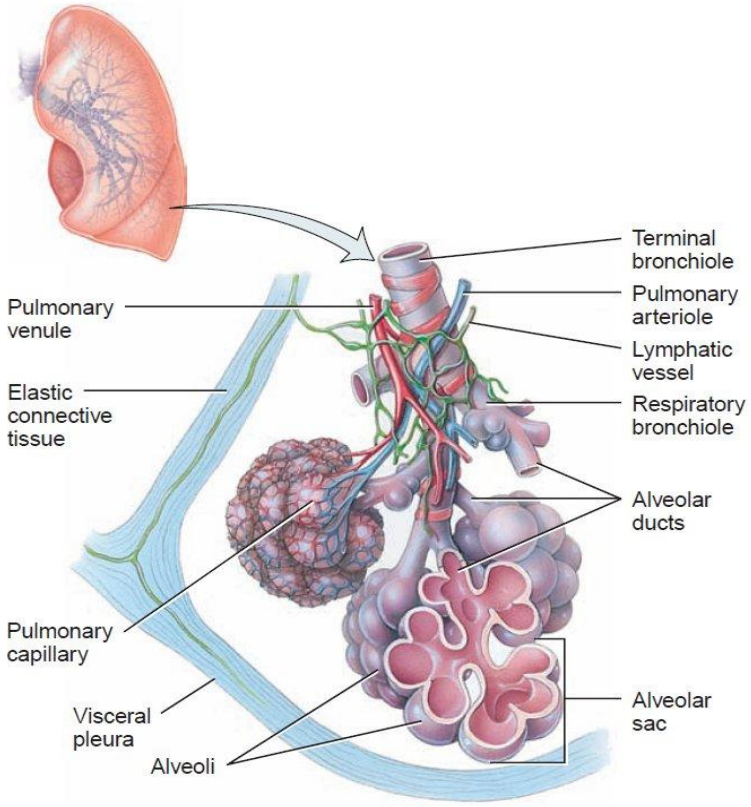

Figure 2.3: Diagram of alveoli with both cross sectional view and external view [4].

Each bronchiole ends in several alveolar ducts which end in alveolar sacs containing a large number of alveoli [7]; these are functions units for the exchange of oxygen and carbon dioxide, a process which is explained in the next section.

2.3 Gas Exchange

As mentioned above the exchange of gases takes place at the level of the alveoli in the lungs and the small blood capillaries. The structure of the lung provides a large surface (about 70 square meters) for this vital exchange to take place. The diameter of capillaries (0.5 micrometers) helps facilitate this exchange further [3].

As shown in Figure 2.4 gases diffuse down their concentration gradient i.e. from an area with a high partial pressure (P) of that gas to an area with a lower partial

pressure. After entering the lungs during inspiration, the oxygen travels to alveoli where its partial pressure (Po_2) is (105mmHg) much higher than that in the adjacent capillaries. For this reason O_2 diffuses from the alveoli into the blood in the capillaries. The oxygen rich blood which travels from here to the rest of the body has a much higher P_{O2} than the surrounding systemic tissue therefore oxygen diffuses out of the blood and into the tissue. Due to the same mechanism, the P_{CO2} in the blood returning from active tissues to the lungs has a much higher P_{CO2} (about 40 mmHg) therefore CO_2 diffuses into the lung capillaries, into the alveoli and out of the body during expiration [6].

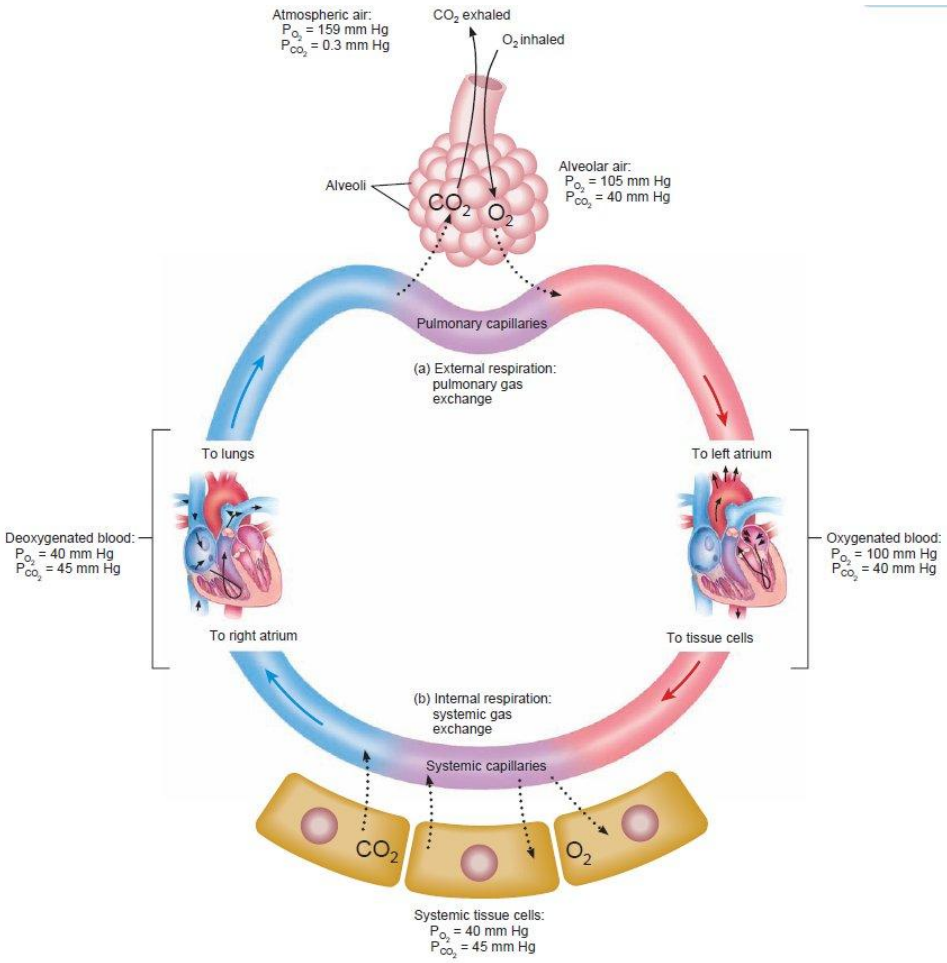

Figure 2.4: Changes in partial pressures of oxygen and carbon dioxide (in mmHg) during external and internal respiration [6].

2.4 **Haemoglobin**

Oxygen travels in the blood bound to Haemoglobin (Hb); a protein found in all red blood cells which contain iron. Hb is used to transport oxygen from the lungs to the rest of the body and also collect carbon dioxide to bring back to the lungs. The iron portion of the haemoglobin both combines and releases oxygen. Whether oxygen is taken up or released depends on many factors such as partial pressures of oxygen, pH and temperature. The higher concentration of oxygen in the alveoli favours the haemoglobin to take up oxygen to become oxyhaemoglobin (HbO_2). This bond however is somewhat unstable therefore for example when HbO_2 passes through tissues with lower concentration of oxygen or a slightly lower pH the bond breaks and the haemoglobin gives up its oxygen to become deoxyhaemoglobin (Hb) [5]. Therefore, the higher the P_{O2}, the higher the oxygen saturation (SaO_2) of haemoglobin, however as oxygen partial pressure decreases so does the SaO_2. Figure 2.5 demonstrates this phenomenon in the well-known sigmoid oxygen dissociation curve where at the arterial point where the P_{O2} is high, about 100mmHg, the SaO_2 is almost 100% saturated. Mixed venous point on the figure represents mixed venous blood, where P_{02} is about 40mmHg and the saturation of haemoglobin is relatively lower but still quite high at 75%.

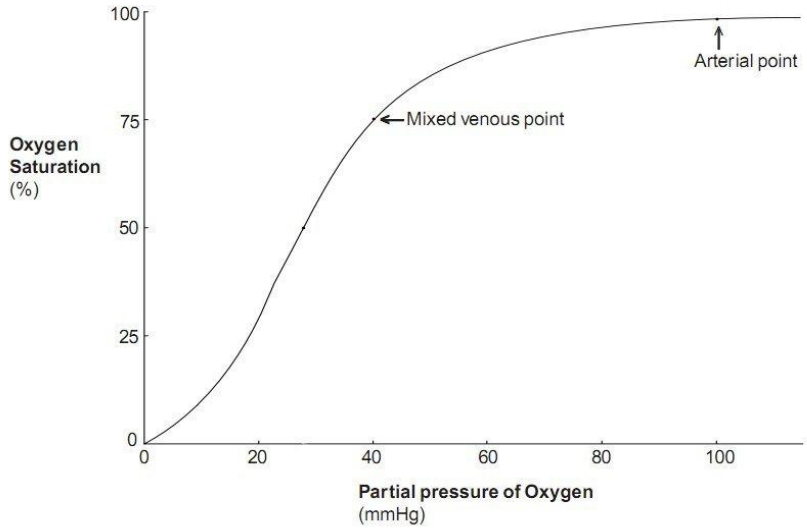

Figure 2.5: Oxygen dissociation curve for adult haemoglobin [8].

It can also be observed from the figure that SaO_2 remains high for much of the curve but it drops to very low levels of around 35% only when the Po_2 reaches 20 mmHg. The partial pressure difference determines the rate and efficiency of diffusion. However, the rate is also dependent on concentration of haemoglobin, the saturation of oxygen and blood flow. It must be considered that no individual parameter or measurement gives a complete picture of cell oxygen consumption [9].

As mentioned in the introduction, successful delivery of oxygen to tissues requires both the respiratory system as well as the circulatory system such as the cardiovascular system. The rest of this chapter will concentrate on how the cardiovascular system contributes to the delivery of oxygen.

2.5 The Cardiovascular System

The cardiovascular system consists of two parts; the heart which pumps the blood throughout the body and the blood vessels through which the blood flows.

The heart which is the strongest muscle in the body is located in the thoracic cavity between the lungs, in order to protect it against any damage by the surrounding bones and organs it is positioned within the rib cage. The heart is a hollow muscular organ about the size of a man's fist between the vertebral column and the sternum (breast bone). The apex of the heart points downwards and is just above the diaphragm to the left of the midline [10]. It is made of four distinct chambers separated from each other by small vessels and sophisticated valves.

In an adult, by beating at approximately 70 beats per minute the heart pumps about 11,000 litres of blood around the body in one day. This rate however varies based on many factors such as age, illness and medications. On average, blood takes about one minute to complete a full circuit around the body and the average body contains 5 litres of blood [9].

Figure 2.6 shows the path that blood takes through the heart where deoxygenated blood from the rest of the body enters the upper chamber of the right side of the heart Such as the right atrium (shown in blue) and is then pumped by the lower chamber, or right ventricle, to the lungs for oxygenation. This blood is then oxygenated in the lungs

and returns to the left side of the heart first into the left atrium and then into the left ventricle.

The oxygenated blood leaves the heart via the largest blood vessel in the body; the aorta. The aorta divides into smaller arteries and arterioles and finally capillaries which transport the oxygenated blood to the cells inside the tissues and organs for exchange of oxygen and carbon dioxide.

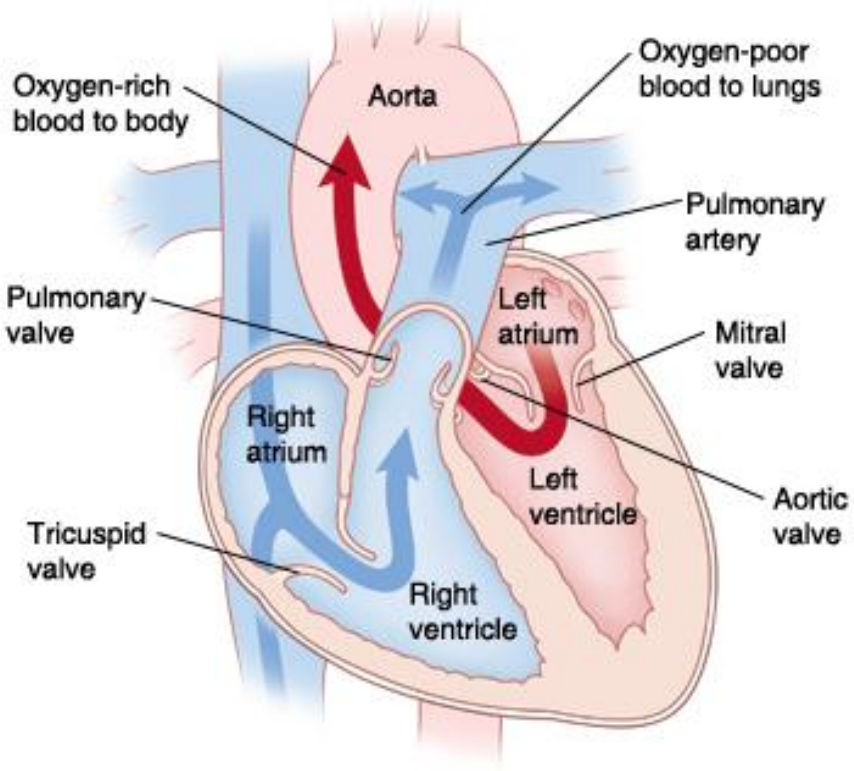

Figure 2.6: Basic anatomy of the heart showing the flow of oxygenated and deoxygenated blood [11].

The amount which reaches different tissues varies based on factors such as temperature where low or high temperature can dilate or constrict the blood vessels.

In the capillary network, blood drains into small venules, which join together to form veins. Veins are the main blood vessels which carry blood back to the heart; they can passively dilate and constrict to vary the amount of blood flow. Veins transport the blood against the gravity hence there are mechanisms helping to move the blood through the veins such as valves. They rely on the surrounding skeletal muscles, for example, calf muscles which contract to squeeze the thin walls of the veins. Blood in

the veins is also carried to the heart by the negative intra-thoracic pressure created on inspiration [12].

The full circuit of blood around the body is soon followed by another through the contraction of the heart. Heart muscle contracts due to a series of electrical impulses produced in the sinoatrial node (SA node) which is located in the wall of the right atrium. The signal causes the atria to contract through depolarization. The signal then travels to the atrioventricular node (AV node) which is located at the centre of the heart between the atria and ventricles and from there to the rest of the heart causing ventricular contraction [12].

As the heart forces blood through the arteries; the blood exerts pressure on the arterial walls, using this phenomenon it is possible to measure blood pressure. The blood pressure is at its highest with each heartbeat during heart contraction which is referred to as systolic blood pressure, the pressure reduces as the heart relaxes before it begins to contract again and the measurement of this is the diastolic blood pressure. The amount of blood pumped out of the heart as well as the heart rate is one of the factors which determine the blood pressure. Another factor affecting the blood pressure is the resistance of peripheral blood vessels to the flow of blood [13].

If the respiratory system or the cardiovascular system fails to function correctly, this will lead to inadequate tissue perfusion which can result in one or more organs of the body beginning to fail as a result of hypoxia. The following section will describe these effects in more detail.

2.6 Inadequate tissue perfusion

Perfusion is the delivery of adequate volume of oxygenated blood to tissues and organs. The major causes of poor tissue perfusion can be due to cardiac, vascular or respiratory failures. These failures can be due to inadequate volume of oxygenated blood caused by hypovolaemia and shock [14].

Some of the respiratory problems which cause poor perfusion are described below:

- Poor lung compliance – e.g. Pneumonia, Acute respiratory distress syndrome (ARDS), lung fibrosis, lung emphysema

- Increased airway resistance – e.g. Asthma, chronic bronchitis, cystic fibrosis
- Low pulmonary diffusion capacity - Emphysema, pulmonary alveolar proteinosis
- Airway obstruction - Choking, secretions from intubation, obstructive sleep apnoea
- Ventilatory muscle weakness - Lead poisoning, trauma to phrenic nerve
- Increased true venous admixture - Congenital heart disease
- Low inspired partial pressure of oxygen - Anaesthesia equipment failure, high altitude [3].

Severe or prolonged lack of tissue perfusion can cause a phenomenon known as “shock”. There are many different types depending on the cause. These are explained below in more detail.

2.6.1 Shock

The lack of oxygen supply which occurs in shock has a catastrophic impact on the cell's mechanisms. For example in cells which normally function aerobically i.e. with the aid of oxygen, will change to function an-aerobically (without oxygen). This can sustain the body for a short amount of time; however it results in the production of lactic acid and lowering of the body's natural pH. Extremely low pH can cause death in a very short amount of time.

Therefore identifying and correcting poor perfusion in a timely manner is paramount to preventing tissue death [15]. As mentioned there are many different types of shock, the most common being septic shock which is caused by bacterial or viral infections. An estimated 31,000 cases a year suffer from severe sepsis with 30-50 % mortality rate in England and Wales and causing more than 100,000 deaths per year in the United States, therefore it is the most common cause of death in hospital critical care units [16].

2.6.2 Ischaemia

As hypoxia which is low levels of oxygen responsible for poor perfusion, ischaemia (poor blood flow) can be equally catastrophic. Ischaemia is caused by blood vessel

constriction resulting in reduction of blood flow to the tissue or complete obstruction of the blood vessel so that the oxygenated blood cannot reach the tissue.

Conditions which can cause ischaemia include:

- Hypoglycaemia -lower than normal levels of glucose
- Tachycardia- abnormally rapid beating of the heart resulting in inadequate pumping function of the heart
- Atherosclerosis - fatty plaques obstructing the lumen of arteries
- Hypotension - low blood pressure, e.g. in septic shock, heart failure
- Thromboembolism - blood clots
- Outside compression of a blood vessel, e.g. by a tumour
- Embolism - foreign bodies in the circulation, e.g. amniotic fluid embolism
- Sickle cell disease - abnormally shaped red blood cells [17].

2.7 **Conclusion**

In this chapter the proper functioning of the delivery of oxygen and removal of carbon dioxide from the body were discussed and the importance of the respiratory system and the cardiovascular system working together to perform this complex action was emphasised.

As discussed, there are many factors which can cause tissue death and organ failure, however the most important of these is low oxygen levels in the body. Therefore monitoring of blood oxygen levels is vital to tissue and organ survival.

As discussed in Chapter 1 the aim of this research is to develop a monitoring technique to enable the continuous monitoring of arterial blood oxygen saturation and changes in volume of blood, during or following specific surgical reconstructive procedures. These surgical procedures will be discussed in the next chapter as well as a discussion on the importance of monitoring of oxygen levels in the body.

Chapter 3

Microsurgery and Free Flap

A free flap is a tissue which is moved from its original site (the donor site) together with its blood supply to a new site on the body (the recipient site). This is done by raising the tissue with its artery and vein still attached; these vessels are then divided, cut and clamped. The tissue is then transferred to the recipient site and the vessels from the donor site are reattached to a suitable artery and vein to the recipient site by microvascular anastomosis in order to re-establish blood supply to the flap [18]. The most common serious complication of this procedure is the reduced arterial and venous flow where both of which could lead to the necrosis of the flap. If necrosis is identified early it may be corrected by surgical re-exploration [19].

Post-operatively the medical staff monitor the free flap closely for signs of necrosis or compromised blood supply. In addition other factors can compromise the blood flow which may include thrombosis within the artery or vein and venous congestion. This chapter explains in detail the use of flaps in reconstructive surgery and their complications.

3.1 Free Flaps in Reconstructive Microsurgery

Autologous tissue transfer (a flap) is possibly the most common technique used by plastic surgeons for reconstructive surgery. Examples of areas where this technique is favourable include radial forearm, head and neck and breast [15]. This project concentrates on the use of this and other techniques as well as pros and cons of each technique in breast reconstructive surgery.

In general there are two main types of flaps depending on the method used during the surgery to re-establish blood flow to the flap. The types include “free flaps” and “pedicled flaps” where free flap is the anastomosis of the blood vessels from the free flap to the vessels in the recipient site whereas in pedicle flaps the vessels supplying

blood to the flap remain attached to the donor site while the flap is transferred to the recipient site.

3.2 Breast Reconstruction

To treat or to prevent breast cancer, mastectomy is often performed where the breast tissue is surgically removed. In a study done by Intergroup Exemestane in 2004 among 4,700 women with early breast cancer in 37 countries, the USA and western and northern Europe had some of the highest rates of mastectomy with 56% and 46% respectively [20].

An option to rebuild the shape of the breast by reconstructive surgery is available in patients undergoing mastectomy, it is believed that reconstructive surgery improves quality of life and psychological and sexual wellbeing for many women. Breast reconstruction is carried out either at the time of the mastectomy (immediate breast reconstruction) or at any time after the mastectomy (delayed breast reconstruction) [16]. Breast reconstruction can be performed using either implants or autogenous tissue from different sites of the body depending on the surgeons' decision; some of these techniques are described below

3.2.1 Implants

Breast reconstruction using implants can be undertaken as either an immediate or delayed procedure following mastectomy. This approach is best suited for patients where there was good preservation of the breast skin and tissue after mastectomy [21].

Following mastectomy the implant is positioned on the chest wall behind the pectoralis major muscle as shown in Figure 3.1. In some patients depending on the amount and quality of the skin of the breast remaining following mastectomy the volume that it can accommodate is identified and the surgeon may use a permanent implant with the desired volume during the initial surgery. The patient will have the definitive breast volume and approximate shape after the first operation without the need for returning post-operatively [22].

Post surgery, once the reconstruction has settled and healed, depending on the quality of the result, further reconstruction may be performed in order to create a more refined breast shape. This is a small surgical procedure which would involve making minor adjustments in contour and the symmetry of the breast [23] .

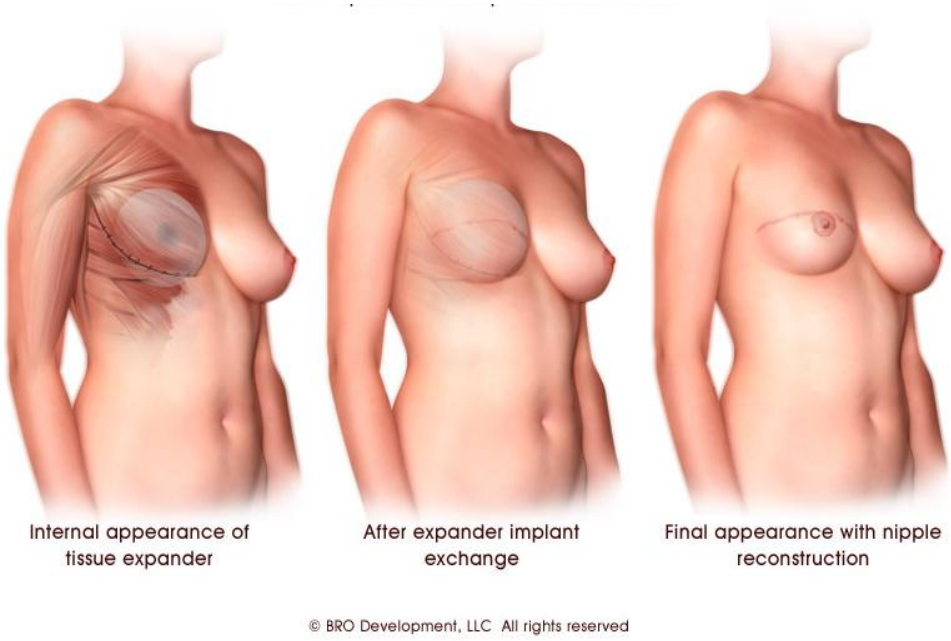

Figure 3.1: Tissue Expander and Implant Post Mastectomy Reconstruction [23].

The complications of using implants include implant deflation, contracture formation, infection, exposure, and ultimately need for exchange or removal of the implant [1]. Use of autologous tissue eliminates some of these complications.

3.3 Autologous tissue flaps in breast reconstruction

Using autologous tissue flap is very commonly used in reconstructing a breast following mastectomy. This involves using the patients' body tissue which can be taken from various sites in the body to create the breast. This method is usually preferable as it is the patients' tissue, there is a reduced risk of infection comparing to using implants. Also unlike implants, it not does deflate or need to be replaced in the future, also in some types of flap surgery as the tissue from the abdomen is used, the end result will be a flatter tummy as well as a reconstructed breast. Some of the different types of flaps which are commonly used for breast reconstructed are described in this section.

3.3.1 Transverse Rectus Abdominus Myocutaneous Flap (TRAM)

The abdomen is a popular donor site used in breast reconstruction surgery as it is supplied by two main vessels, the superior and inferior epigastric vessels.

The conventional (pedicled) transverse rectus abdominis myocutaneous (TRAM) flap was the first effective method of autologous tissue breast reconstruction and still remains one of the most commonly used techniques [1].

In this approach as shown in Figure 3.2, the entire rectus abdominus muscle is used as a tunnel underneath the skin to help move a segment of skin and its underlying adipose tissue together with the muscle and its blood supply from the lower abdomen up into the mastectomy site, the chest wall. The TRAM flap relies on the superior epigastric vessels which provide blood supply to the lower abdomen together with the inferior epigastric vessels as the main blood supply.

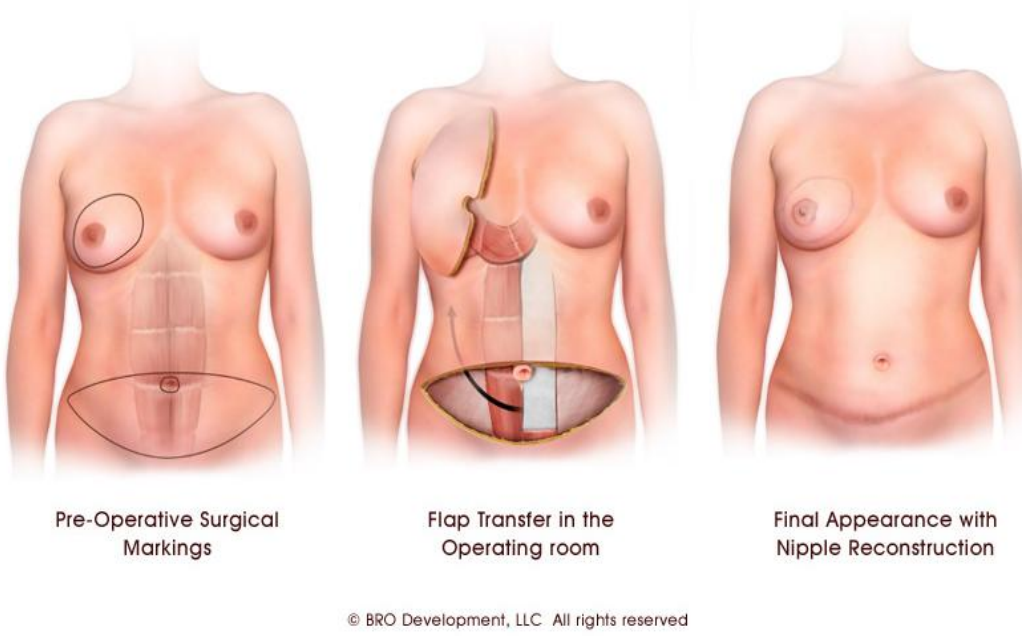

Figure 3.2: TRAM Flap Reconstruction [23].

This technique yields a more natural appearance to the reconstructed breast and has the benefit of a flatter looking abdomen (tummy tuck). Moreover in a patient undergoing unilateral reconstruction, the TRAM flap can potentially offer better symmetry than an implant [23].

The disadvantage to using TRAM flaps is that due to the removal of parts of the abdominal muscle it may weaken the abdominal wall leading to hernias. This can potentially be avoided by using a mesh to fill the defect prior to closing the wound. Moreover patients with already compromised blood vessels such as those with diabetes, mellitus or atherosclerosis and obese and smokers may invariably encounter problems with this type of flap [1].

3.3.2 Deep Inferior Epigastric Perforator (DIEP) Flap

The deep inferior epigastric perforator (DIEP) flap is a distinct variant of the free transverse rectus abdominis myocutaneous (TRAM) flap. In this technique, the lower abdominal skin and the underlying adipose tissue is removed without having to harvest any of the rectus abdominis muscle as shown in Figure 3.3. One or more of the perforating branches of the deep inferior epigastric artery and accompanying veins which are the main blood supply to this part of the body are dissected out of the rectus abdominis muscle and are transported to the recipient site together with the flap [24].

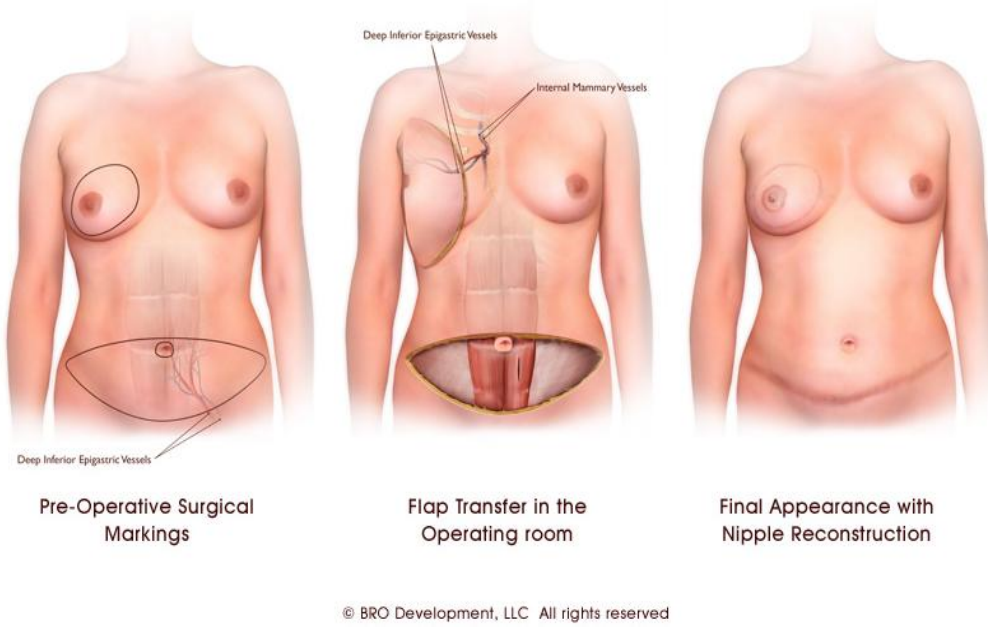

Figure 3.3: DIEP Flap Reconstruction [23].

Despite the fragile appearance of the pedicle, the flap is usually adequately vascularised, although usually not as well as in the standard free TRAM flap [18].

One of the main perforators are clamped and cut, the flap is raised and transferred to the recipient site where the blood vessels of the flap and the blood vessels in the recipient site are anastomosed [1].

In order to avoid using or damaging any muscle, it usually takes longer to harvest a DIEP flap than a TRAM flap. This results in the advantage of minimizing injury to the abdominal wall muscle and a lower risk of abdominal hernias as compared with TRAM flaps [24].

Raising the flap together with its blood supply is a difficult task in which compromising the blood flow and potentially causing necrosis is an issue. The perforating blood vessels are exposed and are more vulnerable to traction injury than in a free TRAM flap where they are surrounded and protected by muscle in their more distal smaller and vulnerable segments. Finally although the entire rectus abdominis muscle may be preserved much of the muscle may still be denervated or devascularised [1].

3.3.3 Latissimus Dorsi Flaps

Latissimus Dorsi (LD) is a flat triangular-shaped muscle located on the posterior trunk as shown in Figure 3.4. This type of flap is a method for breast reconstruction that was first utilized in the 1970's [25]. Breast reconstruction with the latissimus dorsi flap is a simple and reliable technique that gives results that are preferable over implants alone as this type of flap is more stable over time where they will not need to be replaced.

There are relatively few complications with this technique making it one of the benchmarks in breast reconstruction [26]. The latissimus dorsi flap is most commonly combined with a tissue expander or an implant as the tissue used does not contain adequate adipose tissue for a fuller looking breast. This flap provides a source of soft tissue that can help create a more natural looking breast as compared to an implant alone. Occasionally, for a thin patient with a small breast the latissimus dorsi flap can be used alone as the primary reconstruction without the need for an implant [23].

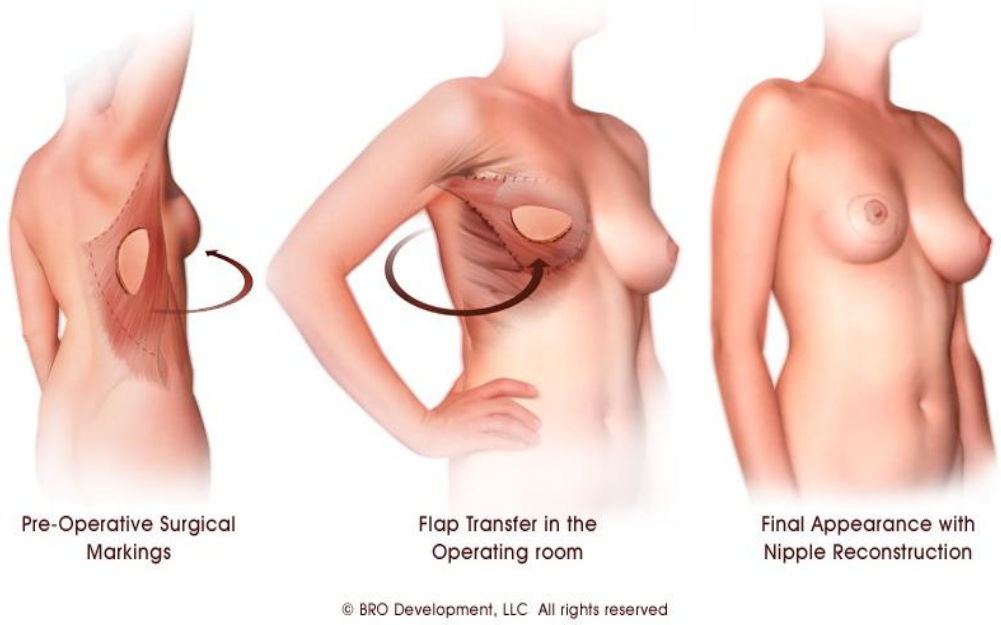

Figure 3.4: Latissimus Dorsi Flap Reconstruction [23].

Some surgeons prefer to only use LD flaps in patients where there is a suspected problem such as soft tissue failure if an implant is used or wound healing. LD flaps can also be used as a salvage procedure for patients who have previously had radiation and who would not be suitable for other breast reconstructive procedures [1]. At the time of breast reconstruction the muscle flap is elevated off of the patient's upper back (donor site) and brought around to the front of the chest wall by tunnelling. As this is a rotational flap, the blood supply to the flap remains attached to the donor site therefore there is no need for anastomosis of the blood vessels. The thoracodorsal artery is the primary source of blood supply to the latissimus dorsi flap. In patients who need more volume an implant can be used which is placed underneath the LD flap where the flap provides soft tissue to allow a more natural looking breast [21].

3.3.4 Superficial Inferior Epigastric Artery (SIEA) Flaps

Another free flap method which utilizes the skin and underlying adipose tissue from the lower abdomen is the superficial inferior epigastric artery (SIEA) flap. As it relies on the superficial rather than the deep blood vessels, the flap does not include muscle or fascia hence reducing the risk of an abdominal hernia [27].

As with the DIEP flap, the SIEA flap is first harvested and then transplanted to the chest wall where the flap vessels and a set of blood vessels in the recipient are anastomosed the flap is then cut and shaped into the breast shape as seen in Figure 3.5 [23]. However unlike the DIEP flap, the SIEA flap relies on a different blood supply and requires less surgical dissection.

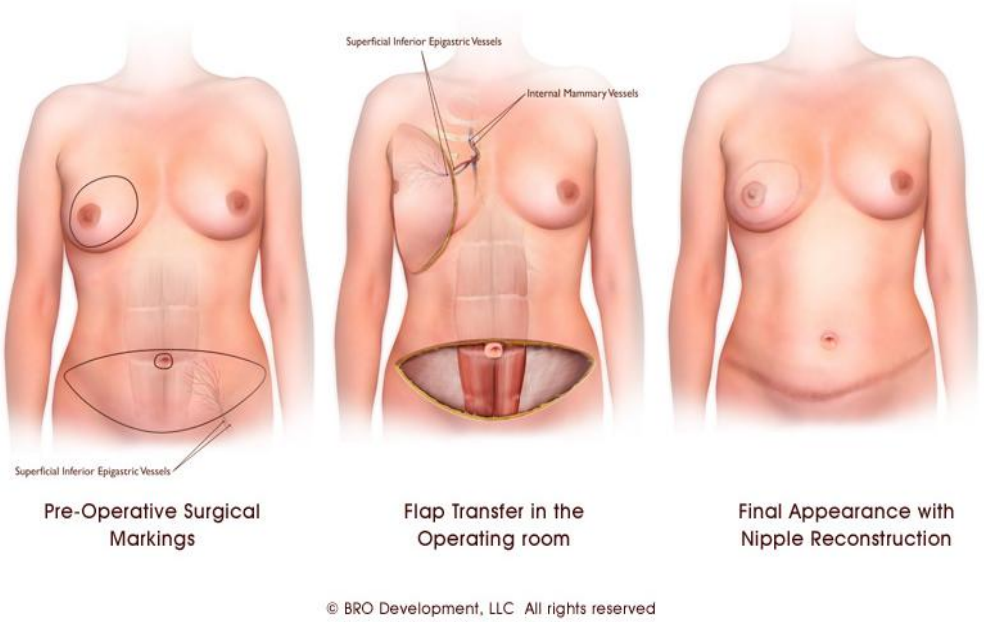

Figure 3.5: SIEA Free flap reconstruction [23].

Unfortunately only a small number of patients are candidates for SIEA flaps. This is due to the superficial vessels being very small in diameter resulting in them often being mismatched with the vessels used in the recipient site which increase the risk of flap necrosis. Moreover SIEP flaps are not suitable in patients with previous surgeries on the lower abdomen such as lower segment caesarean sections and hysterectomies as the superficial vessels may have been irreversibly damaged or dissected [23, 27].

3.4 Microvascular Anastomosis

This procedure is used by plastic surgeons to establish a successful blood supply connection between the existing blood vessels in the recipient site and those found in the transferred tissue, this is invariably vital to the survival of the transferred tissue. [24].

Once the recipient site is available after mastectomy, the defect is evaluated to choose the most suitable type of flap for the reconstruction purposes [27]. The recipient vessels are evaluated prior to flap harvest where factors such as the presence of vessels, their distance to the pedicle as the length of vessel must be long enough for anastomosis purposes, their patency and flow and their general condition i.e. is there any visible damage caused by previous insults such as radiation damage, atherosclerotic change, previous trauma and infection are considered. If the initial vessels are considered to be poor quality, alternative recipient vessels are sought [24].

Free tissue transfer requires a thorough understanding of the anatomy of the relevant donor and recipient sites, their main arterial, venous and nerve supply as well as possibility of major vessel variations and important associated structures which may be prone to damage during the procedure [28].

Ideally the vessels chosen should be of similar diameter to avoid significant size mismatch. The vessels should be handled with care as to minimise mechanical damage to the vessels and anastomosis should be carried out under magnification to ensure accuracy of the anastomosis [28-29]. Orientation of the flap pedicle should be checked to ensure that the anastomosis will not be under excessive tension [28]. As shown in Figure 3.6 double approximating microvascular clamps are used where the donor and recipient vessels are placed within the clamps and the vessel ends are approximated along the direction of the arrows. This technique maintains the correct orientation of the vessels and facilitates suture placement. After the anterior suture line is complete, the clamps are turned over to allow access to the posterior suture line [30].

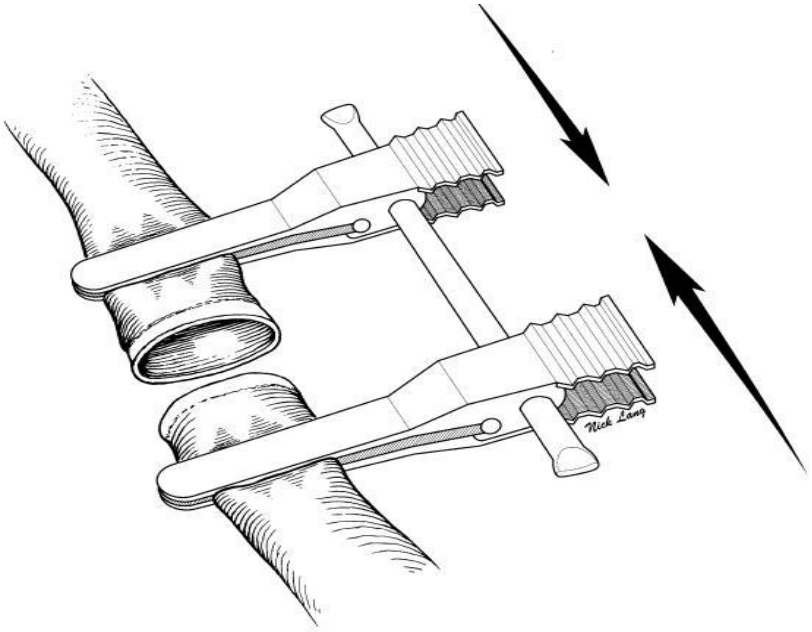

Figure 3.6: Microvascular clamp used in anastomosis [28, 30].

One popular method is to use two orientation sutures placed 180 degrees apart (Figure 3.7 (A)) or three orientation sutures placed 120 degrees apart (Figure 3.7 (B). It has been suggested that it is easier to place the correct number of sutures between the orientation sutures when there are two, whereas the use of three orientation sutures may reduce the risk of including the opposite wall in a suture as this falls away from the anterior suture line with traction on the holding sutures. The remainder of the sutures are then placed (Figure 3.8), usually beginning on the posterior wall to facilitate visualization of the lumen, and ending on the anterior wall [19, 28-29].

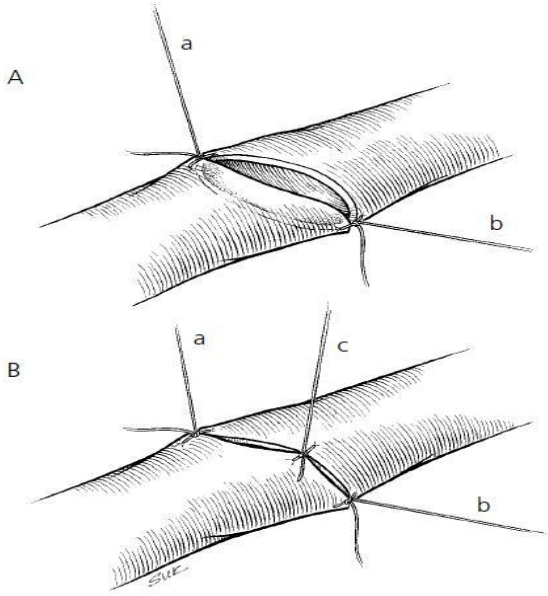

Figure 3.7: A) Sutures "a" and "b" are placed connecting the two vein ends 180 degrees apart. (B) A suture "c" is then placed midway along the venous anastomosis, to be used for traction [1].

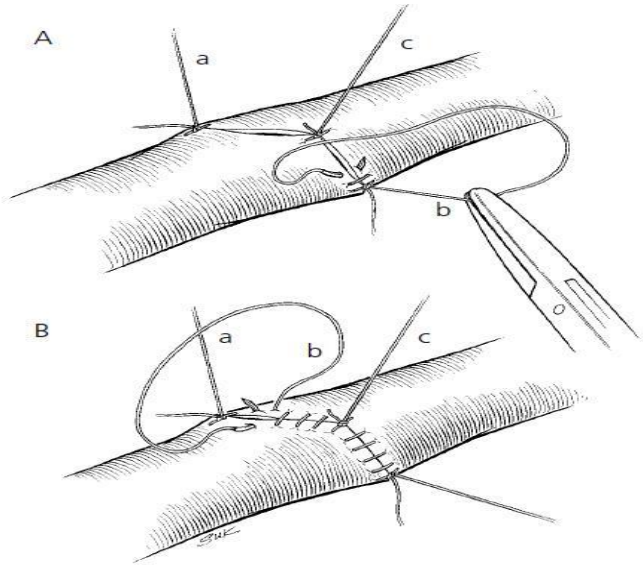

Figure 3.8: (A) During venous anastomosis, the sutures are placed close to the vein edges, using both the running suture "b" and middle traction suture "c" to pull the vein edges away from the back wall. (B) Suture "a" is tied to the loose end of suture "b" [1].

When both anastomosis of the arterial and venous vessel are completed the circulation is restored by removing the clamps, starting with the clamp distal to the venous anastomosis, working back against the direction of flow and finishing with the clamp proximal to the arterial anastomosis. The clamp distal to any anastomosis in the

direction of flow should always be removed first, otherwise the build-up of pressure is liable to result in leakage of blood from the anastomosis and thrombosis may result [1]. When clamps are opened and blood passes across the anastomosis there may be a small amount of blood oozing from between sutures but this should subside quickly. If there is an obvious source of leakage additional sutures should be used to ensure haemostasis. Following the removal of the clamps it may take a few moments for the flap to become perfused. A visible pulsatile artery within the flap, a pink well-perfused appearance and a full vein are all signs of a satisfactory re-established circulation [19].

A healthy flap with a good circulation is the main goal of reconstructive breast surgery. This is of course in addition to the stamina of the flap, its cosmetic appearance and patient satisfaction. As evident in this chapter, free flap surgery is a complex and rigorous procedure which comes with its own complications. These are discussed below in detail.

3.5 Surgery Complications

Surgical complications can be divided into surgical, operator and patient factors.

3.5.1 Surgical Factors

Flap complications which are due to surgical factors are listed below [1, 22-24, 28]:

- **Compromised Blood Supply**

The most common complication of free flap surgery is inadequate circulation in the transplanted free flap. There is a risk of reduced arterial supply with potential flap necrosis and reduced venous return with consequent congestion and again flap necrosis [18].

Microsurgery presents additional complications compared with other techniques, particularly vascular anastomotic failure. In general the blood vessels involved are small hence there is a risk of thrombosis .This risk stands at 2–10% but can rise to 20% in patients with previous exposure to radiotherapy [21]. In cases of thrombosis re-exploration is paramount and if not performed immediately the inadequate blood supply will lead to the loss (usually complete) of the flap.

- **Infection**

As with any surgery particularly with flap surgery where the tissues and skin are exposed for prolonged periods there is a high risk of post operative wound infections. Therefore it is important that all patients receive prophylactic antibiotics and are monitored closely for signs of infections such as erythema around the wound site and fever.

- **Haematoma**

A haematoma which is the localized collection of blood within the tissue that occurs post operatively can cause a lot of pain. This is normally prevented by leaving drains inserted in the operation site for at least 3 days post operatively.

- **Scarring**

Both the TRAM, SEIA and DIEP flap procedures result in a large abdominal scar and scarring around the reconstructed breast [18].

- **Pain**

Experiencing pain after an operation is the body's natural response to trauma and normally settles with good analgesia. Chronic pain i.e. long-term pain can also occur due to the dissection and handling of nerves in donor and recipient areas. Chronic pain is complex and will need specialist input from pain teams and anaesthetists.

- **Abdominal hernias**

These can occur as some of the free flap methods use the abdominal muscle extensively.

- **Limited options for future childbirth**

Pregnancy in women who have flap surgery can be complicated by reduced abdominal muscle strength and presence of abdominal hernias. Delivery procedures such as caesarean-section can be difficult due to previous extensive surgery on the abdomen.

3.5.2 Operator Factors

Free flap surgery is a very complicated procedure and the surgeon's extensive knowledge of anatomy of the sites involved and their previous experience are paramount to achieving a good outcome. However flap complications can arise from operator factors such as:

- **Damage to blood vessels**

The operator must take extra care when dissecting the blood vessels as to minimise damaging the already vulnerable vessels.

- **Infections**

The operator must preserve sterility throughout the operation as the risk of infection is extremely high in free flap surgery.

3.5.3 Patient factors

- **Obesity**

Obese patients face increased risks of almost all the complications. Most important of these include anaesthetic risks, life-threatening post-operative venous thromboembolisms such as pulmonary embolism and impaired wound-healing, In addition partial flap loss is more likely to occur in obese patients.

- **Smoking**

Smokers are more likely to have blood vessels which are already compromised and hence more prone to further damage. Smokers are also more likely to suffer abdominal hernias and impaired wound healing.

- **Previous exposure to radiotherapy**

Patients who have had radiotherapy have fragile blood vessels which may be extra vulnerable to damage by traction and dissection.

- **Patient's age**

Younger patients are more likely to have a faster recovery time.

- **Patient dissatisfaction**

Patient dissatisfaction may occur due to several factors such as poor cosmetic appearance, slow recovery time and failure of the procedure. It is important to assess the patient's expectations prior to surgery so that there is enough time to give the patient all the information needed to make an informed decision and avoid any misinterpretation of what the surgery involves and what the potential outcomes are.

Due to the complications mentioned above, good post-operative monitoring of patients undergoing flap surgery is crucial for a satisfactory outcome. With close postoperative monitoring and subsequent early detection of compromised flap perfusion, easy intervention can result in successful salvage rate in more than 70% of cases [31]. Experienced personnel are essential for monitoring the flap postoperatively as currently the gold standard for assessing viability of the transferred tissue is clinical examination [32]. Identification of a failing or insufficiently perfused flap can occasionally be challenging even for the experienced surgeon which is why a consistent monitoring system is essential. The following chapter will describe some of the currently available technologies used in conjunction with clinical assessment to diagnose flap failure [28, 32].

Chapter 4

Technologies for Monitoring Free Flap Perfusion

In reconstructive microsurgery, post-operative management and continuous monitoring of free flap and early recognition of flap failure is a prerequisite in flap survivability. In a study by Devine et al. where 370 patients who had undergone free flap reconstructive surgery were evaluated, the results confirm the need for continuous monitoring as there was a significant time difference between flaps that were salvaged successfully and those that were not suggesting the importance of identifying any flap compromise without delay. The work presented suggested that in groups where the flap was salvaged, the compromise was recognised 17.5 hours post-surgery compared to the group of patients where the salvage of the flap was unsuccessful as the compromise was identified 51 hours post-operatively [33].

Although many methods for monitoring the perfusion of free flaps are available, there is still no single reliable non-invasive technique used for early detection of venous or arterial compromise resulting in flap failure. In this chapter some of the techniques and technologies used for monitoring the perfusion of free flaps will be described.

4.1 **Clinical Evaluation of Free Flaps**

Most centres rely on a Flap Observation Chart for routine monitoring of the free flap post operatively. This includes monitoring and recording parameters such as surface temperature, colour, texture, pin prick test and capillary refill time.

These clinical examinations are performed on all flaps and recorded on a flap observational chart during post-operative care by the nursing staff in the post-anaesthesia recovery room until up to 3-4 days post-operatively. Various centres perform these clinical observational checks at different frequencies and intervals. The

most common intervals are every 15 to 30 minutes in the first six hours, then every 1 hour for a total of 24 hours post-surgery, followed by every 2 hours for the subsequent 48 hours. In some centres this is performed in conjunction with another monitoring technique such as Doppler ultrasound. Small changes to the flap can be an indicator of the health of the microvascular in the flap, some of these changes are explained below:

- Colour –provides an indication of the health of the flap, i.e. pale flap is an indicator of not enough blood supply (compromised arterial supply) and dark flap can indicate compromised venous return [34];
- Capillary refill time – mild pressure is applied to the surgical flap until it turns white then the time taken for the colour to return once the pressure is released is counted. A 3-second refill is considered normal, no blanch may be an indication of a congested flap and a quick refill indicates a good arterial flow or can be symptomatic of a compromised venous return. If there is no refill it signifies an arterial occlusion [35];
- Texture – similarly this test checks for adequate blood supply to the flap, hard and swollen flap is an indicator of oedema, haematoma or tension and arterial congestion or kinking of the flap may cause sponginess to the flap [35];
- Temperature – assessed with the back of the fingers of the hand where a flap should be the same temperature as the surrounding tissue. A cooling flap may indicate lack of blood supply. Flap temperature is also monitored using a temperature probe;
- Pin prick test- several centres use sterile needles to prick the flap and assess the colour of the bleeding as well as the time taken for the blood to emerge[36]. Excessive exit of dark red blood is caused by venous blockage and no bleeding indicates arterial congestion [37].

However these clinical tests are objective where the colour of the flap is dependent on the brightness of the room by the patients' bed side specially as these tests are initially performed overnight post-surgery, the capillary refill time is rarely timed using a watch and assessing flap temperature with the back of the hand is an objective method of

monitoring flaps. Therefore, these clinical tests are highly subjective, labour intensive and they are dependent on the clinician's experience and opinion.

There have been many studies on reliability of using other techniques in conjunction with the free flap observational chart some of these are presented and discussed in this section.

4.2 Temperature Monitoring

High body temperature has been used as an indication of illness for many years when only the hand was used to detect heat or cold from the skin. Since then, many new techniques have been developed to allow measurement of the core body temperature, local temperature or regional temperature to be used as health indicators.

Some of the key types of temperature measuring systems will be explained below:

- Liquid-in-Glass Thermometers – comprises a capillary tube sealed at both ends with a liquid containing bulb at the basis of the tube which expands inside the tube and raises its height when it gets hot.
- Thermistors – are a type of resistor whose resistance varies with temperature; they can present both reduction and increase of resistance with temperature. Generally, the material used in thermistors is ceramic or polymer.
- Thermocouple – is a device consisting of wires of two different materials (usually metal alloys) which are joined together at one end, that produce a voltage when the metals are subjected to a temperature change.
- Thermography – is a contactless method that is used to detect and measure an objects thermal energy using an IR camera. Since radiation is emitted by all objects, thermal imaging cameras can be used to detect radiation in the infrared range of the electromagnetic spectrum. The amount of radiation emitted by an object increases with temperature, so it is possible to see changes in temperature in that object.

4.2.1 Temperature used in flap monitoring

Neligan et al (1993) showed that surface temperature measurements can provide an indication of compromised perfusion in replanted tissue [32]. Two thermocouples or two thermistor probes were used to measure the temperature difference between the replanted tissue and a control site. An increase in differential temperature was used to alert the surgical team to a potential problem [38]. Salgado et al (2009) noted that a difference in temperature of more than 3°C between the flap and the adjacent skin is an indication of arterial occlusion and a difference of 1°C and 2°C is mostly associated with venous occlusion [34]. In this technique the temperature is relatively slow to respond to change in the blood supply and cannot distinguish between arterial and venous occlusion. Moreover, Stepnick and Hayden (1994) showed that this technique may not be effective with buried flaps due to heat exchange with surrounding tissue [39].

Skin temperature can also be measured by thermography, which uses an infrared camera (Figure 4.1) to record a thermal image of the skin surface.

Figure 4.1: Shows a typical thermography camera [40].

This technique has been used by Salmi et al (1995) and Mercer et al (2010) where thermography was used to record the thermal image of the skin surface by mapping cutaneous perforator vessels pre-operatively and post-operatively [41-42]. Figure 4.2

shows intra-operative thermal image of a Deep Inferior Epigastric Perforator flap used in breast reconstruction.

One of the disadvantages of this technique is that it is operator dependant. It is also an intermittent monitoring technique and is only suitable for surface flaps.

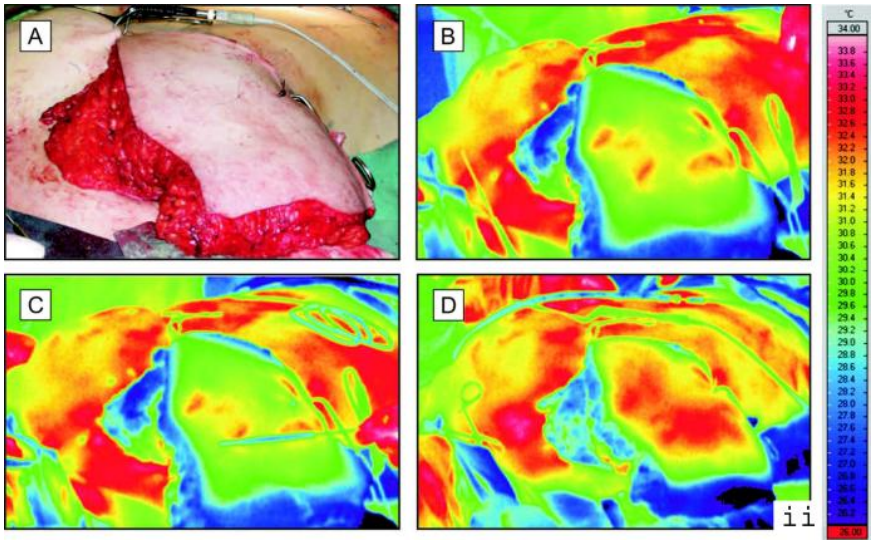

Figure 4.2: (A) Shows a digital photograph of a DIEP flap. (B) and (C) show infrared thermal images of the same flap after successful microsurgical anastomosis. The thermal image in D was taken some minutes after a second vein had been anastomosed to improve flap drainage. An improvement in the rewarming of the flap can be seen in red [40].

4.3 Doppler ultrasound

Doppler ultrasound can be used in detecting the presence, direction and speed of blood flow in vessels by identifying the Doppler shift. The Doppler Effect is a change in the frequency or wavelength of a wave as a result of movement, this is what is used in Doppler ultrasound by emitting an ultrasound beam to the skin and as the sound waves interact with flowing blood, some are scattered and returned to the ultrasound probe. There is a change in the frequency of the wave for an observer (blood) moving relative to the source of the wave (ultrasound probe). The difference between the frequency of the emitted ultrasound and the frequency of the detected ultrasound is the Doppler shift which is proportional to the emitted frequency and to the speed of blood flow [43-44].

If the red blood cell is moving towards the ultrasound source, the reflected frequency is higher than the incident frequency, if the blood is flowing away from the ultrasound source the reflected frequency is lower than the frequency of the emitted ultrasound wave.

One of the older and simpler Doppler ultrasounds is the CW (Continuous Wave) Doppler. This instrument uses a dual-element transducer for transmitting and receiving sound beams continuously. The Doppler shift is made audible through amplification and applied to a loudspeaker. The frequency of the audible sound is proportional to the reflector speed [44].

4.3.1 Doppler Ultrasound used in flap monitoring

Doppler ultrasound (Figure 4.3) is a popular method used for flap monitoring. Preoperatively it is used for locating suitable perforators to supply adequate blood supply to the flap, these perforators are then marked and used for post operative monitoring.

Figure 4.3: Shows a typical handheld Doppler ultrasound [45].

It is common practice in many centres to use Doppler ultrasound in combination with clinical observations for flap monitoring. An audible arterial signal from a Doppler combined with observation of skin colour (to monitor venous return) and capillary

refill, could be used as an indication of the health of the flap. If the Doppler signal disappears, or the skin colour turns dark or blue (suggesting venous pedicle obstruction), it is suggestive of a compromised flap [1].

Hirigoyen et al (1995) used a handheld transcutaneous Doppler probe to confirm the presence of flow in the vessels supplying the flap by taking measurements at regular intervals [46]. Harrison et al (1981) also used this technique and realised one of the disadvantages of this instrument is that it cannot measure dermal blood flow. It was also noted that for continuous measurement of blood from within a vessel requires a frame to hold and maintain the position of the probe accurately over the skin surface. Moreover, assumptions of blood-vessel size and geometry must be made in order to convert flow into absolute values [47].

4.4 Laser Doppler Flowmetry

Laser Doppler Flowmetry (LDF) (Figure 4.4) has been widely used in a clinical setting since 1977 [48-49], this is a non-invasive method to measure blood flow in the microcirculation. LDF works using the Doppler principle which is the change in the frequency of light or sound waves that is reflected from a moving blood cell. This device provides an indirect measurement of the velocity of red blood cells by aiming a monochromatic laser beam at the skin surface under observation with low power laser light from a probe which contains optical fibre light guides. The light is scattered within the tissue and some is reflected back to the probe as shown in Figure 4.4i. The reflected light that is detected from stationary tissue is not shifted and remains at the same frequency as the transmitted light, but the light that is reflected off moving red blood cells undergoes a frequency shift [50]. This produces an oscillation of the measured light intensity. The reflected light which is detected by the photodetector and converted into voltage is then processed to calculate the average velocity of cells. The degree of the frequency shift from the moving blood cells is proportional to the velocity of the blood cell that it interacts with [1].

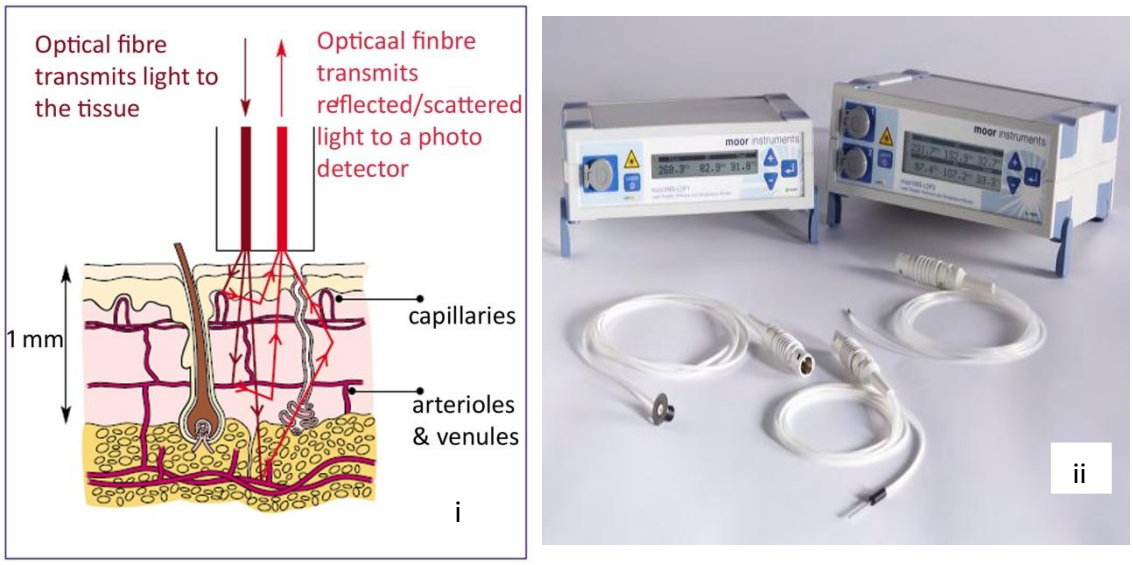

Figure 4.4: i) shows the principle of laser Doppler flowmetry and ii) shows an example of the a single and dual channel device with a variety of probes [51].

The microvascular perfusion can be calculated using this device by multiplying the number of blood cells moving in the tissue by the mean velocity of these cells which results in a value to represent the perfusion (flux).

4.4.1 Laser Doppler Flowmetry used in flap monitoring

Laser Doppler Flowmetry has been widely used to indicate the perfusion of tissue and it has specifically been used as a flap monitoring device. There are many advantages to using LDF as it is non-invasive, portable and many authors have concluded that this method has improved flap survival [52-54]. However, the output of LDF can be affected by probe movement, changes in ambient conditions, fluid collection beneath the probe, and electrical noise [55]. According to Svensson et al. (1993), the recordings of LDF requires careful interpretation and furthermore, Yoshino et al. (1996) after monitoring 37 free flaps were unable to distinguish between arterial and venous occlusion in their cases of flap failure [56-57].

4.5 Laser Doppler Imager

Laser Doppler Perfusion Imaging is a non-invasive technique that produces 2D images of tissue perfusion. A near infrared laser beam scans over the skin surface the depth of penetration of which can be 0.5mm to 2mm depending on the tissue properties. This laser beam moves stepwise over the tissue area under observation. The backscattered light which is partly Doppler shifted due to the moving blood cells in the superficial microvasculature are detected by a photodetector. The output signal that is generated scales linearly with tissue perfusion which is defined as the concentration and speed of flow of blood cells. The perfusion measured can be shown numerically or as a colour coded image by processing the detected signal in order to build a colour map of the blood flow. A digital camera records a photograph simultaneously while processing a colour image of the tissue which corresponds with the blood flow image in both size and aspect [58-60]. Figure 4.5 shows a photograph of a typical Laser Doppler Perfusion Imaging system (PIM 3, Perimed AB, Sweden).

Figure 4.5: A photograph of a Laser Doppler Perfusion Imaging system (PIM) [61].

4.5.1 Laser Doppler Imager in flap monitoring

The use of aser Doppler imaging technique has been investigated as a potential monitor of free flap viability. Tonseth and Tindholdt et al. (2007) evaluated the effect of single and multiple-based perforator flaps on the microcirculation in 17 rats. The

results of this study suggested that laser Doppler imaging was able to identify that the microcirculation in the single-based perforator flap was not reduced after dissection [62]. Schlosser et al. (2010) successfully investigated the feasibility of using a laser Doppler imaging system in detecting ischaemia in 18 free flaps [63]. Tindholdt et al. (2011) monitored 20 patients in order to identify microcirculatory changes in various zones in DIEP flaps using the technique of laser Doppler imager (using the PIM 2 system as shown in Figure 4.6). The technique has proven to be reliable in detecting perfusion levels in the different flap zones [60]. Van den Heuvel et al. (2011) studied 14 patients undergoing DIEP flap reconstructive surgery. With the aid of a laser Doppler imaging system they have showed that flap perfusion did not alter after dissection and that it only changed after flap transplantation when central blood flow increased and peripheral flow decreased [64].

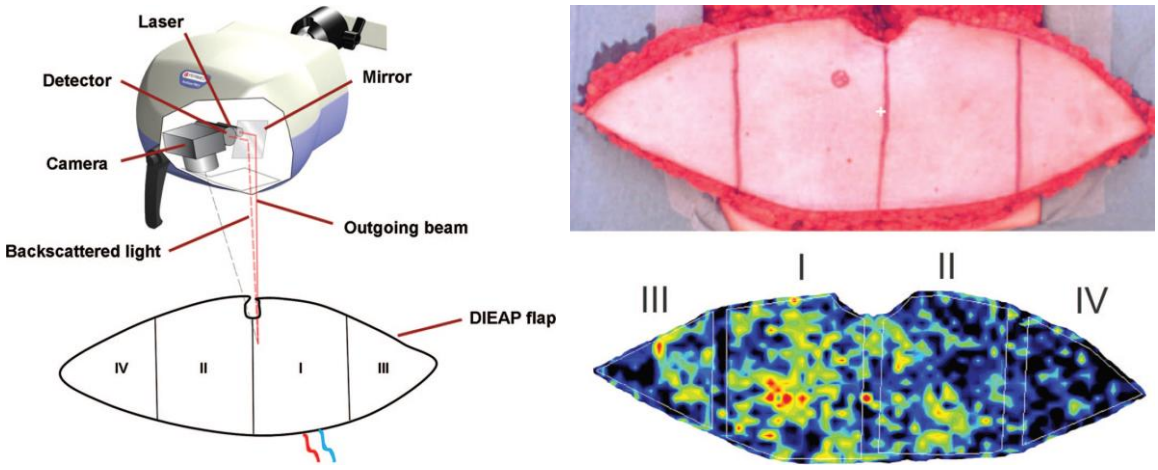

Figure 4.6: i) represents a schematic presentation of the experimental setup; ii) shows the laser doppler imaging colour map of the blood flow according to the skin island of the DIEP flap (with perfusion zones marked) as shown in the photo where red indicates highest perfusion values and black indicating the lowest [60].

Despite the laser Doppler imaging system being successfully used in monitoring flaps as discussed in the above studies, it is not capable of providing a dynamic continuous monitoring of the free flap due to its slow response time [65-66].

4.6 Near infrared spectroscopy (NIRS)

Near Infrared Spectroscopy (NIRS) is used to measure haemoglobin content and oxygenation in local tissue using the principle of optical spectrometry. The tissue under observation is illuminated by shining near infrared light in the spectral range of 700-1100 nm; this light is absorbed by the haemoglobin and other surrounding tissue which results in the reduction of light intensity. Changes in the intensity of the detected light can be said to be due to the changes in the concentration of oxygenated and deoxygenated haemoglobin [67-69].

By calculating the ratio of oxyhaemoglobin and deoxyhaemoglobin it is possible to calculate tissue oxygen saturation (StO_2) which is the percentage of saturated haemoglobin.

4.6.1 Near Infrared Spectroscopy used in Flap monitoring

NIRS has been investigated as a potential monitor of free flap viability in a number of studies. Irwin et al (1995) and Thorniley et al (1998) used near infrared spectroscopy to study flap perfusion in animals (Niro-500, Hamamatsu Photonics, United Kingdom) and were able to detect and characterise the difference between arterial, venous and total occlusion [70-71]. Hayden et al (1996) used a porcine model to assess a dual wavelength near infrared spectrometer for flap monitoring with encouraging results [72]. Stranc et al (1998) monitored an oxygen saturation index in experimental flaps in rats using near infrared spectroscopy. It was found that a fall in the index was associated with dehydration and flap necrosis in the flaps [73]. Keller et al (2007) also used NIRS (T.Ox Tissue Oximeter, ViOptix Fermont, CA), as shown in Figure 4.7, in monitoring free flaps in breast reconstruction.

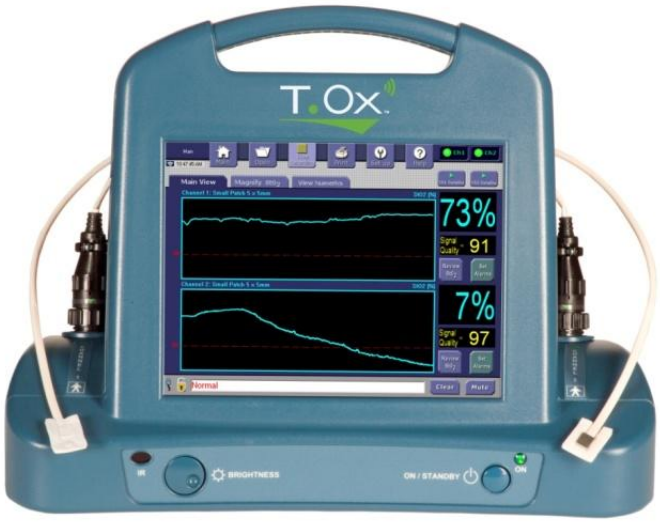

Figure 4.7: Shows a ViOptix Tissue Oximeter (T.Ox) [67].

An example of this device on a Deep Inferior Epigastric Perforator (DIEP) flap can be seen in Figure 4.8. Keller et al (2007) found that the device accurately indicated the drop and rise in oxygen saturation during flap transfer and after blood flow was established [69].

Figure 4.8 In this patient an NIRS monitor is used in postoperative monitoring of the DIEP flap [67].

Over the past decade there have been many papers investigating the use of NIR in flap perfusion and many of these attempts have been successful [68, 74] however due to the high cost of the system it has not become a standard clinical monitoring technique.

4.7 Photoplethysmography

Photoplethysmography (PPG) is a non-invasive optical method used in detecting pulsation which is associated with changes in blood volume in the peripheral vascular bed of tissue [75]. This variation in blood volume in the vessels is detected by emitting light using LEDs onto the tissue and detecting the backscattered light using a photodetector. As haemoglobin is the main light absorber in blood, the intensity of the light detected by the photodetector changes in proportion to the volume of blood in the peripheral tissue, the detected pulsation is synchronized to each heartbeat [76].

The PPG technology has been adapted to monitor a variety of parameters such as measuring arterial blood oxygen saturation (pulse oximeters), estimating blood pressure and cardiac output and also detecting peripheral vascular disease [76]. As photoplethysmography is the technique which will be used in this project, it will be discussed further in Chapter 5.

4.7.1 Photoplethysmography used in flap monitoring

There have been relatively few studies of free flap perfusion using PPG systems. Thorne et al. (1969) was one of the first to use this technique to ascertain flap viability at the time of surgery and this proved to be especially valuable in dark pigmented individuals in whom it is difficult to visually recognise this [77]. Bardach et al. (1978) used a photoplethysmographic system to assess the arterial supply of 100 unipedicle skin flaps in 25 pigs. Eventual necrotic and surviving flaps showed significant differences in signal amplitude as early as 24 hours after transplantation. The study showed that the technique provides a usable measuring technique for skin flap viability prediction [78]. In another study by Harrison et al (1981), 61 free flap transfers were monitored using various techniques, 21 of which were monitored by photoplethysmography. The preliminary results showed a reproducible and consistent waveform in the case of normal circulation and suggested that changes in the shape of

the waveform could allow distinction to be made between arterial and venous obstruction [79]. Stack et al. (1998) studied 22 patients undergoing radial forearm fasciocutaneous free tissue transfers using a green light PPG probe. A well perfused flap spectral analysis of the backscattered light intensity showed a peak at the cardiac frequency for both the unraised and raised flap signals. Within 5 minutes of venous and arterial occlusion, the peak could not be resolved but reappeared after the occlusion was removed. The authors concluded that photoplethysmography appears to be a promising technology for tissue perfusion monitoring [80].

Galla et al. (1999) monitored flap perfusion of abdominal cutaneous island flaps in 16 rats, simultaneously using laser Doppler flowmetry (LDF) and photoplethysmography to identify intentionally occluded vessels. In this study, either the artery or the vein was clamped while perfusion was simultaneously monitored with LDF and PPG to identify the occluded vessel. The LDF signal decreased promptly after arterial clamping, however after the venous clamping, a slow decrease was noted. The LDF amplitude differed significantly between arterial and venous clamping only up to 90 seconds after occlusion but not thereafter, allowing no further distinction between the two types of vessel occlusion. In contrast, PPG measurements demonstrated significant differences between both perfusion disorders throughout the entire observation period [81]. Futran et al. (2000) also noticed changes in characteristics of measured signals between flaps with venous and arterial occlusion [55]. A further study done by Stack et al (2003) compared results from a PPG monitor with a conventional surveillance protocol that included observation, bleeding to pin prick and bedside Doppler ultrasound monitoring of the vascular pedicle. Ischemic events were detected by the PPG monitor and the monitor was able to correctly predict the survival of a flap even when the Doppler ultrasound monitor indicated an absence of perfusion [82].

4.8 **Pulse Oximetry**

Pulse oximetry (Figure 4.9) has been used in clinical practice to non-invasively monitor the arterial blood oxygen saturation (SpO_2) and heart rate by using the principle of photoplethysmography [83].

Figure 4.9: Shows a typical handheld pulse oximeter with a finger probe (Nellcor Puritan Bennett Incorporated, USA) [84].

The principle of operation of this device is based on the absorption of light by haemoglobin in the blood which is varied with oxygen. This is due to the fact that oxygenated haemoglobin and deoxygenated haemoglobin have different optical spectra in the wavelength range of 500-1000nm [85]. Two LEDs with different wavelengths of red (600-700nm) and infrared (800-1000nm) are placed on the skin to transmit light to the tissue under observation; the light can either be reflected back from the tissue or it can be transmitted through tissue and detected using a photodiode depending on the type of probe used. As the light with red and infrared wavelengths interacts with the blood some of these lights are absorbed by the oxy-haemoglobin and deoxyhaemoglobin components in blood. The light which is either reflected or transmitted through the tissue is detected by a photodiode. The detected light is made up of the pulsatile arterial blood, venous blood, tissue and bones. Using the detected signal arterial blood oxygen saturation values can be calculated.

4.8.1 Pulse Oximetry used in flap monitoring

Graham et al (1986) used pulse oximetry as a monitoring device for replanted or re-vascularised digits. During this study it was noted that vascular occlusion was detected with 100% accuracy and arterial and venous occlusion could be differentiated by changes in the oxygen saturation. It was concluded that digits with saturation values of

below 85% were associated with venous occlusion and those with no saturation represented arterial occlusion [86]. Menick et al (1988) successfully used this technique for monitoring a free latissimus muscle flap for seven days with positive results of pulsatile arterial flow and O_2 saturation [87]. Lindsey et al. (1991) proposed that the absence of PPG signal or oxygen saturation below about 80% should be taken as an indication for re-exploring the flap [88]. The principles of operation of this technique are discussed in more detail in Chapter 5.

4.9 **Conclusion**

Many different surgical techniques are available to reconstruct a breast following full mastectomy. Deep Inferior Epigastric Perforator free flaps are one of the most commonly used in breast reconstructive surgery. These flaps reduce recovery times and complication rates comparing to the other available breast reconstructive procedures. However there are drawbacks to this technique like most other surgical operations. One of the main complications of a free flap surgery is tissue necrosis which is mainly due to compromised blood supply to the tissue. If this is identified early surgical exploration can often salvage the flap. To date, flap perfusion monitoring has been relying on intermittent clinical observation. In 1995 a survey was taken in North America to find the most commonly used technique in monitoring flaps [46], the result from this survey show that Doppler ultrasound, Laser Doppler velocimetry and surface temperature measurements were the most commonly used techniques, all used in conjunction with regular clinical inspection. Another survey taken in the UK [36] presented similar results, where Doppler ultrasound and surface temperature monitoring were some of the most frequently used techniques. However, all these techniques have drawbacks. Doppler ultrasound can be used to observe blood flow in the vascular pedicle but not in the more peripheral portions of the flap and this technique cannot be used continuously. Laser Doppler flowmetry has been used in many studies and has shown some positive results but as yet it provides no absolute measurement of blood flow and its output requires expert interpretation [36, 89].

There is a need for an objective, continuous, non-invasive, safe, easily managed and interpreted by medical and nursing staff, inexpensive and a clear indicator of flap

perfusion. Photoplethysmography and pulse oximtery have shown some promise in recent studies due to its non-invasive nature. Also, with recent advances in technology pulse oximeters have become cost effective, also the PPG signal is easily interpreted by medical and nursing staff as well as providing an objective result. Using photoplethysmography in conjunction with pulse oximeter provides information on the change in volume of blood in the tissue under observation as well as the arterial blood oxygen saturation levels in the tissue. The principles of photoplethysmography and pulse oximetry and its use as a potential free flap monitoring technique will be described in more detail in following chapters.

Chapter 5

Photoplethysmography and Pulse Oximetry

5.1 Review of Photoplethysmography

A new free flap sensor based on multi-wavelength photoplethysmography has been developed for monitoring flap perfusion. This chapter describes the basic principles of photoplethysmography and pulse oximetry.

Photoplethysmography (PPG) is an optical measurement technique that can be used to detect blood volume changes in the microvascular bed of tissue [75]. It has widespread clinical applications, with the technology utilized in commercially available medical devices, for example in pulse oximeters, vascular diagnostics and blood pressure measurement systems [76].

In 1937 Alrick Hertzman and his colleagues were one of the first to establish this technique for measuring blood volume changes in the fingers and toes by exercise and exposure to cold [90].

In more recent decades there have been significant advancements in this technique to build a small, reliable, low cost, non-invasive and user friendly device. Recent developments in semiconductor technology i.e. light-emitting diode (LED) and photodiodes, have made improvements to the size and reliability of PPG probes [76].

5.2 Principle of Photoplethysmography

As commented above, Photoplethysmography (PPG) is a non-invasive, low cost, simple and easy to use technique that can be used to detect changes in arterial blood volume in the microvascular bed of tissue [76].

As light interacts with biological tissue it can be transmitted, reflected, refracted, scattered, and/or absorbed. Bone, skin pigmentation, arterial and venous blood are the primary absorbers of light with haemoglobin being the main components of blood which absorbs light passing through tissue. The absorbance of haemoglobin depends on its chemical binding and the wavelength of the light it is interacting with; oxygenated and deoxygenated haemoglobin absorb most of the light at higher wavelengths (Near Infrared wavelengths) [91].

As the heart pumps blood to the periphery, the arteries and arterioles change in diameter due to the pulsation of the blood and the volume of blood changing in the vessels. This variation of blood volume in arteries is detected by illuminating the tissue under observation using LEDs, which is usually in the range of 600-940 nm, and detecting the backscattered light using a photodetector which is sensitive to the emitted wavelengths.

During systole the volume of blood in the arteries increase, causing an increase in absorbance of light, as the cardiac cycle continues. During diastole the volume of blood in the arteries decrease resulting in lower concentration of haemoglobin, which means less light is absorbed. The intensity of light detected by the photodetector changes in proportion to the volume of blood in the tissue illuminated. The resulting information from the photodetector is a time varying signal which is known as the photoplethysmographic signal [91-92].

The detected PPG signal (Figure 5.1) is made of two components;

- A dc component which an almost constant voltage due to the absorption by venous blood, bone, tissue and skin pigmentation and non-pulsating arterial blood. A low frequency modulation can frequently be seen on the dc component which is attributed to respiration.
- An ac component which is the pulsatile part of the total absorbance often attributed to the cardiac cycle and the change of volume in the arteries. The shape of the ac PPG signal can be used as an indicative of vessel compliance and cardiac performance. The amplitude of the ac component usually does not exceed 1-2% of the dc component [83, 91].

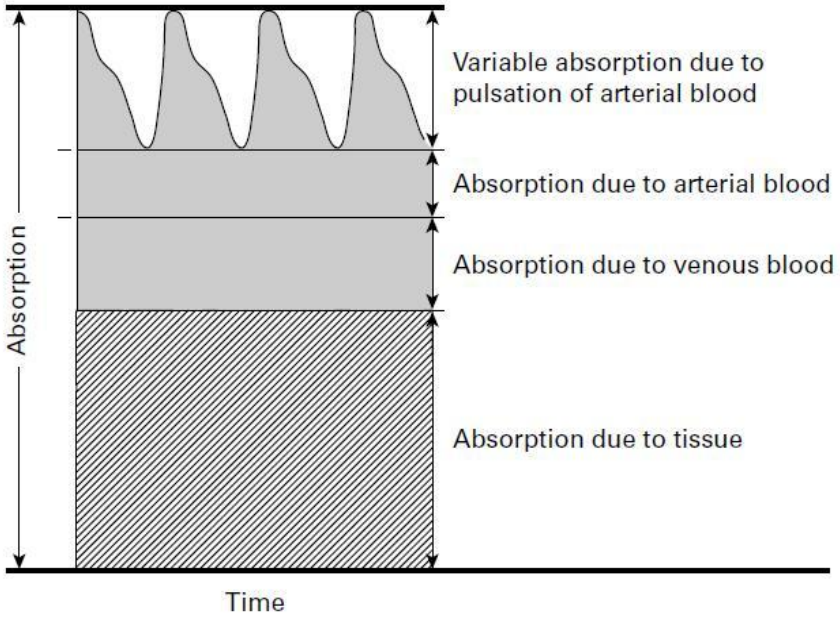

Figure 5.1: Photoplethysmographic waveform with ac (variable absorption due to arterial pulsation) and dc (absorption due to tissue, venous and non-pulsatile arterial blood) components [92].

The PPG technology has been used in a wide range of medical devices which are used for measuring arterial blood oxygen saturation (pulse oximeters) and also detecting peripheral vascular disease [76].

5.3 Pulse Oximetry

Pulse oximetry is one of the most significant technological advances in clinical patient monitoring over the last few decades [91]. It utilizes PPG measurements to determine the oxygen saturation of arterial blood (SpO_2) as well as heart rate by using two light emitting diodes (LEDs) which emit light at two different wavelengths of red (660 nm) and infrared (940 nm) and measuring the light absorption of blood where by identifying the pulsatile signal from the two wavelengths it is possible to differentiate between absorbance of arterial blood and other absorbers [76, 92-93].

In 1935 Matthes developed the first device to measure O_2 saturation, his first attempt was with red and green filters which he then changed to red and infrared filters. Pulse oximetry was developed in 1972 by Takuo Aoyagi where he was able to calculate oxygen saturation without calibration by using the ratio of red to infrared light through

the pulsating component (arteries) of blood. During the early 1980s this technology was commercialised by two companies, Ohmeda (Biox) and Nellcor [91].

In the past three decades there have been major advancements in size reduction, cost and development of multiple site probes. In 1995 Masimo introduced a technology used for signal processing to accurately measure O_2 saturation during patient motion and low perfusion states. The principle of using pulse oximetry for determining arterial oxygen saturation will be described in more detail in this chapter.

5.3.1 Wavelengths used for pulse oximetry

The principle of operation of a pulse oximeter is based on emitting light with wavelengths of red and infrared and measuring the absorbance of tissue. Oxygenated haemoglobin has a higher absorption at red wavelength (660 nm) and deoxygenated haemoglobin has a higher absorption at infrared wavelength (940 nm). This is due to the large differences in the extinction coefficients of oxy and deoxy-haemoglobin at these wavelengths as shown in Figure 5.2 which is the reason they are the most common choice of wavelengths used in pulse oximetry.

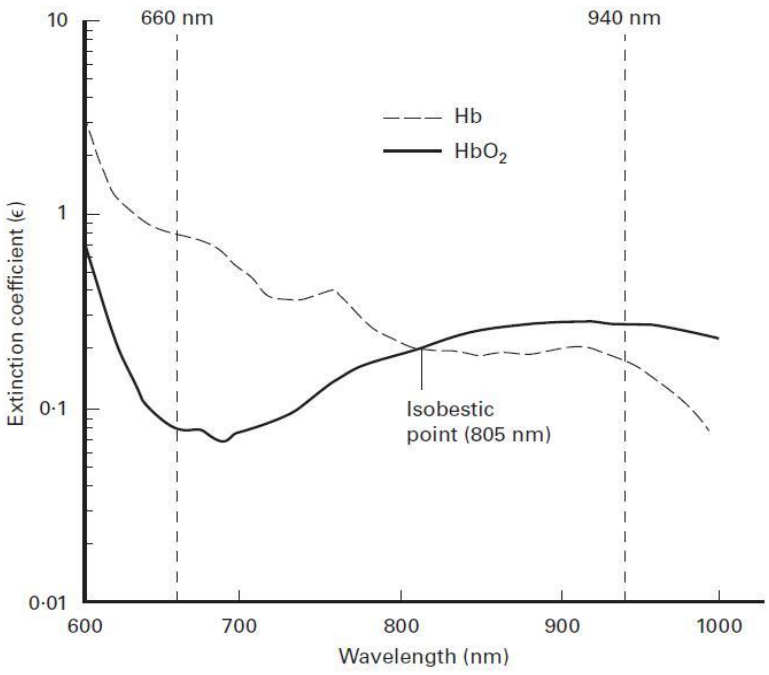

Figure 5.2: Absorption spectra of oxygenated and deoxygenated haemoglobin showing the two most commonly used wavelengths, the isobestic point is where the absorbance of oxy and deoxy-haemoglobin is equal [92].

Another reason for the choice of these wavelengths is the flatness of the absorption spectra at these wavelengths which ensures that there is no shift in the peaks at these wavelengths which would result in errors [91-92].

Pulse oximeters estimate arterial oxygen saturation by shining light at red (R) and infrared (IR) wavelengths through vascular tissue. The factors described above contribute to the choice of these wavelengths greatly. Photoplethysmographic signal is obtained by illuminating the skin and detecting the light not absorbed by pulsatile arterial blood, venous, tissue and bone. As described previously the ac component of the PPG signal is assumed to be solely due to the pulsatile blood in the arterial vessels. The amplitude of the red and infrared signals depends on arterial oxygen saturation as oxygenated and deoxygenated haemoglobin absorb different amounts of the emitted lights. By measuring the amplitudes of the ac PPG signals from red and infrared wavelengths and the corresponding dc signals, the arterial oxygen saturation value can be estimated. Therefore, the principle of light absorption is crucial in understanding the basis of estimating arterial oxygen saturation (SpO_2). In conventional practice the sensor and the system are empirically calibrated to account for the effects of light scattering. However, in order to provide a better understanding of the absorbance of light through tissue, the principles of the Beer-Lambert law will be explained in the following section.

5.3.2 Beer Lambert Law

The relationship between the absorption of light and haemoglobin concentration was first described by Johann Heinrich Lambert in his publication dated 1706. These ideas were then further investigated by August Beer who then published the Beer-Lambert Law in 1851 [92].

Beer's Law describes the attenuation of light passing through a uniform medium which contains an absorbing substance.

$$I = I_0 \, e^{-\varepsilon(\lambda) c d} \tag{5.1}$$

As shown by Equation (5.1), if monochromatic incident light of intensity I_0 enters the medium, a part of this light is transmitted through the medium and another part of this light is absorbed. This effect causes the intensity I of light travelling through the medium to decrease exponentially with distance [91].

In pulse oximetry the dc component of the signal from the tissue absorb a constant amount of the incident light I_0 from skin pigmentation, bone, venous blood and the non pulsatile part of the arterial blood. During diastole the arteries have a decreased volume of blood, therefore the optical path length through the arteries is at a minimum and the light intensity detected at the photodiode is at a maximum level. During systole, due to increased volume of blood in the arteries, the optical path length reaches a maximum and therefore there is more haemoglobin to absorb the light which causes the light reaching the photodiode to be at a minimum level [91].

Although the Beer-Lambert law is used in pulse oximetry it doesn't take into consideration many physiological conditions which occur during the cardiac cycle, such as variable path length, existence of many other substances in the tissue and blood other than haemoglobin and other effects of light on tissue such as diffusion, refraction and reflection. These effects are accounted for by empirically calibrating the pulse oximeter. However, assumptions made during an empirical calibration are only valid for a limited range of saturations [83].

From the amplitude of the ac component and the constant voltage of the dc component of the PPG signal at these two wavelengths, the R/IR ratio is calculated and the resulting value is compared to a "look-up" table which is based on calibration curves derived from healthy subjects at various SpO_2 levels [92].

The calibration curve of the pulse oximeter is empirical which means that it is based on human volunteer experimental data. This calibration procedure involves desaturating the subjects by breathings a gas mixture and collecting measurements at different oxygenation levels.

Equation (5.2) is used to derive the R value:

$$R = \frac{AC_{660}/DC_{660}}{AC_{940}/DC_{940}} \quad (5.2)$$

The calculated R value is then used to compute the arterial oxygen saturation using (5.3).

$$SpO_2 = 110 - 25\,R \quad (5.3)$$

A typical relationship between the ratio (R) (Equation (5.2) and SpO_2 is shown in Figure 5.3 as the calibration curve used for pulse oximeters. One of the problems associated with pulse oximeter calibration is the ethical issue of deliberately desaturating any subjects below 85% due to the risk of brain damage, and therefore because of this limitation, it is necessary to estimate (extrapolate) the calibration curve for SpO_2 values below 85% [92].

At approximately 85% oxygenated haemoglobin and deoxygenated haemoglobin absorb the same amount of light, therefore the amplitudes of their signals are the same, resulting in R/IR=1 [4].

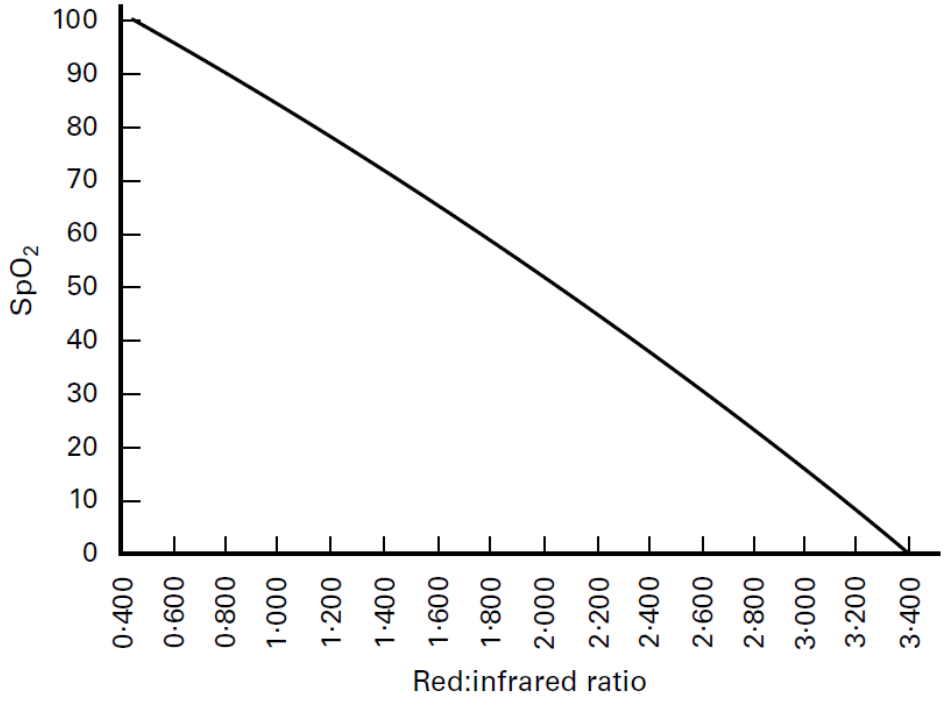

Figure 5.3 relationship between R (Red : infrared ratio) and SpO_2 values [92].

5.3.3 Types of optical probes used in pulse oximetry

Pulse oximeters can measure SpO_2 using both the reflection and transmission modes of operation [94].

Transmission pulse oximetry probe is what is used by majority of commercially available pulse oximeters which consists of the light-emitting diodes mounted opposite the photodetector where light will pass through the tissue and the amount of light transmitted through will be detected by the photodetector. This is shown diagrammatically in Figure 5.4 but it is important that it is a snug fit, with a constant but light pressure on the tissues, and that the energy cannot bypass the tissues. The whole sensor must be protected from ambient light over the range of wavelengths to which the detector is sensitive to avoid errors [92].

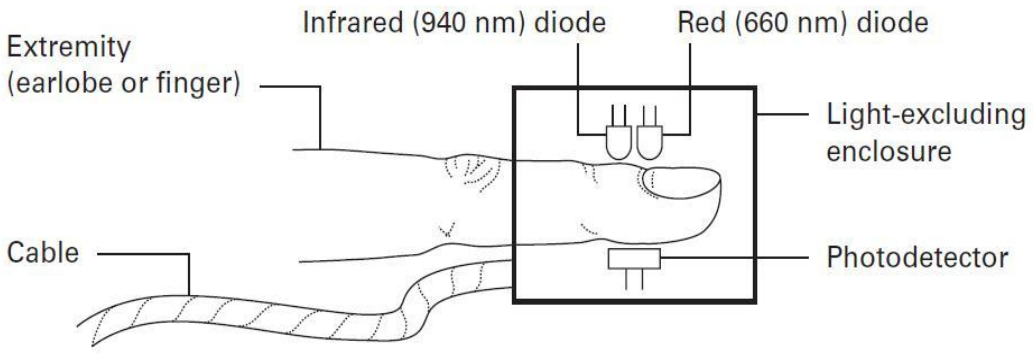

Figure 5.4: Transmission pulse oximeter sensor [92].

Reflectance pulse oximetry probes have recently been introduced by several companies. As shown in Figure 5.5 in this design the LEDs and the photodetector are mounted side by side where the intensity of the reflected light from the tissue is used to measure SpO_2.

From a clinical point of view a reflection pulse oximeter has the advantage that it can be used at more sites than the transmission type, for example the forearm, thigh, chest, forehead and cheeks. This means that its saturation readings can be made in patients with poorer perfusion and in those who are hypothermic [91-92]. This probe design will be used in this project for monitoring perfusion of flaps.

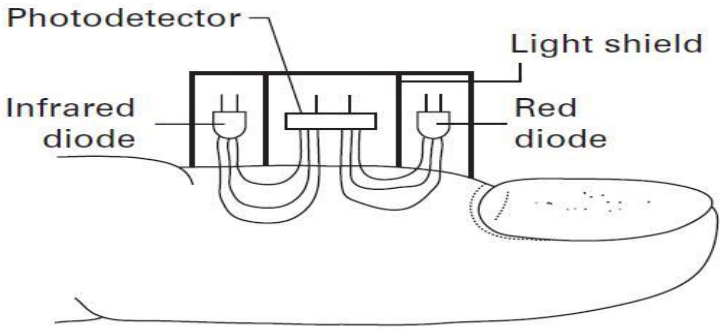

Figure 5.5: Reflective pulse oximeter sensor [92].

One of the important factors to take into consideration when designing a reflectance probe is the distance between the LEDs and the photodetector. In 1988 Mendelson and Ochs revealed that the intensity of the backscattered light decreases in direct proportion to the square of the distance between the photodetector and the emitters. A separation distance of 4-5mm was suggested to provide the best sensitivity and PPG signals with adequately large amplitudes [94].

5.4 Conclusion

In conclusion the principles of photoplethysmography and its application in pulse oximetry have been discussed in this chapter where it has been noted that the pulsatile PPG signal (ac) is assumed to be attributed to the variations in the arterial blood. It has also been shown that the amplitudes of the red and infrared ac PPG signals are sensitive to arterial blood oxygen saturation levels due to the differences in the light absorption of oxygenated and deoxygenated haemoglobin at the two wavelengths. By taking advantage of this phenomenon the ac and dc PPG signals provide the capability of estimating arterial blood oxygen saturation levels (SpO_2).

In an attempt to investigate changes in volume of arterial blood pulsating in flaps as well as the oxygenation of that blood, this technology was developed. The following chapter describes how photoplethysmography and the principle of pulse oximetry are used to develop a three wavelength optical sensor to be used in monitoring the perfusion of flaps.

Chapter 6

Development of a reflectance photoplethysmographic flap sensor

6.1 Introduction

To overcome the limitations of current techniques to assess flap viability as described in Chapter 4 a new flap reflectance PPG sensor was developed. This sensor was used in clinical trials to investigating the feasibility of detecting PPG signals and estimating blood oxygen saturation of flaps in 20 patients.

In addition to the flap PPG sensor, a finger PPG sensor was also developed using identical optical components which was placed into a modified commercial pulse oximeter clip. This additional sensor will enable comparison of the estimated oxygen saturation and PPG signals from both the flap and the finger. Details of the construction of both of these sensors as well as evaluation tests are presented in this chapter.

6.2 Three wavelength flap photoplethysmographic sensor

A new reflectance, three-wavelength photoplethysmographic sensor was developed which consists of two infrared (IR), two red (R) and two green ceramic chip surface mount LEDs and a surface mount photodiode. An illustration of the developed sensor is shown in Figure 6.1. For the measurement of PPG signals from flaps, the optical components were configured in the reflectance mode instead of the more commonly used configuration of transmission mode. As transmission mode requires the tissue under investigation to be placed in between the light source and the detector which would have restricted the monitoring sites.

The shape of the sensor was decided to be circular and was designed to be small enough with a diameter of 20mm in order to be accommodated on the exposed part

of the flaps (mainly DIEP flaps) during and after the operation. Also, shown in Figure 6.1 is a diagram representation of the probe inside the black sensor cover, which was specifically designed to prevent penetration of surrounding light and their interference with the PPG signal. A separation distance of 4-5mm was applied between the photodiode and each LED to provide the best sensitivity and PPG signals with adequately large amplitudes [94]. The cover also facilitates in securing the sensor on the flap which will be discussed later on in this chapter.

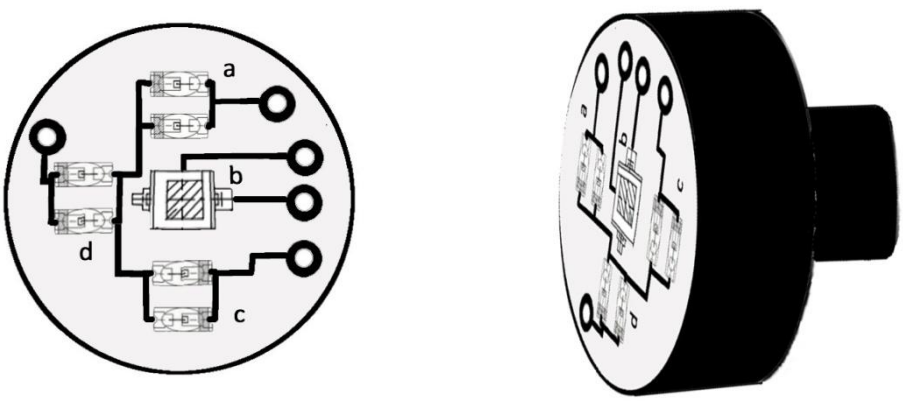

Figure 6.1: Diagram of the reflectance photoplethysmographic flap sensor; a: IR surface mount LED; b: PIN photodiode in flat plastic package; c: red surface mount LED, d: green surface mount LED.

The optical components of the sensor are driven using a developed photoplethysmographic processing system, therefore the PPG sensor is connected to the PPG processing system using a multicore cable with PVC insulation.

6.2.1 Optical Components

The optical components selected for the flap PPG sensor was based on specific requirements for estimating blood oxygen saturation values as discussed in previous chapters. As seen in Figure 6.2 oxygenated haemoglobin and deoxygenated haemoglobin have widely different absorptions at red and infrared wavelengths which make them suitable for use in pulse oximetry. The figure also suggests that green light is strongly absorbed by haemoglobin which results in its short depth of penetration to provide a means to monitor changes in blood volume in the dermal capillaries, hence the use of these wavelengths for flap monitoring.

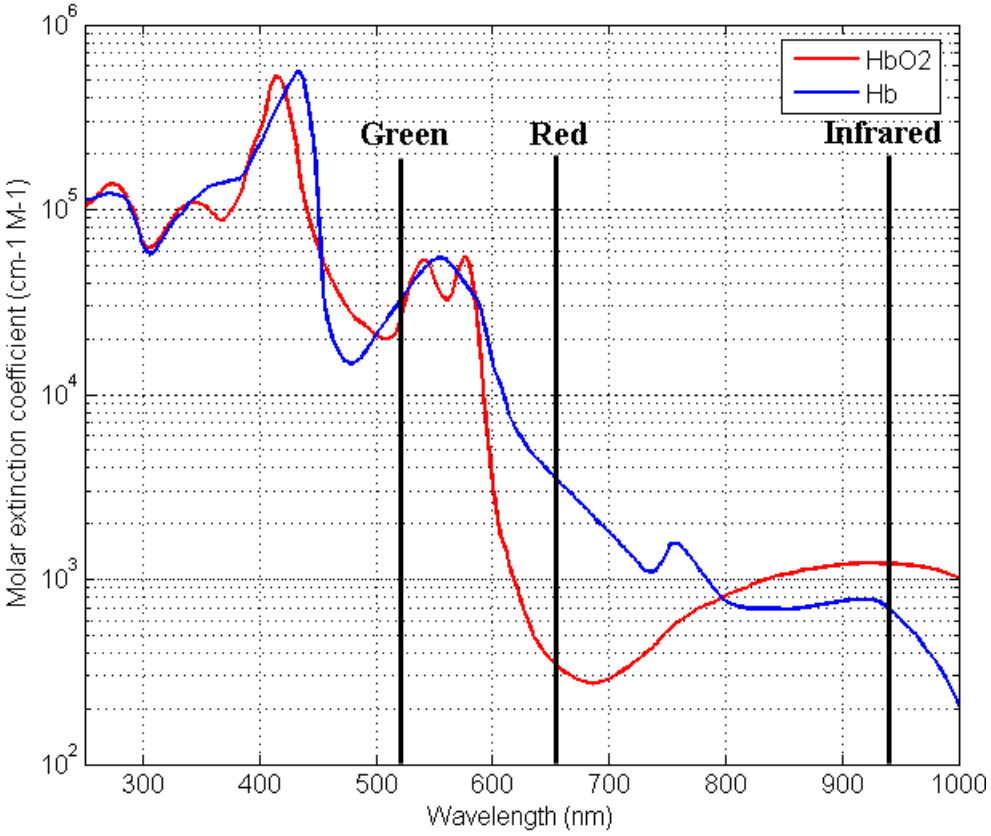

Figure 6.2: Showing absorption spectra of oxygenated haemoglobin and deoxygenated haemoglobin at the three chosen wavelengths.

The reflectance photoplethysmographic flap sensor was constructed using two infrared with peak emission wavelength at 940nm and dimension of 2.0 x 1.25mm (AP2012F3C, Kingbridght), two red with peak emission wavelength at 660nm and dimension of 2.0 x 1.25mm (EM20UR, EUROLED) and two green with peak emission wavelength of 520nm and dimension of 3.0 x 1.20mm (CR60G, CERLED) surface ceramic chip surface mount LEDs. The opto-electronic characteristic and illustrations of the infrared (IR), red (R) and green used for the sensor are shown in Table 6.1, Table 6.2 and Table 6.3 respectively.

Table 6.1: Optical, electrical and package characteristics of the IR emitter (940nm).

Electrical/ Optical Characteristics at T_A=25°C	
Power dissipation	100 mW
Peak forward current	1.2 A
Continuous forward current 1/100 Duty Cycle, 0.1ms Pulse width	50 mA
Storage temperature	-40°C to 85°C
Operating temperature	-40°C to 85°C
Soldering temperature	245°C
Peak emission wavelength	940 nm
Spectral half bandwidth	50 nm
Forward voltage	1.6 V
Reverse leakage	10µA
Reverse voltage	5 V
Light emission angle	120°

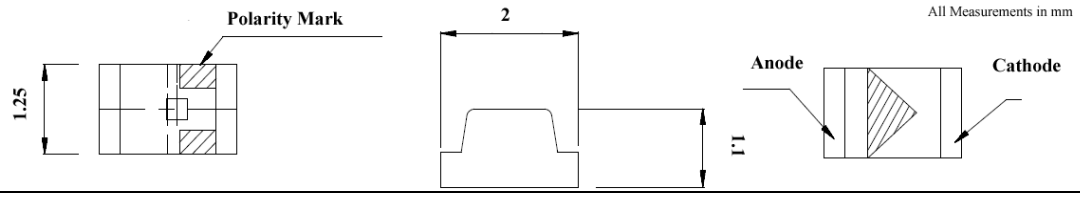

Table 6.2: Optical, electrical and package characteristics of the Red emitter (660nm).

Electrical/ Optical Characteristics at T_A=25°C	
Power dissipation	100 mW
Peak forward current 1 / 10 Duty Cycle, 0.1 ms Pulse Width	150 mA
Continuous forward current	30 mA
Junction temperature	120°C
Storage temperature	-40°C to 85°C
Operating temperature	-40°C to 85°C
Luminous intensity	70 mcd
Peak emission wavelength	660 nm
Spectral half bandwidth	20 nm
Forward voltage	2.5 V
Reverse leakage	10µA
Reverse voltage	5V
Light emission angle	120°

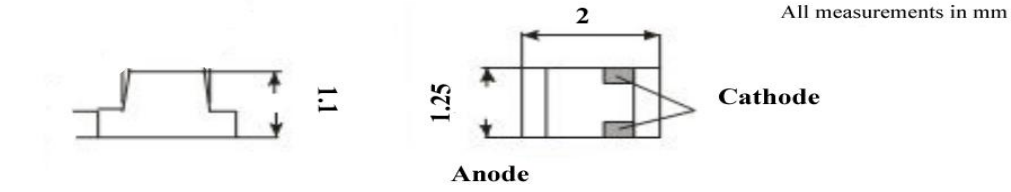

Table 6.3: Optical, electrical and package characteristics of the green emitter (520nm).

Electrical/ Optical Characteristics at T_A=25°C	
Power dissipation	130 mW
Peak forward current, 0.1ms Pulse Width	100 mA
Continuous forward current	30 mA
Junction temperature	120°C
Storage temperature	-20°C to 120°C
Operating temperature	-20°C to 80°C
Soldering temperature	240°C
Luminous intensity	180 mcd
Peak emission wavelength	525nm
Spectral half bandwidth	35nm
Forward voltage	3.8V
Reverse leakage	10µA
Reverse voltage	5V
Light emission angle	170°

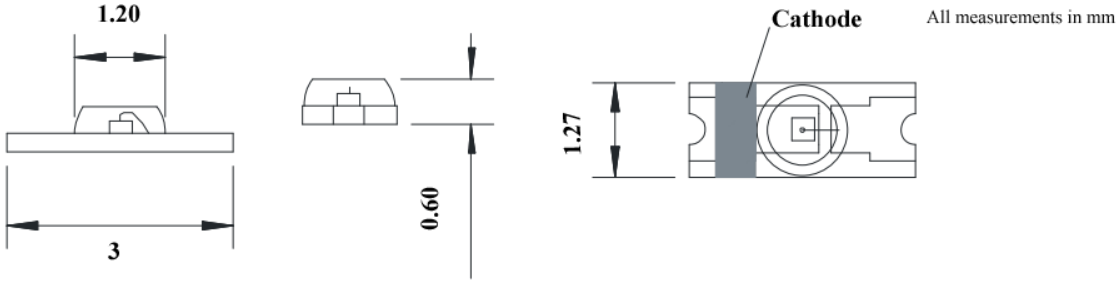

To detect the backscattered light from the tissue a photodiode is used where its characteristics, absolute maximum ratings and illustrations of the photodiode are shown in Table 6.4.

Table 6.4: Characteristics, absolute maximum ratings and illustrations of the photodiode used on the PPG flap sensor (VBPW34S).

Basic Characteristics at T_A=25°C	
Forward voltage	1.3 V
Breakdown voltage	60 V
Reverse dark current	30 nA
Open circuit voltage	350 V
Reverse light current	55 µA

Angle of half sensitivity	±65°
Wavelength of peak sensitivity	940 nm
Range of spectral bandwidth	430 to 1100 nm
Rise time and Fall time	100 ns
Absolute Maximum Ratings at T_A=25°C	
Reverse voltage	60 V
Power dissipation	215 mW
Junction temperature	100 °C
Operating temperature range	-40to + 100 °C
Storage temperature range	-40 to + 100 °C
Soldering temperature	260 °C
Thermal resistance junction/ambient	350 K/W

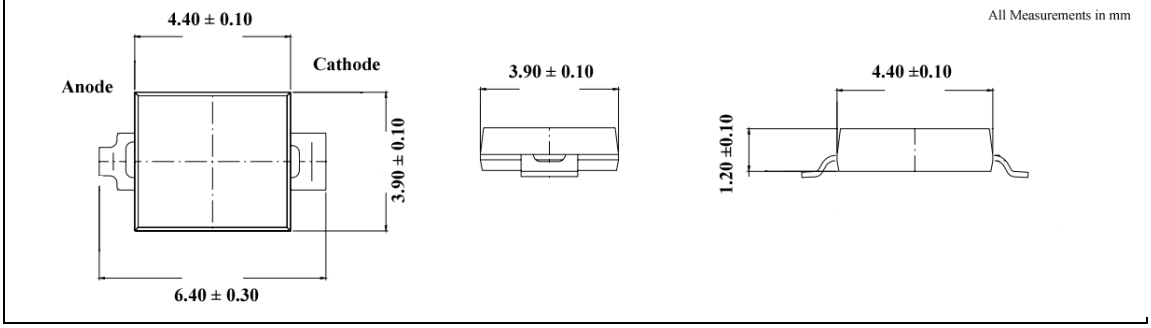

The selected detector is a surface mount silicon PIN photodiode (VBPW34S) which is a high speed with high sensitivity and an active area of 7.5 mm^2 with dimensions of 6.4 x 3.9 x 1.2 mm. Its wide range of sensitivity bandwidth of 430-1100 nm was used as this photodiode allows the detection of all three wavelengths of 520nm, 660nm and 940nm which were used in the constructed sensor.

6.2.2 Mechanical Construction of the Flap Sensor

The reflectance photoplethysmographic flap sensor was designed using printed circuit board (PCB) technology utilizing the commercial software package Altium Designer (Altium Limited, Sydney, Australia) [95]. As some of the components were not included in the Altium libraries, the symbol and footprints of components were designed using their datasheets for the dimension sizes and a component library was built to include all the components to be used on the sensor. The schematic diagram was then drawn on the schematic sheet as shown in Figure 6.3.

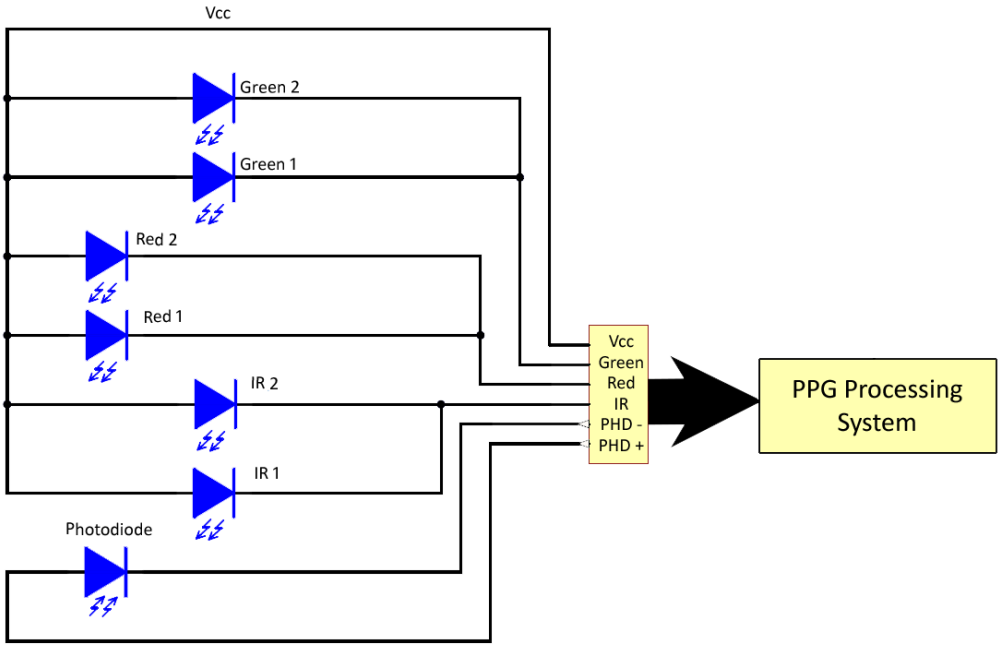

Figure 6.3: Schematic diagram of the three wavelength PPG flap sensor.

The schematic diagram was then transferred to the board layout stage to design a printed circuit board (PCB) after setting the board details such as its shape and size and the design rules such as the track width which was set at 0.4 mm, with the via hole size of 0.5 mm for the connector wires and a minimum track clearance of 0.4 mm were used. The layout of the design, the position of the components and the routing of the PCB design were repositioned until satisfied with the final artwork (shown in Figure 6.4).

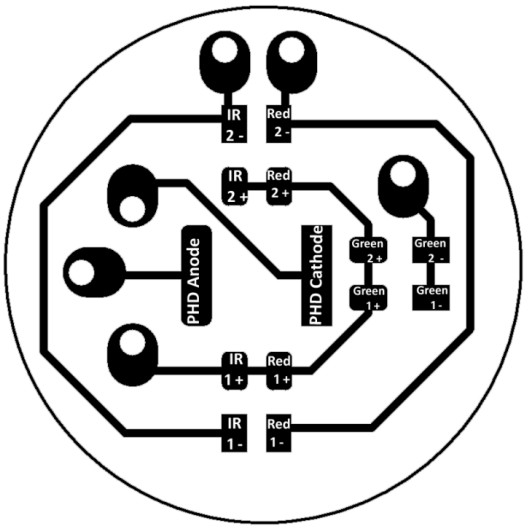

Figure 6.4: The designed PCB artwork using Altium Designer.

A positive (where black is copper) UV translucent artwork film was then generated on a transparent sheet (Laserstar, 895-945 Farnell, 100062) using a laser printer with a high resolution. The prototype PCB board (FR4 Laminate) used was made of epoxy resin impregnated glass fibre matt with electrodeposited copper coated with high quality pre-coated positive photosensitive. The panel was protected by a blue film which is also light proof to allow the board to be cut into size using a guillotine without fracturing the photoresist layer. The basic characteristics of the board used for the PCB of the PPG sensor are shown in Table 6.5.

Table 6.5: Basic characteristics of the FR4 board used for the PPG sensor.

Characteristics of FR4 Laminate	
Thickness	1.6mm
Copper foil	35 microns
Dissipation factor	35
Dielectric Constant	5.4
Solderbath resistance (260º)	20 secs.
Resist thickness	5 microns
Spectral response	350 – 450 nm
U.V. light energy required approx.	50ml / cm
Shelf life	1 year at 15 – 20ºC
Developer	3204996
Etchant	Ferric chloride pellets or liquid and fine etch crystals.

As a single sided PCB was used, the printed artwork was placed on the glass of the ultra-violet instrument (3M, Scotchal exposure unit) and after peeling the blue protective layer of the board, it was then placed on top of the artwork on the photoresist side and the hinged lid of the exposure unit was closed and secured. Following the exposure of the board to UV for approximately 3-4 minutes, it was then taken out and placed inside an empty and clean tray and the recommended diluted photoresist (Developer: 3204996, 1:4 photoresist developed: water) was poured on top to cover the board. Once the board was developed it was then taken out and placed inside the heated bubble etch tank (Mega electronics, bubble etch tank, PA104) which was filled with ferric chloride etchant previously dissolved in warm water. The

tank was then switched on and left for approximately 10 minutes or until the PCB tracks were clearly visible and all exposed parts of the board were removed. The board was then rinsed with water and dried.

The developed PCB board was then tin plated by pouring adequate volume of tinning solution in a tray to cover the PCB it was then left in place at room temperature for approximately one minute. The board was then rinsed and dried and using a vertical drill stand the holes for the connectors were drilled using a 1mm drill bit.

For soldering the surface mount components to the PCB, a forced convection reflow oven (C.I.F, FT02, France) was used. This oven is designed to work with high temperature alloys while the heat is distributed by forced convection and monitored by microprocessors. A solder paste, which is a mixture of powdered solder and flux, was used to attach the components to the contact pads on the PCB. The board was then placed inside the oven to melt the solder and permanently connect the joint of the SMD components to their pads on the PCB by subjecting the prototype to selected temperatures for specifically programmed times for the different parts of the process as shown in Table 6.6.

Table 6.6: Details of the heating times and temperatures used for soldering the SMD components onto the sensor.

Process	Temperature/Time
Waiting temperature	90°C
Preheating temperature	180°C
Preheating time	3 min
Reflow temperature	255°C
Reflow time	2 min 30 seconds

Following the end of the heating procedure, the board was then left to cool and removed from the oven. The sensor was coated using medically graded light curable clear epoxy (Dymax, OP-29, Ct, USA). A UV light curing system (Electro-lite, ELC-410, Ct, USA) was used for curing the optical adhesive. The basic specifications of the UV light curing system used are shown in Table 6.7.

Table 6.7: Specifications of the UV curing system used for the adhesive coating on the PPG sensor.

Specifications of Electro-Cure-410 UV Spot Curing	
UV Output	90 mW/cm^2 at 365nm
Power Input	120 V/60 Hz
Lamp Input	75 W Halogen
Lamp Life	800-1000 hrs

Coating the sensor with the epoxy provides adequate shielding and minimises excess electrical impedance caused by direct skin contact of the optical components and it also avoids any damage to the optical components of the sensor. The OP-29 series adhesive was selected based on its advantages of it being optically clear, resilient, resists yellowing and has high light transmission in the wavelengths of interest (500-1000nm) as shown in Figure 6.5.

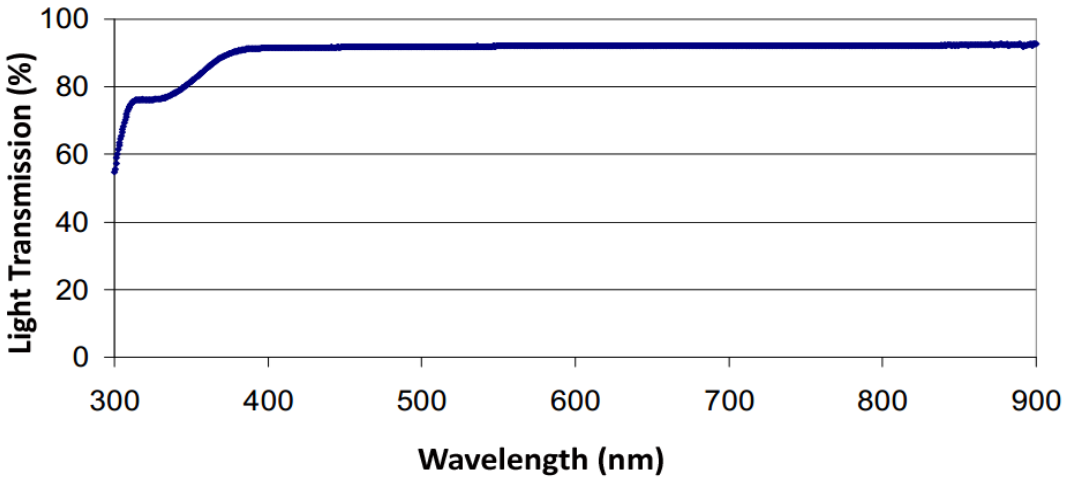

Figure 6.5: Light transmission of the OP-29 adhesive at wavelengths 300 nm to 900 nm

The adhesive was evenly spread across the sensor by using a 45° blunt end dispensing tip (Adhere, Intertronics, IJFH560085-45, Oxfordshire, UK) on the adhesive syringe. The sensor was then placed under the UV curing system for the duration of approximately 20 minutes with an approximate distance of 2cm between the sensor and the UV curing gun. UV protective spectacles were worn to provide protection from harmful UV

radiation emitted from the UV curing device. The curing speed is dependent upon the intensity of the lamp, the distance from the light source and the thickness of the cure. The sensor was then left undisturbed for 24 hours to avoid any markings on the epoxy.

Figure 6.6 shows photographs of the developed three wavelengths reflective PPG flap sensor with the LEDs on and off. In Figure 6.6 (b) the PPG sensor is covered with a sterile transparent sheath, this transparent medical dressing will be used when monitoring signals in the *in vivo* evaluation of the system to avoid cross contamination between patients and ease sterilisation and cleaning of the sensor. This will be described in more detail in future chapters.

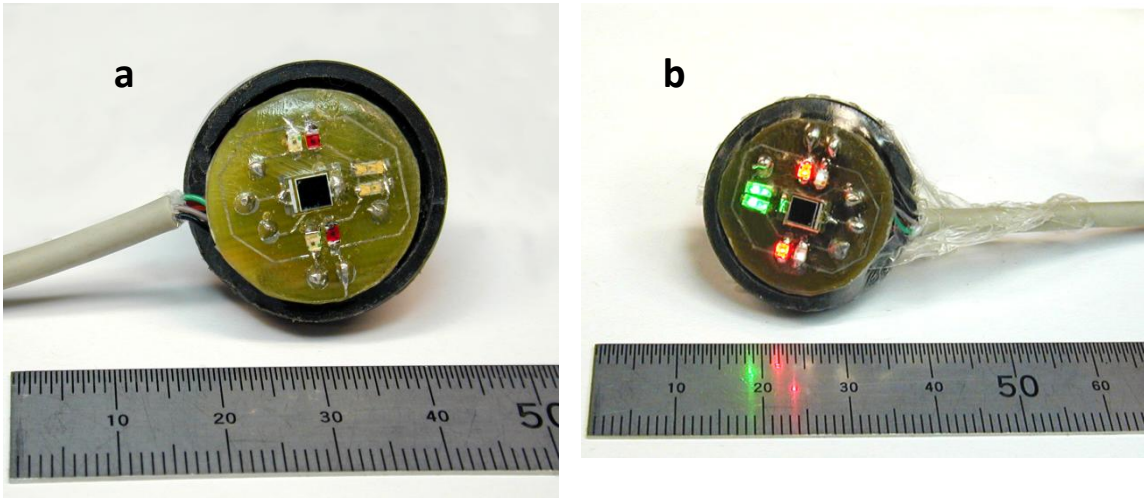

Figure 6.6: a) Shows the developed three wavelengths PPG flap sensor; b) Shows the illuminated PPG flap sensor covered in sterile transparent sheath which will be used in the *in vivo* evaluation of the sensor.

6.2.3 Evaluation of flap PPG Sensor

The functionality of the reflectance flap photoplethysmographic sensor was evaluated in the laboratory. The red, infrared and green LEDs are driven by three independent variable LED current drivers on the PPG processing system, which allows the flexible adjustment of the driving currents on demand. The photodiode on the sensor detects the energy backscattered by the tissue and gives an output current proportional to the intensity of the light detected and the transimpedance amplifier on the processing system convert this current into voltage. Following filtering and amplification of the PPG signal on the processing system, the digitization of the acquired signal was then

achieved using a 12-bit data acquisition card (DAQCard-6024E) by National Instruments (Texas, U.S). A Virtual Instrument (VI) implemented in LabVIEW was also developed for acquisition, displaying, analysis and storing of all the acquired PPG signals.

As described previously in order to avoid cross contamination as the same sensor is used in all patients, the reflectance PPG flap sensor was covered using an adhesive transparent film dressing (Tegaderm film, 3M Health Care, Germany) with dimensions of 10cm x 12cm, therefore during the *in vitro* evaluation the sensor was also covered to conform with the protocol which will be followed in the *in vivo* evaluation. The covered sensor was then connected to the developed PPG processing system which will be described in detail in the next chapter.

Red, infrared and green photoplethysmographic signals were acquired by a volunteer placing an index finger on the sensor. Figure 6.7 shows a ten second window of good quality red, infrared and green ac PPG signals from the index finger.

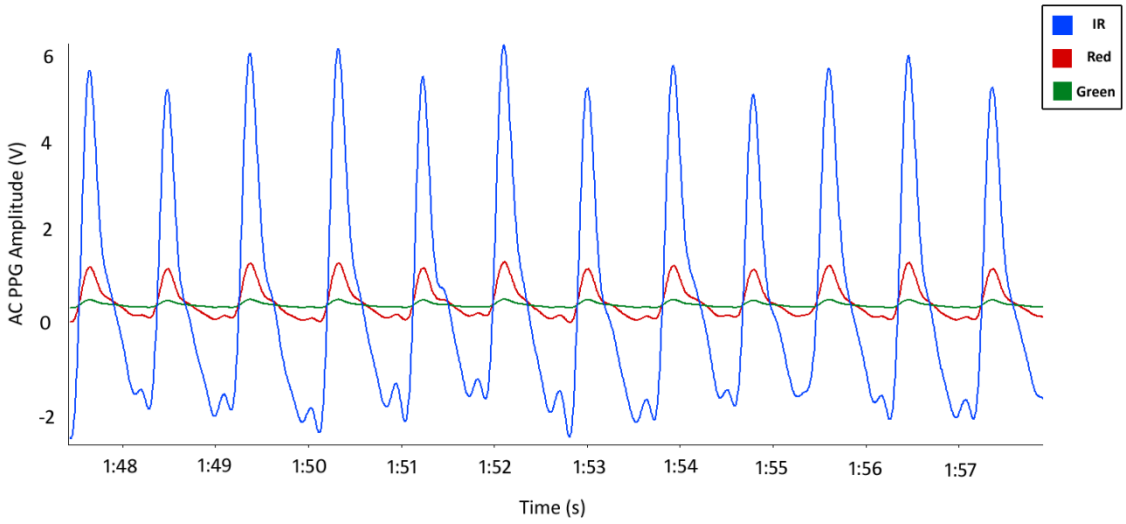

Figure 6.7: Red, infrared and green ac PPG signals from the index finger.

6.2.4 Thermal Evaluation on the flap PPG sensor

As the LED intensities can be changed according to the area being monitored, it was deemed necessary to perform a thermal evaluation of the sensor by driving all the LEDs at the same current of 70mA. This LED driving current is almost half of the

maximum forward current indicated in the datasheets which will be the starting current for all patients and will only be varied if difficulties in detecting signals arise. To verify that the red, infrared and green LEDs will not cause any thermal damage to skin during measurements, *in vivo* measurements were conducted to investigate the possibility of any excessive rise in skin surface temperature associated with the LEDs. The *in vivo* measurements were made on one healthy volunteer. The flap sensor was covered using the adhesive transparent film dressing (Tegaderm film) for sterility to simulate the conditions of the post-operative measurements which will be carried out on patients. A precision centigrade temperature sensor (LM35, Texas Instruments, USA) was used for temperature measurements; this was placed over the photodiode to ensure an equal separation distance to all the LEDs. Surgical tape (3M™ Transpore™) was used to secure the PPG sensor as well as the temperature sensor onto the volunteer's arm. The LM35 used is a precision integrated-circuit temperature sensor whose output voltage is linearly proportional to the temperature (Celsius), its absolute maximum ratings and electrical specifications are shown in Tables 6.8 and 6.9 respectively.

Table 6.8: Table showing the absolute maximum ratings for the temperature sensor (LM35) indicating limits beyond which damage to device may occur.

Absolute Maximum Ratings	
Supply Voltage	+35V to -0.2V
Output Voltage	+6V to -1.0V
Output Current	10Ma
Storage Temperature	-60° C to +150° C
Lead Temperature (Soldering, 10 seconds)	260° C
Specified Operating Temperature Range: T_{MIN} to T_{MAX}	-55° C to +150° C

Table 6.9: Showing the electrical characteristics, connection configuration and bottom view of the connection diagram of the temperature sensor used for thermal evaluation of the PPG sensor.

Electrical Characteristics		
Parameter	Conditions	Typical values
Accuracy	T_A=+25° C	±0.4° C
	T_A=-10° C	±0.5° C
	T_A= T_{MAX} & T_{MIN}	±0.8° C
Nonlinearity	T_{MIN} ≤T_A ≤T_{MAX}	±0.3 ° C
Sensor Gain	T_{MIN} ≤T_A ≤T_{MAX}	+10 mV/° C
Quiescent Current	Vs=+5V, +25° C	56 µA
Minimum temperature for rated accuracy	In circuit of figure below	+1.5° C
Long Term Stability	T_J=T_{MAX}, for 1000 hours	±0.08° C

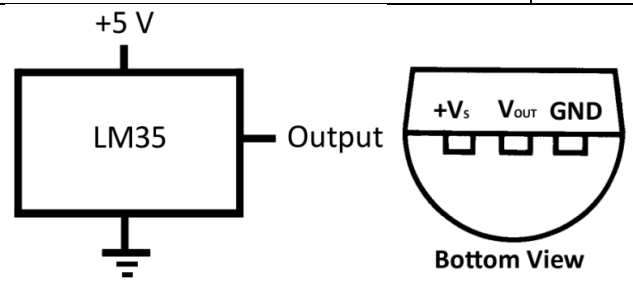

The temperature sensor was connected to a single power supply of positive 5 volts and the output of the temperature sensor was connected to the data acquisition card (DAQCard 6024E, National Instruments) and the acquired temperature measurements were displayed and saved using a Virtual Instrument implemented in LabVIEW. Initially the thermal evaluation of each LED was carried out separately and a final measurement was performed to measure the temperature rise of all LEDs together. For each measurement the temperature sensor was switched on and a baseline temperature was achieved prior to switching on the LEDs, subsequently the temperature rise was monitored until steady state conditions were achieved. In Figure 6.8 a section of the temperature trace is shown where the infrared emitters were switched on where the rise in skin temperature was captured. The measurement was also repeated for both red and green LEDs shown in Figure 6.9 Figure 6.10 respectively. The rise in skin temperature due to excessive heat caused by the LEDs were observed at 0.9°C for infrared, 0.6°C for red, 1.29°C for green and 2.2°C for all LEDs being switched at the same time (shown in Figure 6.11).

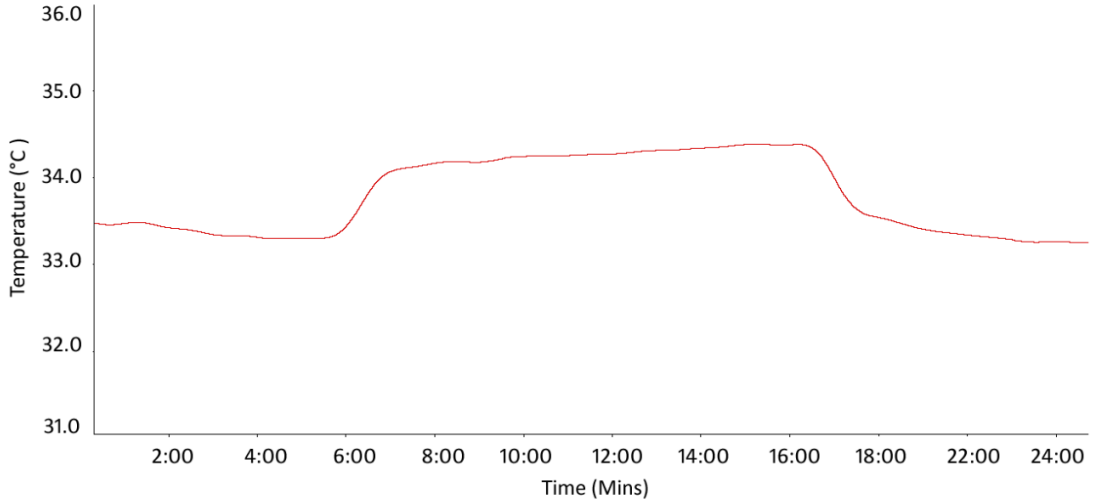

Figure 6.8: The temperature rise of the infrared LED when switched on for 12 minutes.

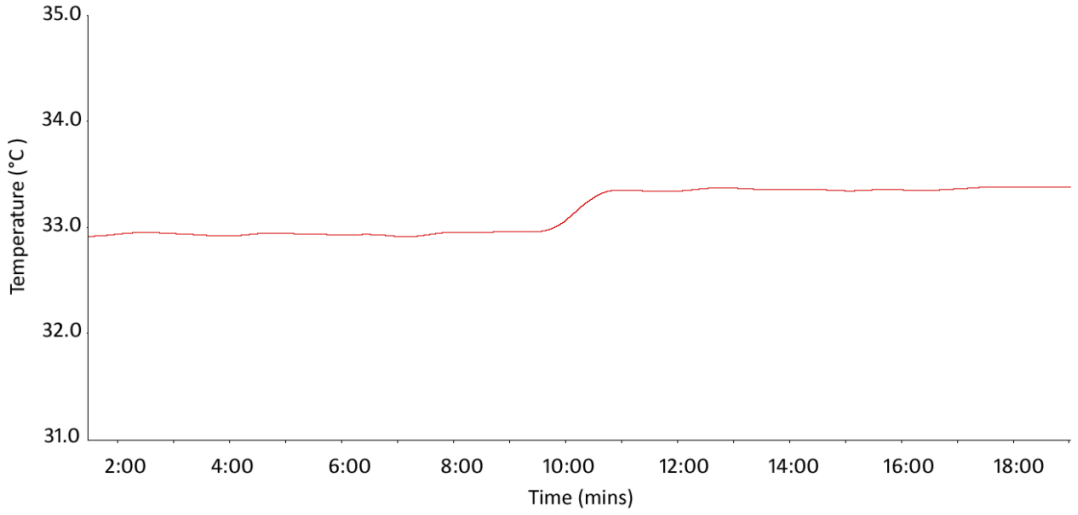

Figure 6.9: Showing the temperature rise of the red LED when switched on for 10 minutes

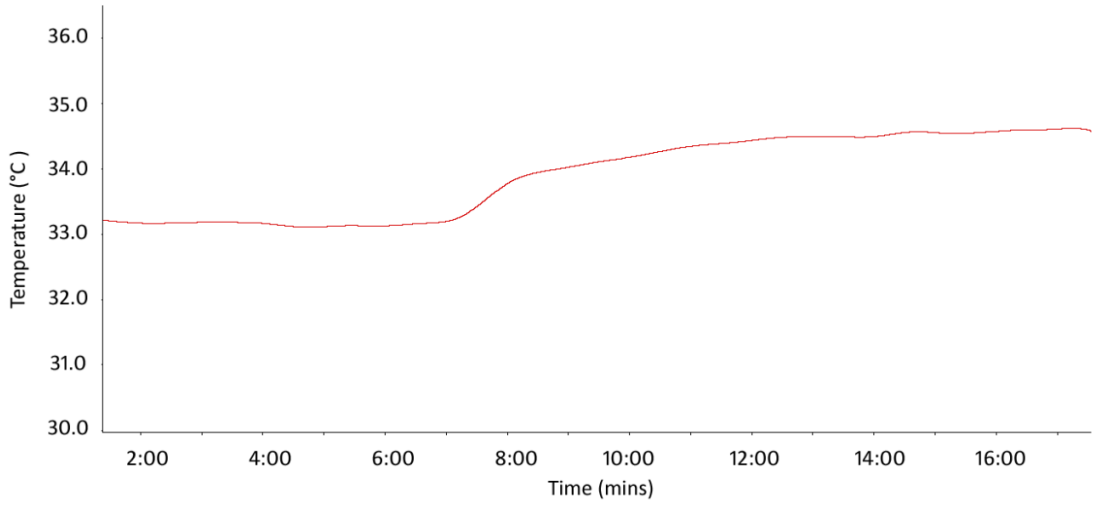

Figure 6.10: Showing the temperature rise of the green LED when switched on for 10 minutes.

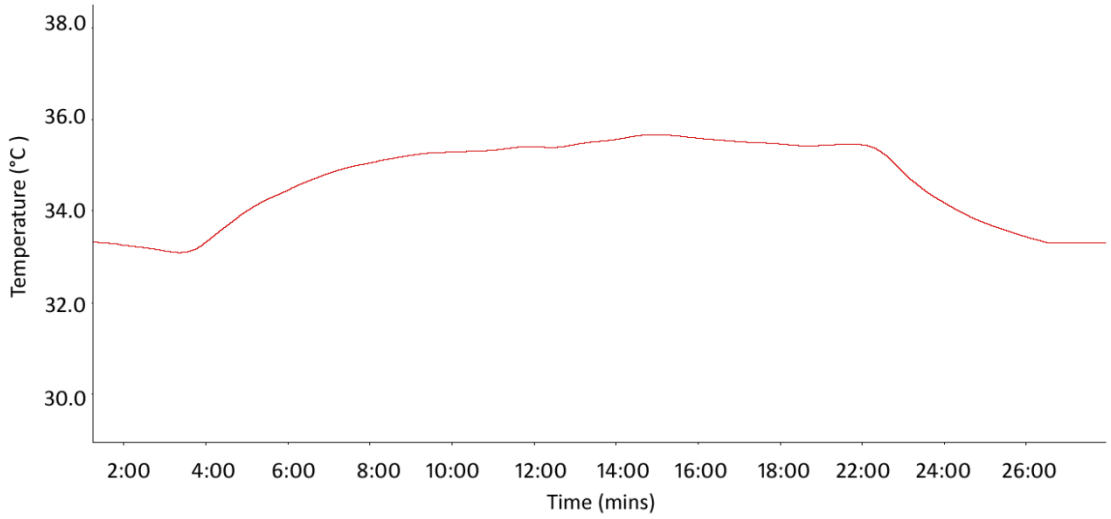

Figure 6.11: Showing the temperature rise when all three LEDs are switched on for 24 minutes.

Following discussions with our clinical collaborators, none of these temperature rises would be expected to result in thermal injury to the skin.

6.3 Reflectance finger photoplethysmographic sensor

A reflectance finger PPG sensor which was optically and electrically identical to the three wavelength flap PPG sensor was also designed and developed. The design of this

finger PPG sensor was to enable the simultaneous detection and comparison of the estimated oxygen saturation values and the PPG signals from both the flap and the finger.

6.3.1 Optical Components

The finger PPG sensor comprised of two infrared, two red and two green LEDs and a surface mount photodetector identical to the flap PPG sensor described above. The optical, electrical and package characteristics of the selected components are shown in Section 6.2.1

6.3.2 Mechanical construction of the finger sensor

The techniques and technologies used for the development of the printed circuit board, the mechanical construction of the sensor and the epoxy coating of the sensor were identical to the flap sensor. Following removal of the cable and optical components of a commercial pulse oximeter finger clip, the finger PPG sensor was then accommodated inside the clip and secured using a multipurpose adhesive as seen in the photograph in Figure 6.12.

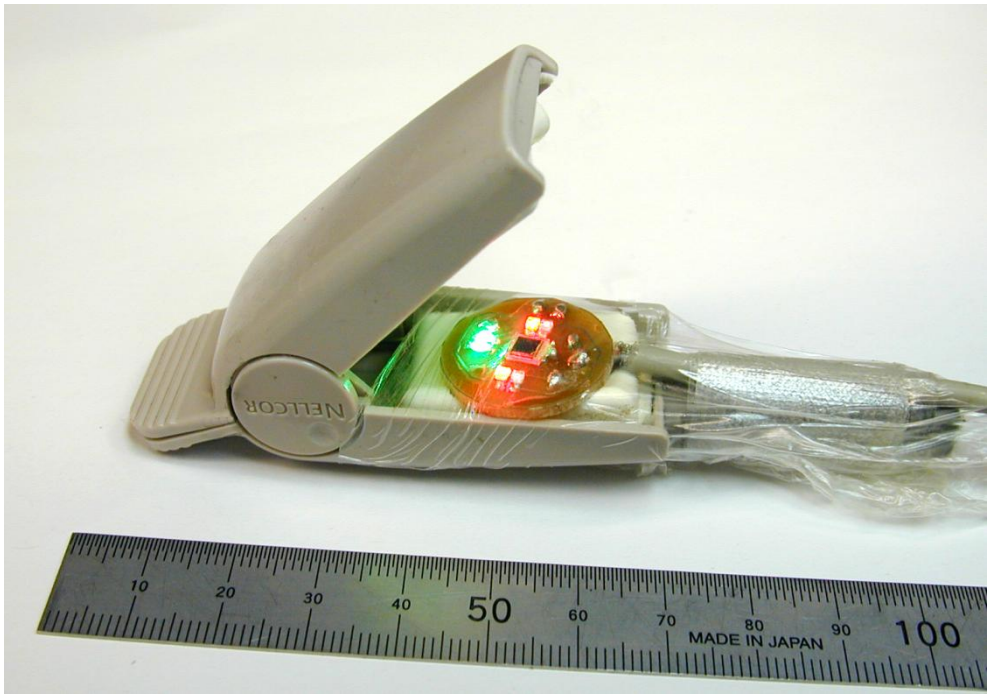

Figure 6.12: Photograph of the developed finger PPG sensor fixed into the commercial finger clip and covered with adhesive transparent film dressing with the LEDs switched on.

6.3.3 Evaluation of the finger PPG sensor

The functionality of the finger PPG sensor was evaluated in the laboratory on a healthy volunteer. As was the case with the flap sensor, the LEDs and the photodiode on the finger sensor were illuminated and the backscattered energy was then detected by the PPG processing system. The sensor was then covered using the transparent film dressing. To acquired PPG signals, the volunteer's finger was placed inside the clip ensuring the pulp of the finger covers all of the optical components on the sensor as shown in Figure 6.13.

As described in section 6.2.3 in order to evaluate the sensor a developed PPG processing system was used to drive the optical components on the sensor which will be described in details in Chapter 7. Also a Virtual Instrument was implemented in LabVIEW to acquire, display, analyse and store the photoplethysmographic signals, the developed software will be explained further in Chapter 8.

Figure 6.13: Photograph showing the finger PPG sensor on a volunteers' index finger for evaluation.

The acquired signals were of large amplitudes and high signal-to-noise ratio. Figure 6.14 shows typical traces of infrared, red and green PPGs using the reflectance finger photoplethysmographic sensor.

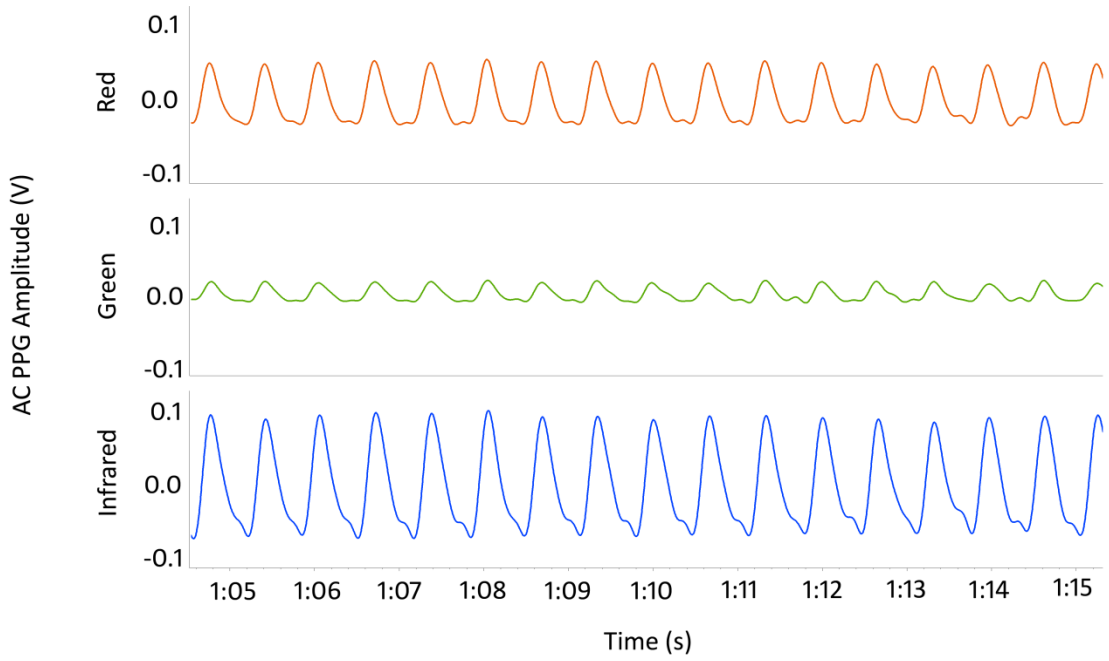

Figure 6.14: Shows a 10 second window of typical traces of red, IR and green PPG from finger.

Using a developed PPG processing system, the designed and developed flap and finger PPG sensors were successfully evaluated *in vitro*. The design and development of the PPG system will be explained in the next chapter.

Chapter 7

Development of a three wavelength free flap photoplethysmography processing system

7.1 Introduction

An ideal free flap monitoring technique is required to be objective, continuous, non-invasive, safe and easily managed and interpreted by medical and nursing staff.

In earlier chapters limitations of the techniques and technologies which are currently used in monitoring flaps were discussed. In order to overcome some of these limitations a three wavelength photoplethysmographic (PPG) processing system was designed and developed. This system consisted of two separate PPG processing systems, as shown in Figure 7.1, to allow the simultaneous monitoring of the flap and finger using the PPG sensors discussed in the previous chapter.

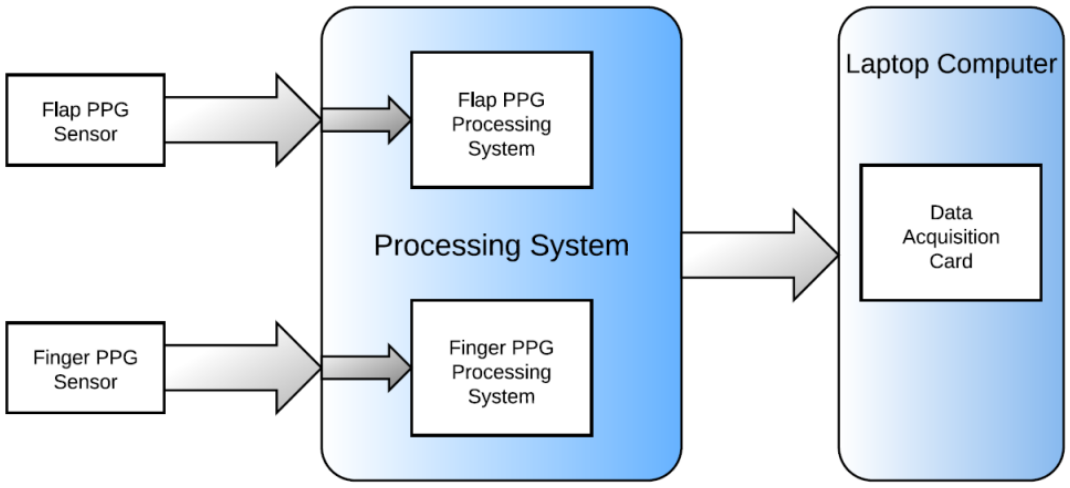

Figure 7.1: Block diagram of the two channel three wavelength PPG process system.

The PPG processing system drives the optical components of the sensor and is also used to detect and pre-process the PPG signals which will then be displayed, analysed and stored on a laptop computer. As the two PPG channels are electrically identical, the technical details of the construction and the performance evaluations of the flap PPG processing system will be presented in this chapter.

7.2 Instrumentation

A detailed block diagram of one of the three wavelength photoplethysmographic processing systems is illustrated in Figure 7.2.

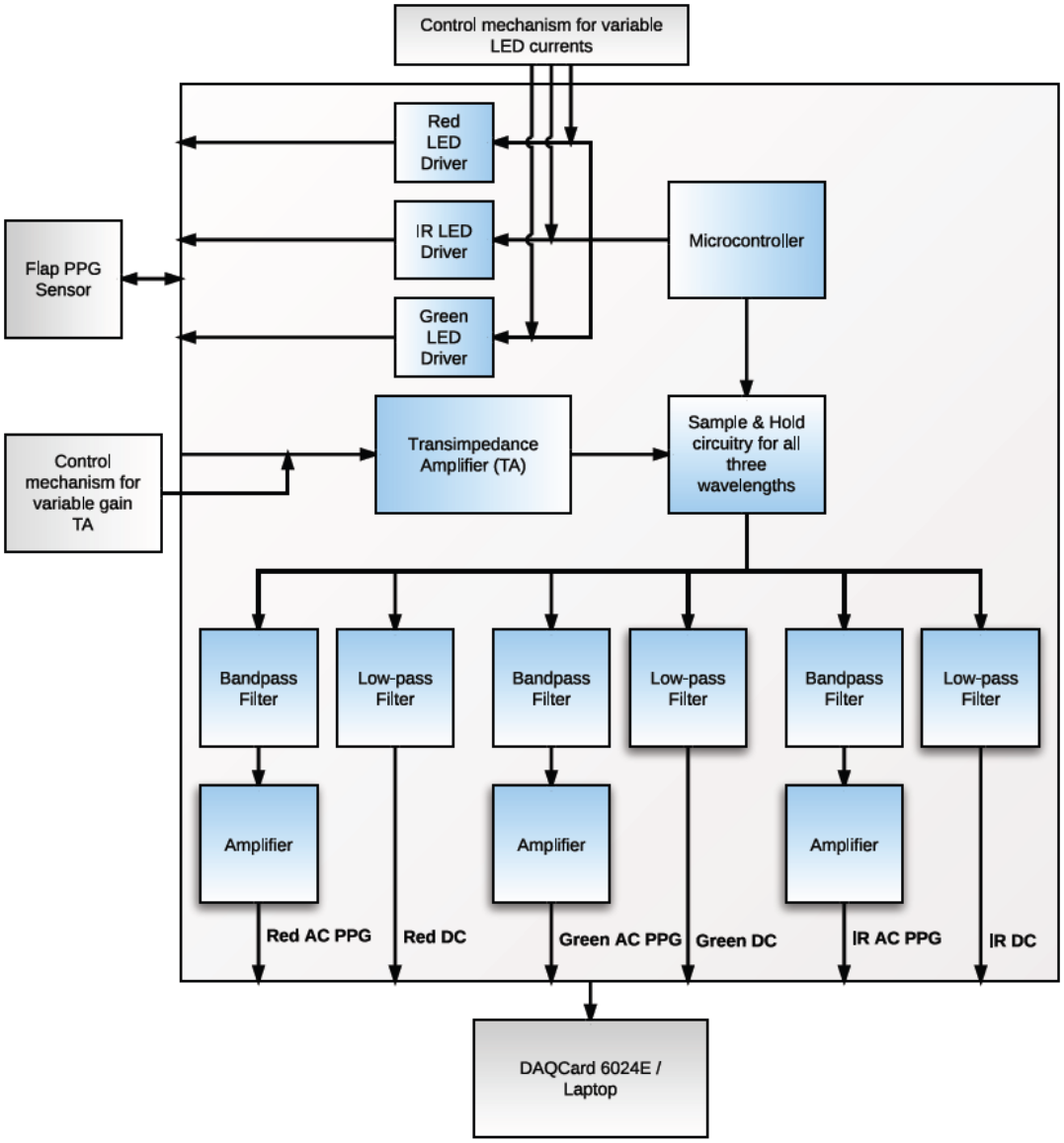

Figure 7.2: Detailed block diagram of the three wavelengths flap PPG processing system.

The three separate LED drivers on the developed PPG processing system drive the optical components on the flap PPG probe. Following the detection of the backscattered energy by the photodiode on the flap PPG probe, the output is then processed and the signal is then separated into its red, infrared and green PPG components on the battery powered PPG processing system. Following the filtering of the PPG signals and splitting them into their ac and dc components, the outputs are then digitised using a DAQCard (National Instruments) which is connected to the laptop computer where the signals can then be displayed, analysed and stored using the developed virtual system implemented in LabVIEW (Chapter 8).

Detailed descriptions of each of the main blocks shown in Figure 7.2 are presented in the following sections.

7.2.1 LED Driver

The red, infrared and green LEDs on the flap probe must be driven by identical variable current sources, as shown in Figure 7.3 to allow the user to vary the output light intensity to facilitate the flexibility of utilising the flap probe on different tissue types without saturating the signal. The current sources were multiplexed using a microcontroller to ensure the LEDs are never on at the same time.

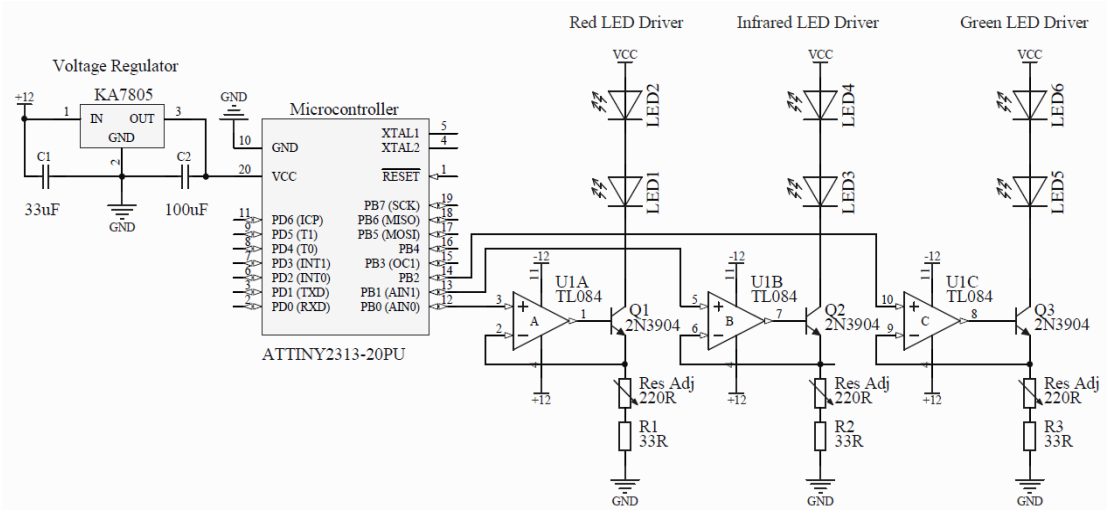

Figure 7.3: Schematic drawing of the LED current driver circuit.

The red, infrared and green LEDs were driven by their individual LED driver circuit which consists of a variable current source comprising a low power operational amplifier (TL084, Texas Instruments, Dallas, Texas, USA) and a series NPN transistor (2N3904). The current source is driven by a switching timing signal provided by the microcontroller.

The low-power 8-bit microcontroller, ATtiny2313, (Atmel, CA, USA) with 2K bytes in-system programmable flash used for providing the timing signal for multiplexing the LED drivers is based on the AVR architecture. To program the microcontroller the AVR STK500 (Atmel, CA, USA) development system for the AVR flash microcontroller from Atmel Corporation was used. A code was written in C, as shown below, which was implemented in the Atmel Studio (Version 4, Atmel); the software that is the integrated development environment for developing applications for the ATtiny2313 microcontroller.

```
#include <avr\io.h>
#include <util\delay.h>

int main (void)

{
        DDRB=0x07;                          //0,1&2 of port B are set as output
        const float freq = 100;             //set the frequency of 100 Hz
        const float time = freq*6;          //set time as frequency multiplied for
                                              the 6 events
        const float delay = 1/time;         //set the delay time
        const float delayus = delay*1000000;  //delay time of 1.666 ms

        while (1)
        {
                PORTB = 0b00000001;             //port B0 switched on
                _delay_us(delayus);             //port B0 on for 1.666ms
                PORTB = 0b00000000;             //all ports are off
                _delay_us(delayus);             //all ports off for 1.666ms
                PORTB = 0b00000010;             //port B1 switched on
                _delay_us(delayus);             //port B1 on for
                PORTB = 0b00000000;             //all ports are off
                _delay_us(delayus);             //all ports off for 1.666ms
                PORTB = 0b00000100;             //port B2 switched on
                _delay_us(delayus);             //port B2 on for 1.666ms
                PORTB = 0b00000000;             //all ports off
                _delay_us(delayus);             //all ports off for 1.666ms
        }
}
```

As mentioned previously the microcontroller provides the control signals to drive each of the LED driving circuit for each wavelength where square waves with frequency of 100 Hz is produced as illustrated in Figure 7.4. The timing of the pulsations is critical as the photodiode cannot distinguish between different wavelengths of light therefore it relies on the pulsations provided by the microcontroller to synchronise the pulsation of the LEDs with the samples taken so that the detected signal by the photodiode can be attributed to the correct LED signal.

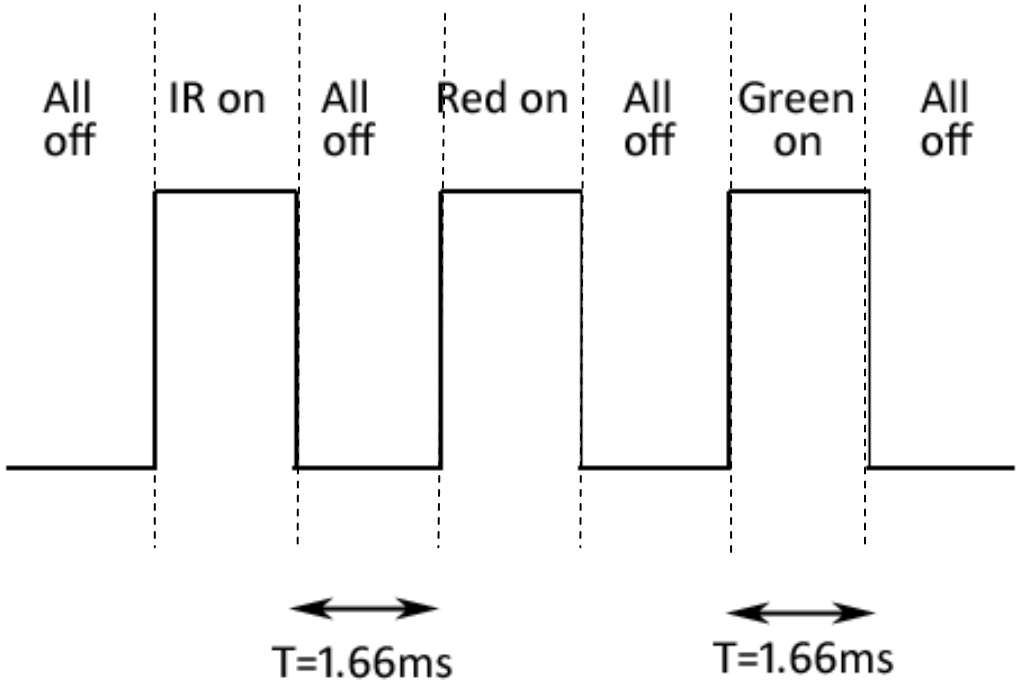

Figure 7.4: Timing diagram of the multiplexing signals used in the PPG instrumentation.

The program written in C is designed to switch each LED on and off using three different clock signals with duty cycle of $^1/_6$ for each wavelength as illustrated in Figure 7.4 ensuring that the LEDs are never on at the same time although during part of the switching cycle all LEDs are off to allow the photodiode to detect ambient light. The same signal is also used to distinguish between the different signals subsequent to their detection by the photodiode.

When the Red is high (5V), transistor Q1 is turned on, allowing current to flow from the positive supply to the red LED anode, therefore the red LED is turned on. When the

clock signal is low (0V), the transistor is switched off and no current will flow through it, resulting in the red LED switching off. The same process also occurs for the IR and green LEDs with transistors Q2 and Q3 respectively acting as switches when a high or low signal is detected from the microcontroller resulting in sequentially pulsing of the LEDs.

Light emitting diodes can transmit large intensities of light proportional to the amount of drive current. Many of the pulse oximeters on the market today provide up to 50 mA of pulse current to each LED where in the commercial pulse oximeters the amount of current supplied to the LEDs is automatically changed by the microcontroller according to the absorption of the tissue under observation. Factors such as skin pigmentation, skin thickness and optical path length determine the absorption of the tissue. The microcontroller adjusts the current to the LEDs as needed to ensure adequate light is detected to excite but not saturate the photodiode [91]. As the PPG instrumentation developed is intended for use on various types of flaps a panel mounted potentiometer (P16, Vishay, PA, USA) was incorporated in the LED driver circuit to enable adjustments to the LED intensity. The chosen potentiometer provides a resistance of up to 200Ω with a tolerance of ±20% and power rating of 1W at +40°C.

To avoid damaging the LED by exceeding the predetermined (as shown in Table 7.1) maximum forward current value, the maximum current through each LED varies according to the characteristics of each LED therefore the drive current is limited according to the suggested values in the datasheets.

Table 7.1: The maximum current required to drive the LEDs as stated in the relevant datasheets

Wavelength (nm)	Forward Current (mA)	Peak Forward Current
660	30	150mA, 0.1ms Pulse width
525	30	100mA, 0.1 ms Pulse width
940	50	1.2A, 0.1ms Pulse width

For the flap PPG processing channel the maximum pulsed current of 151mA will be used for all three wavelengths where Equation (7.1) is used to determine the resistor value needed to make certain that the LED never draws a current more than the maximum value set. Using:

$$I_{Emitter} = \frac{V}{\mathrm{R}} \tag{7.1}$$

where R is 33Ω to 200Ω for resistor values which determine the maximum and minimum currents used to drive the LEDs. Therefore, with a voltage of 5V the range of LED driving current is 25-151mA providing a sufficient current to switch on the LED and detect good quality signals without saturating the photodiode.

7.2.2 Transimpedance amplifier

The photodiode is the main input in the photoplethysmography system; this component is found on the PPG sensor, as described in the previous chapter, where the intensity of the reflected light from the LED after its interaction with the tissue under observation is detected. The photodiode produces an output current which is linearly proportional to the intensity of light detected [91].

To pre-process and display the detected signal a transimpedance amplifier which works as a current-to-voltage convertor was used in both the flap and finger PPG channels as shown in Figure 7.5.

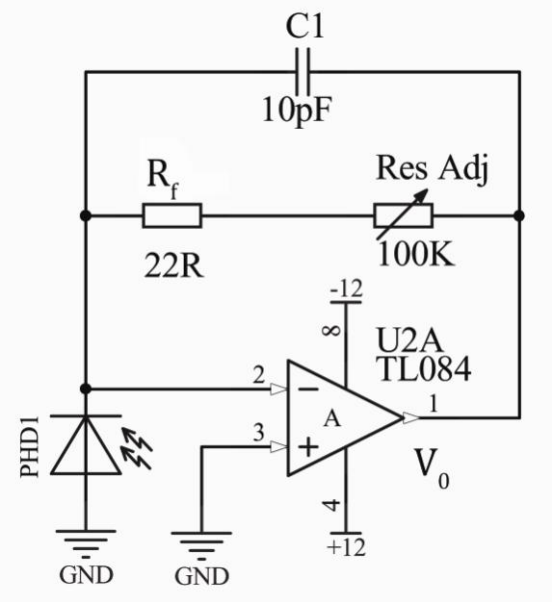

Figure 7.5: Circuit diagram of a transimpedance amplifier with a photodiode.

Because of the virtual ground, the op amp maintains zero voltage across the photodiode. Current flows through the feedback resistor (R_f) and a voltage (V_o) is created at the output that is proportional to the light intensity (I_d) as given by [91]:

$$V_o = I_d R_f \tag{7.2}$$

The transimpedance gain is then equal to the value of the feedback resistor. To enable the use of the PPG sensor on various flap types as well as an adjustable LED intensity, the value for the feedback resistor is required to be modified to avoid saturating the photodiode. A surface mount knob potentiometer was used providing a maximum resistance of 100KΩ. The feedback resistor should be made as large as possible to minimize noise, as this is the main source of noise in the circuit. This thermal (Johnson) noise increases as a function of the square root of the value of the feedback resistance [91].

$$Thermal\ Noise = \sqrt{4kTBR} \tag{7.3}$$

where k is Boltzmann's constant, T is absolute temperature, B is the noise bandwidth (Hz), R is the feedback resistance (Ω), while the signal voltage increases as a function of R. Therefore the signal-to-noise ratio improves by the square root of the feedback resistance as the feedback resistance is increased [91].

The capacitor in the feedback loop minimizes gain peaking and improves stability. To calculate the capacitance value when using photodiodes with relatively large surface area where the junction capacitance is much larger than the feedback capacitor Equation (7.4) is used [91].

$$C_f = \sqrt{\frac{C_I}{2\pi R_f f_c}} \tag{7.4}$$

where f_c is the unity gain frequency of the op amp, C_I is the total input capacitance = photodiode junction capacitance + op amp input capacitance, R_f is the feedback resistance. For small photodiode junction capacitances a more general formula is used [4]:

$$C_f = \frac{1}{4\pi R_f f_c}\left(1 + \sqrt{1 + 8\pi R_f C_I f_c}\right) \tag{7.5}$$

A FET op amp is also a requirement for this configuration, a TL084 (Texas Instruments, Dallas, USA) was used with a low bias current providing a higher sensitivity.

7.2.3 Demultiplexer

The output of the transimpedance amplifier is the obtained signal from the tissue under observation. As the photodiode cannot distinguish between the different wavelengths, the signal is a mixed photoplethysmographic signal of red, infrared and green wavelengths. In order to separate the three wavelength PPG signals, the output of the transimpedance amplifier is fed into a demultiplexer consisting of the three timing signals generated by the ATtiny2313 microcontroller connected to three LF398 sample-and-hold circuits (National Semiconductor Inc., Santa Clara, CA, USA) as shown in Figure 7.6.

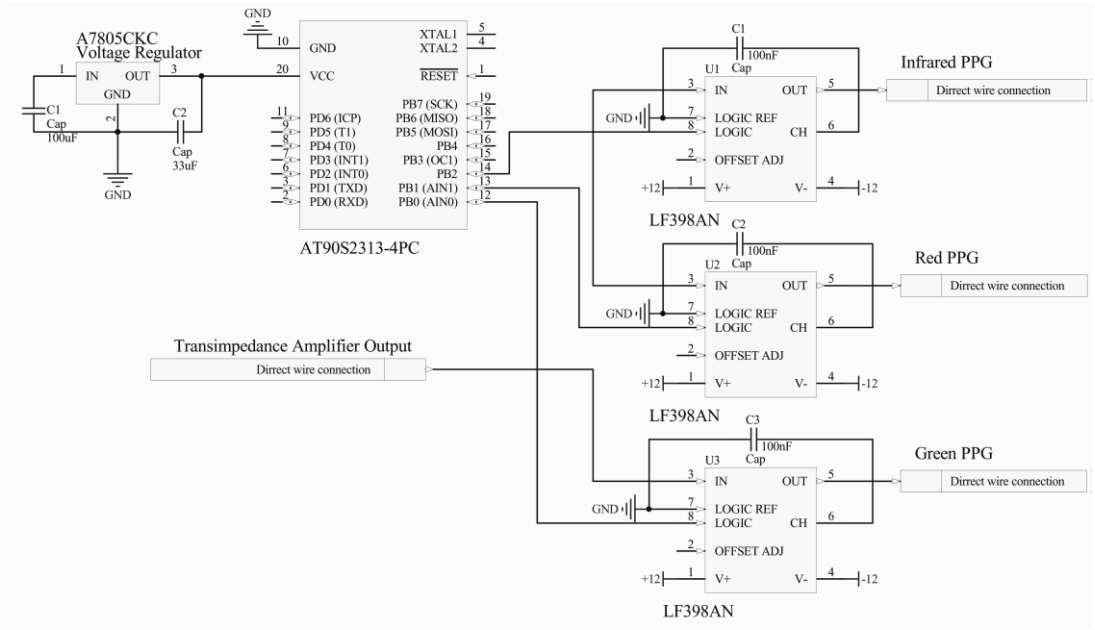

Figure 7.6: Schematic diagram of the three demultiplexing circuits.

The timing signal is used to trigger the sample-and-hold circuits to sample the output of the transimpedance amplifier signal at appropriate times in order to extract the red, infrared and green PPG signals as illustrated in Figure 7.7. Each of the sample-and-hold circuits are triggered using the same timing signals which were used to switch the LEDs on, so the voltages corresponding to the reflected signals originating from the red, infrared and green LEDs are the output of these LF398s.

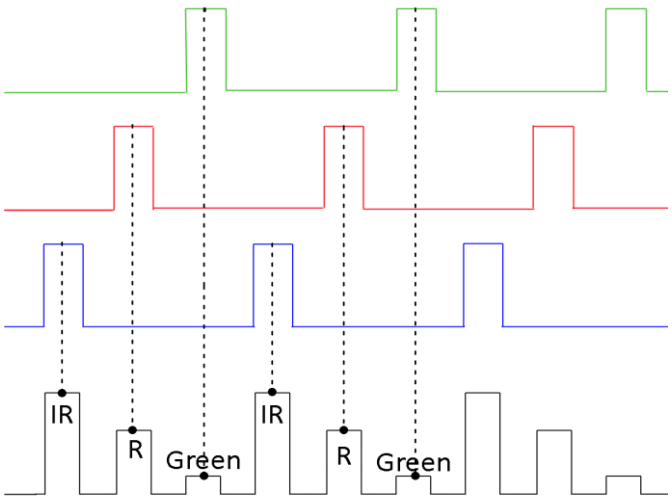

Figure 7.7: Demultiplexer timing diagram, the dotted lines indicate the timing of LF398s sampling the photodiode output.

Once the demultiplexer separates the photodiode signal into its three components of red, infrared and green signals, the waveforms representing the light levels are reconstructed from the output signal.

7.2.4 Filters

The outputs of the sample-and-hold circuits for red, infrared and green wavelengths are signals consisting of both ac and dc PPG components. These components (for all three wavelengths) are separated using filters.

To extract the ac component of the PPG signal band pass filters were used. These filters were designed using a 2nd order active low pass and a 2nd order active high pass filter using a Sallen and Key topology as shown in Figure 7.8. The cut-off frequencies of 0.4Hz and 20Hz were chosen to ensure that the pulsatile component of the PPG signal, which is approximately 1Hz, is not distorted while the high pass filter was used to eliminate the dc component of the PPG signal and the high frequency switching noise from the demultiplexer was attenuated using the low pass filter.

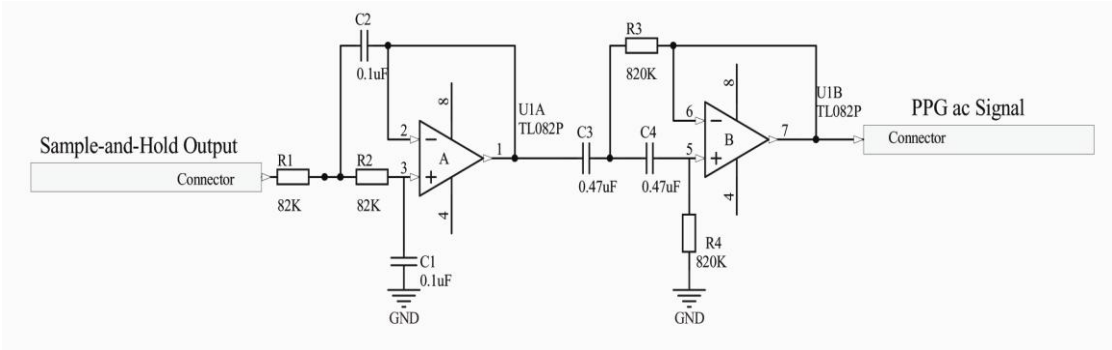

Figure 7.8: Band pass filter circuit: low-pass filter followed by a high-pass filter to separate ac component from the red and IR PPG signal.

The cut-off frequencies for the high pass and low pass filters were calculated using:

$$f_{cLP} = \frac{1}{2\pi\sqrt{R_1 R_2 C_1 C_2}} \tag{7.6}$$

$$f_{cHP} = \frac{1}{2\pi\sqrt{R_3 R_4 C_3 C_4}} \tag{7.7}$$

where R_1, R_2, R_3, R_4 and C_1, C_2, C_3, C_4 are chosen to give $f_{cHP} = 0.4Hz$ and $f_{cLP} = 19.4Hz$ as shown in Figure 7.8.

The frequency response of the band pass filter was simulated using Multisim (National Instruments, USA) as shown in Figure 7.9.

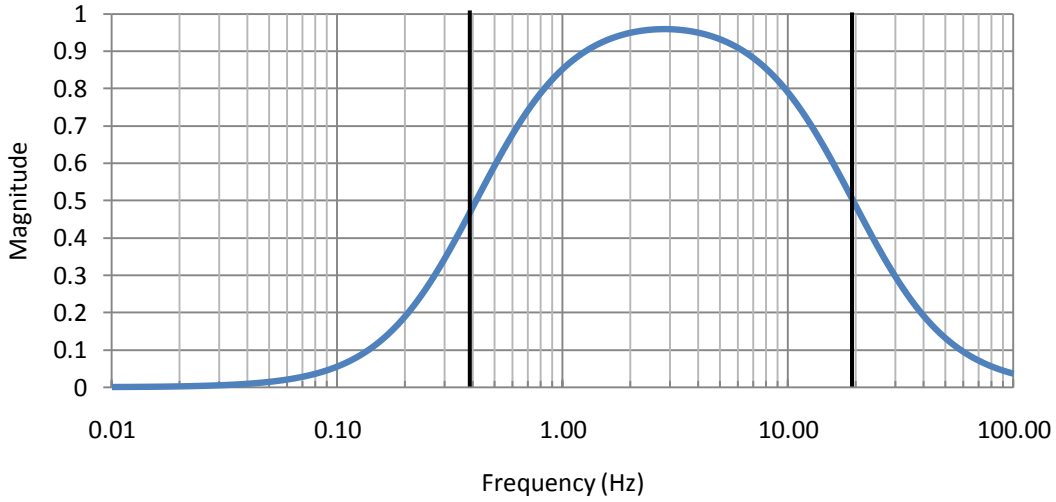

Figure 7.9: Simulated magnitude of the PPG band pass filter.

The output of the sample-and-hold circuits were connected to six identical band pass filters to extract the ac components of each of the six PPG signals to output R_{ac} flap, IR_{ac} flap, G_{ac} flap, R_{ac} finger, IR_{ac} finger and G_{ac} finger.

To attenuate and eliminate the high frequency noise as well as the pulsatile component of the PPG signal and to extract the dc component of the PPG signal a 2nd order low pass filter using a Sallen and Key topology was designed, as illustrated in Figure 7.1.

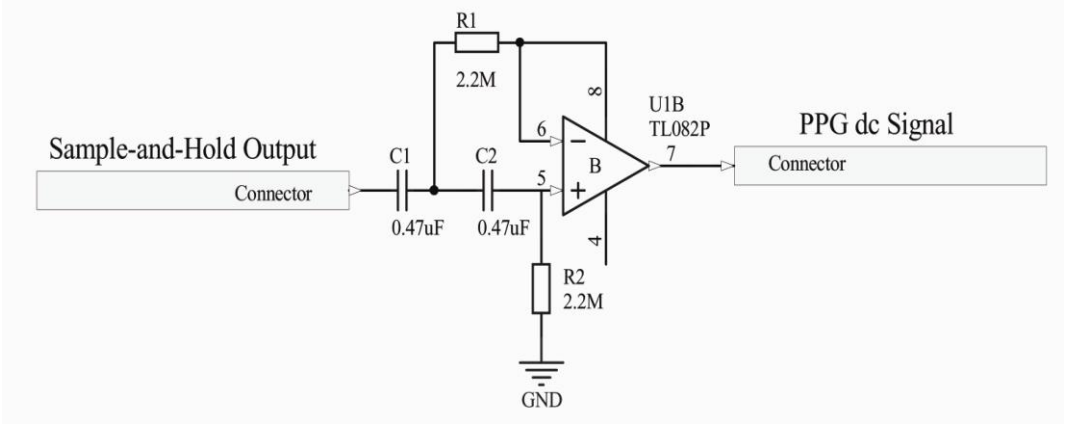

Figure 7.10: Low-pass Butterworth filter to extract the dc components of the PPG signal

The cut-off frequency used for the low pass filter is calculated as follows:

$$f_{cLP} = \frac{1}{2\pi R_1 R_2 C_1 C_2} \tag{7.8}$$

where R_1, R_2, C_1 and C_2 are chosen to give $f_{cLP} = 0.15Hz$ as shown in Figure 7.10.

Prior to constructing the low pass filter on a board it was designed on Multisim (National Instruments, USA) and evaluated by performing frequency response analysis in order to confirm the accuracy of the filter in its ability to cut off the unwanted signals below the cut off frequency of 0.15 Hz as shown in Figure 7.11.

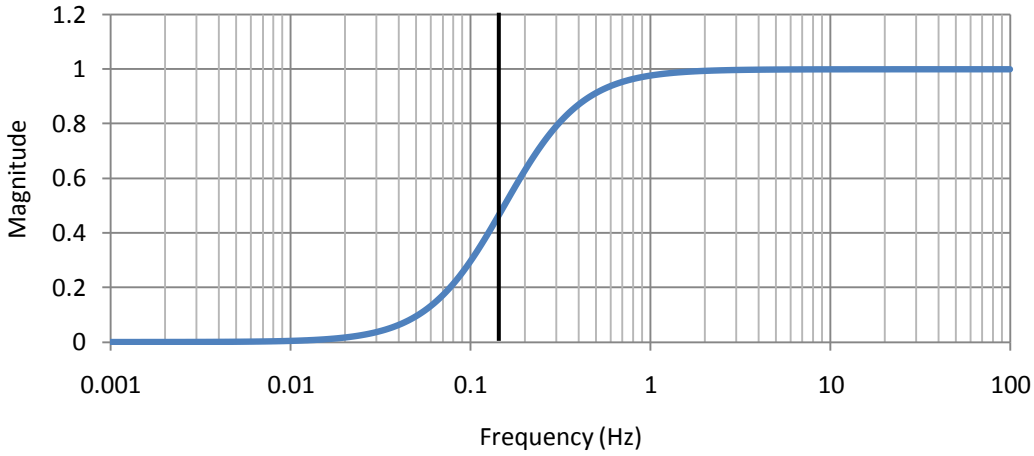

Figure 7.11: Simulated frequency response of the low pass filter used to extract the dc component of the PPG signal.

To extract the six dc component of R_{dc} flap, IR_{dc} flap, G_{dc} flap, R_{dc} finger, IR_{dc} finger and G_{dc} finger from the PPG signal, the output of the sample-and-hold circuits were connected to six identical low pass.

7.2.5 Non-inverting amplifier

After the red, infrared and green photoplethysmographic signals were separated into their ac and dc components, the ac PPG signals were amplified, using a non-inverting amplifier, prior to digitisation. The schematic diagram of the non-inverting amplifier is illustrated in Figure 7.12.

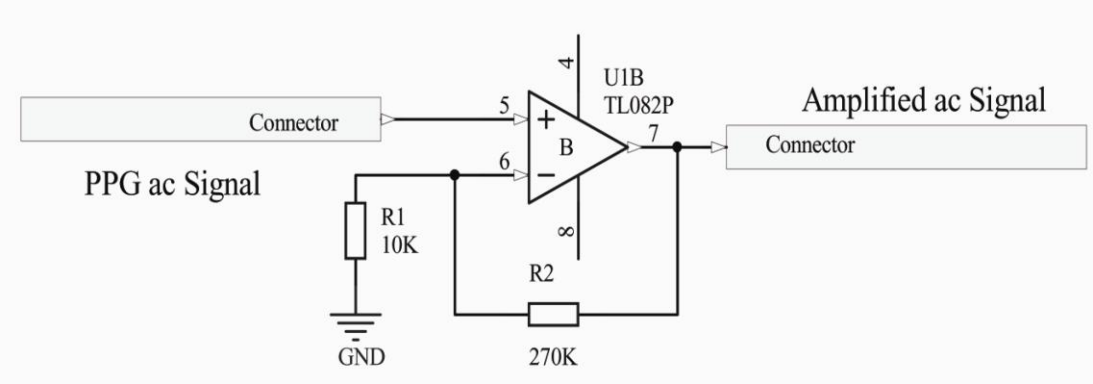

Figure 7.12: Schematic diagram of the non-inverting amplifier.

The amplification of the ac signal was adequate to enable the user to easily view the signal on an oscilloscope or the personal laptop while keeping within the ±10V range of the data acquisition card which will be described in the following chapter. The same gain of 27 was applied to all three flap ac PPG signals using:

$$V_{out} = V_{in}\left(1 + \frac{R_2}{R_1}\right) \tag{7.9}$$

The amplifier was simulated on Multisim using a sine wave as shown in Figure 7.13 where a sine wave with amplitude of 300 mV was used as an input as shown in blue and the amplified signal of 8 V is shown in red.

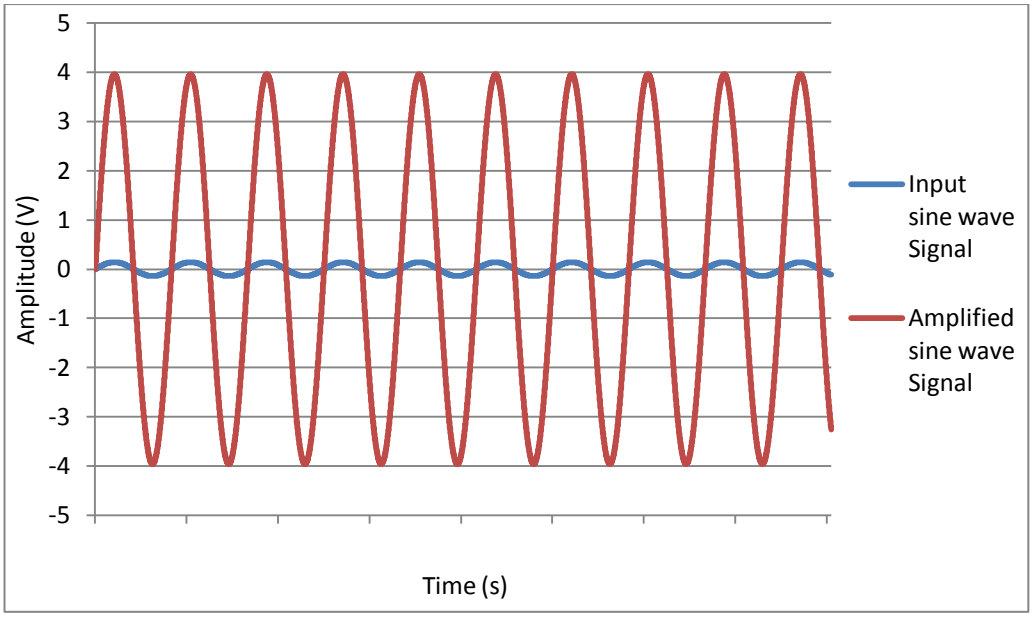

Figure 7.13: Simulated non-inverting amplifier on Multisim.

7.3 Instrumentation

Two identical flap and finger photoplethysmographic channels were constructed on a prototyping strip-board (dimensions: 160mm x 100mm x 1.6mm) using soldering techniques.

The processing system was enclosed in an ABS plastic instrument case with tongue and groove construction to provide protection against dust and water as well as ventilation grills on the top cover (Maplin, KC61R). With internal dimensions of 170mm x 122mm x 50mm the enclosure case could easily accommodate the two prototyping strip-boards horizontally, where the flap PPG channel was secured to the bottom and the finger PPG channel was secured to the top of the enclosure case using plastic nuts, bolts and spacers as shown in Figure 7.14.

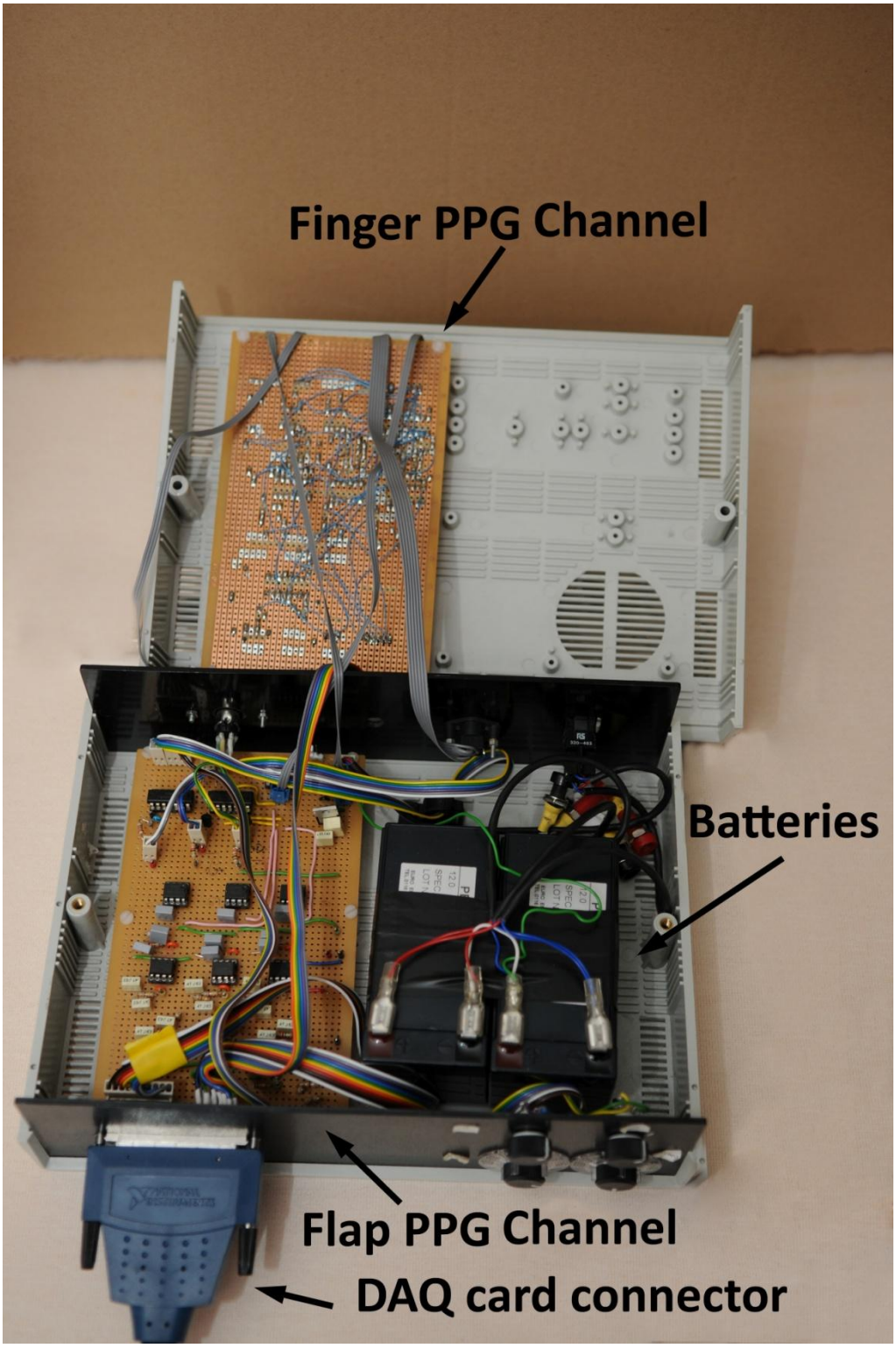

Figure 7.14: The constructed finger and flap PPG processing channels secured inside the PPG processing system.

The front panel of the instrument case consisted of, an on/off power rocker switch, two six-way mini DIN sockets to connect the flap and finger PPG sensors shown in Figure 7.15.

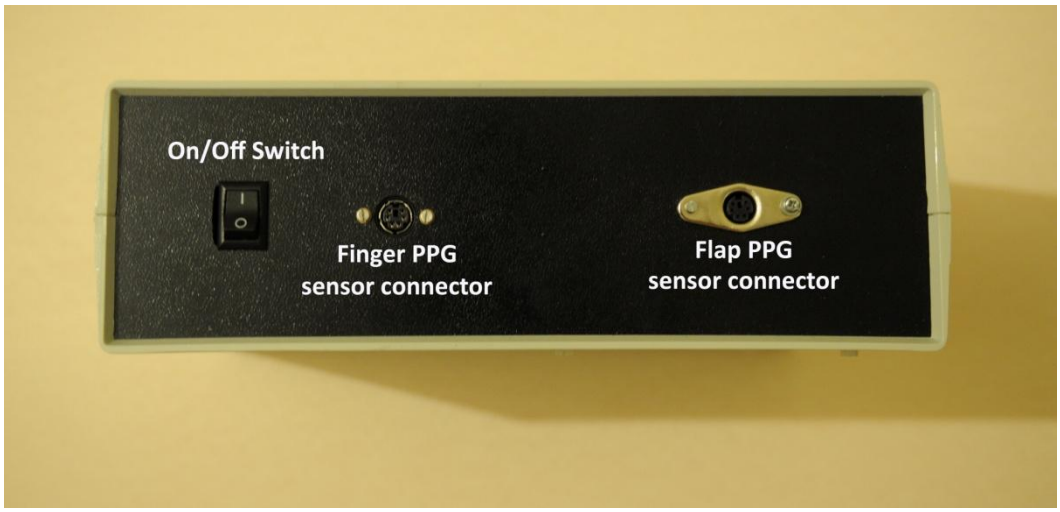

Figure 7.15: Front panel of the instrument case with the finger and flap channel sockets and the on and off power switch.

The rear panel of the processing system shown in Figure 7.16, consisted of three panel mounted potentiometers (200Ω) for adjusting the LED intensities, one panel mounted potentiometer (100KΩ) to change the gain of the transimpedance amplifier and a 68-pin vertical PWB mounting connector for the data acquisition card (P/N 777600-01, National Instruments, Texas, USA).

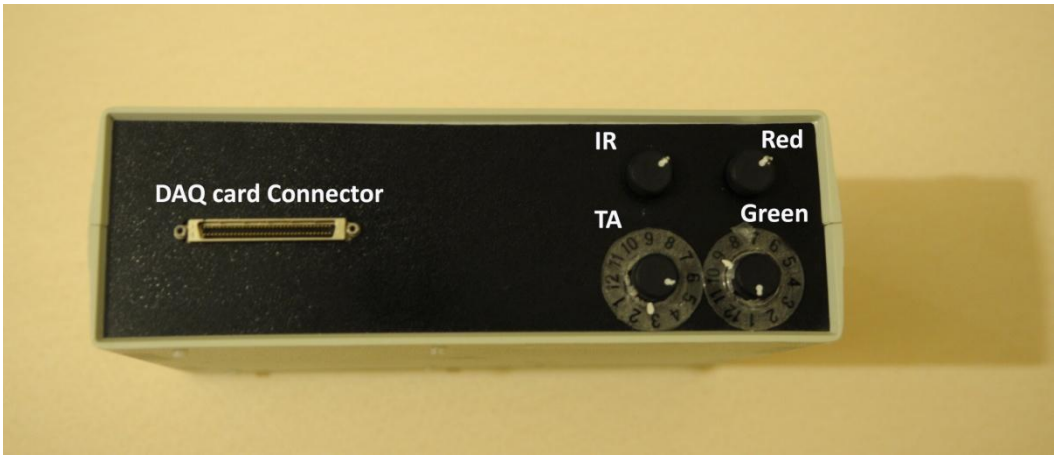

Figure 7.16: Rear panel of the developed PPG processing system with four potentiometers as well as the 68-pin DAQ card connector.

To power the PPG processing system two 6 volt rechargeable lead-acid batteries with 1.2 Ah capacity (NP 1.2-6, Yuasa, PA, USA) were used with dimensions of 97mm x 55mm x 47 mm each. The discharge characteristic curve of the battery is shown in Figure 7.17.

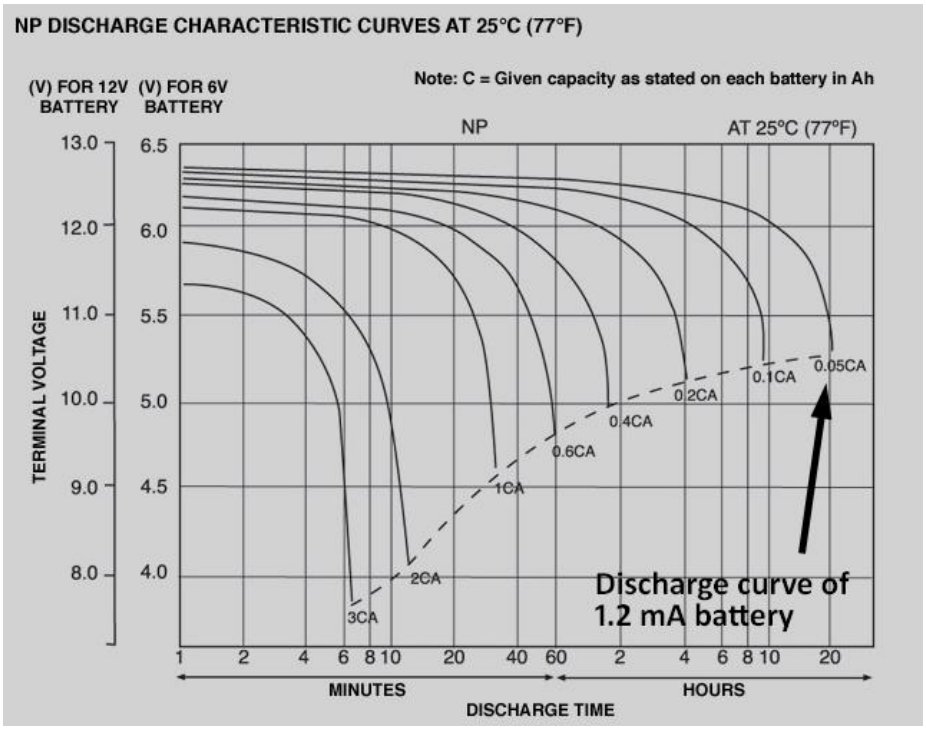

Figure 7.17: Discharge characteristic curve of the batteries used in the PPG processing system.

The batteries were interconnected to produce the positive (+12V) and negative (-12V) rails required by the PPG processing system.

7.4 Evaluation of the PPG processing system

To ensure the correct and accurate performance of the developed PPG processing system, each section of the system was evaluated. The timing signals accurately switched on the LEDs at the programmed frequency of 100Hz as observed on an oscilloscope (Tektronix TDS 3014B, USA) shown in Figure 7.18, also the intensities were correctly adjusted using the potentiometers.

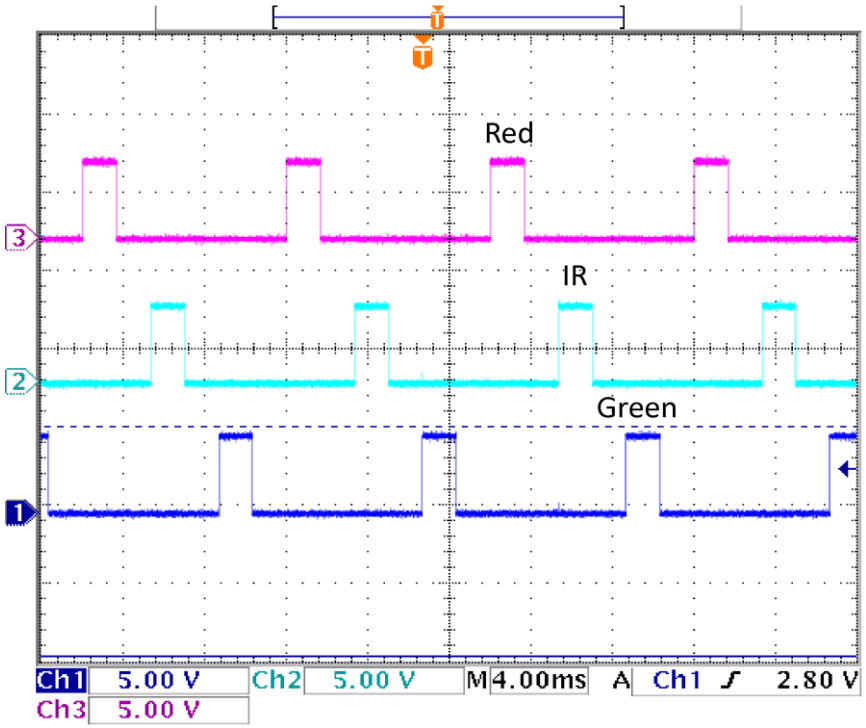

Figure 7.18: The timing signals used for driving the LEDs and demultiplexing the output of the transimpedance amplifier as observed on an oscilloscope.

The signal observed at the output of the transimpedance amplifier was a mix of all three wavelengths seen in Figure 7.19.

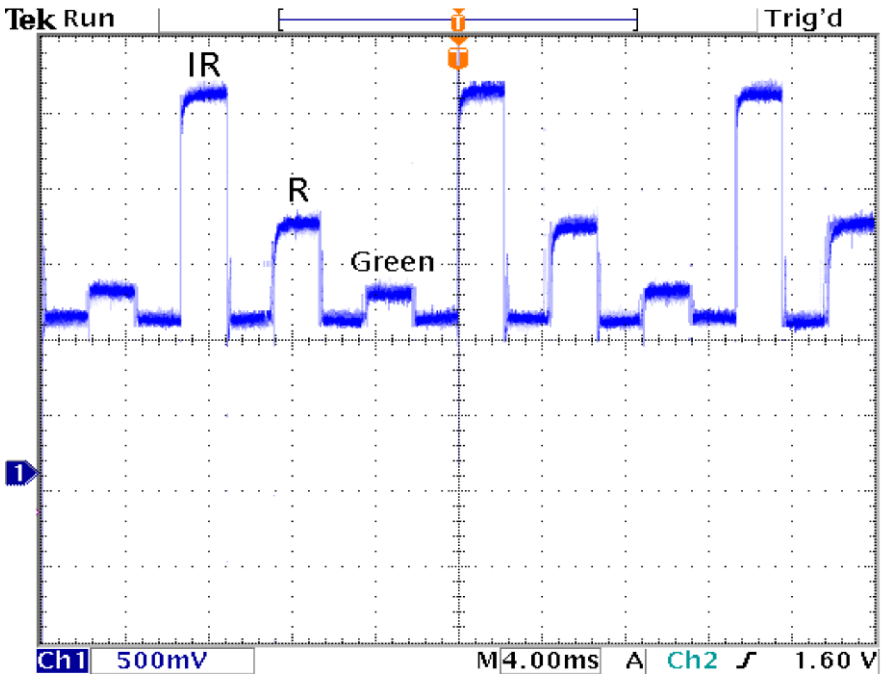

Figure 7.19: Output of transimpedance amplifier showing the mixed PPG infrared, red and green signals

Once the three sample-and-hold circuits were validated and it was ensured that the PPG signals of the three wavelengths were successfully separated, the band pass and low pass filters were also evaluated. The frequency responses of the filters were measured in the laboratory as shown in Figure 7.20 for the band pass filter and Figure 7.21 for the low pass filter. The experimental values for the cut-off frequencies of the band pass filter were 0.5Hz (lower cut-off frequency) and 15Hz (upper cut-off frequency) at -3 dB as shown in the figure. Also, the experimental value for the cut-off frequency of the low pass filter was 0.1Hz at -3dB.

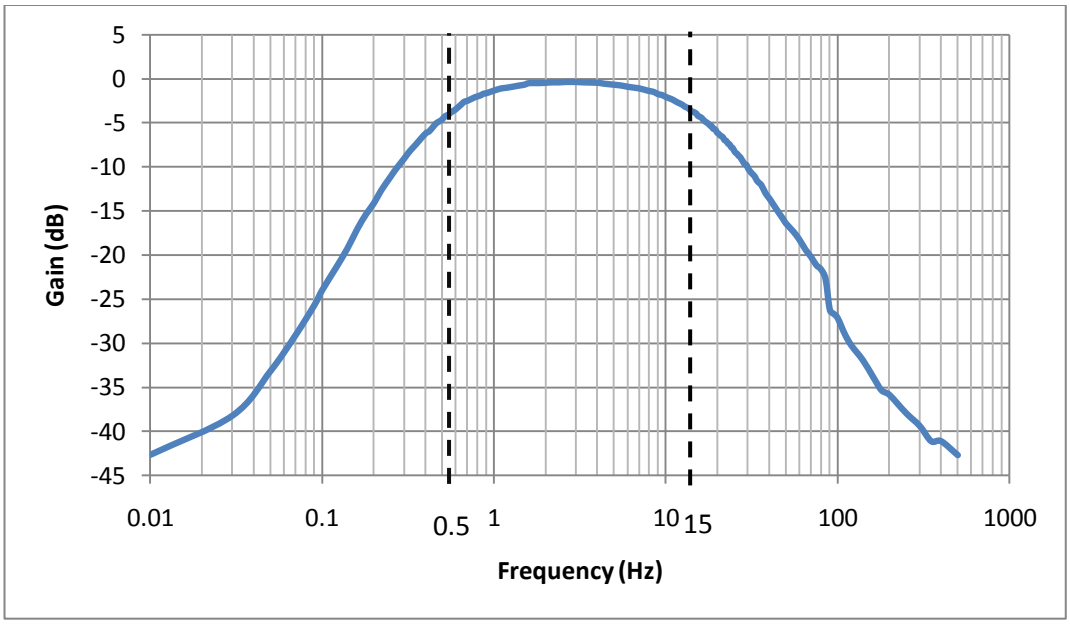

Figure 7.20: Experimental frequency response of the band pass filter.

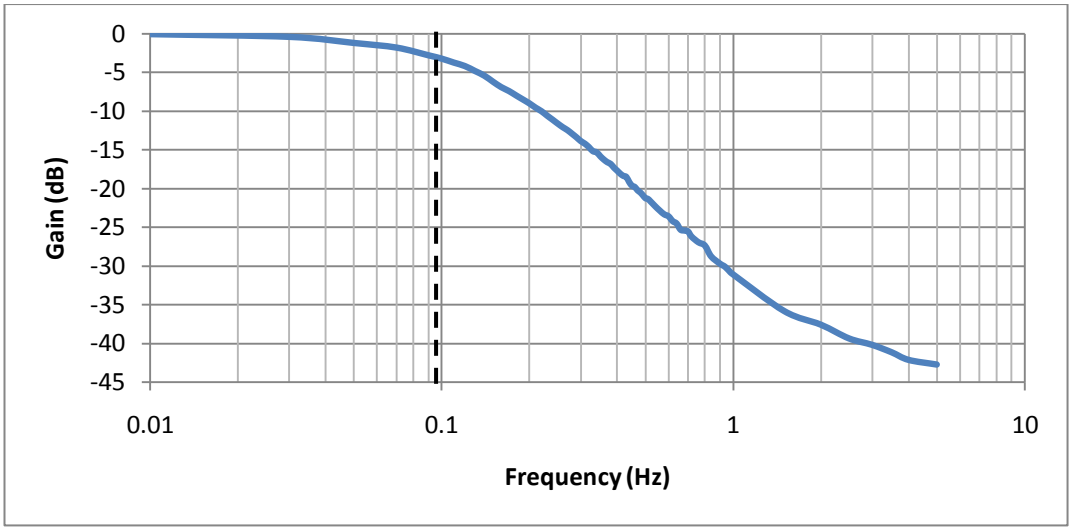

Figure 7.21: Experimental frequency response of the low pass filter.

The experimental frequency sweep analysis of the band pass filter was executed by an input signal of 0.01Hz-1000Hz while both the input signal and the output of the filter was observed on the oscilloscope as shown in Figure 7.22.

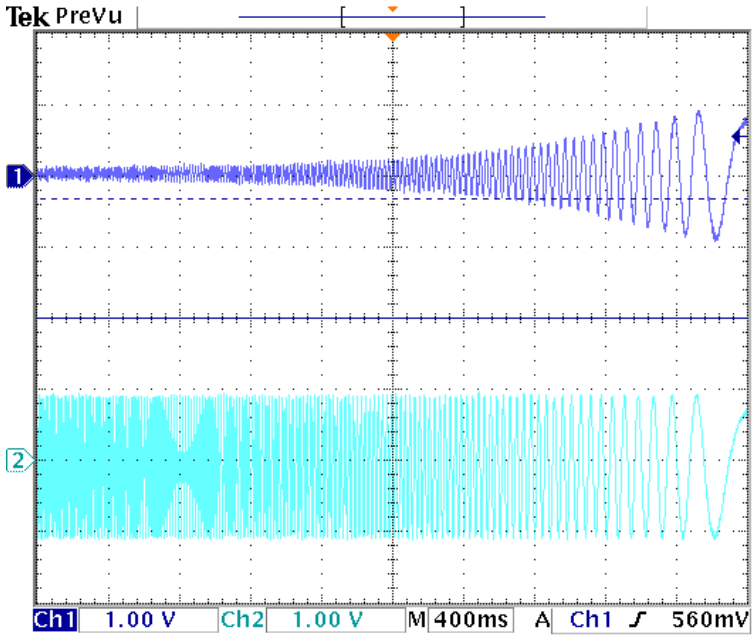

Figure 7.22: Experimental frequency sweep of the band pass filter, trace 2 displays the input frequency and trace 1 displays the output of the filter.

As the PPG processing system is battery operated, the battery consumption was evaluated to determine the length of time the system can operate until the battery potential drops to a level which causes the PPG processing system to cease to operate

within its specifications. The PPG sensor was connected to the PPG processing system and switched on whilst the battery voltage was continuously recorded using LabVIEW software. As shown in Figure 7.23 the battery voltage drops to 6 volts at the positive voltage rail (T1) after operating for four hours, at this point electrical interference is observed on the instrument output. The output of the instrument is detecting signals from the photodiode on the PPG sensor. At this voltage the processing system is incapable of providing adequate voltage in order to activate the LEDs and the photodiode as necessary which results in the electrical interference. After six hours into the experiment the battery voltage decreases to zero volts shown as T2 in the figure.

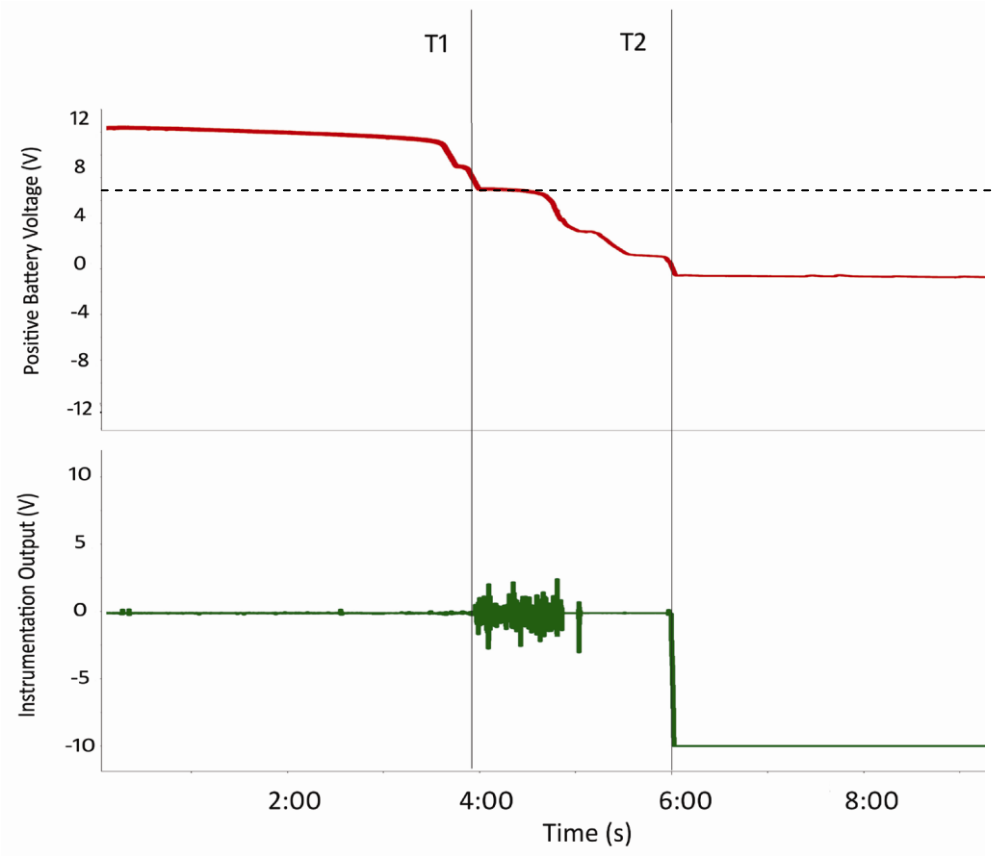

Figure 7.23: Battery consumption of the PPG processing system, T1 represents the time the processing system ceases to function; T2 represents the time when the output of the battery is zero.

The PPG processing system with the finger PPG sensor was evaluated on a volunteer where the sensor was secured on the volunteers' index finger by placing the PPG sensor inside a modified pulse oximeter probe as described in the previous chapter.

The system was connected to a personal laptop as shown in Figure 7.24 where the PPG signal was displayed using LabVIEW software, which will be explained in more detail in the following chapter.

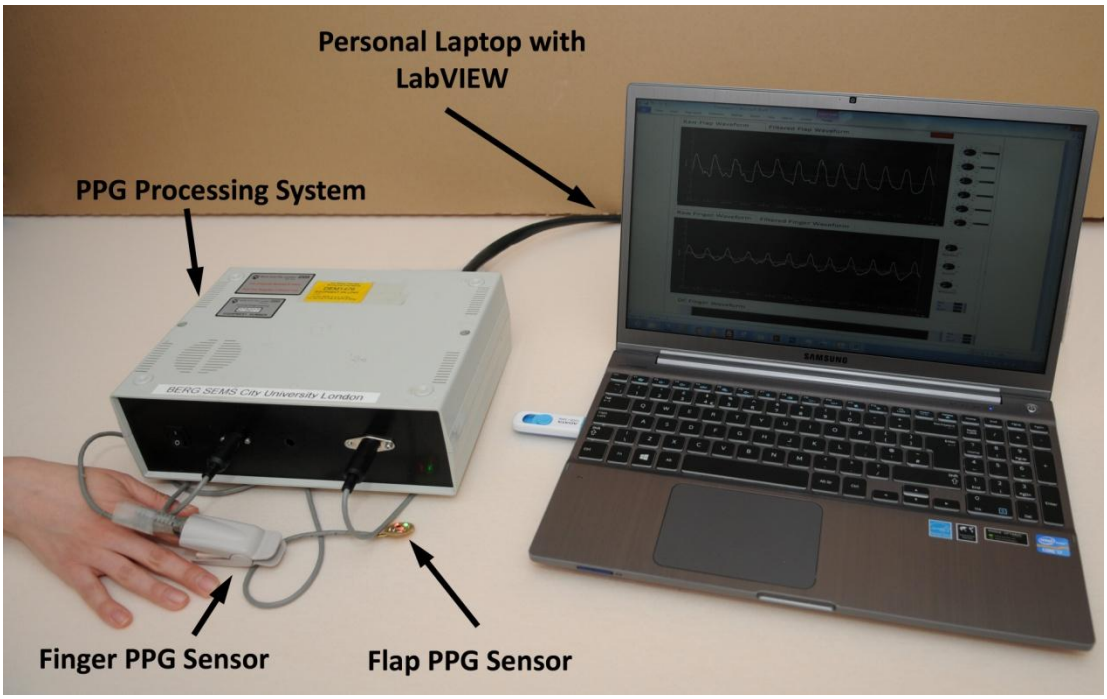

Figure 7.24: Photograph demonstrating the setup of the developed PPG processing system and sensor on a volunteer.

Red, infrared and green ac PPG signals were successfully acquired in the laboratory on a volunteer as shown in Figure 7.25 where the typical PPG morphology is clearly observed.

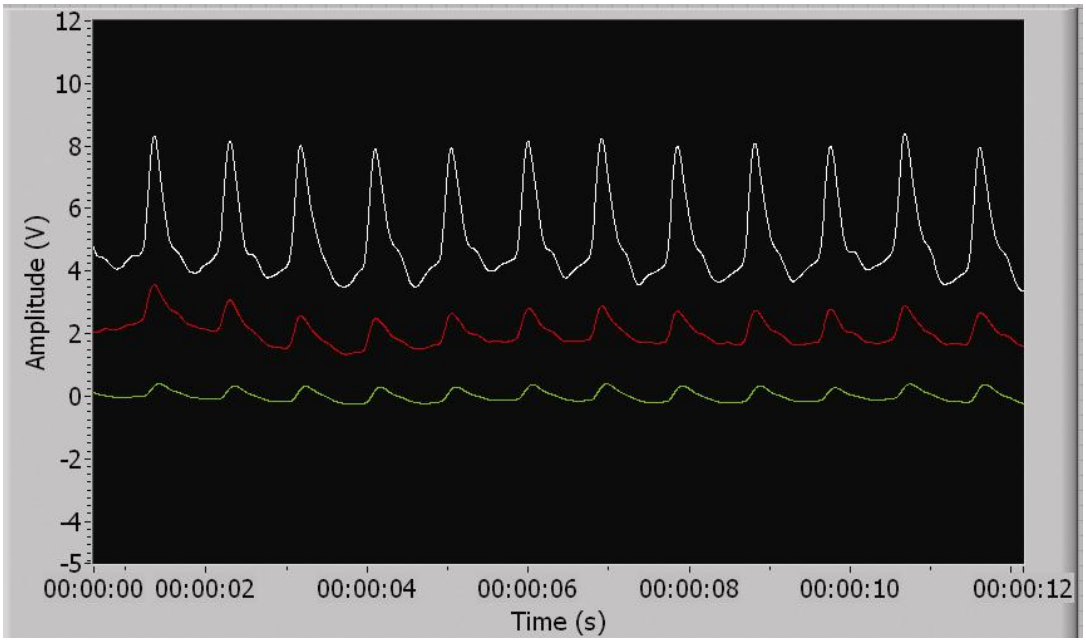

Figure 7.25: Infrared, red and green ac PPG signals are shown in white, red and green colour waveforms respectively.

7.5 Conclusion

A two channel three wavelength photoplethysmographic processing system was successfully designed and developed in the laboratory to monitor PPG signals from both a free flap and a finger. The ac and dc components of the PPG signals from all wavelengths were successfully displayed.

Following the display of the PPG signals on an oscilloscope the PPG system is then connected to a personal laptop using a DAQcard-6024E where the signals can be displayed, analysed and stored for future analysis using LabVIEW.

Chapter 8

Signal Acquisition Using LabVIEW

8.1 Introduction

The developed photoplethysmography system uses a Virtual Instrument (VI) to record, process, display and store the data for further offline analysis. The processing system provides 14 output signals for ac PPG (pulsatile arterial component) and dc PPG signals (non-pulsatile PPG component from venous, skin and bone) for Red (R), Infrared (IR) and Green (G) wavelengths which are as follows: R_{ac} flap, IR_{ac} flap, G_{ac} flap, R_{dc} flap, IR_{dc} flap, G_{dc} flap, R_{ac} finger, IR_{ac} finger, G_{ac} finger, R_{dc} finger, IR_{dc} finger, G_{dc} finger and +ve and –ve battery voltages. These outputs are then digitised using a data acquisition card (National Instruments) which is connected to the laptop computer where the signals can then be displayed, analysed and stored using the developed virtual VI. The required VI was implemented in a software program named, LabVIEW, on a laptop computer. Figure 8.1 illustrates the main functions of the developed VI.

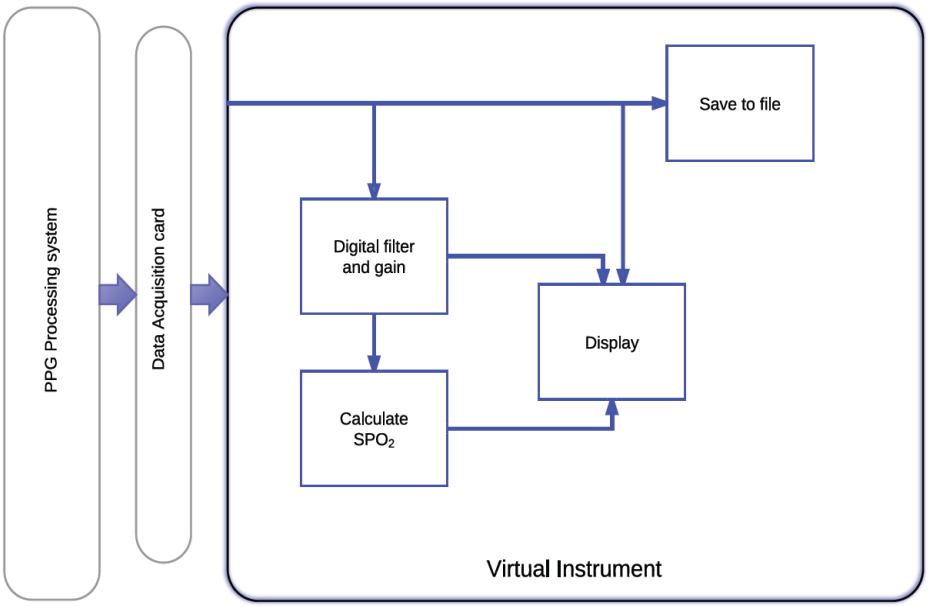

Figure 8.1: Block diagram of the virtual instrument illustrating its main functions of acquisition, analysis, display and storage of data.

In this chapter an introduction to LabVIEW and the development and evaluation of the virtual instrument for data acquisition, storage and data analysis are detailed.

8.2 Introduction to LabVIEW

Laboratory Virtual Instrument Engineering Workbench (LabVIEW) is a platform and development environment for a visual programming language from National Instruments (US, Texas). LabVIEW uses a programming language, G, which uses block diagrams to create programs. The software relies on graphical symbols and icons instead of lines of textual language as C and Java use to create applications. It also uses dataflow programming where the order of execution of the program is determined by the sequential order of the elements of the program.

This programming system consists of many libraries with a wide range of functions for data acquisition, signal generation, data storage, signal conditioning and data analysis [96]. Programmes developed in LabVIEW are called virtual instruments (VI) because their appearance and operation can imitate actual instruments. Each VI consists of three main parts, the user interface (front panel), the source code (block diagram) and subVIs which are used as subprograms within another program.

These aspects of VIs are as follows:

- Front Panel, is the interactive user interface where the users can control the program, change inputs and see the displayed data update in real time. This is also where the controls are used for inputs and indicators are used for outputs.
- Block diagram, contains the code to control the front panel objects which is added using graphical representations of functions. Every front panel indicator or control has a corresponding terminal that is located on the block diagram. The icons are connected together using wires and data travels on these wires from controls through functions to indicators on the front panel.
- SubVIs, are VIs that are used within another VI which consist of a front panel and a block diagram.

In order to measure signals with a personal computer or laptop a data acquisition (DAQ) system is required. This system consists of a sensor with a current or voltage output, DAQ measurement hardware and a computer with a programmable software or LabVIEW.

Analogue signals cannot be manipulated or displayed on a personal computer without a DAQ device. One of the primary functions of a DAQ device is its ability to work as an analogue to digital convertor (ADC) to digitise the photoplethysmographic signals acquired from the PPG sensors and transferring the signals to the computer over a computer bus which serves as the communication interface between the DAQ device and the computer. More details on the specifications of the data acquisition card have already been discussed in the previous chapter.

8.3 Development of virtual instruments using LabVIEW

Following digitisation of the PPG signals, a virtual instrument was implemented in LabVIEW version 8.5 (National Instruments, Austin, Texas, USA) as shown in Figure 8.2. The VI was developed to acquire all signals, further process and filter the acquired signals, calculate SpO_2 values, display all ac and dc signals in graphical format as well as the calculated SpO_2 values for both flap and finger PPG channels and to finally save the data in a spread sheet format. Each segment of the VI, as identified in Figure 8.2 (orange blocks) will be described in the following sections.

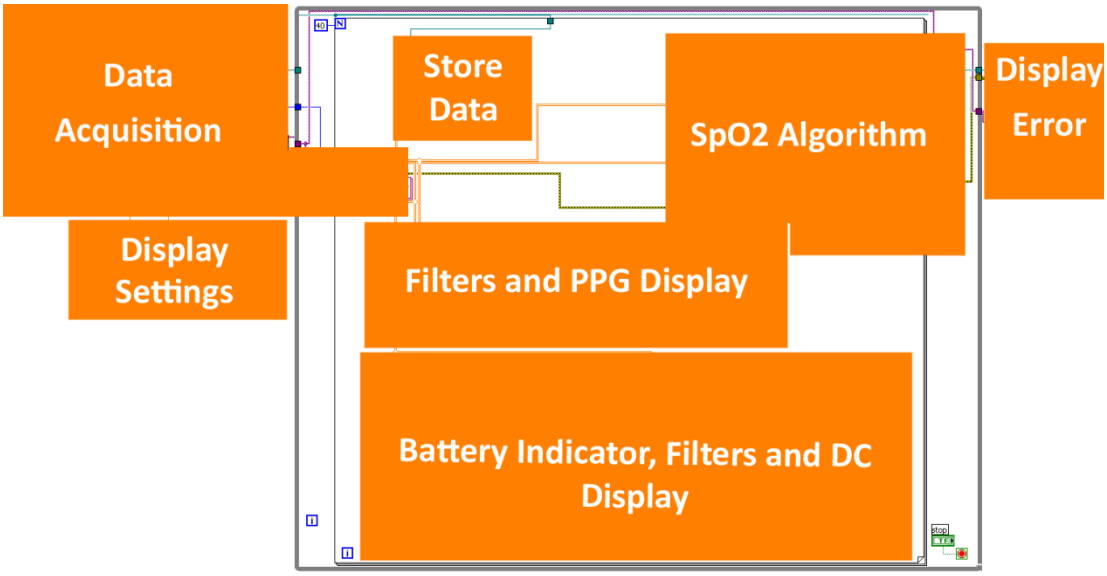

Figure 8.2: Block diagram of the developed Virtual Instrument.

8.3.1 VI for Data acquisition

Following the detection of signals by the photodiode, the signals are demultiplexed and filtered to their corresponding ac and dc PPG components of each wavelength as described in Section 7.2.4. All PPG analogue signals are then transmitted to the DAQ system for display purposes and further analysis as shown in Figure 8.3.

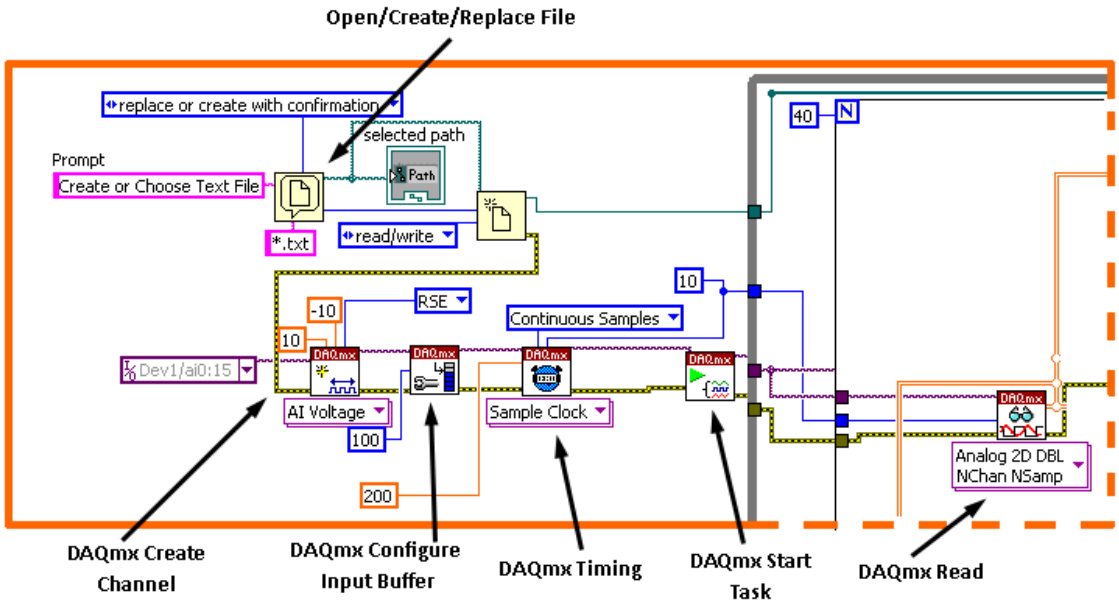

Figure 8.3: Data acquisition section of the developed Virtual Instrument.

As seen on the top section of the figure, prior to initialising data acquisition an *Open/ Create/ Replace File* function is used to create a new file to store the acquired data, this will be described in more detail in the following sections. The VI developed to continuously acquire all PPG signals also comprise of a *DAQmx create Channel* to create sixteen virtual channels required for measuring the voltage output from the PPG processing system where the output is created as a task. A task is a collection of one or more virtual channels with different information such as timing and triggering.

These virtually created channels correspond to the physical channels or terminals, *ai0-ai15* (analogue input 0 – analogue input 15) on the DAQ device to which the outputs from the PPG processing system have been connected. The terminal configurations are set to referenced single ended (RSE) mode and the minimum and maximum voltages of expected measurements are set to -10 V and +10 V [97].

As shown in Figure 8.3 to avoid an overflow error the *DAQmx Configure Input Buffer VI* is added to the DAQmx task code where the function is used to override the automatic input buffer allocation which the NI-DAQmx sets as the value of the samples per channel which in this case was set to 10 samples. The input buffer was overridden and increased to 100 samples per channel.

DAQmx Timing Sample Clock VI is also added to the DAQmx code to configure the number of samples to acquire which is set to 10 samples at a sampling rate of 200 Hz and the sample mode on the function is set so it continuously acquires samples until the VI is stopped.

DAQmx Start Task function is used to transition the task created to the running state to start the measurement. The task is then passed into a *while loop* then into a *for loop* where the *DAQmx Read* function reads samples from the task and the format of samples it is required to return is specified as analogue “2D DBL NChan NSamp”, to read multiple samples from multiple channels and output the data as a two dimensional array of double precision numbers.

The VI developed is based on a repeating loop where during each cycle the VI acquires a specified number of samples from each channel. As shown in Figure 8.3 the *DAQmx Read* function is in a *for loop* which is in turn in a *while loop*. The *for loop* is

programmed to run forty times for every iteration of the *while loop.* As the *DAQmx Read* is set to obtain 10 samples for each iteration, and the *for loop* is specified to execute its subdiagram 40 times, the number of samples acquired for each iteration of the *while loop* is 400. The while loops repeats the subdiagram inside it until the conditional terminal receives the set *Boolean value*. The *while loop* will always execute at least once, the condition set for the *while loop* to stop running is for the conditional terminal to receive a true Boolean value, this will only occur once the user has pressed the STOP button on the front Panel which will terminate the DAQmx program.

Since the *DAQmx Start Task VI* is used to begin the task, the task is changed from an "idle" state to a "running" state.

8.3.2 VI for data filtering

Despite the filtering process (hardware) which takes place in the processing system the acquired PPGs might still have some noise on them and therefore further digital filters (software) implemented in LabVIEW have been employed to remove any unwanted signals from the PPGs.

As mentioned previously the *while loop* consists of *DAQmx Read* function which reads the samples from the virtual channels created and specified. The VI returns an array of 2-dimensional samples where each row corresponds to a channel in the task and each column corresponds to a sample from each channel.

To allow filtering of the acquired PPG signals, the acquired array of all 14 channels must be separated. As shown in Figure 8.4 a *DAQmx Index Array VI* is used to extract the 2D array into 1D sub-arrays, as each row corresponds to a channel, the VI is programmed to separate the 14 channels. In the array connected to the DAQmx Index Array function, each column in the array represents a channel connected to the DAQcard. By wiring a constant value which represents the required channel to the column index input of the function, the data from that specified channel can be extracted from the output of the function. The separated channels represent the ac and dc components of the signal including the 2 channels used for displaying the battery voltage of the processing system.

To provide the user with the option of viewing the filtered and unfiltered PPG signals a *Case Structure* was used. The *case structure*, shown in Figure 8.4, can have two or more subdiagrams where only one subdiagram is shown at a time and each case is executed once at a time. Using an *enum* control on the front panel, the user can control which subdiagram is executed, in this VI the user is provided with two options, to view the PPG signals in the raw or the filtered format.

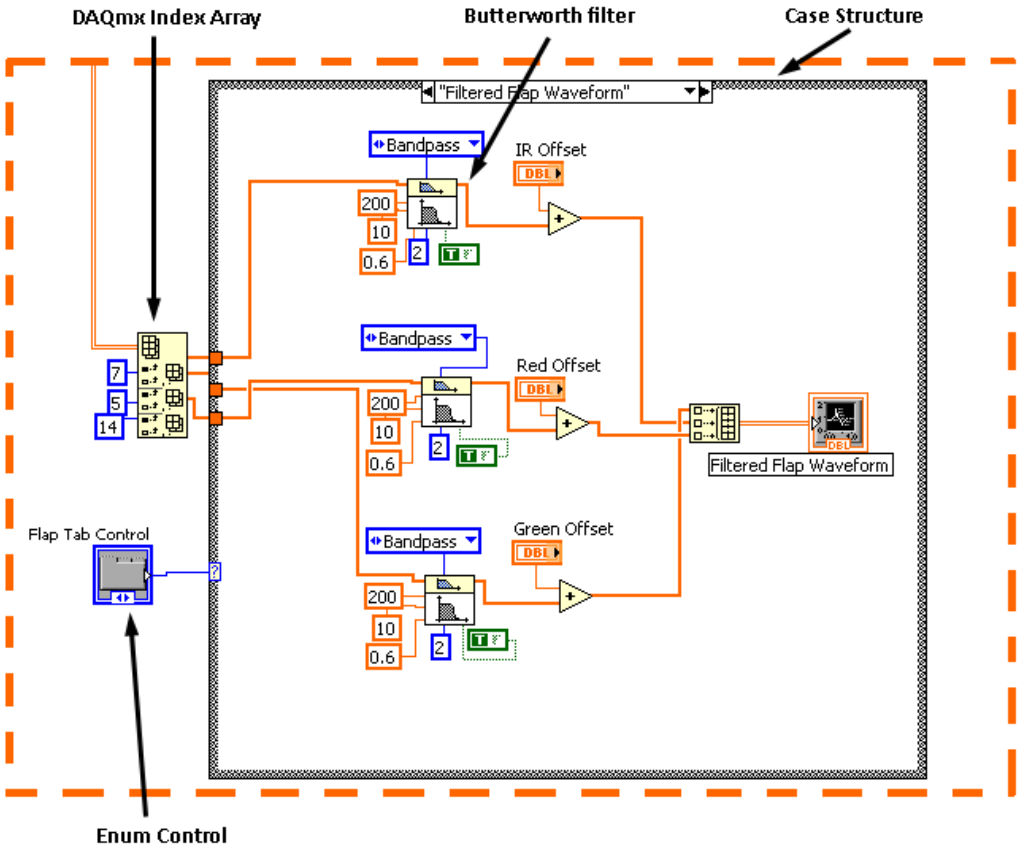

Figure 8.4: showing the Virtual instrument of the filtering of the acquired data (flap ac PPG).

To remove any noise from the PPG signals an Infinite Impulse Response (IIR) filter was used which works with the current and previous input and output values. To filter the acquired photoplethysmographic signals a second order *Butterworth filter VI* was placed within a case structure in the block diagram. This VI generates a digital Butterworth filter by calling the Butterworth Coefficient VI. This specific filter was chosen for its smooth, monotonically decreasing frequency response in the transition

region. Figure 8.5 illustrates the performance of the filter used to eliminate frequencies outside of the chosen pass band.

Identical parameter settings were chosen to filter all the flap ac red, infrared and green PPG signals and finger ac red, infrared and green PPG signals using cut off frequencies of 0.6-10Hz for the band pass filter with sampling rate of 200Hz. Similarly the flap and finger dc PPG signals for red, infrared and green wavelengths were filtered using a low pass second order *Butterworth filter VI* with a cut off frequency of 0.15Hz and a sampling rate of 200Hz.

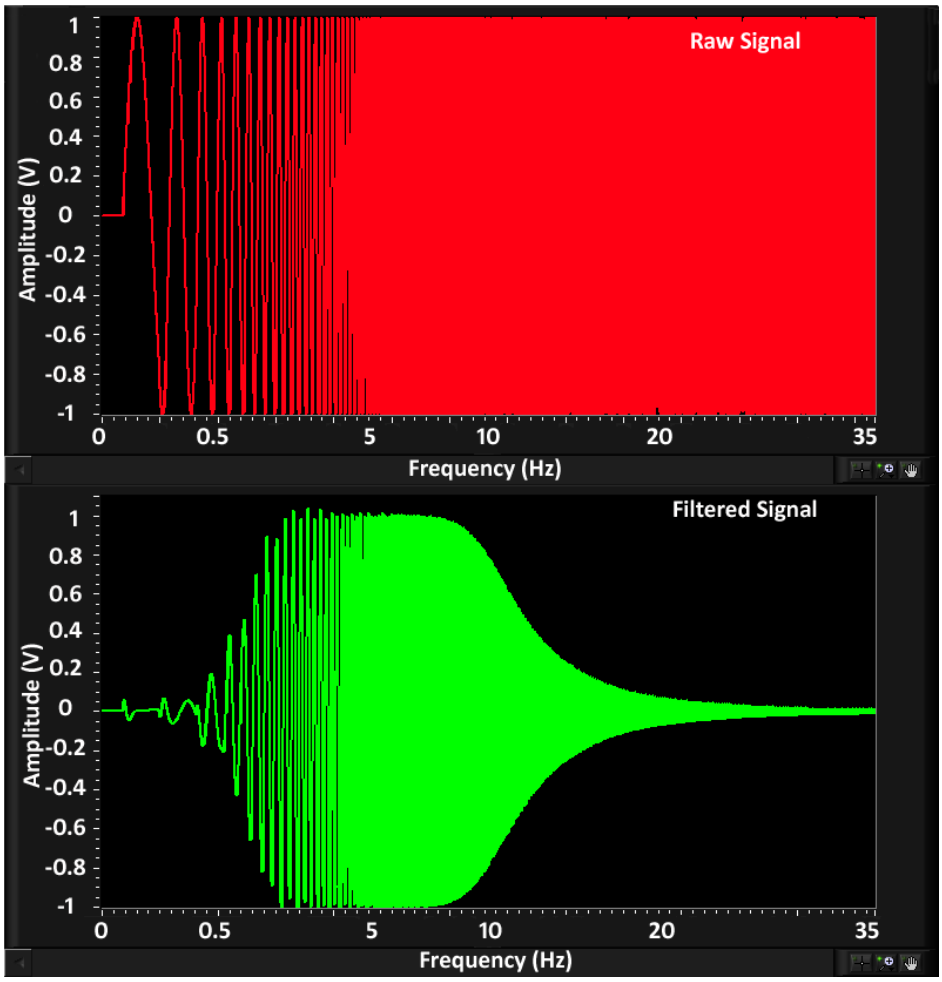

Figure 8.5: Shows the Butterworth filter eliminating the frequencies outside of the 0.6-10Hz cut off frequency.

8.3.3 VI for display of Photoplethysmographic signal

Once the signals have been separated and the user has chosen to view the waveform in either the filtered or unfiltered format on the front panel as seen in Figure 8.6, the

user can subsequently modify the gain of the signal and change the offset according to their preference in order to allow all signals to be easily viewed. An *Index Array VI* is used to return the subarrays as shown in Figure 8.4.

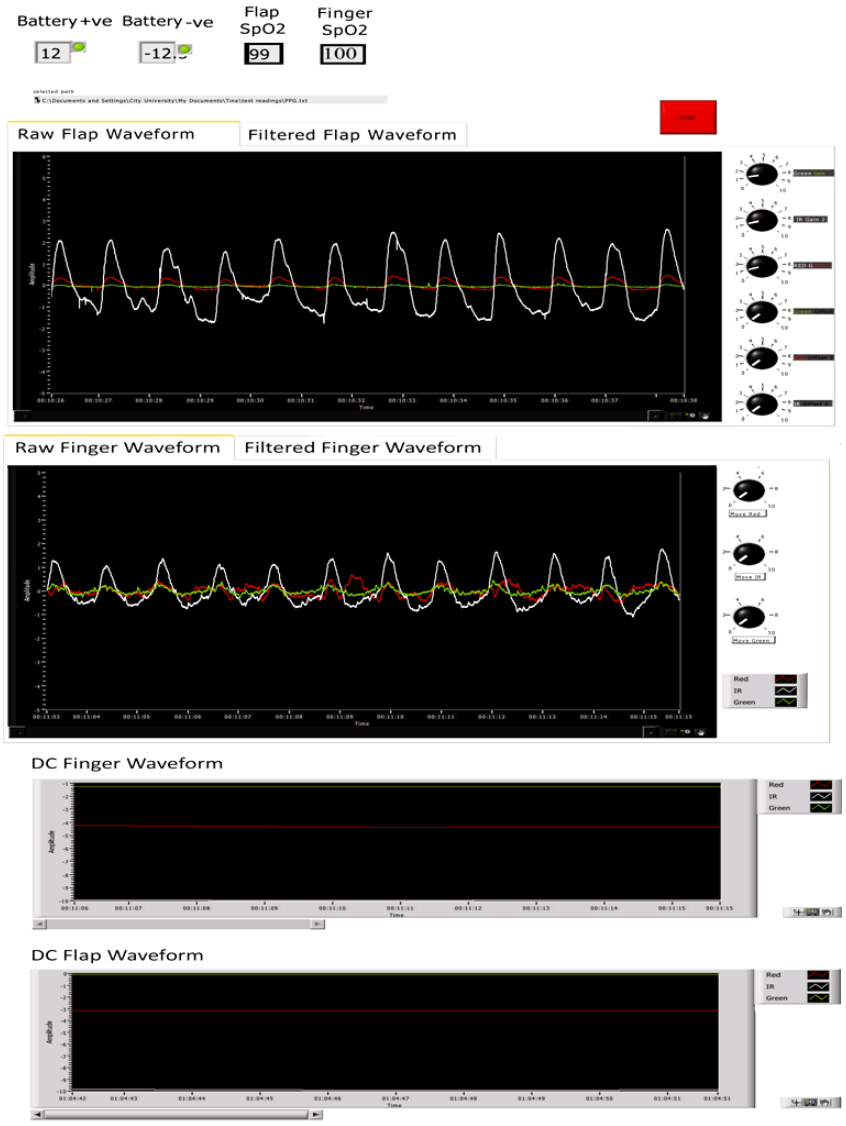

Figure 8.6: The front panel of the virtual instrument used to display the acquired three wavelength ac and dc PPGs from free flap and finger.

As each row corresponds to a channel, the VI is programmed to separate each channel; these channels represent the ac and dc components of the signal where each channel can be filtered and adjusted separately as desired. As shown in Figure 8.4 a *Build Array VI* is then used so the strings are combined to form one array to be able to display the R_{ac} flap, IR_{ac} flap and G_{ac} flap PPG signals on one chart, R_{ac} finger, IR_{ac} finger and G_{ac}

finger on a second chart followed by the relevant dc values of flap and finger on two separate charts as shown in Figure 8.6.

The front panel of the virtual instrument is implemented to show the continuous display of flap PPG waveforms consisting of red, infrared and green wavelengths and finger PPG waveforms consisting of red, infrared and green wavelengths. The dc flap and finger waveforms are also displayed. The VI is also implemented to show estimated SpO_2 values and the state of the batteries situated at the top of the VI, as seen in Figure 8.7.

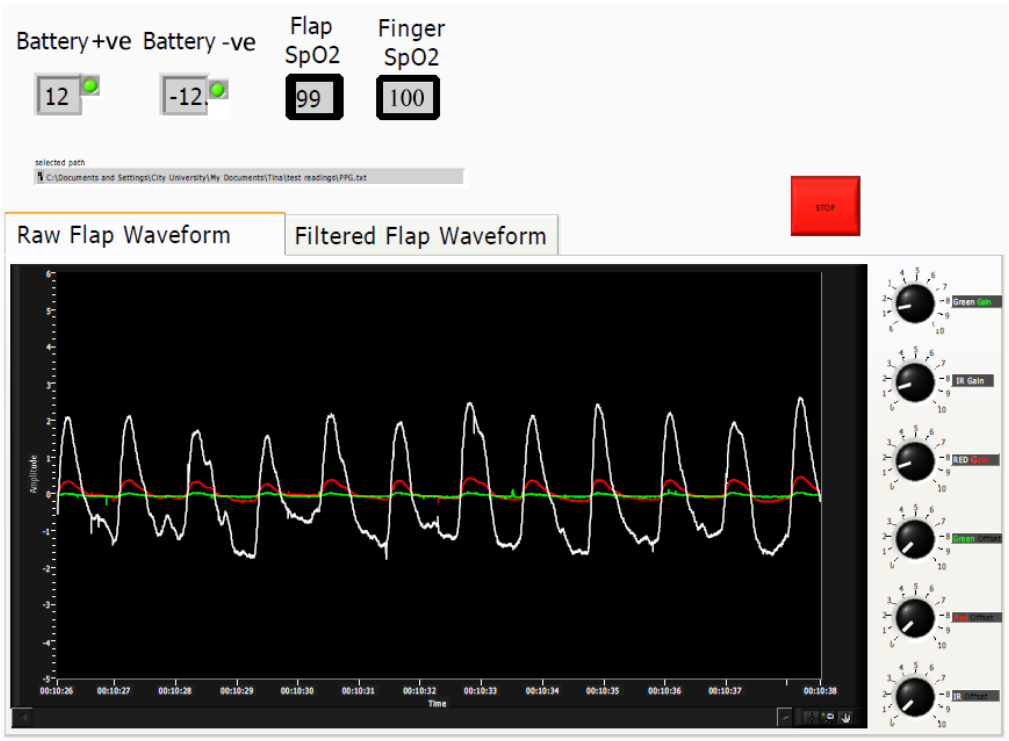

Figure 8.7: Front panel utilized for observing real-time flap PPG signals with adjustable gain and offset.

Waveform chart is a special type of numeric indicator that displays plots of data acquired at a constant rate which in this case was 200Hz. This function remembers and displays a certain number of points by storing them in a buffer. As the data points are acquired, the chart displays the received data as well as the already existing points allowing real-time, continuous display of the acquired PPG signals. By altering the length of the *Chart History buffer* (in the waveform chart options), the number of points the chart will remember and display can be changed.

The user has an option to adjust the gain and offset (DC level shifting) of the signals from the front panel as observed in Figure 8.7 (on the right of the figure). This provides the option to change the offset and gain during real-time display of the flap ac PPG signals. The offset value of the finger ac PPG signals can also be changed, enabling the user to view the red, green and infrared signals separately. However as the finger PPG signals are typically considerably larger in amplitude than the flap PPGs, the option to increase the gain of the finger PPG signal was not provided.

As shown in Figure 8.8, by using the Build Array function the flap red, infrared and green PPG signals are appended to one array which is then plotted on the same *waveform.* The control of the gain was accomplished by connecting the output of each channel to one of the inputs on the *multiply* numeric function, while a numeric control function located on the front panel as a rotating knob was connected to the second input of the *multiply* numeric function which then returns the product of two inputs.

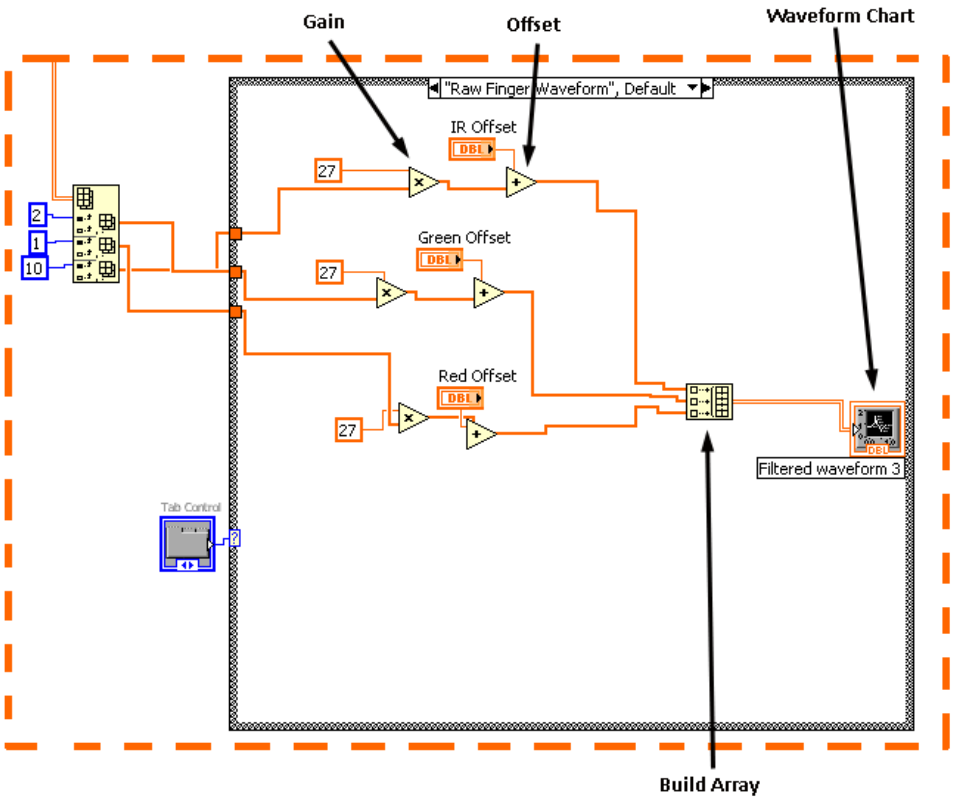

Figure 8.8: The adjustable gain and offset of red, infrared and green ac flap PPGs.

After multiplication of the signal by the chosen value, the output is then connected to an *add* numeric function which computes the sum of the two inputs. A numeric control located on the front panel was also connected to the other input of the *add* numeric function which enables the user to level shift the signal on the chart display by choosing the desired value on the rotating knob control.

In *waveform chart* display the *x* value is not specified and it is automatically incremented as the provided *y* value is appended to the chart which means that the PPG amplitude is plotted against the number of samples acquired [97]. By utilising the *Multiplier property node* for the *x*-axis (seen in Figure 8.9), the scaling information can be adjusted. *Property nodes* allow the properties of a front panel object to be programmatically controlled. By changing the input of the multiplier value to $\frac{1}{f_s}$, where f_s is the sampling frequency which in this VI is 200Hz, the *x*-axis is changed to show the signal in real-time (seconds).

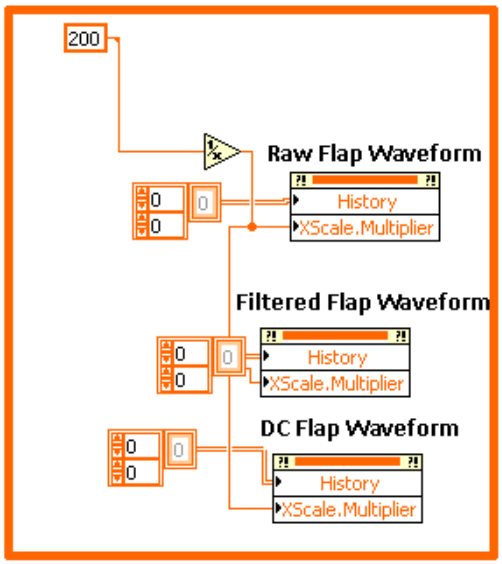

Figure 8.9: History data and XScale Multiplier property nodes.

In order to alert the user of a low battery condition on the front panel, an algorithm was developed. As mentioned in section 8.3.1 the minimum and maximum voltages of expected measurements for the DAQ device are set to ±10V, however the rechargeable lead acid batteries used in the photoplethysmographic processing system are ±12V, therefore a voltage divider was used on the processing board to half the

output voltage of the batteries prior to connecting them to the DAQcard. Consequently, once the battery voltage has been separated from the 2D array of the data acquired, the signal is then multiplied by 2 using a *multiply* numeric function; this is shown in Figure 8.10. The output voltages of the batteries are then displayed using a *numeric indicator* on the front panel as Battery +ve and Battery –ve representing the remaining positive and negative battery voltage.

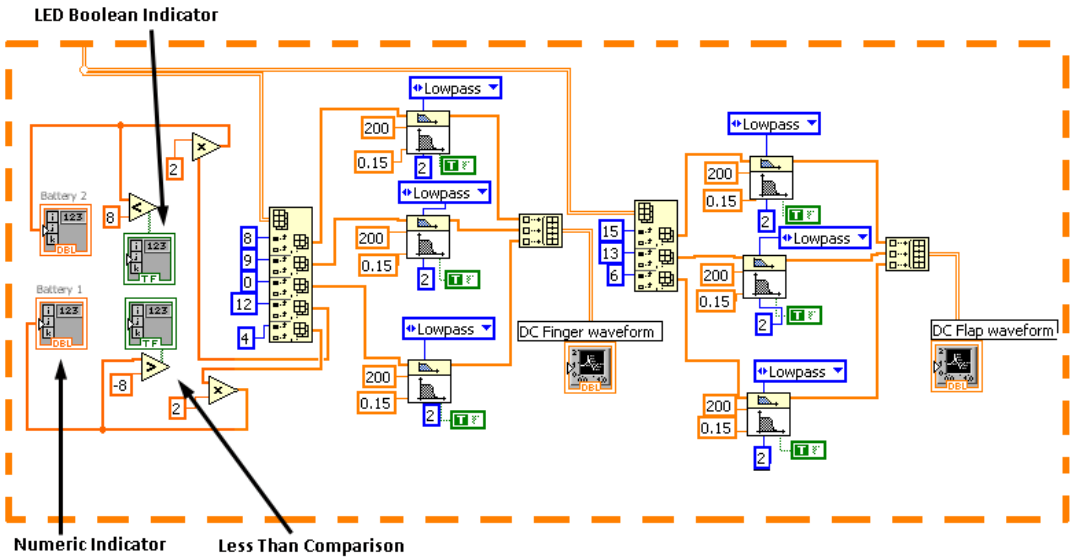

Figure 8.10: Battery alert and PPG dc display section of the developed virtual instrument.

A *Less than comparison* function is used to compare the detected battery voltage with a constant value of +8 for the positive battery and -8 for the negative battery. The output of the comparison function will return true if the battery voltage is less than the constant value. A round *LED Boolean indicator* is also used to alert the user if the battery voltages drop below +8V or -8V. The LED indicator is set up to show a green light providing the battery value is higher, once the battery voltage drops to below the set limit of +8 or -8V the LED indicator light changes to red as a low battery warning to the user. The motive for this chosen limit is explained further in the previous chapter.

8.3.4 Estimation of flap and finger SpO_2

Algorithms for estimating flap and finger arterial blood oxygen saturation (SpO_2) values were also developed. As the algorithms used to estimate the flap and finger SpO_2 values are identical, only the flap algorithm will be discussed in this section.

To derive estimations for SpO_2 values, initially the ratio (R) of the quotients of the ac and dc amplitudes of the red and infrared wavelengths (the green wavelength was not used for this algorithm) are calculated using:

$$R(ratio) = \frac{ac_R / dc_R}{ac_{IR} / dc_{IR}} \tag{8.1}$$

The arterial oxygen saturation is then computed using an empirically derived linear equation which is frequently used in commercial pulse oximeters:

$$SpO_2 = 110 - 25R \tag{8.2}$$

To be able to calculate the ratio ac/dc of red and infrared wavelengths and ultimately calculate the SpO_2 of flaps the VI shown in Figure 8.11 was implemented using equations (8.1) and (8.2).

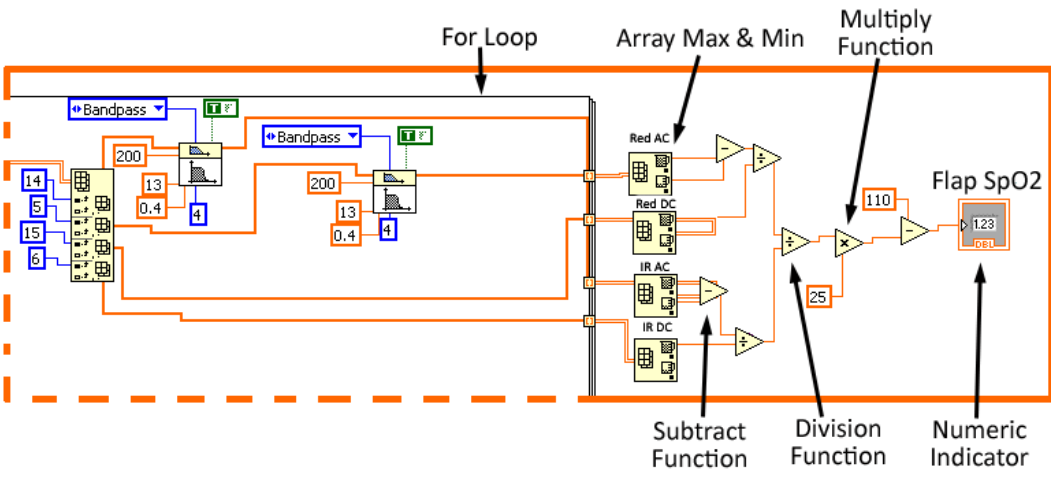

Figure 8.11: Illustration of the algorithm used for calculating the ratio for the flap PPG channel.

As explained in previous sections, the VI is programmed to run continuously and acquire 10 samples at a sampling rate of 200Hz, the acquired data is then passed into a *while loop* followed by a *for loop* where its iteration is set to 40. Therefore, after forty iterations of the *for loop*, 400 samples have been acquired which equals to 2 seconds (approximately 2 PPG cycles), considering the sampling frequency of 200Hz which enabled the continuous collection of enough data for calculating the ratio. Following the filtering of the ac and dc PPG signals of red and infrared wavelengths, the four signals are then passed outside the *for loop* and into the input of four *Array Max & Min* functions as illustrated in Figure 8.11. This function returns the maximum and minimum values found in the numeric array input. For the ac PPG data the maximum values which represent the peak and the minimum values which represent the valleys of the waveform were found and using a *subtract* numeric function the two values of were then deducted to find the amplitude of the pulsatile PPG component of the signals for both red and infrared wavelengths. Two additional *Array Max & Min* functions were used to detect the maximum values for the dc component of the PPG for both wavelengths.

The calculated amplitude of the ac PPG and the maximum value for the dc PPG were then used to calculate the ratios of ac_R/dc_R and ac_{IR}/dc_{IR} using two *division* numeric functions. Subsequently to compute the R value a third division numeric function was used to divide the quotients of the ac and dc values at the red and infrared wavelengths. The calculated R value is then multiplied by 25 using a *multiply* numeric function and a constant, the output is then subtracted from a constant value of 100 using a *subtract* numeric function where the output is the estimated SpO_2 value which is updated every 2 seconds. The estimated blood oxygen saturation for the Flap SpO_2 and Finger SpO_2 are numerically displayed on the front panel as shown in Figure 8.11.

8.3.5 VI for saving acquired data

All the acquired PPG signals were saved to a text file to enable their further offline analysis. At the start of the VI an *Open/Create/Replace Fil*e function was used with a *File Dialog* function connected to its *File Path* input. Once the user clicks on the *Run Button* on the front panel to run the VI, a dialog box is displayed requesting the user to

select the path where the user desires to create or choose an existing text file to save the acquired data onto, otherwise the user has the option of entering the file path in a *File Path Control* on the front panel prior to running the program.

The VI generates an output *refnum out* which is the reference number of the open file. This is then connected to *Write to Spreadsheet VI* which is located inside the *for loop* to indicate the path the file is to be saved into. Additionally as mentioned in previous sections, the *DAQmx Read VI* presents the acquired data as a 2D array which contains all the raw data that needs to be saved. Prior to storing the acquired data, the *Transpose 2D Array* function is used to rearrange the elements of the created 2D array such that each row and the corresponding columns are interchanged where a 2D array $[i, j]$ becomes a transposed array $[j, i]$ where each column of data will represent a channel . As shown in Figure 8.12 the output of this function is then connected to the input of the *Write to Spreadsheet VI* which then converts the acquired 2D array of double-precision numbers to a text string and writes the string to the chosen new or existing file. The format which the numbers are converted to characters is a string containing the number with three digits to the right of the decimal point.

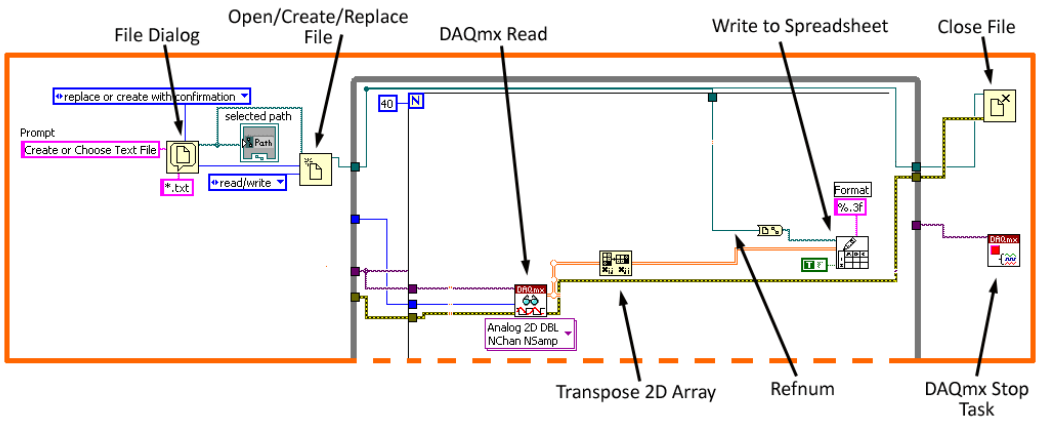

Figure 8.12: Block diagram of the data storing virtual instrument.

Once the user presses the Stop Button on the front panel, control exits the while loop and the *Close File* Function closes the open file which is specified by the refnum. Starting from *DAQmx Create Channel* through to the *Close File* function the error in and error out connections of the VI functions were wired together so in the event of that the VI encounters an error, the message can be displayed using a dialog box.

The *DAQmx Stop Task* VI is used outside the *while loop* to stop the task in the data acquisition program and returns it to the "idle" state. The *Close File* function is also used to close the open file which was created using the *Open/Create/Replace File* function, the file path is specified by refnum and the *Close File* function returns the path to the file associate with the refnum.

The Error input and outputs of the VIs and functions have been wired to enable the error to be displayed for the user once the task has stopped.

8.4 **Conclusion**

Using a data acquisition card (DAQCard-6024E) and a personal laptop computer, a Virtual Instrument was successfully developed in LabVIEW to acquire, filter and display all acquired signals of flap R_{ac}, flap IR_{ac}, flap G_{ac}, flap R_{dc}, flap IR_{dc}, flap G_{dc}, finger R_{ac}, finger IR_{ac}, finger G_{ac}, finger R_{dc}, finger IR_{dc}, finger G_{dc}, Battery +ve and Battery –ve. The developed photoplethysmographic processing system was connected to the data acquisition card using a 68 pin, shielded cable SHC68-68-EPM (National Instruments). The developed VI was successfully evaluated and good quality PPG signals were recorded and displayed on the personal laptop. Additionally SpO_2 values were calculated and displayed using red and infrared PPG signals from both channels and the values were displayed on the front panel to enable the user to detect any changes in SpO_2 levels. Also, the battery condition algorithm executed successfully by displaying the status of the battery voltage on the front panel. All signals were displayed on *waveform charts* following the removal of noise using *Butterworth filters* where good quality waveforms were produced to allow the user to observe any changes to the morphology and the amplitudes of the PPG signals in real time.

Following the successful implementation of the virtual instrument and its detection of PPG signals from the developed photoplethysmographic processing system the clinical evaluation of the system will be presented in the following chapter.

Chapter 9

In vivo evaluation of the photoplethysmographic system on DIEP flaps

As discussed in the previous chapters, the functionality of the developed photoplethysmographic system, the reflectance three wavelengths PPG sensor and the virtual instrument were successfully evaluated in the laboratory. Since good quality PPG signals were acquired from all three wavelengths from volunteer index fingers, it was decided to begin preliminary clinical measurements.

The aim of these measurements was to assess the reliability of the PPG system in monitoring PPGs and SpO_2s of flaps prior, during and following reconstructive surgery with a focus in the investigation of PPGs during all operative periods in patients undergoing Deep Inferior Epigastric Perforator (DIEP) flap reconstructive surgery. In these preliminary clinical measurements pre-operative PPG measurements were made from the donor site (the abdomen); intra-operative measurements were made from the flap after it was re-sited and the vessels had been anastomosed; post-operatively flap measurements were performed for up to 12 hours in order to detect changes in PPG amplitude and arterial blood oxygen saturation.

This chapter also provides an outline of the protocol which includes the patient recruitment procedure and methods used for obtaining pre, intra and post-operative measurements. The methodology used to analyse the data acquired will then be presented, followed by a detailed discussion of the results.

The developed photoplethysmographic (PPG) processing system and sensor were inspected and electrically safety tested by the Biomedical Engineering Department in

Mid Essex Hospital. As the developed PPG processing system was battery powered, the device was considered electrically safe for use on patients.

Ethical approval (see Appendix i) was obtained for the study in July 2010 from the East London Research Ethics Committee and the project was approved by the Mid Essex Hospital Services NHS Trust to use the developed system on patients aged 18 to 70 years old undergoing Deep Inferior Epigastric Perforator flap reconstructive surgery. Prior to recruiting patients for the study approval was obtained from the surgeons involved

In total fifteen adult female patients with average age (±SD) of 54 (±8.9) undergoing elective breast reconstructive surgery using DIEP flap were recruited to the study.

9.1 Pre-operative protocol and *in vivo* assessment in DIEPs

The recruited patients were induced with Midazolam 2mg intravenously and TIVA (total intravenous anaesthesia) using target controlled 2% propofol and target controlled remifentanil, followed by a muscle relaxant (atracurium, rocuronium or vecuronium). The airway was maintained using either a Proseal laryngeal mask or endotracheal tube as indicated. The lungs were mechanically ventilated with oxygen enriched air and anaesthesia was maintained using TIVA. Routine monitoring such as ECG, blood pressure, pulse oximetry, cardiac output using oesophageal Doppler probe, temperature (core and peripheral), and urine output were monitored throughout the operation.

During these types of operations the routine practice is to use hand held Doppler ultrasound, after the patient is anaesthetised, in order to identify the main perforators in the donor site and to ensure there is good blood supply to the donor segment.

As a proof of concept the flap PPG sensor was also, in a similar way as the Doppler probe, used on five patients to achieve baseline PPG measurements prior to surgery and to investigate whether the PPG sensor will have the capability of also identifying the main perforators. The investigation of PPG signals from the donor site commenced in the anaesthetic room. As the same sensor is used in all patients, to ease sanitisation of the sensor and avoid cross-contamination between patients, for each patient the

flap PPG sensor was covered with a sterile transparent adhesive film dressing (3M™ Tegaderm™ Film). The PPG sensor was then placed on the abdomen of the patient and secured in place using a transparent and perforated plastic surgical tape (3M™ Transpore™ surgical tape).

In some patients the exact site to place the sensor was mapped by locating the section on the abdomen where a good quality PPG signal was displayed on the laptop, this was normally the PPG signal with the highest amplitude.

Flap ac and dc photoplethysmographic signals from red, infrared and green wavelengths were acquired using the PPG processing system and recorded for up to two minutes for each patient. The developed virtual acquisition system on LabVIEW was used to acquire, display and store the signals for further offline analysis. A Patient log file was also prepared for each patient where patient information such as the patient's date of birth, weight and date of surgery as well as the recording of the SpO_2, heart rate, blood pressure and any temperature measurements taken are documented.

9.1.1 Pre-operative results

Good quality red (n=5), green (n=4) and infrared (n=6) PPG signals with typical PPG morphology were acquired in the pre-operative period. It was not possible to perform pre-operative measurements in all patients as there was not enough time and this study had no intention to delay the surgical procedure. Figure 9.1 depicts ac PPG signals from all wavelengths for a 10 second period recorded from the abdominal site (donor site) of one patient.

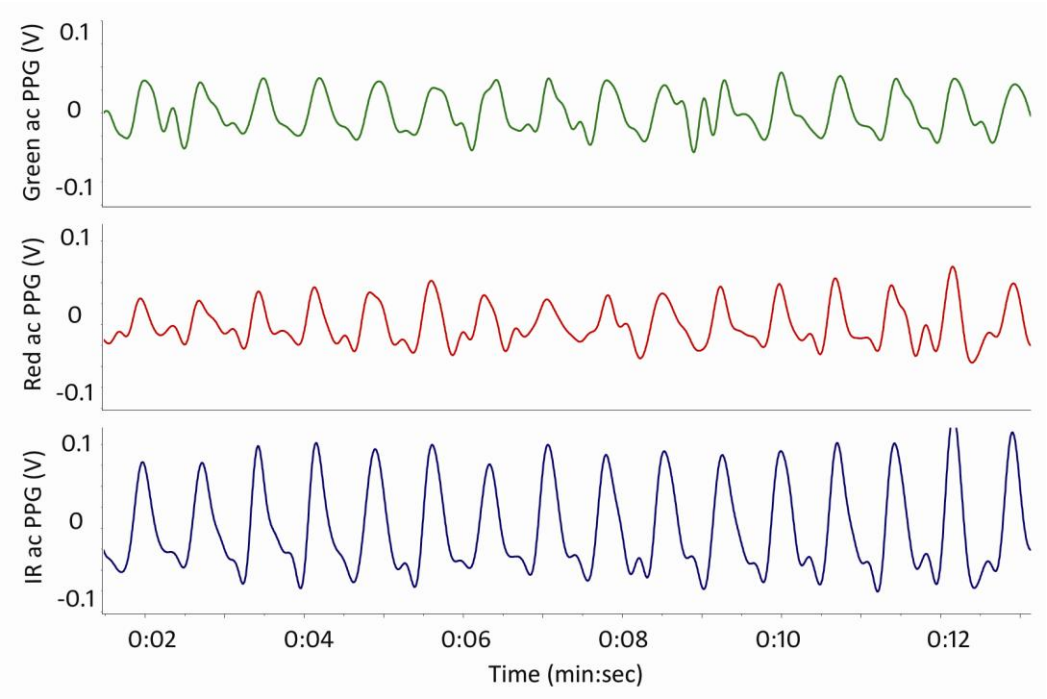

Figure 9.1: shows ac PPG signals from the abdominal donor site obtained pre operatively.

In order to investigate how ac PPG amplitudes of red, infrared and green wavelengths differ between patients, the mean (± SD) of ac PPG signals from each wavelength were calculated, and these are presented in Table 9.1.

Table 9.1: Basic analysis of the PPG ac amplitudes from all patients at all wavelengths.

Patient	ac Red (n=5) (mV)	ac Green (n=4) (mV)	ac IR (n=6) (mV)
1	53.8	53.1	161.1
2	284.9	104.7	268.1
3	128.5	93.8	317.1
4	70	__	133.2
5	__	__	52.2
6	76.3	66.9	166.3
Mean	**122.7**	**79.6**	**183**
±SD	**94.9**	**23.8**	**95.5**

The PPG processing system failed to detect good quality green wavelength PPG signals in patients 4 and 5 and red PPGs in patient 5. These were possibly caused by incorrect placement of the sensor in relation to the main perforators or movement artefact caused by the surgical team handling the patient. Also, some of the difficulties in detecting PPGs from the patient's abdomen could be due to the patients' body habitus as the amount of adipose tissue in the abdomen reduces the penetration of red and green wavelengths. Also, as the primary blood supply to the abdominal wall is from the deep vasculature it is more difficult to detected the pulsatile arterial flow in these vessels.

9.2 Intra-operative protocol and *in vivo* assessment in DIEP flaps

As commented above, in order to avoid delaying the surgical procedure, intra-operative measurements were carried out in six out of the fifteen patients recruited. The reconstructive surgery commenced once the patient was fully prepped. Patients underwent immediate breast reconstructive procedure where the surgeons perform full mastectomy on the affected breast and the mastectomy specimen was recorded for weight in order to use the correct weight of flap for reconstructing the breast. Following this procedure, appropriate recipient vessels were identified in the chest and prepared where the vein and artery were dissected free for several centimetres and clamped, ready for anastomosis. Subsequently another team of surgeons dissected a large segment of skin and the subcutaneous adipose tissue from the abdomen; this was done by elevating the tissue from lateral to medial and identifying the perforator vessels. Once the appropriate perforators were chosen the vessels were then dissected to ensure they are of sufficient length and quality. These vessels were then clamped and cut from the donor site. The skin, adipose tissue and the dissected deep inferior epigastric blood vessels were then cut to the appropriate size and weight to form the flap prior to its transfer to the chest. The surgeon then used temporary sutures to hold the flap in place in the chest whilst the flap vessels and the vessels in the recipient site were joined using anastomosis while avoiding any twists or kinks in the vessels.

The anastomosis was performed by joining the arterial and venous blood vessels of the flap to the arterial and venous blood vessel in the axilla or to those behind the breastbone. To capture the reperfusion of the flap (in very few cases) the PPG sensor was secured on the flap. Prior to contact to the patient the PPG sensor was placed inside a sterile transparent adhesive film dressing (3M^{TM} Tegaderm^{TM} Film) and then taped on the free flap exposed skin. The multicore cable which connects the sensor to the processing system was also covered using a sterile camera sheath (EASI-DRAPE, Leonhard Land^{LTD}).

Once the sensor was secured in place using intra-operative sterile tape (OP-Tape, Winner Medical Group Inc) the PPG processing system was switched on and signal acquisition commenced using the LabVIEW program on the laptop. An initial recording of 2 to 5 minutes was made in order to establish a baseline or detect any signals from surrounding vessels to distinguish any interference with the PPG signal from the flap. With the flap loosely secured in place the surgeon then removed the venous clamps followed by the arterial clamps and confirmed the flow of blood through the vessels.

The signal acquisition continued for a further 5 to 10 minutes to enable the detection of any changes in the signal during the reperfusion of the flap, i.e. change in amplitude or morphology of the signal. The length of the recording depended on the time taken for the surgical team to prepare, contour and secure the flap to the chest wall, ensuring no interference was caused to the surgical procedure; also simultaneously the abdomen was closed by another surgical team. Once satisfied with the signal detected from the flap the signal acquisition was stopped and the signal was stored whilst the required notes were made on the patient log file for future analysis of the signals. The flap wound was then closed with either sutures or surgical glue. At the end of surgery gauze dressing was placed on both the reconstructed breast and the abdomen.

9.2.1 Intra-operative results

Figure 9.2 demonstrates the reperfusion of the flap following the anastomosis of the vessels and the removal of the arterial and venous clamps thus resulting in blood flow through the free flap.

The figure depicts the PPG signals before and after the release of the arterial clamp. As displayed, low amplitude noise can be seen where no PPG was observed in the first segment of the acquired signal. As the clamps were removed at approximately 0:50 seconds, a noticeable rise in amplitude was observed and within the first minute after the clamp removal the photoplethysmographic signals increased in amplitude which suggests successful reperfusion of the flap.

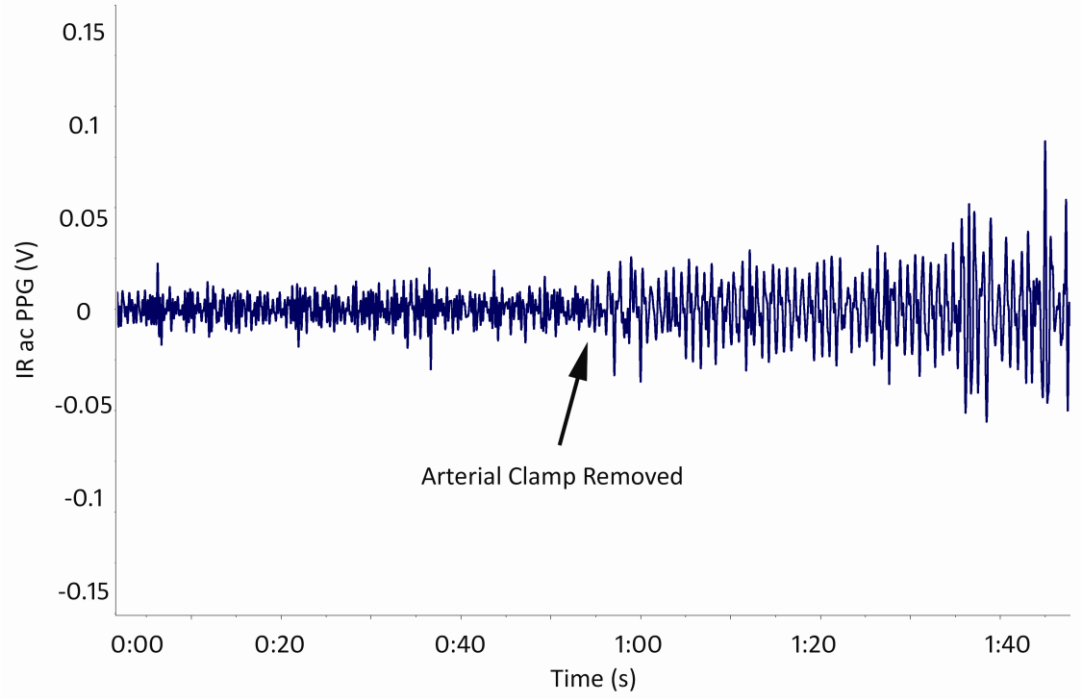

Figure 9.2: Free flap IR ac PPGs after the venous and arterial clamps were removed.

Once the venous and arterial clamps were removed, the recording was continued for a further ten minutes. Figure 9.3 illustrates a 10 second period of red and infrared ac PPGs eight minutes post clamp removal where high amplitude PPG signals are detected. No green PPG signals were detected in the intra-operative period except in one patient. The factors contributing to this could be that there is no capillary flow through the flap as the blood supply has just been established through the main perforators and hence as the green wavelength cannot penetrate deep enough it is incapable of detecting any PPG signals. As seen in the figure the red and infrared signals are significantly smaller in comparison with the pre-operative signal. This is expected as the measurements are from a tissue which has just been anastomosed. These signals are also noisy, and this was due to movement artifact as the signal was

acquired while the surgical team was closing the abdominal wound, causing movement and jittering to the unsecured flap.

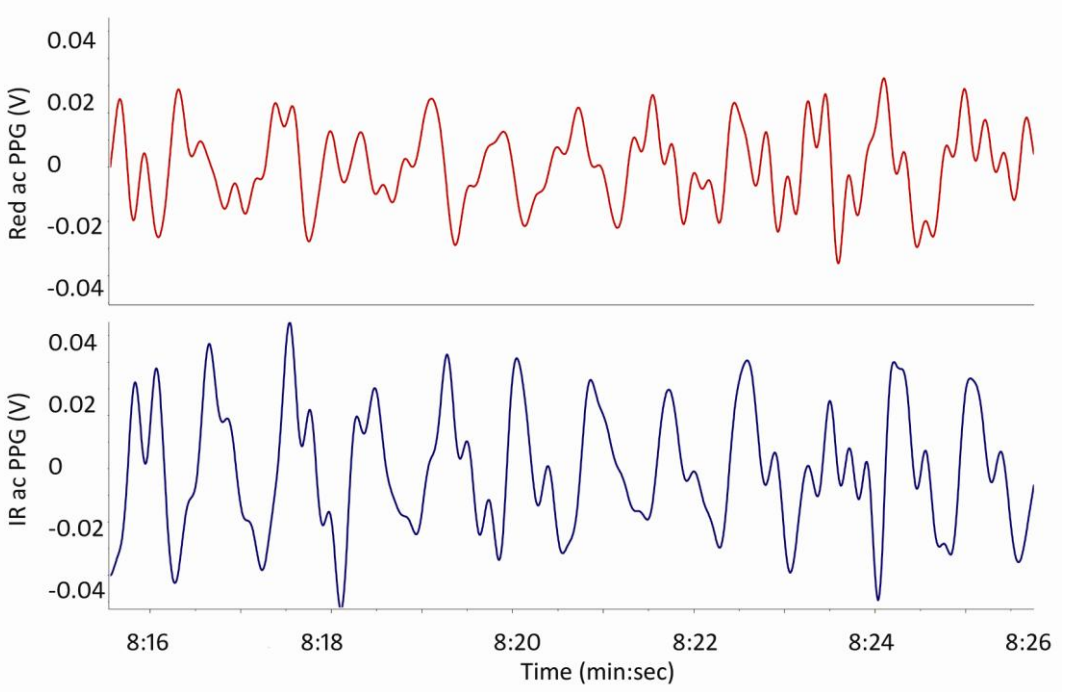

Figure 9.3: DIEP IR ac PPG signals eight minutes post clamp removal.

Table 9.2 shows the mean of all the PPG amplitudes acquired from the red (n=6), green (n=1) and infrared (n=6) wavelengths in the intra-operative period.

Table 9.2: Red, green and infrared ac PPG amplitudes in the intra-operative period

Patient	ac Red (n=6) (mv)	ac Green (n=1) (mv)	ac IR (n=6) (mv)
1	40.0	__	80.9
2	16.5	16.5	15.6
3	148.5	__	163.3
4	64.5	__	210.6
5	20.0	__	43.5
6	22.3	__	25.6
Mean	51.9	__	89.9
±SD	50.6	__	82.0

There is a large variability in PPG amplitudes across all patients resulting in large standard deviation values. This could be due to the free flap thickness being different from patient to patient where it is assumed that flaps with increased adipose tissue produce lower amplitude signals and vice versa. In addition, perforators and their thickness vary between patients, which would result in different volumes of blood flowing through the flap.

These preliminary results suggest that PPGs can be used as an indicator of reperfusion of the flap in the intra-operative period. Following the intra-operative measurement period the patient was then followed to the post-anaesthesia patient recovery room where the bulk of the PPG monitoring took place.

9.3 Post-Operative Protocol and in vivo assessment in DIEP flaps

Fifteen patients were monitored in the post-operative period utilising the newly developed flap PPG sensor. The post-operative measurements commenced in the post-anaesthesia care unit after the patient was extubated and stabilised.

As mentioned in previous chapters, there are many techniques and technologies used to monitor the viability of the free flap post-operatively. These include Doppler ultrasound, temperature monitoring, laser Doppler flowmetry and Near Infrared Spectroscopy (NIRS). Most centres use these techniques alongside clinical observations where a flap chart is followed and completed where parameters such as the flap's colour, temperature, capillary refill time, texture and pin-prick test are recorded. In Mid Essex hospital where the clinical trials were carried out the clinical team routinely use flap chart where the flap is examined at 15 minute intervals for the first 2 hours, 30 minute intervals for the following four hours and hourly for the next 12 hours. Where there was doubt as to the viability of the flap, a Doppler was used by the medical staff to confirm blood flow through the flap where the strength of blood pulsating through the flap was evaluated.

The PPG measurements were obtained at the same intervals as the routine qualitative assessment of the free flap in the post-operative period. This ensured that the PPG

study did not add any extra complication in the procedure and prevented any further disturbance to the patient and also enabled a comparison/correlation of the obtained PPG signals with the qualitative assessment of the free flap. To avoid any wound contamination the free flap PPG sensor was covered with a sterile transparent adhesive film dressing (3M™ Tegaderm™ Film). The PPG sensor was placed away from the area which was marked as having the main perforator supply in the pre-operative period. This was to avoid the PPG sensor being moved by the medical or nursing staff when they use Doppler to assess flow to ensure repeatability of the measurement by keeping the sensor in the same position and orientation relative to the blood vessels being monitored. Initially the PPG sensor was hand held on the exposed skin of the free flap as shown in Figure 9.4 while making a recording. However, this approach caused motion artifacts which resulted in noisy PPG signals.

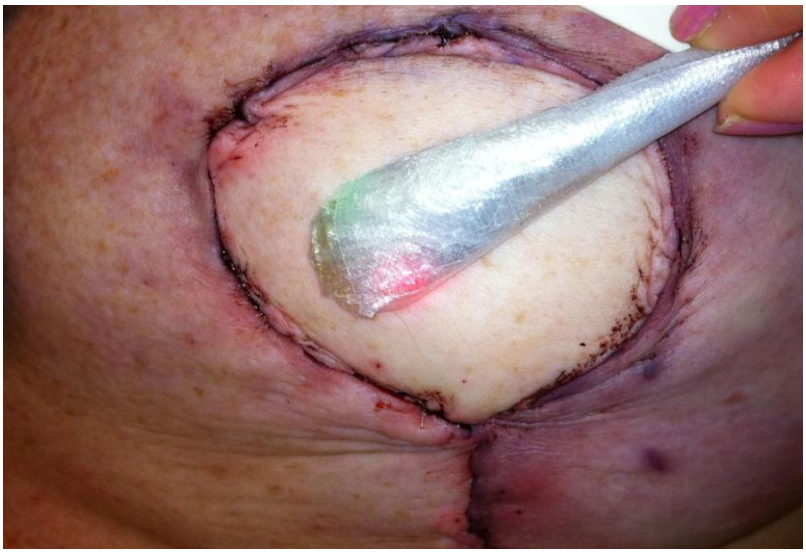

Figure 9.4: PPG sensor hand held on the free flap.

To ensure repeatability of measurements in terms of the position and orientation of the sensor each time a recording was made it was decided to secure the probe on the free flap as shown Figure 9.5. As before the PPG sensor was secured using surgical tape (3M™ Transpore™).

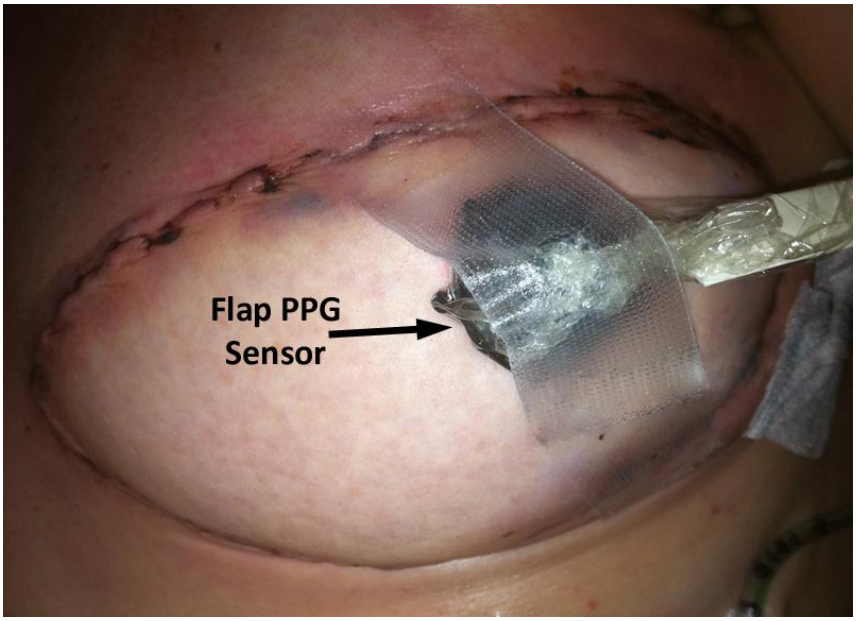

Figure 9.5: Three wavelength reflectance PPG sensor taped on the exposed skin of the DIEP free flap during the post-operative period.

In order to compare the qualitative assessment of free flaps (done with the flap chart) with the recorded PPGs the flap chart results were collected by the researcher as well as other general observations such as blood pressure, temperature, heart rate and SpO_2 levels. Any factors which could affect the quality and amplitude of the signal such as temperature was also recorded on the patient log file for future analysis, i.e. use of patient warmer blanket.

9.3.1 Post-operative results

The initial measurements were obtained in the post-anaesthesia care unit from all recruited patients followed by acquisition of signals at intervals of every 15 minutes in the first two hours, every 30 minutes for the following four hours and hourly for the subsequent 12 hours for up to 11 hours post-operatively. During these intervals PPGs were continuously acquired for 1 minute per interval. The length of stay of each patient in the post-anaesthesia care unit varied depending on the time taken for the critical assessment and stabilisation of the patient. To normalise the data, results are presented as "Recovery" where the first measurement was recorded followed by data recorded at hourly intervals post-operatively. A typical signal acquired one hour post-operatively is illustrated in Figure 9.6 where good quality PPG signals from all three

wavelengths are presented. In this figure it can be observed that the PPG signals from the red and infrared wavelengths are slightly modulated by a spontaneous breathing artifact at 0.32 Hz (19 breaths per minute). In the offline analysis of the PPG signal this artifact was filtered out.

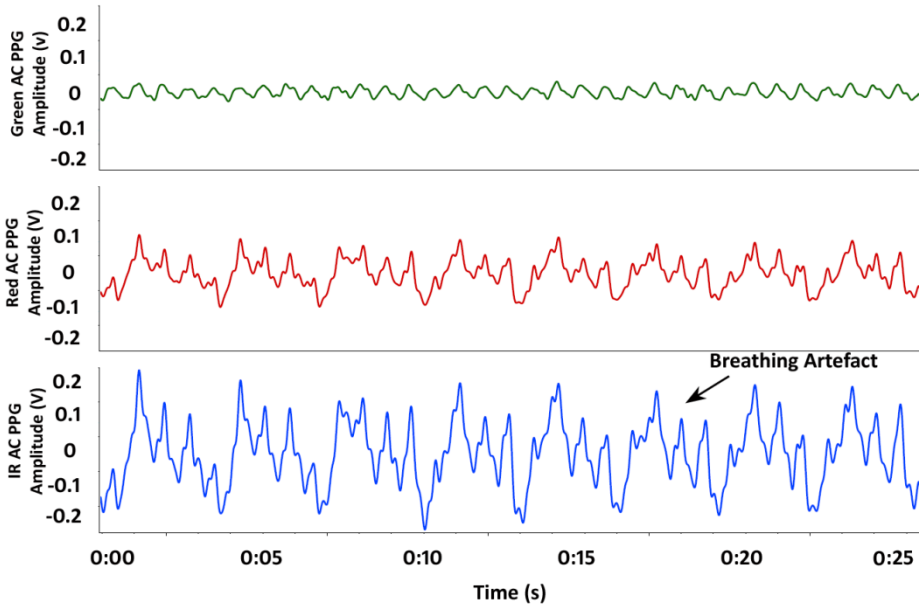

Figure 9.6: PPG signals at one hour post-operatively from all three wavelengths.

Also as demonstrated in the figure, the PPG signal detected from the infrared is larger in amplitude than that of the red and green wavelengths. Interestingly no noticeable breathing induced motion artifact can be seen in the obtained green PPG, and this can be due to its low penetration in tissue. To evaluate the system for its capability in monitoring and detecting any changes in the volume of blood pulsating in the flap, the ac PPG amplitudes were examined. To perform this analysis the detected signals were filtered to remove the respiration artifact. Figure 9.7, Figure 9.8 and Figure 9.9 show 10 second periods of the infrared, red and green PPG signals obtained at all post-operative intervals from one patient. In each patient the heart rate was also calculated (from the PPG signal) offline and compared with the recorded measurement from the commercial pulse oximeter to confirm the capability of the developed system in also measuring heart rate. The calculated heart rate values from our PPG system were compared with the heart rate values recorded from the commercial pulse oximeter as shown in Figure 9.7.

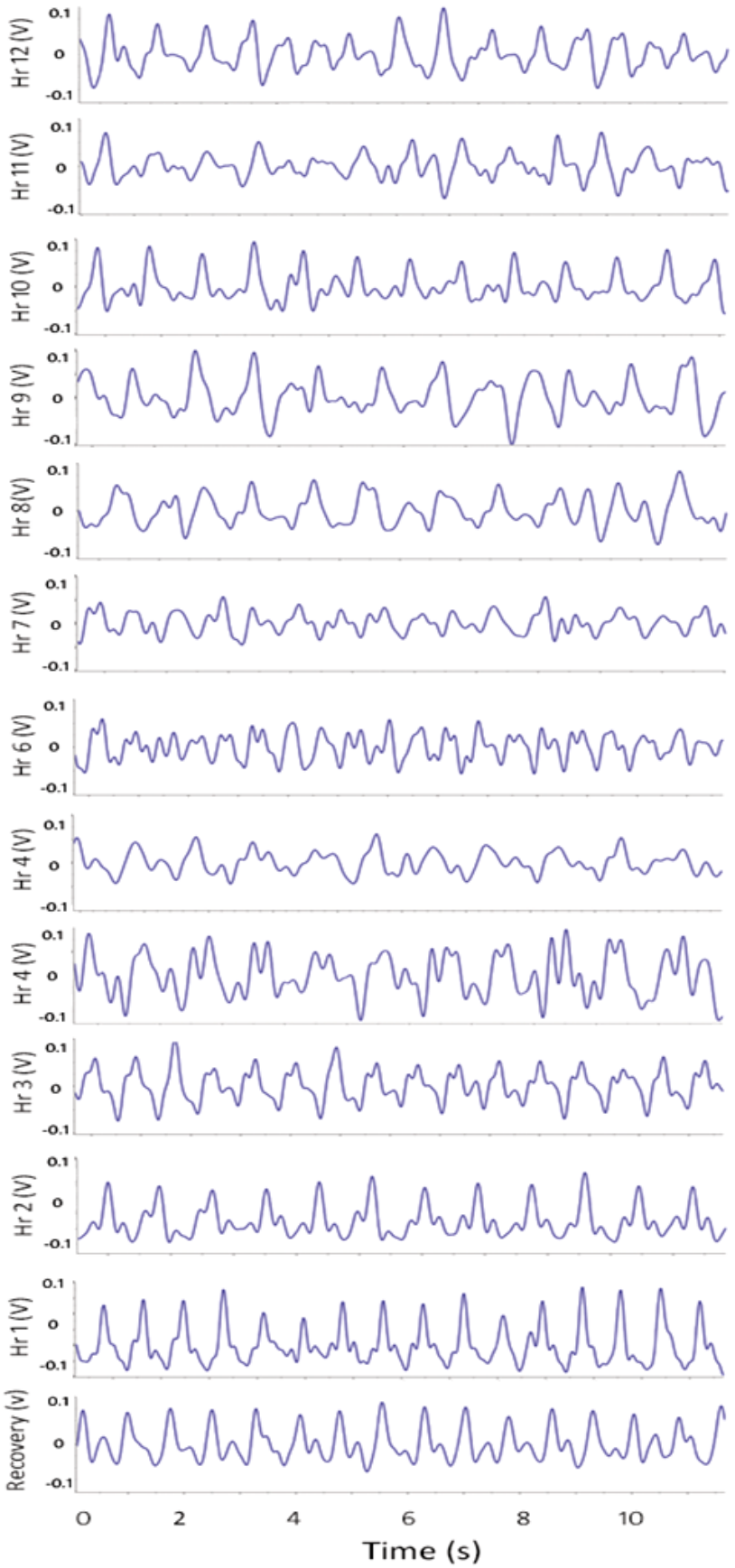

PPG HR	Oximeter HR	Amplitude (mV)
79	80	139.9
67	66	108.2
66	63	149.8
72	71	148
66	65	158.6
82	80	69.1
102	100	84.7
57	57	97.6
60	61	147.3
84	83	230.7
63	62	182.1
84	84	229
81	81	120.4

Figure 9.7: Infrared ac PPGs at all post-operative intervals from one patient with heart rate.

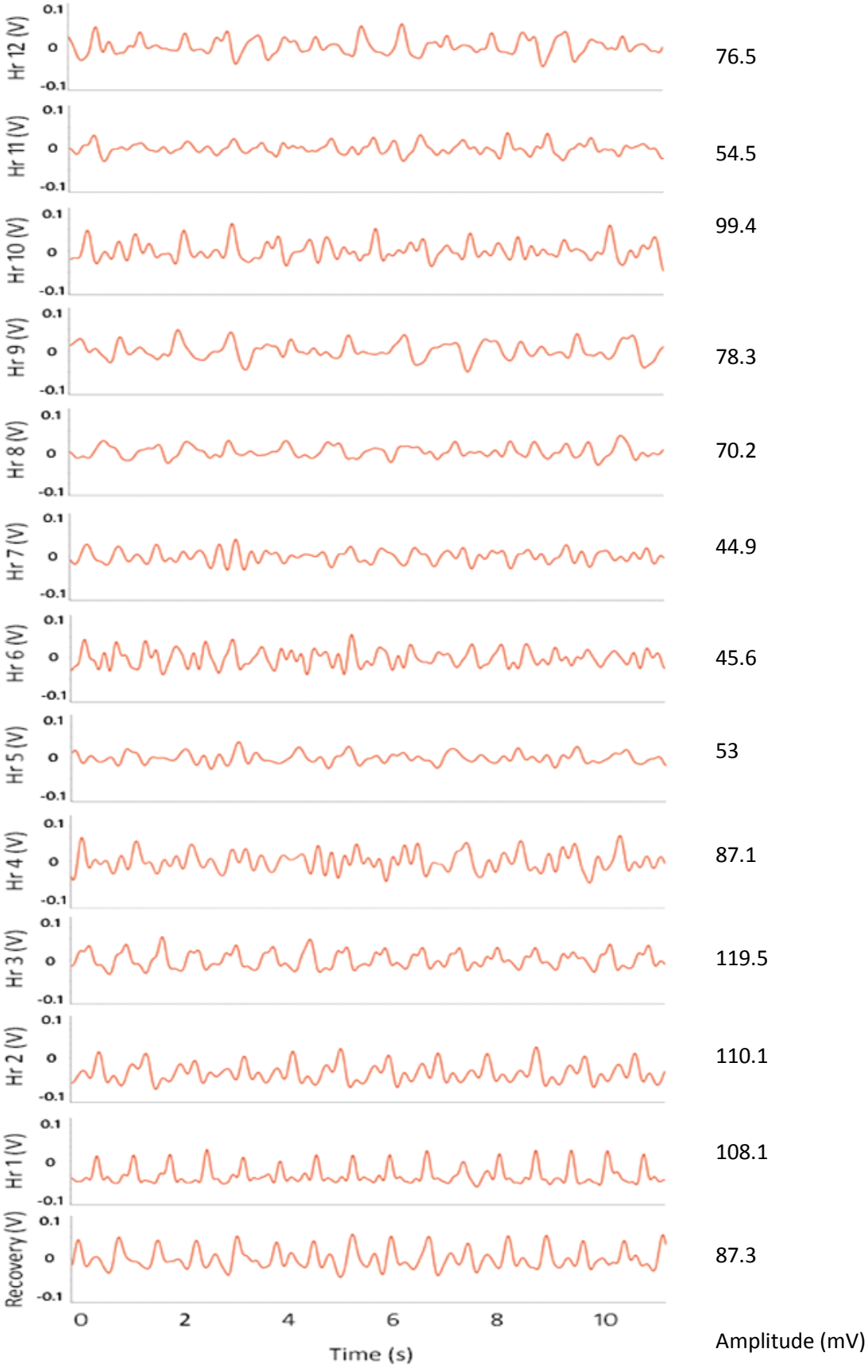

Figure 9.8: Red ac PPG signals from one patient at all post-op interval with amplitude.

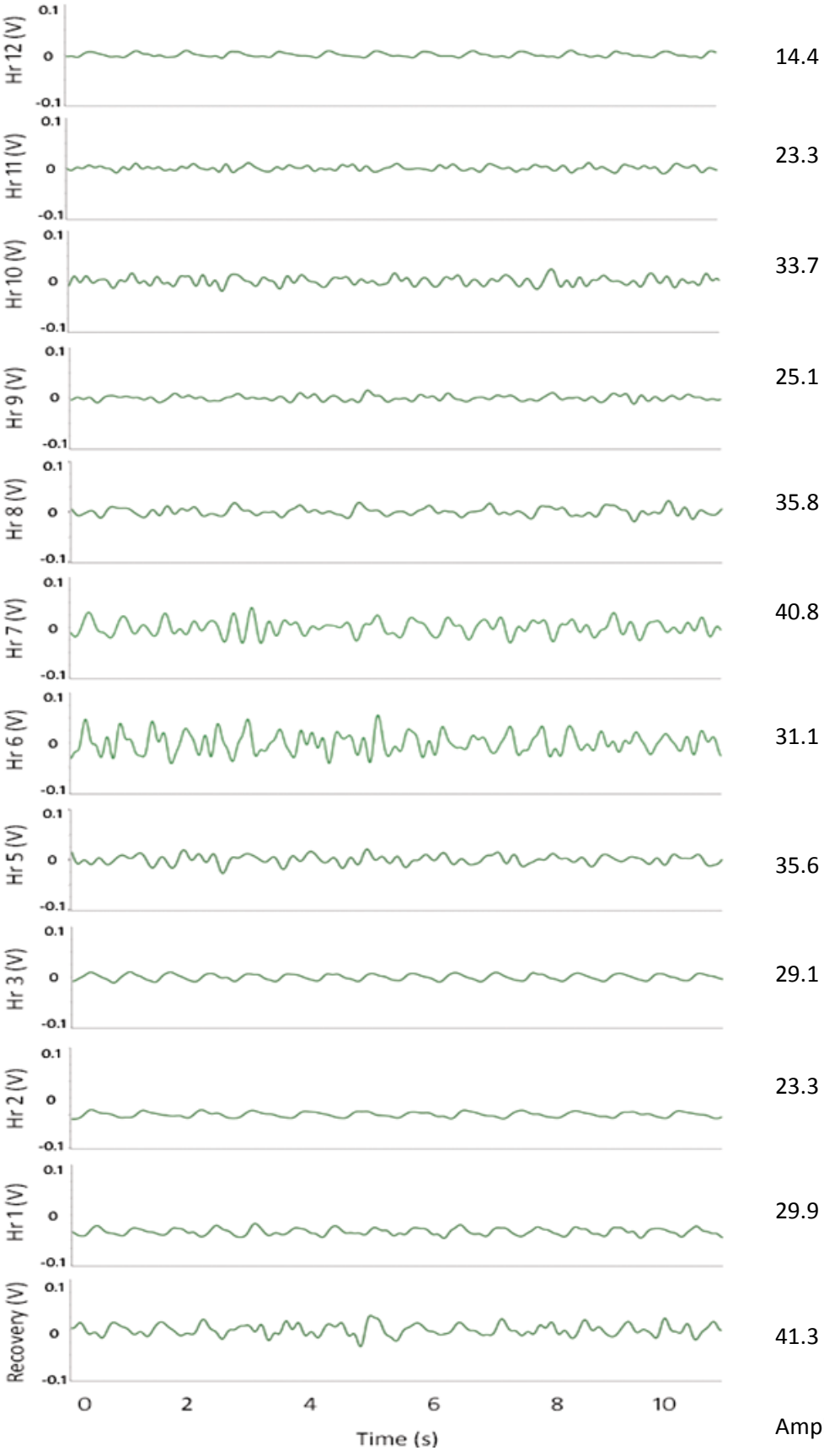

Figure 9.9: Green ac PPGs from one patient at all post-operative interval with amplitude.

From the figures it can be noticed that there is an increase in the PPG amplitude one hour subsequent to transferring the patient to the post anaesthesia recovery room; this could be an indication of improved blood flow to the flap. At approximately 5 hours post-operatively a reduction in the amplitude is seen, the reduction could be due to environmental factors such as temperature since at 8 hours post-operatively the patient warmer blanket was switched on as this resulted in the increase of the PPG amplitude which can be seen in the figure. In the post-operative period some patients speak due to confusion or pain, this and the patients deep breathing will result in motion artifact in the PPG signals during measurement acquisition. These unwanted artifacts to the signal can be seen in Figure 9.8 at 4, 6 and 10 hours post-operatively in the red ac PPG signals. As seen in Figure 9.9 the green PPG signals detected from the flap are lower in amplitude comparing to the red and infrared signals. In both the red and infrared ac signal an increase in the PPG amplitude can be observed once the patient warmer blanket was turned on, resulting in an increase in the temperature of the flap, however this change cannot be seen in the green PPG. There is a continuous reduction in the green PPG amplitude in the post-operative period, although there is a noticeable change to the quality of the signal at approximately the same hour (5 hours post-operatively) that the amplitude of red and infrared PPGs are reduced. Also, at approximately 12 hours post operatively the quality of the signal has improved. No green PPG signal could be obtained at 4 hours post-operatively and a sudden deterioration of the signal quality can be seen. This poor signal quality could be due to vasoconstriction of the blood vessels, particularly the capillaries as the flap gets cold, hence reducing the blood flow to the area.

In order to analyse and investigate how the PPG amplitudes changed during the post-operative period, the mean PPG amplitude at each time interval is calculated from each wavelength. The mean of PPG values from all fifteen patients are presented graphically in Figure 9.10.

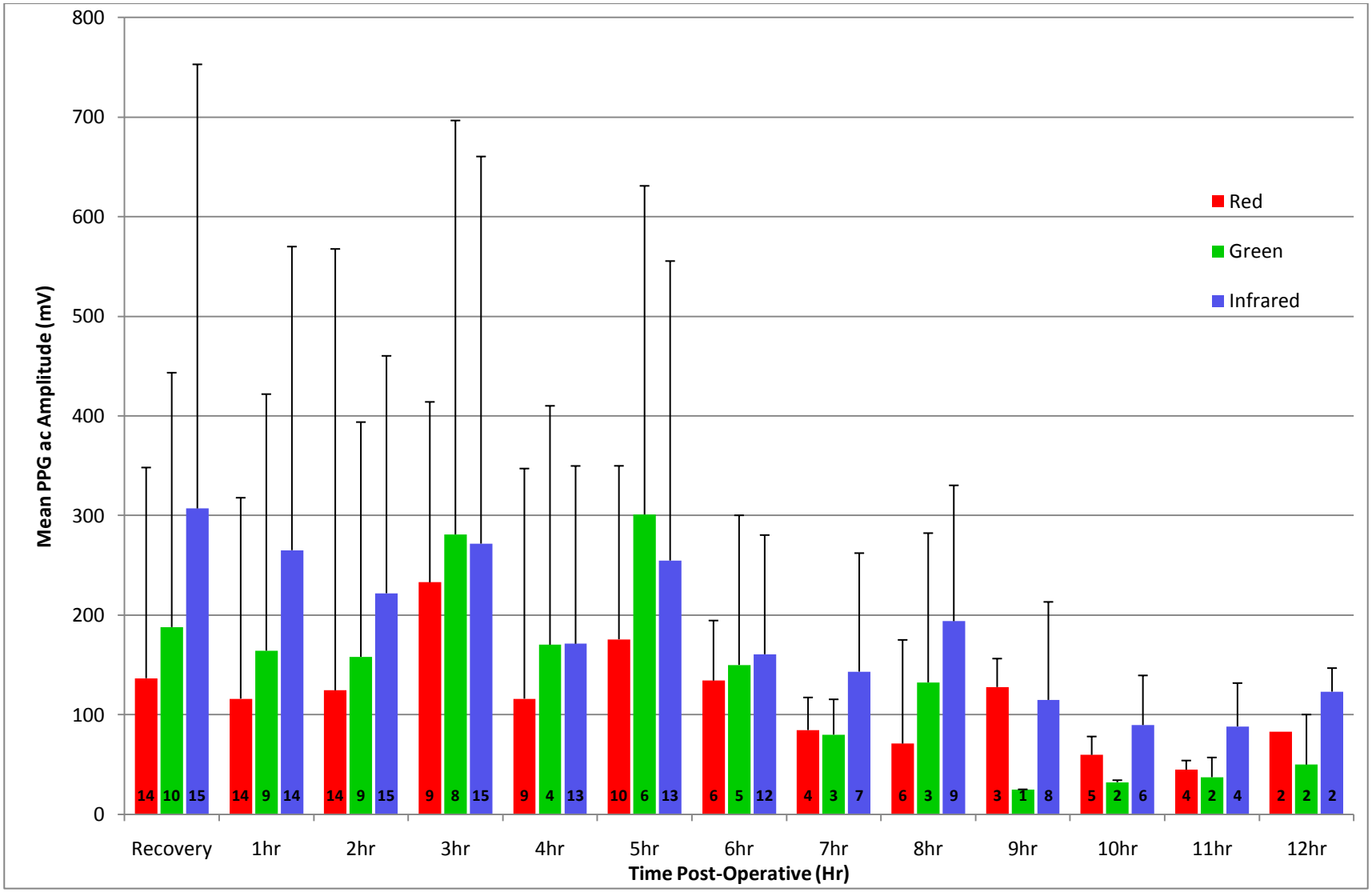

Figure 9.10: The mean amplitude of ac PPGs acquired post-operatively at hourly intervals.

By observing Figure 9.10 , it can be seen that there is a decrease in the mean PPG amplitude after 6 hours in the post-operative period in all three wavelengths. In order to confirm if this reduction in the amplitude is statistically significant the data was analysed using SigmaPlot 12 (CA, USA) and Microsoft Excel.

9.3.2 Statistical analysis on post-operative PPG amplitude

The PPG amplitudes were examined in order to investigate whether there are any statistical significant differences in the mean amplitude of the PPGs at all durations in the post-operative period. By observing Figure 9.10, it can be seen that the mean of the means ac PPG amplitude were larger in amplitude comparing to those seen from 6 hours post-operatively up to 12 hours post operatively. In order to choose the appropriate test the data were checked to ensure they are normally distributed. A data set is said to be normally distributed when the frequency distribution of the values is evenly distributed around the mean in a symmetrical fashion where if the data is plotted as a histogram this will result in a bell curve. The frequency distribution of the mean of the infrared ac PPG amplitudes from all patients was plotted in a histogram as shown in Figure 9.11.

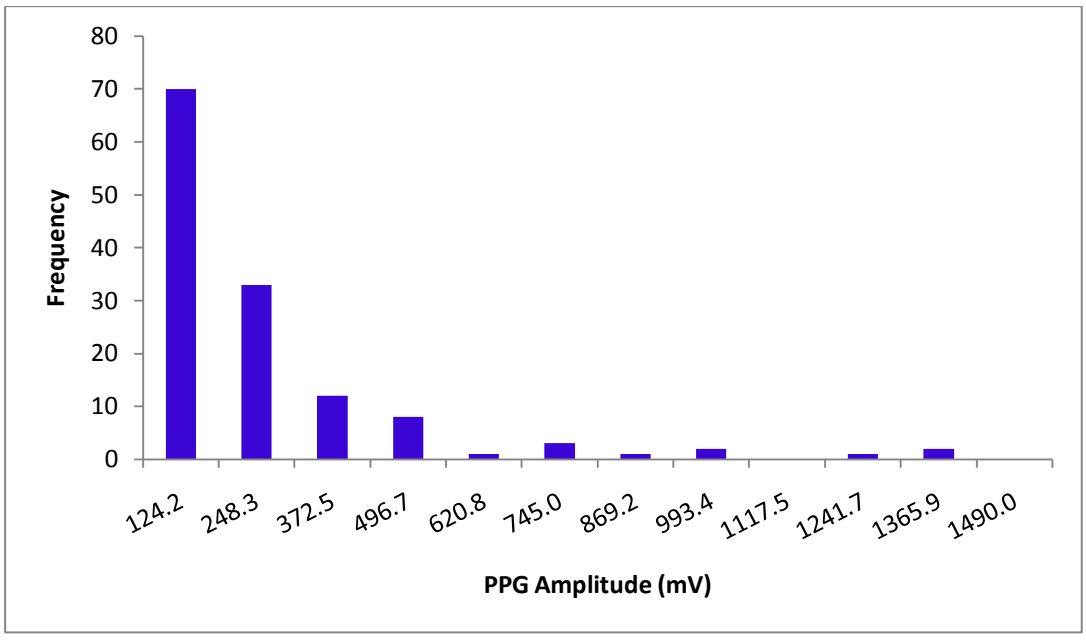

Figure 9.11: Frequency distribution of the infrared ac PPG amplitude.

It is observed from the histogram in Figure 9.11 that the obtained signals are not normally distributed; to confirm this numerically the infrared ac PPG data were tested for normality using the Kolmogorov-Smirnov (K-S) statistical test. The K-S tests the data by comparing the values in the sample to a normally distributed set of samples with the same mean and standard deviation. If the deviation from the normally distributed data set is not significantly different the data is said to be normally distributed. The results from the Kolmogorov-Smirnov test performed on the mean amplitude of infrared ac PPG signals from all patients at each interval are presented in Table 9.3.

The results show that the distribution of the PPG signals recorded at 7, 8, 10, 11, 12 hours post-operatively is not significantly different from a normal distribution, i.e. these data are normally distributed. However, the data from the Recovery period until 6 hours post-operatively as well as the data from 9 hours post-operatively were found to be non-normal as the deviations between the recorded samples and the comparable normal distribution values were too large.

Table 9.3: Results from the Normality Test performed on the amplitude of infrared ac PPG signals at each monitoring interval.

Post-operative period	K-S Distance	P Value	Normality Test Result
Recovery:	K-S Dist. = 0.330	P < 0.001	Failed
Hr 1 post-op:	K-S Dist. = 0.245	P = 0.016	Failed
Hr 2 post-op:	K-S Dist. = 0.277	P = 0.003	Failed
Hr 3 post-op:	K-S Dist. = 0.320	P < 0.001	Failed
Hr 4 post-op:	K-S Dist. = 0.275	P = 0.008	Failed
Hr 5 post-op:	K-S Dist. = 0.283	P = 0.005	Failed
Hr 6 post-op:	K-S Dist. = 0.262	P = 0.022	Failed
Hr 7 post-op:	K-S Dist. = 0.168	P > 0.200	Passed
Hr 8 post-op:	K-S Dist. = 0.180	P > 0.200	Passed
Hr 9 post-op:	K-S Dist. = 0.335	P = 0.009	Failed
Hr 10 post-op:	K-S Dist. = 0.266	P > 0.200	Passed
Hr 11 post-op:	K-S Dist. = 0.176	P > 0.200	Passed
Hr 12 post-op:	K-S Dist. = 0.260	P > 0.200	Passed

The p value for the normality test determines the probability of being incorrect in assuming that the data is not normally distributed. If the chosen p value is set to 0.01 then data with greater deviations from normality will still be considered as normality distributed, therefore it was decided for this study to set the p value to 0.05. If the computed p value is greater than 0.05 the test passes, whereas if it is smaller, the value is shown in the table and the test fails concluding the data is not normally distributed.

The quantile-quantile (Q-Q) plot is also useful in graphically interpreting and determining the deviation of the data points from the normally distributed data set. As seen in Figure 9.12 in the 4th hour of the post-operative period the recorded data deviate greatly from the line which represents the data not being normally distributed, however 7 hours post-operatively the data points do not significantly deviate from the line resulting in the data set being normally distributed. This is consistent with the higher significance value of the 4th hour on the K-S distance.

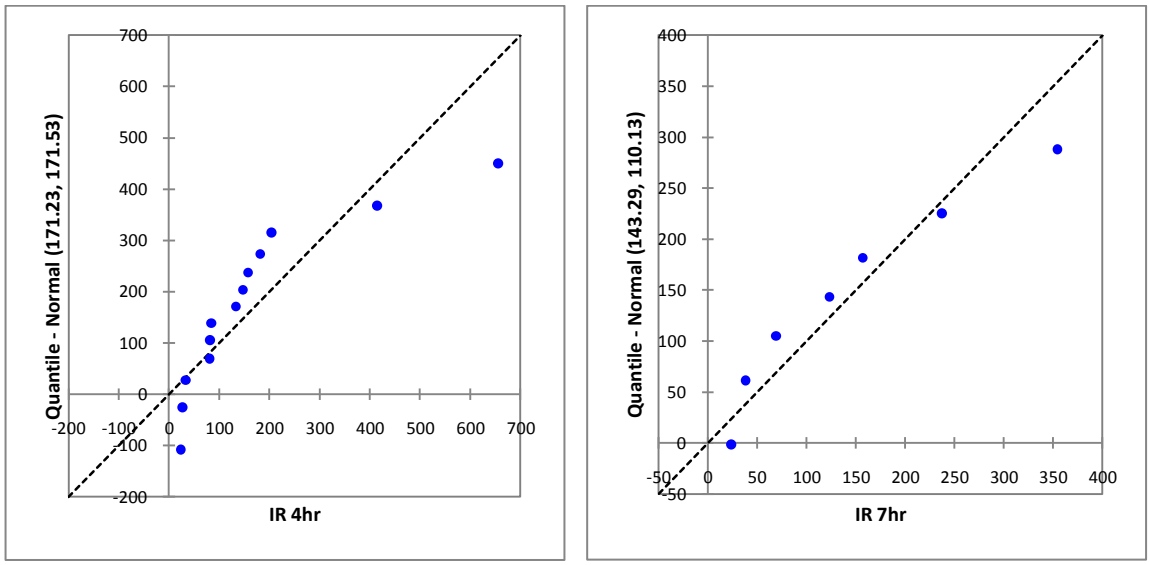

Figure 9.12: Q-Q plot of the data at 4 and 7 hours post-operatively.

As shown in Table 9.4

Table 9.5 this process was repeated for both red and green ac PPG amplitudes recorded at the hourly intervals following the transfer of the patient to the recovery

room for up to 12 hours post-operatively. The computed K-S distance and the p value are also presented in the table as well as if the data pass the normality test.

Table 9.4: Results from normality test performed on mean of red ac PPG amplitudes from all patients at all post-operative intervals.

Post-operative period	K-S Distance	P Value	Normality Test Result
Recovery:	K-S Dist. = 0.333	P < 0.001	Failed
Hr 1 post-op:	K-S Dist. = 0.398	P < 0.001	Failed
Hr 2 post-op:	K-S Dist. = 0.283	P = 0.003	Failed
Hr 3 post-op:	K-S Dist. = 0.342	P = 0.002	Failed
Hr 4 post-op:	K-S Dist. = 0.374	P < 0.001	Failed
Hr 5 post-op:	K-S Dist. = 0.400	P < 0.001	Failed
Hr 6 post-op:	K-S Dist. = 0.394	P = 0.004	Failed
Hr 7 post-op:	K-S Dist. = 0.344	P = 0.102	Passed
Hr 8 post-op:	K-S Dist. = 0.228	P > 0.200	Passed
Hr 9 post-op:	K-S Dist. = 0.349	P = 0.163	Passed
Hr 10 post-op:	K-S Dist. = 0.229	P > 0.200	Passed
Hr 11 post-op:	K-S Dist. = 0.421	P = 0.013	Failed
Hr 12 post-op:	K-S Dist. = 0.260	P > 0.200	Passed

Table 9.5: Results from normality test performed on mean of green ac PPG amplitudes from all patients at all post-operative intervals.

Post-operative period	K-S Distance	P Value	Normality Test Result
Recovery:	K-S Dist. = 0.336	P = 0.002	Failed
Hr 1 post-op:	K-S Dist. = 0.358	P = 0.001	Failed
Hr 2 post-op:	K-S Dist. = 0.343	P = 0.003	Failed
Hr 3 post-op:	K-S Dist. = 0.350	P = 0.004	Failed
Hr 4 post-op:	K-S Dist. = 0.402	P = 0.008	Failed
Hr 5 post-op:	K-S Dist. = 0.385	P = 0.006	Failed
Hr 6 post-op:	K-S Dist. = 0.324	P = 0.094	Passed
Hr 7 post-op:	K-S Dist. = 0.273	P > 0.200	Passed
Hr 8 post-op:	K-S Dist. = 0.360	P = 0.137	Passed
Hr 9 post-op:	K-S Dist. = 0.000	P < 0.001	Failed
Hr 10 post-op:	K-S Dist. = 0.260	P > 0.200	Passed
Hr 11 post-op:	K-S Dist. = 0.260	P > 0.200	Passed
Hr 12 post-op:	K-S Dist. = 0.260	P > 0.200	Passed

Table 9.4 shows the results from the normality test (Kolmogorov-Smirnov) performed on the mean amplitude of red ac PPG amplitudes from all fifteen patients at all post-operative hours. The data from 7, 8, 9, 10 and 12 hours post-op were found to be normally distributed. Results in

Table 9.5 show that the green PPG signals recorded in the 6, 7, 8, 10, 11, 12 hours post-operatively have passed the normality test which is an indication that the PPG data match the expected pattern if the data was from a sample with a normal distribution, therefore it is assumed that the data collected at these hours are normally distributed.

Typically if a data set is normally distributed a parametric test such as a *t*-test is performed to investigate if there is a statistically significant different between two data sets. However, if the data is not normally distributed a non-parametric test is used where these tests do not assume if the population is normally distributed. Parametric tests are based on the assumption that the data are normally distributed, although parametric tests are preferred over non-parametric tests as these are more powerful. It must also be noted that with smaller data sets the normality tests are not powerful enough to detect small deviations from the comparable normal distribution data set. Therefore, it was decided to conduct a multiple paired *t*-test on the red, green and infrared PPG amplitudes to evaluate if there is any statistically significant difference in the mean between each two intervals.

A value of $p < 0.05$ was considered as statistically different in each post-operative interval. The results from the paired *t*-tests obtained from the mean PPG amplitudes of all patients at all monitoring intervals on the red, green and infrared ac PPG data are presented in Table 9.6 to 9.8 respectively. Where there was deemed to be a statistically significant difference between two intervals compared, the p value is presented. In cases where there was no statistically significant difference it is noted by NS.

Table 9.6 show that for red ac PPG signals there is a statistically significant difference between 8 hours post-operatively with 6 and 7 hours as well as between 9 and 10 hours in the post-operative periods. Given that the 7, 8, 9 and 10 hours were

considered normally distributed, we can accept that there is a statistically significant difference obtained from red ac PPG data between 7 and 8 hours and 9 and 10 hours in the post-operative period. However, there was found to be no significant difference between the other intervals which is as expected since the *t*-test assumes the data compared are normally distributed.

From the results in Table 9.7 it can be seen that there are no significant differences between any intervals except 5 and 12 hours post-operatively. This could be due to the small sample number as it is more difficult to detect any statistically significant difference in limited populations. Results of the paired *t*-test are shown in Table 9.8 where the ac PPG signals at each interval are compared for statistically significant difference. It is observed that there is a significant difference between 9 hours with 6 and 8 hours post-operatively, 8 and 10 hour intervals and 11 and 12 hours post-operatively where the p values are presented in the table. As with the red ac PPG there was found to be no significant difference between intervals which are not normally distributed.

These results confirm the reduction in PPG amplitude in Figure 9.10, where the *t*-test results suggest that there is a statistically significant difference between the time intervals after 7 hours post-operatively. Also, as the standard deviation of the signals are high and the amplitudes of the signals vary between patients significantly which could also result in finding no statistical difference at each interval.

Table 9.6: Results of paired *t*-test comparison on red ac PPG signals from all intervals.

	Recovery	1 hr	2 hr	3 hr	4 hr	5 hr	6 Hr	7 hr	8 hr	9 hr	10 hr	11 hr	12 hr
Recovery	-	NS	NS	NS	NS	NS	NS	NS	NS	NS	NS	NS	NS
1hr	NS	-	NS	NS	NS	NS	NS	NS	NS	NS	NS	NS	NS
2hr	NS	NS	-	NS	NS	NS	NS	NS	NS	NS	NS	NS	NS
3hr	NS	NS	NS	-	NS	NS	NS	NS	NS	NS	NS	NS	NS
4hr	NS	NS	NS	NS	-	NS	NS	NS	NS	NS	NS	NS	NS
5hr	NS	NS	NS	NS	NS	-	NS	NS	NS	NS	NS	NS	NS
6hr	NS	NS	NS	NS	NS	NS	-	NS	P= 0.047	NS	NS	NS	NS
7hr	NS	NS	NS	NS	NS	NS	NS	-	P= 0.040	NS	NS		
8hr	NS	NS	NS	NS	NS	NS	P=0.047	P= 0.040	-	NS	NS	NS	NS
9hr	NS	NS	NS	NS	NS	NS	NS	NS	NS	-	P=0.002	NS	
10hr	NS	NS	NS	NS	NS	NS	NS	NS	NS	P= 0.002	-	NS	NS
11hr	NS	NS	NS	NS	NS	NS	NS		NS	NS	NS	-	NS
12hr	NS	NS	NS	NS	NS	NS	NS		NS		NS	NS	-

Table 9.7: Results of paired *t*-test comparisons on green ac PPG signals at all intervals.

	Recovery	1hr	2hr	3hr	4hr	5hr	6hr	7hr	8hr	10hr	11hr	12hr
Recovery	-	NS	NS	NS	NS	NS	NS	NS	NS	NS	NS	NS
1hr	NS	-	NS	NS	NS	NS	NS	NS	NS			
2hr	NS	NS	-	NS	NS	NS	NS	NS	NS			
3hr	NS	NS	NS	-	NS	NS	NS	NS	NS			
4hr	NS	NS	NS	NS	-	NS	NS	NS				
5hr	NS	NS	NS	NS	NS	-	NS	NS	NS	NS	NS	P=0.004
6hr	NS	NS	NS	NS	NS	NS	-	NS		NS	NS	NS
7hr	NS	NS	NS	NS	NS	NS	NS	-	NS			
8hr	NS	NS	NS	NS		NS		NS	-			
10hr	NS					NS	NS			-	NS	NS
11hr	NS					NS	NS			NS	-	NS
12hr	NS					P=0.004	NS			NS	NS	-

Table 9.8: Results of paired *t*-test comparisons on infrared ac PPG signals at all intervals.

	Recovery	1hr	2hr	3hr	4hr	5hr	6hr	7hr	8hr	9hr	10hr	11hr	12hr
Recovery	-	NS	NS	NS	NS	NS	NS	NS	NS	NS	NS	NS	NS
1hr	NS	-	NS	NS	NS	NS	NS	NS	NS	NS	NS	NS	NS
2hr	NS	NS	-	NS	NS	NS	NS	NS	NS	NS	NS	NS	NS
3hr	NS	NS	NS	-	NS	NS	NS	NS	NS	NS	NS	NS	NS
4hr	NS	NS	NS	NS	-	NS	NS	NS	NS	NS	NS	NS	NS
5hr	NS	NS	NS	NS	NS	-	NS	NS	NS	NS	NS	NS	NS
6hr	NS	NS	NS	NS	NS	NS	-	NS	NS	P=0.045	NS	NS	NS
7hr	NS	NS	NS	NS	NS	NS	NS	-	NS	NS	NS	NS	
8hr	NS	NS	NS	NS	NS	NS	NS	NS	-	P=0.028	P=0.034	NS	NS
9hr	NS	NS	NS	NS	NS	NS	P=0.045	NS	P=0.028	-	P=0.218	NS	NS
10hr	NS	NS	NS	NS	NS	NS	NS	NS	P=0.034	NS	-	NS	NS
11hr	NS	NS	NS	NS	NS	NS	NS	NS	NS	NS	NS	-	P=0.001
12hr	NS	NS	NS	NS	NS	NS	NS		NS	NS	NS	P=0.001	-

9.4 Photoplethysmographic signals from finger and flap

In a small group of patients (five of the fifteen recruited patients) the flap PPGs from the post-operative period were compared with the finger PPGs using the identical custom made finger probe as described in earlier chapters. During this comparative study the finger PPG sensor was secured on the patient's index finger.

Simultaneous PPG monitoring of the flap and finger were performed in the post-operative period beginning in the recovery room for up to 11 hours post-surgery. Typical red, infrared and green ac PPG signals obtained at one hour post-operatively are shown in Figure 9.13. The ac PPG signals from the three wavelengths detected from the patients' finger are shown on the top of the graph followed by the ac PPG signals from green, red and infrared presented at the bottom of the graph. The PPG signals from the finger are approximately more than double the amplitude of the PPG signals from the flap and this was due to the good blood supply and perfusion in the finger compared to the flap.

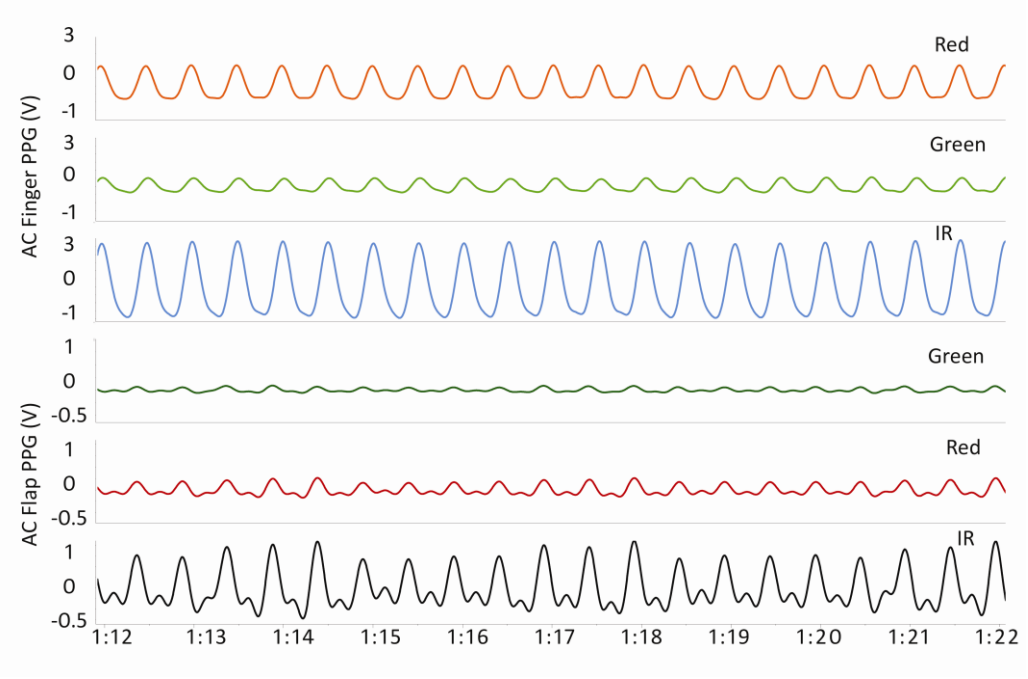

Figure 9.13: Typical ac photoplethysmographic signals obtained one hour post surgery from all three wavelengths from finger (top graph) and flap (bottom graph).

The mean of the means (±SD) of the ac PPG amplitudes (finger and flap) from all patients at each interval are presented for each wavelength of red, green and infrared

in Figure 9.14,Figure 9.15 and Figure 9.16 respectively. Initial observations show that there is a large difference in the amplitude of the PPG signals obtained from the custom made finger and flap sensors in the red, green and infrared histograms. The main reason for such difference is the level of perfusion of the two different sites (finger and free flap).

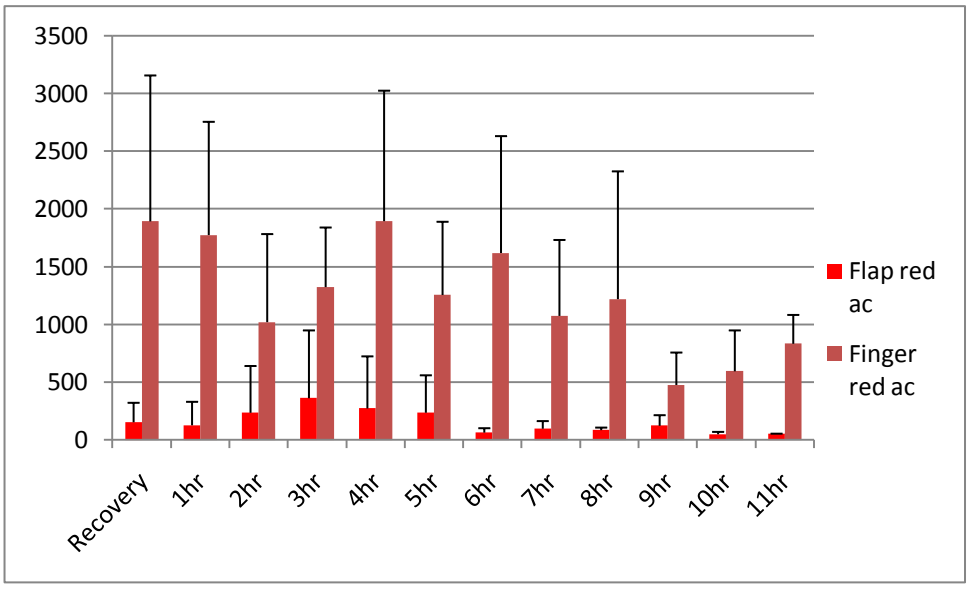

Figure 9.14: Mean of the means (±SD) of red ac PPG amplitudes from the custom made flap and finger sensors from 5 patients at 12 one hour intervals in the post-operative period.

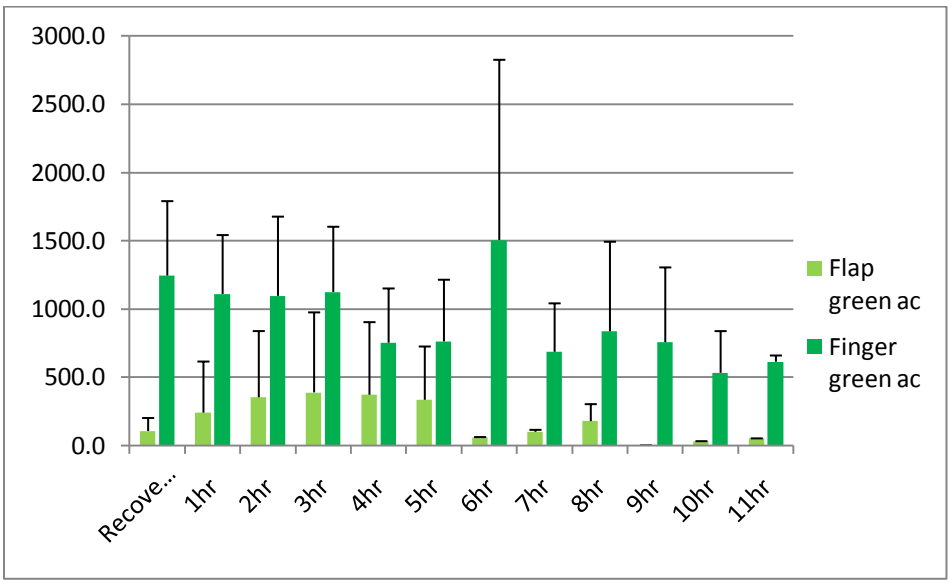

Figure 9.15: Mean of the means (±SD) of green ac PPG amplitudes from the custom made flap and finger sensors from 5 patients at 12 one hour intervals in the post-operative period.

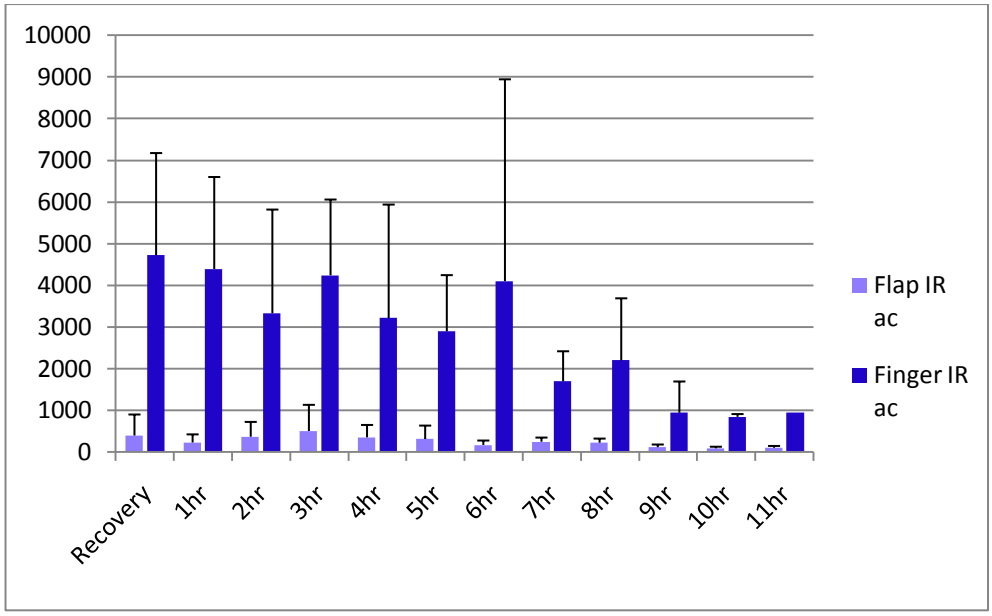

Figure 9.16: Mean of the means (±SD) of infrared ac PPG amplitudes from the custom made flap and finger sensors from 5 patients at 12 one hour intervals in the post-operative period.

To determine if the difference between the finger and flap ac PPGs are considered to be statistically significantly different the required statistical tests were performed.

9.4.1 Statistical analysis on finger and flap PPG

Before commencing the statistical analysis of the data, the signals were initially tested for normality using the Kolmogorov-Smirnov normality test on SigmaPlot. The results of the K-S test used on mean of means of infrared flap and finger ac PPG amplitudes from all patients are shown in Table 9.9. It was found that the data from the finger PPG are normally distributed at all intervals except at 9, 10 and 11 hours post-operatively. The normality test performed on the free flap PPG on the five patients also show that at intervals of 3, 6, 9 and 10 hours the signals detected from the flap vary significantly from a comparable normally distributed data set resulting in failing the normality test.

The normality test was repeated on the green and red ac PPG signals from the finger and flap to investigate if the data collected are normally distributed as shown in Table 9.9, 9.10 and 9.11.

Table 9.9: Results of the Kolmogorov-Smirnov normality test on ac PPG signals at infrared obtained from both finger and flap from all patients at each interval.

	Results of normality test on flap PPG			Results of normality test on finger PPG		
Post-operative period	**K-S Distance**	**P Value**	**Normality Test Result**	**K-S Distance**	**P Value**	**Normality Test Result**
Recovery:	K-S Dist. = 0.271	P>0.200	Passed	K-S Dist. = 0.350	P= 0.099	Passed
Hr 1 post-op:	K-S Dist. = 0.214	P>0.200	Passed	K-S Dist. = 0.289	P> 0.200	Passed
Hr 2 post-op:	K-S Dist. = 0.342	P=0.057	Passed	K-S Dist. = 0.268	P> 0.200	Passed
Hr 3 post-op:	K-S Dist. = 0.383	P=0.016	Failed	K-S Dist. = 0.228	P> 0.200	Passed
Hr 4 post-op:	K-S Dist. = 0.292	P=0.174	Passed	K-S Dist. = 0.265	P> 0.200	Passed
Hr 5 post-op:	K-S Dist. = 0.314	P=0.111	Passed	K-S Dist. = 0.370	P= 0.118	Passed
Hr 6 post-op:	K-S Dist. = 0.387	P=.014	Failed	K-S Dist. = 0.380	P= 0.097	Passed
Hr 7 post-op:	K-S Dist. = 0.216	P>.200	Passed	K-S Dist. = 0.371	P= 0.114	Passed
Hr 8 post-op:	K-S Dist. = 0.294	P=0.169	Passed	K-S Dist. = 0.341	P= 0.109	Passed
Hr 9 post-op:	K-S Dist. = 0.347	P=0.049	Failed	K-S Dist. = 0.387	P= 0.037	Failed
Hr 10 post-op:	K-S Dist. = 0.407	P=0.020	Failed	K-S Dist. = 0.407	P=0.020	Failed
Hr 11 post-op:	K-S Dist. = 0.260	P>0.200	Passed	K-S Dist. = 0.000	P< 0.001	Failed

Table 9.10: Results of the Kolmogorov-Smirnov normality test on ac PPG signals at green obtained from both finger and flap from all patients at each interval.

	Results of normality test on flap PPG			Results of normality test on finger PPG		
Post-operative period	**K-S Distance**	**P Value**	**Normality Test Result**	**K-S Distance**	**P Value**	**Normality Test Result**
Recovery:	K-S Dist. = 0.326	P=0.088	Passed	K-S Dist. = 0.178	P>0.200	Passed
Hr 1 post-op:	K-S Dist. = 0.425	P=0.011	Failed	K-S Dist. = 0.243	P>0.200	Passed
Hr 2 post-op:	K-S Dist. = 0.372	P=0.113	Passed	K-S Dist. = 0.258	P>0.200	Passed
Hr 3 post-op:	K-S Dist. = 0.392	P=0.031	Failed	K-S Dist. = 0.348	P=0.166	Passed
Hr 4 post-op:	K-S Dist. = 0.379	P=0.100	Passed	K-S Dist. = 0.319	P>0.200	Passed
Hr 5 post-op:	K-S Dist. = 0.383	P=0.092	Passed	K-S Dist. = 0.183	P>0.200	Passed
Hr 6 post-op:	K-S Dist. = 0.260	P>0.200	Passed	K-S Dist. = 0.234	P>0.200	Passed
Hr 7 post-op:	K-S Dist. = 0.260	P>0.200	Passed	K-S Dist. = 0.260	P>0.200	Passed
Hr 8 post-op:	K-S Dist. = 0.186	P>0.200	Passed	K-S Dist. = 0.344	P=0.054	Passed
Hr 9 post-op:	K-S Dist. = 0.000	P<0.001	Failed	K-S Dist. = 0.266	P>0.200	Passed
Hr 10 post-op:	K-S Dist. = 0.000	P<0.001	Failed	K-S Dist. = 0.260	P>0.200	Passed
Hr 11 post-op:	K-S Dist. = 0.000	P<0.001	Failed	K-S Dist. = 0.260	P>0.200	Passed

As seen in Table 9.10 the green finger PPG signals were found to be normally distributed at all intervals, subsequently for Table 9.11 it can be seen that the red finger PPG signals were found to be normally distributed at all intervals except at 8 and 9 hours in the post- surgery period.

Table 9.11: Results of the Kolmogorov-Smirnov normality test on ac PPG signals at red obtained from both finger and flap from all patients at each interval.

	Results of normality test on flap PPG			Results of normality test on finger PPG		
Post-operative period	**K-S Distance**	**P Value**	**Normality Test Result**	**K-S Distance**	**P Value**	**Normality Test Result**
Recovery:	K-S Dist. = 0.344	P=0.053	Passed	K-S Dist. = 0.205	P>0.200	Passed
Hr 1 post-op:	K-S Dist. = 0.439	P=0.002	Failed	K-S Dist. = 0.287	P=0.191	Passed
Hr 2 post-op:	K-S Dist. = 0.462	P<0.001	Failed	K-S Dist. = 0.294	P=0.167	Passed
Hr 3 post-op:	K-S Dist. = 0.383	P=0.016	Failed	K-S Dist. = 0.372	P=0.056	Passed
Hr 4 post-op:	K-S Dist. = 0.441	P=0.002	Failed	K-S Dist. = 0.239	P>0.200	Passed
Hr 5 post-op:	K-S Dist. = 0.400	P=0.009	Failed	K-S Dist. = 0.278	P>0.200	Passed
Hr 6 post-op:	K-S Dist. = 0.318	P>0.200	Passed	K-S Dist. = 0.228	P>0.200	Passed
Hr 7 post-op:	K-S Dist. = 0.328	P>0.200	Passed	K-S Dist. = 0.373	P=0.111	Passed
Hr 8 post-op:	K-S Dist. = 0.217	P>0.200	Passed	K-S Dist. = 0.428	P=0.003	Failed
Hr 9 post-op:	K-S Dist. = 0.260	P>0.200	Passed	K-S Dist. = 0.381	P=0.017	Failed
Hr 10 post-op:	K-S Dist. = 0.263	P>0.200	Passed	K-S Dist. = 0.267	P>0.200	Passed
Hr 11 post-op:	K-S Dist. = 0.260	P>0.200	Passed	K-S Dist. = 0.260	P>0.200	Passed

As most of the data set was found to be normally distributed, paired *t*-tests were carried out to determine if the amplitude of finger ac PPGs and flap ac PPGs can be considered to be statistically significantly different in all wavelengths. The results from the t-tests for all wavelengths are presented in Tables 9.12, 9.13 and 9.14 respectively. In each case a value of $p < 0.05$ was considered to be statistically significant.

Table 9.12: Results of paired t-test comparisons on red ac PPG signals from the custom made finger and flap sensor.

Recovery	Hr 1	Hr 2	Hr 3	Hr 4	Hr 5	Hr 6	Hr 7	Hr 8	Hr 9	Hr 10	Hr 11
P= 0.030	P= 0.025	NS	P= 0.020	P= 0.047	P= 0.022	NS	NS	P= 0.036	P= 0.034	NS	NS

Table 9.13: Results of paired t-test comparisons on green ac PPG signals from the custom made finger and flap sensor.

Recovery	Hr 1	Hr 2	Hr 3	Hr 4	Hr 5	Hr 6	Hr 7	Hr 8	Hr 9	Hr 10	Hr 11
P= 0.006	P= 0.011	P= 0.045	NS	NS	NS	NS	-	NS	-	-	-

Table 9.14: Results of paired t-test comparisons on infrared ac PPG signals from the custom made finger and flap sensor.

Recovery	Hr 1	Hr 2	Hr 3	Hr 4	Hr 5	Hr 6	Hr 7	Hr 8	Hr 9	Hr 10	Hr 11
P= 0.0397	P= 0.0379	NS	P= 0.0319	NS	NS	NS	NS	P= 0.0679	NS	P= 0.0003	-

In comparisons where there was deemed to be no significant difference NS is noted, "-" is used where the test could not be conducted due to limited number of samples in the group and in comparisons where a statistically significant difference was found, the p value is noted. Red, green and infrared ac PPG signals from the finger compared to the flap were found to be statistically significant in the recovery and 1 hour post-operatively. Red PPGs between finger and flap were found to be significantly different in more than half of the post-surgery intervals. However, green ac PPG signals from the flap and the finger were either deemed not statistically significant or the test could not be performed due to limited number of samples in the population. The infrared signals were found to be significantly different in the recovery, 1, 3, 8 and 10 hour intervals following DIEP free flap surgery.

These tests indicate that the amplitude of ac PPG signals from the finger are statistically significantly larger than the amplitude of the ac PPG signals obtained from the flap at most intervals in the post-operative hours.

Using the red and infrared ac and dc PPG signals, SpO_2 values were estimated in order to investigate the feasibility of using the developed PPG processing system and sensor for monitoring arterial blood oxygen saturation levels of the free flap. These preliminary findings are presented in the following sections.

9.5 Blood Oxygen Saturation (SpO_2) estimations in DIEP free flap

As described in previous chapters, an estimation of blood arterial oxygen saturation can be obtained using red and infrared ac and dc PPG signals. Even though the developed flap pulse oximetry system is an uncalibrated system, preliminary SpO_2 values were estimated offline using the patients' flap red and infrared, ac and dc PPG signals from the various periods of monitoring.

9.5.1 Pre-operative SpO_2 estimations

Estimation of arterial blood oxygen saturation levels commenced using the PPG signals obtained in the anaesthetic room prior to the start of the reconstructive surgery. The SpO_2 values estimated were used as a baseline prior to harvesting the flap. SpO_2 values were estimated using two seconds of the obtained PPG signals. These were then compared with the simultaneously recorded SpO_2 values from the commercial pulse oximeter. The mean ± SD of the estimated donor site SpO_2 and the recorded finger SpO_2 values were calculated for the five patients in the preoperative period and presented in Figure 9.17.

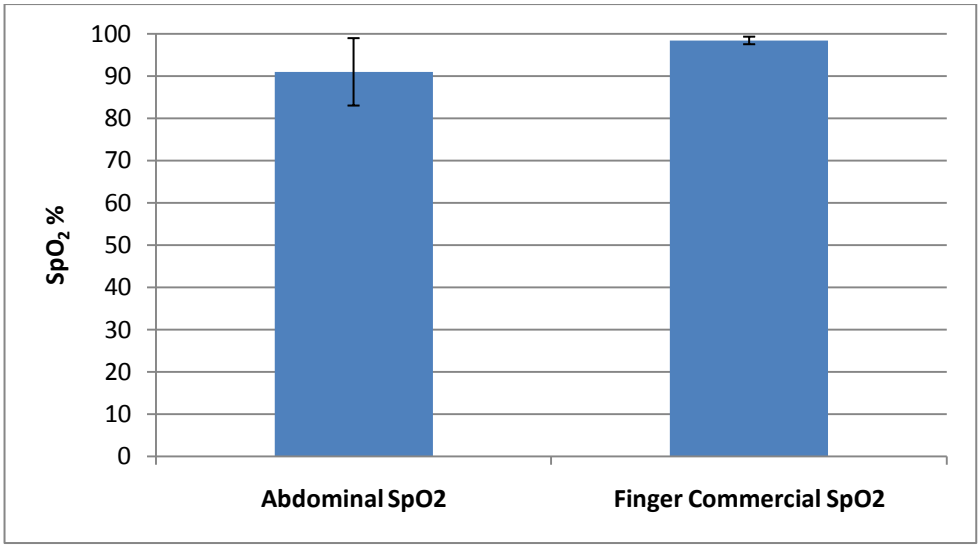

Figure 9.17: Mean (±SD) SpO_2 values from the abdomen (PPG sensor) and the commercial pulse oximeter (n=5).

The calculated blood oxygen saturation values from the donor site were found to be 7.4% lower than those obtained simultaneously from the finger pulse oximeter. It is speculated that the main reason for the lack of agreement between the two pulse oximeters was the uncalibrated nature of the custom made flap pulse oximeter, hence the under estimation. The difference could also be due to the increased adipose tissue presented in the abdomen.

Following the successful estimation of SpO_2 in the 5 patients in the preoperative period, the system was then evaluated further in order to provide an indication of the system's ability to estimate arterial blood oxygen saturation levels in intra-operatively.

9.5.2 Intra-operative SpO_2 estimation

Good quality red and infrared PPG signals were successfully detected intra-operatively from the free flap following the removal of the arterial and venous clamps in all six patients. Using the detected red and infrared ac and dc PPG signals from the free flap, SpO_2 values were estimated. In order to assess the accuracy of the PPG system and its capability in correctly estimating the percentage of blood arterial oxygen saturation of the free flap, the values were then compared with the SpO_2 values recorded from the commercial finger pulse oximeter.

Intra-operative measurements were recorded continuously for 5 to 10 minutes. The mean and standard deviation of the free flap SpO_2 and the pulse oximeter SpO_2 recorded from the commercial pulse oximeter were calculated and are shown in Figure 9.18.

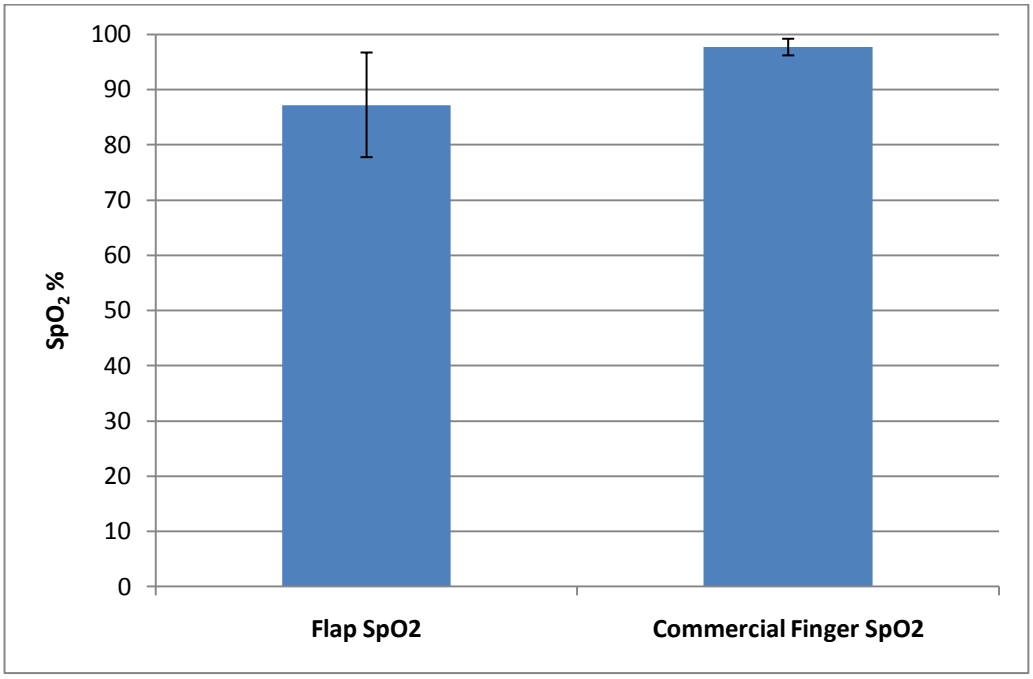

Figure 9.18: Mean and ±SD SpO_2 values from the free flap and the finger pulse oximeter recorded intra-operatively following removal of vessel clamps (n=6).

As was the case in the pre-operative period the SpO_2 values from the free flap are lower than that of the commercial pulse oximeter which could be due to the uncalibrated nature of the custom made system and also on a more physiological level the differences in saturations could be due to the newly anastomosed flap vessels and lack of collateral blood supply.

Following successfully estimating SpO_2 levels of the free flap in the intra-operative period the post-operative ac and dc signals from the red and infrared wavelengths were then used to investigate arterial blood oxygen saturation levels of the free flap commencing in the recovery room for up to 12 hours post-operatively.

9.5.3 Post-operative SpO_2 estimations

In this section the estimated arterial blood oxygen saturation levels from the custom made flap pulse oximeter as well as the recorded values from the commercial finger pulse oximeter (N560, Covidien, Ireland) will be presented. In order to provide an indication of how the SpO_2 values from the flap and the commercial SpO_2 differ, the mean of all values at all intervals from the flap sensor are plotted against the mean of the means of the commercial SpO_2 as shown in Figure 9.19.

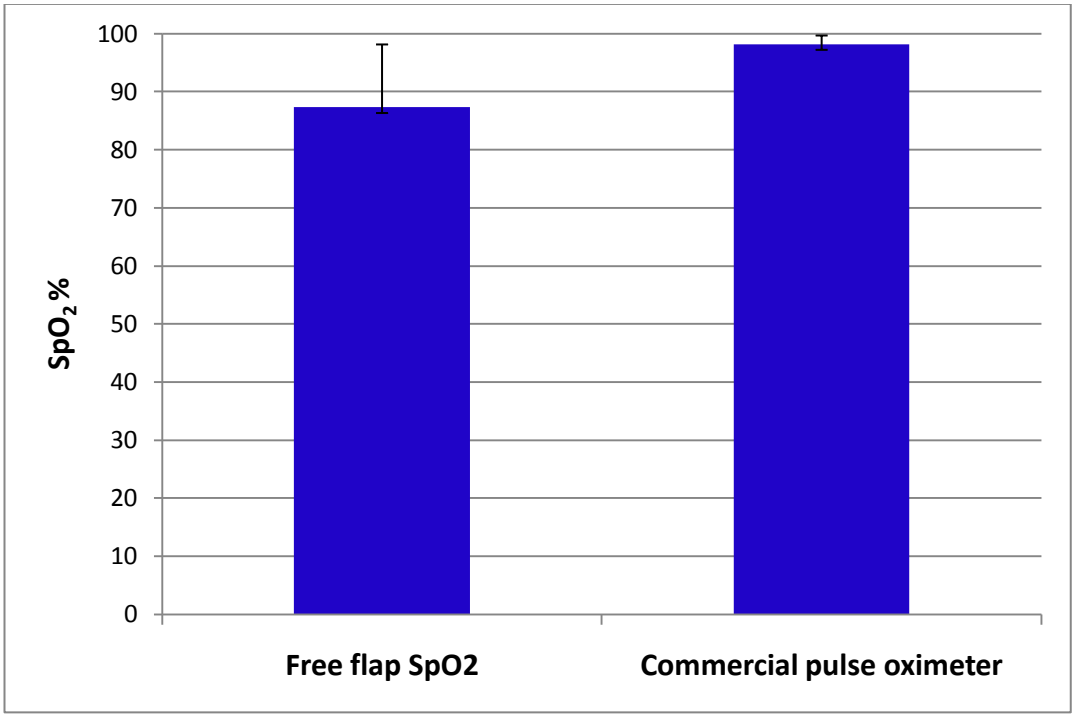

Figure 9.19: Comparison of the mean (±SD) of all SpO2 values at all intervals from custom made flap sensor with the commercial pulse oximeter.

The SpO_2 values were estimated for all intervals in the post-operative period, the mean of the means of the values as well as the values from the commercial pulse oximeter are shown in Figure 9.20.

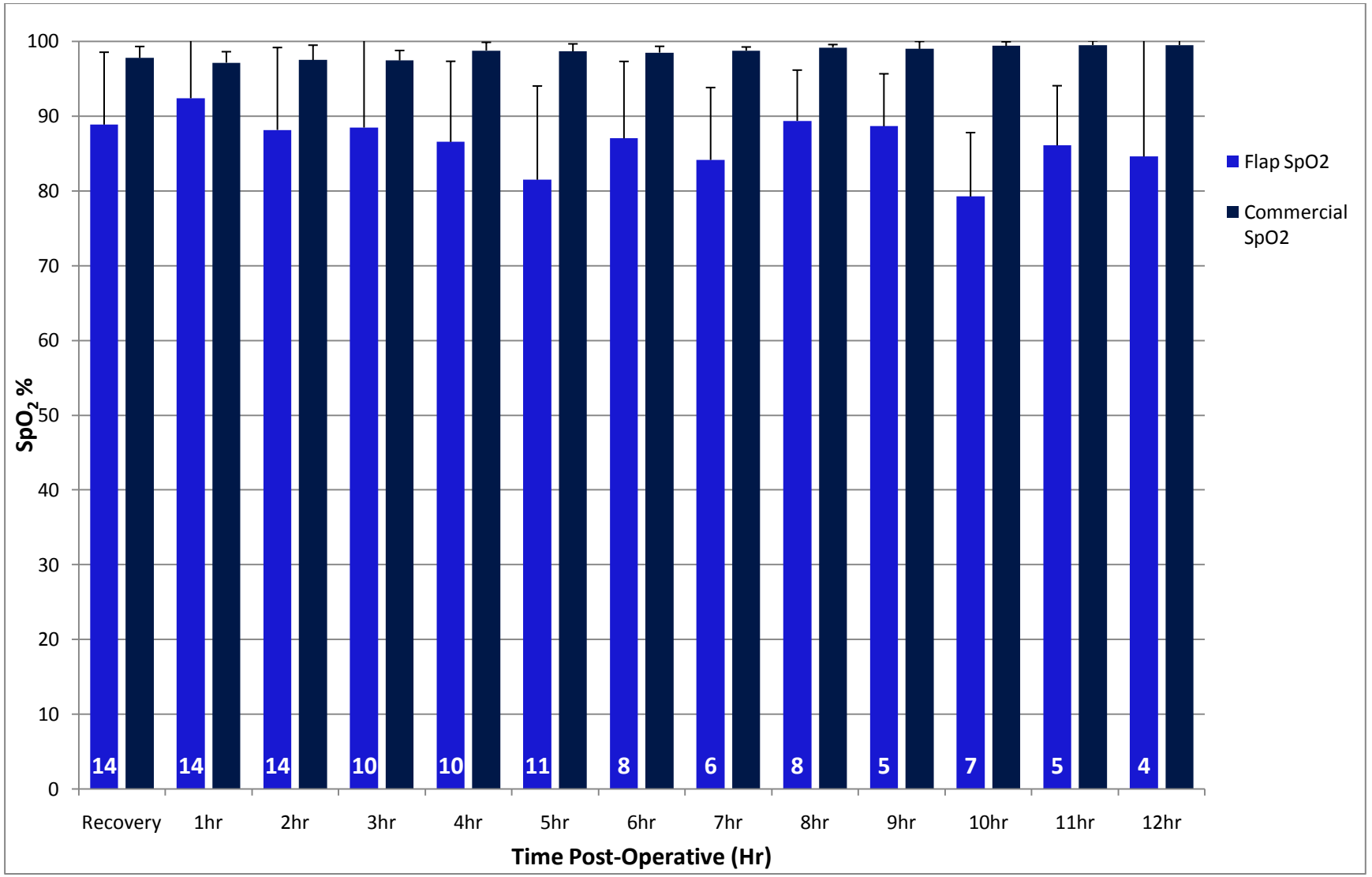

Figure 9.20: Mean of the means SpO_2 (±SD) values for custom made flap sensor and commercial pulse oximeter from finger.

As shown in the figure the SpO_2 values from the flap are in broad agreement (with a consistent underestimation) with the values from the commercial finger pulse oximeter. Observations from the plotted histogram suggest that the estimated arterial blood oxygen saturation levels from the flap are generally lower that the recorded values from the commercial pulse oximeter from the finger. To confirm that the lower SpO_2 values in the flap are statistically significant and if the PPG processing system can be used as a pulse oximeter for free flap monitoring, the data were statistically analysed which are presented in the following section.

9.5.4 Statistical analysis on Post-operative SpO_2 estimations

In order to determine if there was any statistically significant difference between the estimated SpO_2 values and the recorded values from the commercial pulse oximeter a paired *t*-test was performed. Prior to testing the data for normality the frequency distribution was plotted to graphically ascertain if the estimated SpO_2 values from the free flap are normally distributed. Figure 9.21 shows the frequency distribution of the estimated arterial blood oxygen saturation of the free flap. The histogram indicates a slight deviation from normal as the data is not symmetrical which suggest a skewed distribution of -0.42.

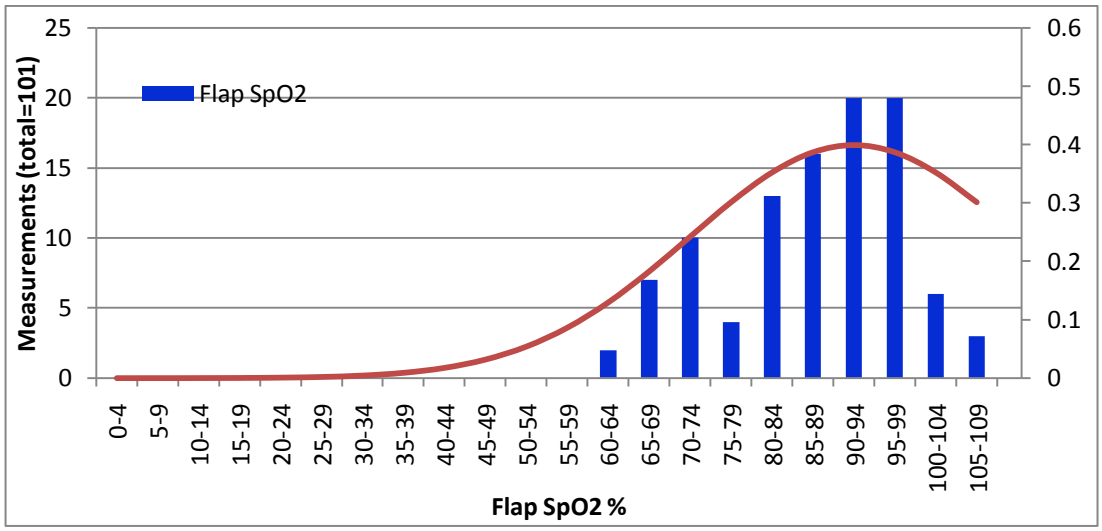

Figure 9.21: Frequency distribution of the estimated SpO_2 values with an overlying Gaussian curve for comparison.

The data were then tested for normality using the Kolmogorov-Smirnov test where the results are presented in Table 9.15. The mean of estimated arterial blood oxygen saturation levels from all patients were found to be normally distributed at each interval except in hour 3 of the post-operative period.

Table 9.15: Results of Kolmogorov-Smirnov normality test on estimated SpO_2 values from the free flap at each post-operative interval.

Post-operative period	K-S Distance	P Value	Normality Test Result
Recovery:	K-S Dist. = 0.197	P = 0.148	Passed
Hr 1 post-op:	K-S Dist. = 0.145	P > 0.200	Passed
Hr 2 post-op:	K-S Dist. = 0.141	P > 0.200	Passed
Hr 3 post-op:	K-S Dist. = 0.366	P = 0.001	Failed
Hr 4 post-op:	K-S Dist. = 0.220	P = 0.183	Passed
Hr 5 post-op:	K-S Dist. = 0.207	P > 0.200	Passed
Hr 6 post-op:	K-S Dist. = 0.267	P = 0.196	Passed
Hr 7 post-op:	K-S Dist. = 0.295	P > 0.200	Passed
Hr 8 post-op:	K-S Dist. = 0.220	P > 0.200	Passed
Hr 9 post-op:	K-S Dist. = 0.361	P = 0.136	Passed
Hr 10 post-op:	K-S Dist. = 0.250	P > 0.200	Passed
Hr 11 post-op:	K-S Dist. = 0.316	P = 0.172	Passed
Hr 12 post-op:	K-S Dist. = 0.260	P > 0.200	Passed

Table 9.16: Results of Kolmogorov-Smirnov normality test on recorded SpO_2 values from the commercial pulse oximeter from the finger at each post-operative interval.

Post-operative period	K-S Distance	P Value	Normality Test Result
Recovery:	K-S Dist. = 0.270	P = 0.007	Failed
Hr 1 post-op:	K-S Dist. = 0.227	P = 0.065	Passed
Hr 2 post-op:	K-S Dist. = 0.187	P > 0.200	Passed
Hr 3 post-op:	K-S Dist. = 0.217	P > 0.200	Passed
Hr 4 post-op:	K-S Dist. = 0.358	P = 0.001	Failed
Hr 5 post-op:	K-S Dist. = 0.192	P > 0.200	Passed
Hr 6 post-op:	K-S Dist. = 0.392	P = 0.004	Failed
Hr 7 post-op:	K-S Dist. = 0.441	P = 0.006	Failed
Hr 8 post-op:	K-S Dist. = 0.492	P < 0.001	Failed
Hr 9 post-op:	K-S Dist. = 0.175	P > 0.200	Passed
Hr 10 post-op:	K-S Dist. = 0.367	P = 0.026	Failed
Hr 11 post-op:	K-S Dist. = 0.307	P > 0.200	Passed
Hr 12 post-op:	K-S Dist. = 0.260	P > 0.200	Passed

The SpO_2 values recorded from the commercial pulse oximeter at each interval were also tested for normality using the SigmaPlot software. The results from the K-S normality test are shown in Table 9.16. The data were found not to be normally distributed at Recovery, 4, 6, 7, 8 and 10 hours post operatively. Paired t-tests performed on the flap and finger pulse oximeter SpO_2 values show statistically significant differences between the two devices at more than half the time intervals in the post-surgery period. However, the mean of the mean SpO_2 values estimated from the flap were found to be not significant to the commercial SpO_2 values obtained at 1, 3, 7,9 and 12 hours in the post-operative period.

Table 9.17: Results of paired t-test comparisons SpO_2 values from the custom made flap sensor and the commercial pulse oximeter.

Recovery	Hr 1	Hr 2	Hr 3	Hr 4	Hr 5	Hr 6	Hr 7	Hr 8	Hr 9	Hr 10	Hr 11	Hr 12
P= 0.004	NS	P= 0.010	NS	P= 0.014	P= 0.004	P= 0.044	NS	P= 0.016	NS	P= 0.007	P= 0.038	NS

In order to compare and determine the feasibility of using the developed PPG processing system for monitoring flap SpO_2 levels interchangeably with the established commercial pulse oximeter the Bland and Altman between-method-difference analysis is used. The Bland and Altman method suggests that by graphically plotting the difference between the two measurements from each method against their mean, if the new method agrees sufficiently with the standardised method, the old method may be replaced. This is done by calculating the bias, estimated by the mean difference (d) and the standard deviation of the differences (s). Provided the differences within d±2s would not be clinically important, we could use the two methods or instruments interchangeably [98].

Figure 9.22 shows the plot of the difference between the custom made flap pulse oximeter and the SpO_2 value recorded from the commercial pulse oximeter against their mean. The computed limits of agreement are 11.5% and -33%, these would suggest that the SpO_2 values obtained from the custom made PPG processing system may be 11.5% above or 33% under the SpO_2 values obtained from the commercial pulse oximeter from the finger suggesting that the free flap custom made SpO_2

monitoring device underestimates the arterial blood oxygen saturation levels from the flap.

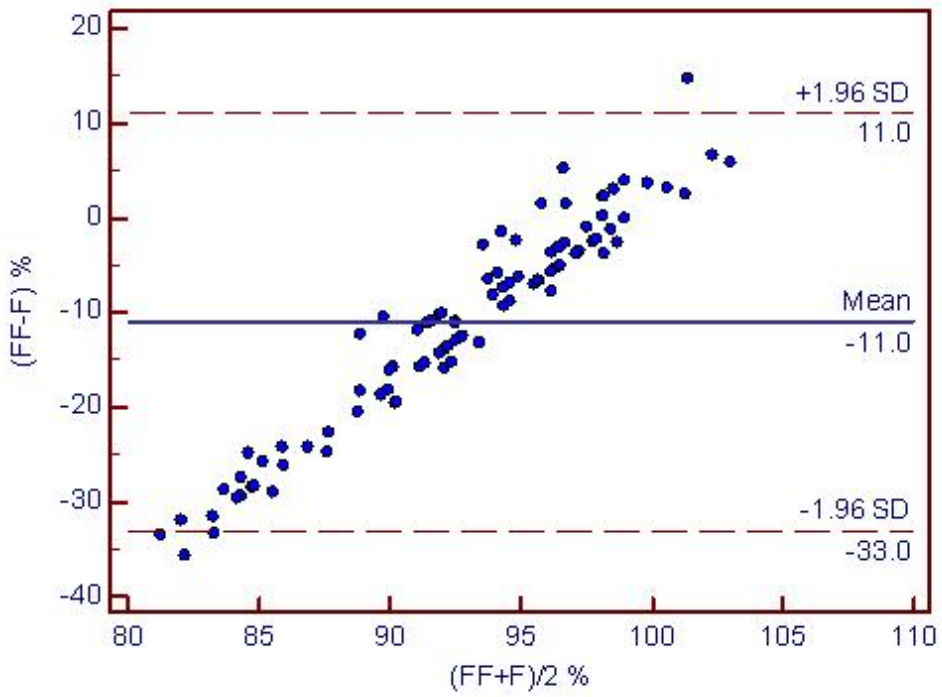

Figure 9.22: Difference against mean for SpO_2 data obtained from the free flap (FF) PPG sensor and the finger (F) using the commercial pulse oximeter.

9.5.5 Statistical analysis and estimation of SpO_2 from flap and finger

A comparison of the SpO_2 results from the 5 patients where the custom made finger sensor was used in conjunction with the commercial finger pulse oximeter and the flap sensor are presented in this section.

Figure 9.23 shows the plot of the mean and standard deviation from all patients at all post-operative periods with the number of patients observed noted as *n* on the x axis. This figure represents the difference between the estimated flap and finger SpO_2 values from both the developed PPG processing systems and the SpO_2 readings recorded from the commercial pulse oximeter which is routinely used by medical staff for the observational check. All three SpO_2 recordings were obtained simultaneously.

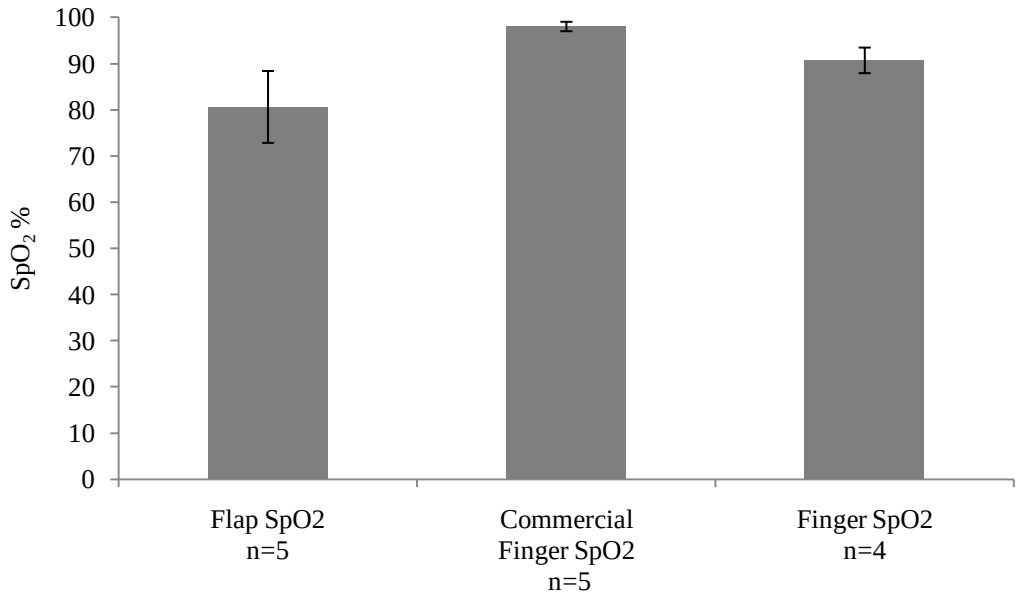

Figure 9.23: Mean SpO_2 (±SD) values from the flap sensor, custom made finger sensor and commercial pulse oximeters from all patients.

The results shown in Figure 9.23 suggest that the SpO_2 results from the finger PPG processing system were in broad agreement with the blood oxygen saturation values obtained from the commercial pulse oximeter. The estimated flap SpO_2 values were moderately lower than the custom finger SpO_2 values which is expected due to newly anastomosed vessels and general poor perfusion of the flap immediately after free flap surgery. Furthermore, the larger standard deviation of the flap SpO_2 levels compared to the finger oxygen saturation levels is due to change in the health of the anastomosed arterial and venous blood vessels during the post-operative period.

The Bland and Altman method was repeated on SpO_2 values obtained from the custom made finger pulse oximeter and the SpO_2 values from the commercial finger pulse oximeter. The results (from 4 patients) from the comparison of the custom made finger SpO_2 and the commercial pulse oximeter are presented in Figure 9.24.

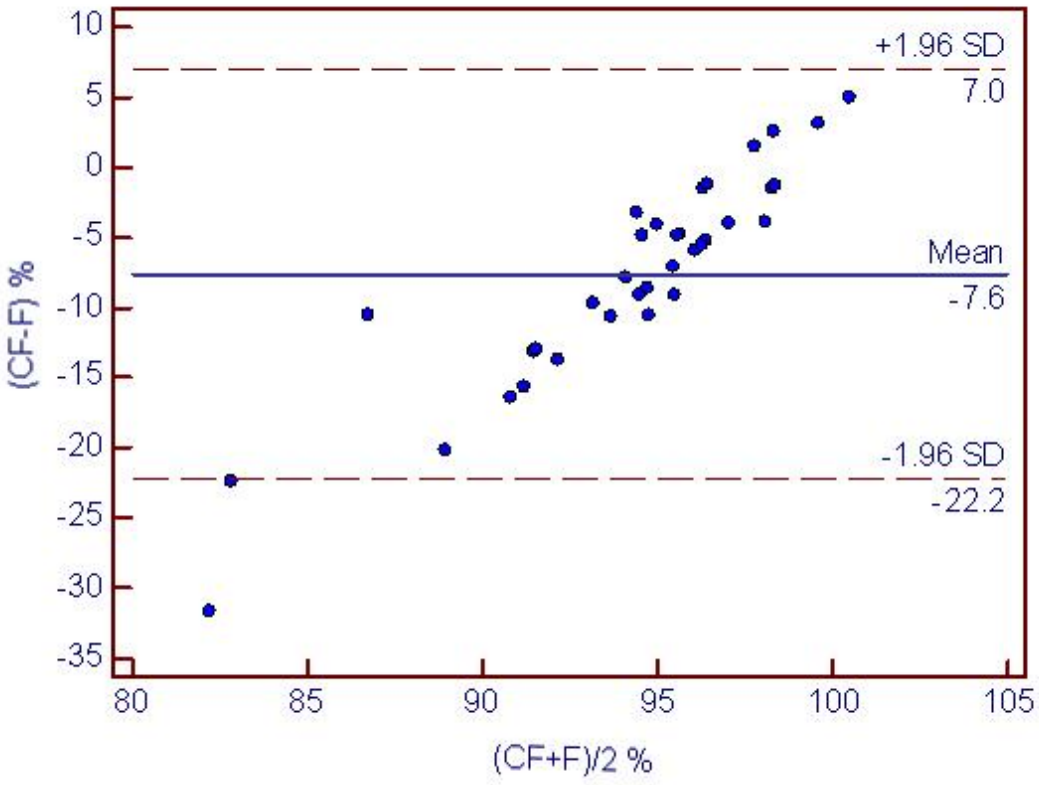

Figure 9.24: Difference against mean for SpO_2 data obtained from the custom finger PPG sensor (CF) and the commercial pulse oximeter (F).

The limits of agreement between the custom made finger SpO_2 values and the commercial pulse oximeter are -22% and 7%. Which confirms the underestimation of the custom made finger pulse oximeter.

In summary, a non-invasive flap PPG pulse oximetry monitoring system has been successfully developed and evaluated in preliminary clinical trials in patients undergoing DIEP free flap surgery.

Chapter 10

Case Studies: Investigation of PPG and SpO_2 from Latissimus Dorsi and head and neck flaps

In this chapter unique and isolated case studies that were performed on head and neck flaps such as: jejunum free flap and Vertical Rectus Abdominis Musculocutaneous (VRAM) flap for head and neck reconstruction and pedicle flaps such as Latissimus Dorsi (LD) which is used in breast reconstruction will be presented. These pilot studies were performed as a proof of concept study at St Bartholomew's and The Royal London Hospital as part of the approved study. As there is a small population of patients studied with these flaps, this chapter will present each flap as a case study.

10.1 Case Study 1: PPG and SpO_2 of Latissimus Dorsi flap

Mastectomy is often performed in women who have been diagnosed with breast cancer. However this is often associated with psychological trauma as it is often damaging to the womans' self image and the need for special clothing following mastectomy. Breast reconstructive surgery is an option to restore a normal form of breast in order to improve quality of life for those afflicted with breast cancer [1].

Breast reconstruction with autologous tissue is the preferred option as it gives a more natural look and feel to the breast. Latissimus Dorsi flap is one of the reconstructive options available for patients who are not suitable for DIEP or TRAM free flap surgery. This procedure involves using an ellipse of tissue and skin from the upper back to create a reconstructed breast. However as this flap lacks volume for a normal and natural breast expander or implants are often added under the flap.

10.1.1 Latissimus Dorsi Flap for Breast Reconstruction Surgery

In patients undergoing immediate breast reconstruction the mastectomy is performed prior to beginning the reconstructive surgery as the patient must be turned to her side in order to provide the surgeon with easy access to the latissimus muscle in the upper section of the patients' back [27]. In the Latissimus Dorsi (LD) flap (as shown in Figure 10.1) an ellipse shape of skin paddle with the underlying fat and muscle are dissected where care is taken to preserve the main blood vessels supplying nutrients to the LD flap. A tunnel is then created from the axilla to the chest where the mastectomy defect is located. The tunnel is enlarged in order to allow rotation of the pedicle of the LD flap to the mastectomy wound.

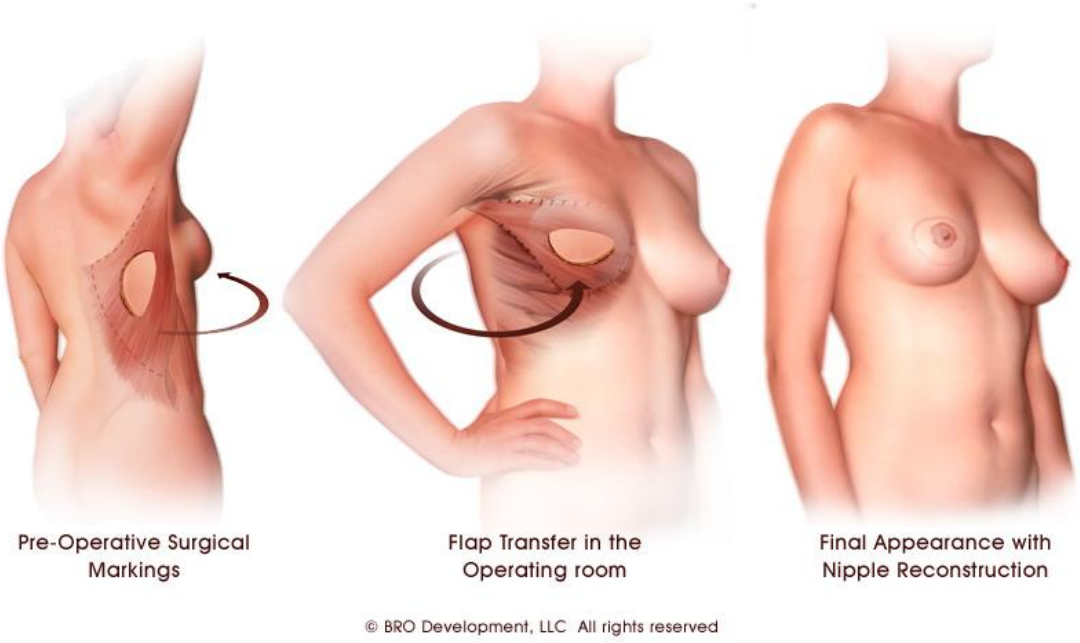

Figure 10.1: Latissimus Dorsi flap reconstruction following mastectomy.

The wound on the back is then closed followed by securing of the flap to the chest wall and an implant or expander is then placed under the flap.

As the main blood vessels remain attached to the flap the vascularity of the flap is robust therefore fat necrosis or vascular compromise rarely occurs. However as any flap reconstructive surgery there are risks of complications such as haematoma or

partial or total flap necrosis due to kinking or twisting of the blood vessels. Therefore flap monitoring is imperative in ensuring its survival. Techniques and technologies used for post-operative monitoring of flaps in breast reconstruction have been discussed in previous chapters. However clinical examination of the flap using a flap chart (as shown in appendix (i)) as well as occasional use of hand-held Doppler ultrasound still remain as the most commonly used post-operative monitoring techniques. As these techniques are operator dependent, biased depending on experience, and environmental factors such as room temperature and lighting can affect the result of these clinical observations there is still a need for a reliable, continuous, objective monitoring technique.

As the designed and developed photoplethysmographic processing system and sensor were successfully evaluated in monitoring DIEP free flaps in breast reconstruction, it was decided to assess the capability of the system in monitoring other types of flaps such as a pedicle flap e.g. LD flaps.

10.1.2 Preliminary in vivo evaluation of Latissimus Dorsi flap

In vivo evaluation of the PPG processing system and free flap PPG sensor were performed on fifteen patients undergoing breast reconstruction using DIEP free flap. As the system was previously used in Mid Essex Hospital, it was electrically safety tested in the medical physics department of the NHS trust. Prior to using the system on patients undergoing breast reconstructive surgery using LD flaps the system was inspected in the Clinical physics department at the St Bartholomew's and the Royal London Hospital patients will be recruited for the study. A substantial amendment approval was obtained on the original ethics approval from City & East National Research Ethics Service in order to monitor patients undergoing reconstructive surgery using all types of flaps as well as adding the Barts and The Royal London Hospital as an additional site where patients will be recruited into the study (appendix i). As this is a proof of concept study two patients undergoing breast reconstructive surgery with latissimus dorsi pedicle flap with implants were recruited for assessment of photoplethysmographic signals intra and post-operatively.

10.1.2.1 Intra-operative PPG measurement protocol and results

In order to prepare the PPG system for the initial intra-operative measurement, the PPG sensor was covered with a sterile transparent adhesive film dressing (Tegaderm™ Film) and the multicore cable which connects the sensor to the processing system was also covered using a sterile camera sleeve (EASI-DRAPE, Leonhard Lang[LTD]). Once the patient was anaesthetised and prepped, the surgical procedure commenced by the surgical team performing a mastectomy on the affected breast. The patient was then rotated in order to ease access to her upper back where the latissimus dorsi muscle is located. Upon dissection of the LD flap and its preparation for insetting and prior to its transfer to the recipient site the PPG sensor was taped onto the flap using intra-operative sterile tape (Op-Tape, Winner Medical Group Inc). A 15 second period of the intra-operative measurement from the donor site is shown in Figure 10.2.

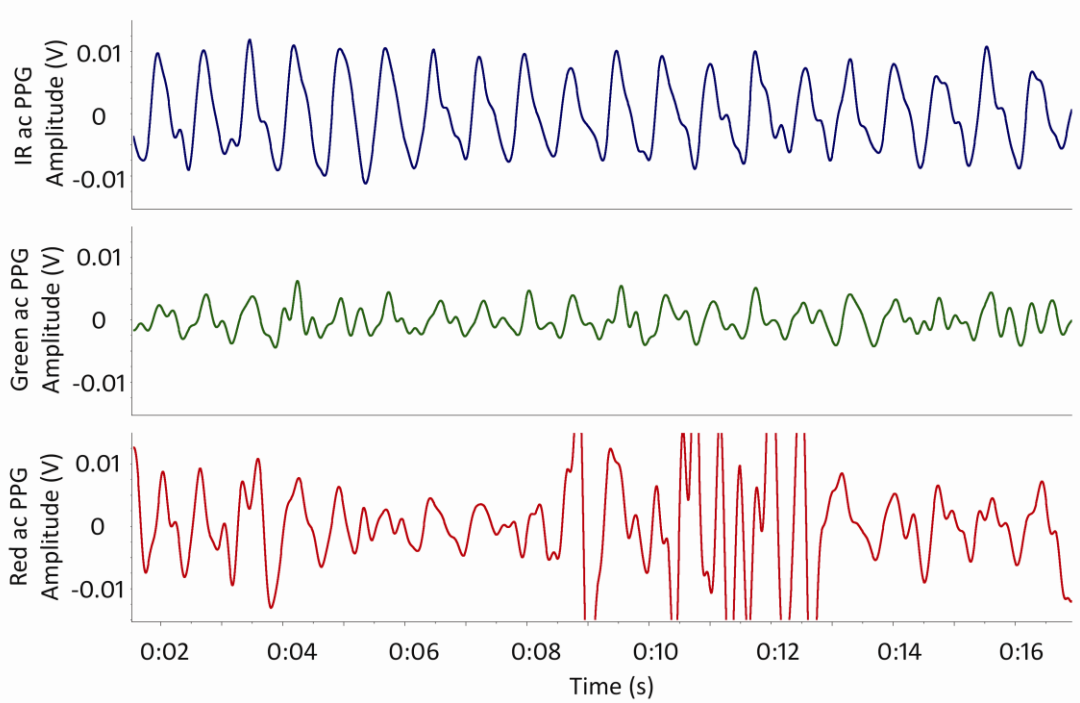

Figure 10.2: Typical red, green and infrared ac PPG signals from the LD flap prior to its transfer.

Good quality infrared and green PPG signals were detected with typical morphology of an expected PPG waveform. Red ac PPG signals with clarity of a typical PPG waveform

can be observed in the first and last 2 seconds of the recorded waveform, however electrical interference can be observed from 9-13 seconds of the recording which was due to a loose wiring in the PPG processing system.

Once the recording was stopped the PPG sensor was removed and the surgeon continued with the surgical procedure by dissecting a skin tunnel from the axilla to the mastectomy wound. The pedicle flap was then passed through to the mastectomy site where the second intra-operative measurement was acquired. The PPG sensor was taped onto the flap using Op-Tape and the finger PPG sensor was also attached to the patients' finger. Red, green and infrared PPG signals were acquired from both the LD flap and the finger. As seen in Figure 10.3 good quality ac PPG signals were detected from all three wavelengths from the patients' finger. However minor modulations can be observed in the ac PPG signals detected from the LD flap which is due to motion artifact as the flap had not yet been secured in the recipient site.

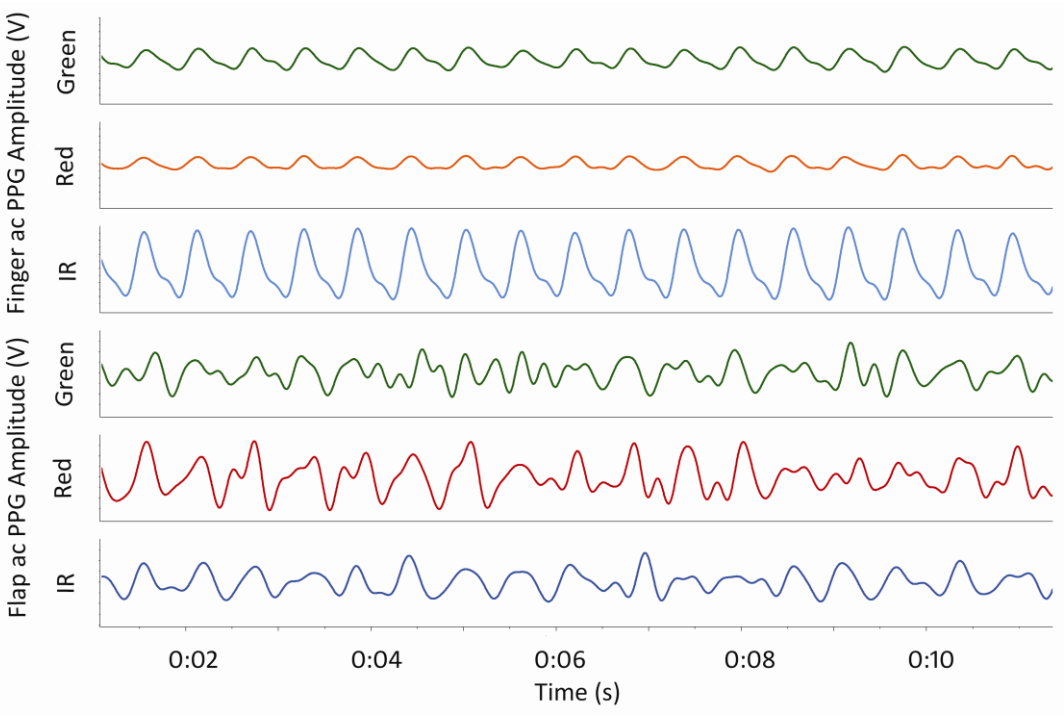

Figure 10.3: Infrared, red and green ac PPG signals obtained intra-operatively from the pedicle flap.

Upon successful acquisition of PPG signals in the intra-operative period the recording was stopped and the surgeons continued with securing the LD flap in the mastectomy site while ensuring to avoid any twist, kink or tension to the main blood vessels. The

plastic surgeon then inserted an implant under the pedicle flap in order to add volume to the breast. The wounds were then closed and breast was then loosely covered with sterile gauze. The patient was then transferred to the post-anaesthesia patient recovery room where the post-operative PPG monitoring commenced.

10.1.2.2 Post-operative PPG measurement protocol and results

The nursing staff commenced post-operative monitoring of the free flap in the recovery room then in the ward by examining the colour, texture, capillary refill and temperature of the flap at regular intervals of every 15 minutes in the first 2 hours, every 30 minutes in the following 4 hours and hourly in the following 24-48 hours following surgery. The first post-operative PPG measurement was performed in the recovery room once the patient was extubated and stabilised. The PPG sensor was placed on the LD flap and secured in place as it was taped onto the skin surrounding the flap using surgical tape (3M™ Transpore™); sterile gauze was also used on the wound edges to ensure the surgical tape does not adhere directly to the sutured edges. To minimise causing further inconvenience to the patient the PPG post-operative measurements were obtained immediately following the routine flap observational examinations carried out by the nursing staff at the same regular intervals beginning in the post-anaesthesia patient recovery room followed by monitoring of the patient in the ward overnight for up to 8 hours post surgery.

Figure 10.4 shows an approximately 25 second period of a typical red, green and infrared ac PPG signal obtained in the post-operative period.

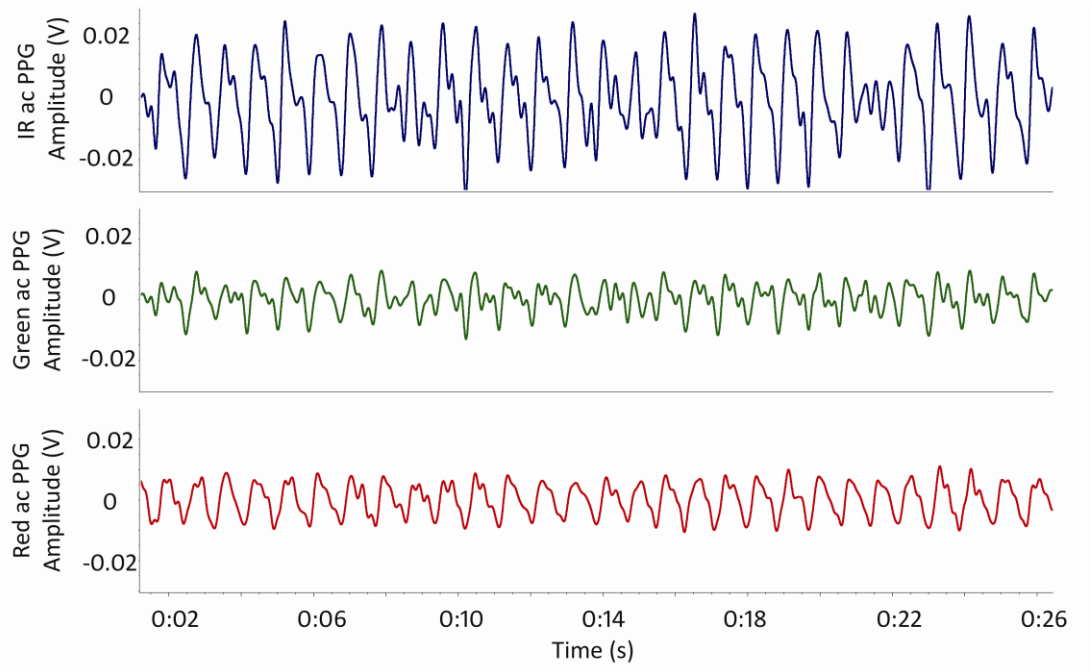

Figure 10.4: Typical red, green and infrared ac PPG signals obtained from the LD flap 1 hour following surgery.

Initial observations suggest that good quality PPG signals with high amplitude can be obtained from LD flaps. Two patients were monitored for 8 hours post-operatively at 15 minute intervals for the first 2 hours, every 30 minutes for the following 4 hours and hourly for the subsequent 24-48 hours. In order to identify any trend in the ac PPG amplitude following LD flap reconstructive surgery the mean (±SD) of data recorded at hourly intervals from both patients plotted in a histogram as shown in Figure 10.5.

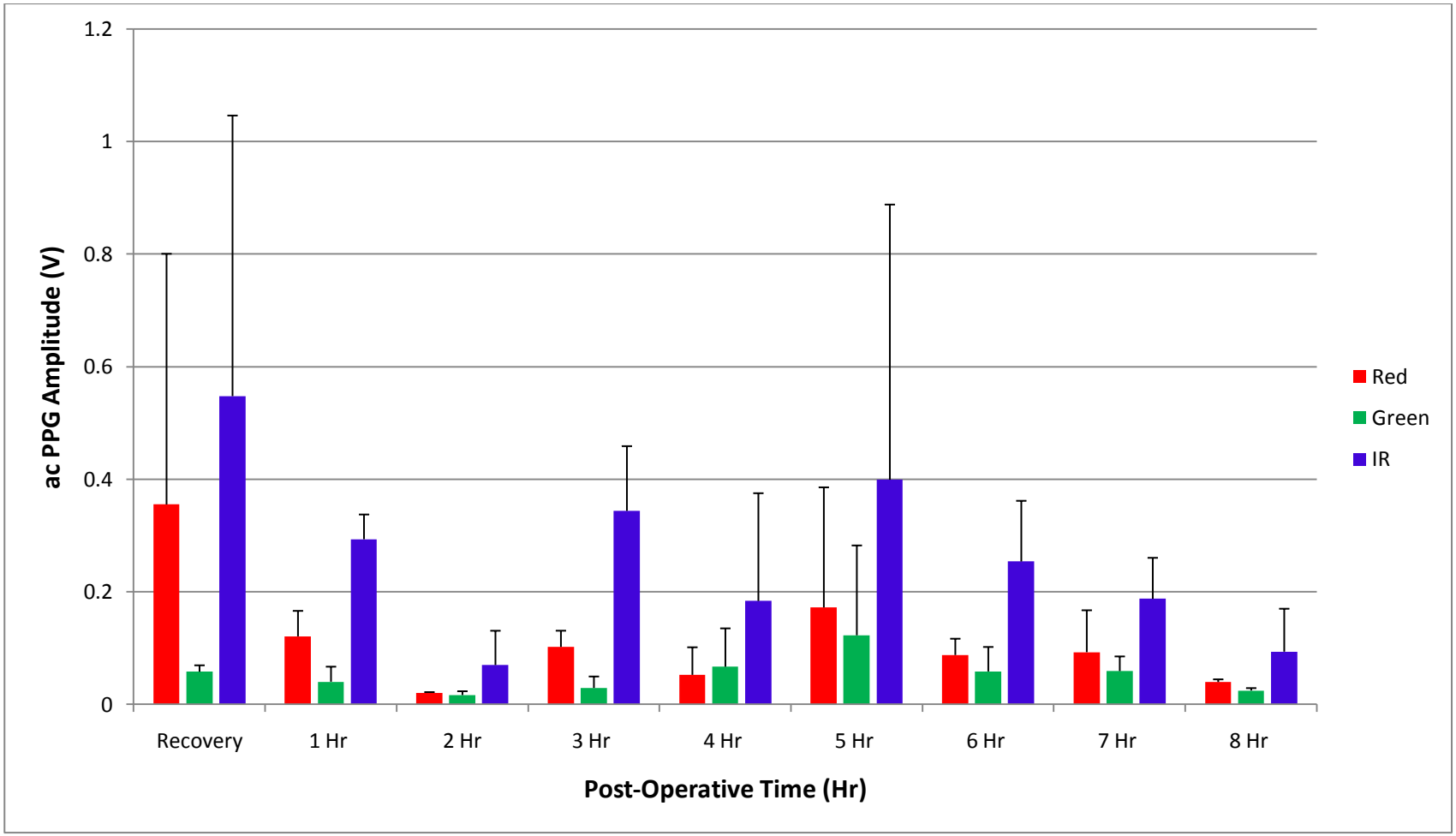

Figure 10.5: Mean (±SD) of red, green and infrared ac PPG amplitudes obtained from two patients in the post-operative period following breast reconstruction using LD flap.

As this was a pilot study with the aim of evaluating the capability of the system in detecting photoplethysmographic signals intra and post-operatively, only two patients were recruited into the study. Therefore the small population size prevents carrying out statistical analysis on the data in order to determine if the decrease in PPG amplitude observed in the first 3 hours and the last 4 hours can be considered to be statistically significant or if the difference is due to chance. Also with small sample sizes it is difficult to detect a difference even when one exists. The large standard deviations observed are due to different PPG amplitudes detected from each patient, the cause of this could be environmental factors such as the temperature of the flap being different in each patient or the difference in thickness of the adipose tissue in the flaps.

Following successfully detecting good quality PPG signals from all three wavelengths the red and infrared ac and the red and infrared dc PPG signals are utilized in order to estimate the LD flap blood arterial oxygen saturation values at all post-operative intervals in both patients.

10.1.2.3 Post-operative SpO_2 estimations

The percentage of oxygen saturation of arterial blood in the LD flap were estimated using the detected red and infrared, ac and dc PPG signals from both patients. The SpO_2 values from the commercial pulse oximeter routinely used for monitoring patient observations were manually recorded simultaneously with each post-operative measurement interval.

Figure 10.6 shows the mean (±SD) of the estimated SpO_2 values with SpO_2 values recorded from the commercial pulse oximeter attached to the patients' finger from both patients at all post-operative intervals. Observations from the histogram plot suggest that the flap SpO_2 measurements are lower than those from the finger estimated by the commercial pulse oximeter. It was calculated that the oxygen saturation of the arterial blood pulsating through the flap is on average 17% lower than the SpO_2 from the finger from the commercial device. This difference could be because two different sites are being monitored by two different devices; also it must be taken into consideration that the developed PPG processing system is not a calibrated system.

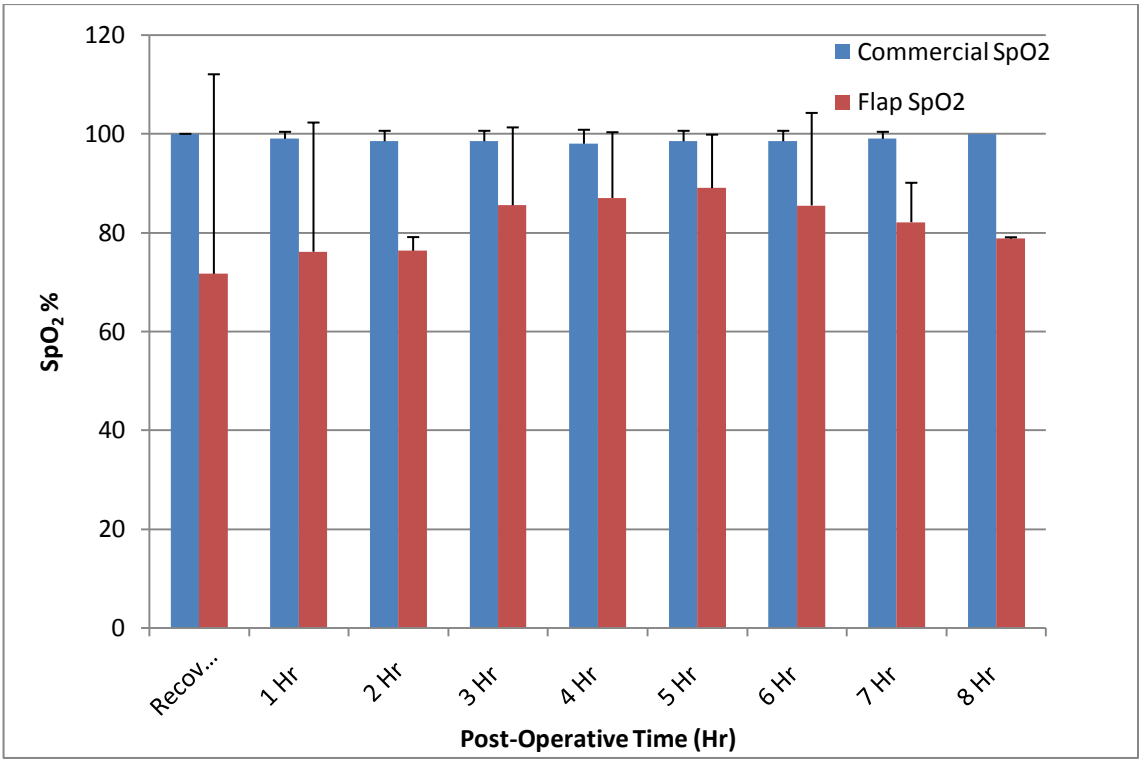

Figure 10.6: Mean (±SD) of estimated flap SpO_2 and commercial SpO_2 values in both patients at all post-operative intervals.

In summery as the developed PPG processing system and sensor is versatile, it has the potential to be used in pedicle flaps as well as free flaps. Good quality red, infrared and green PPG signals were successfully obtained intra and post-operatively which enables the system in estimating SpO_2 values from the flap either real-time or offline.

This is the first time that such a system with the capability of monitoring for any change in PPG signals intra-operatively and post-operatively, as well as estimating the arterial oxygen saturation levels from LD flaps.

10.2 Case study 2: PPG and SpO_2 of head and neck

In patients suffering from cancer of the head and neck, reconstructive surgery using free flap is commonly used following removal of the tumours. The type of flap used is dependent on the extent and size of the defect. The main focus in this section is cancer of the ear and use of free flaps for cosmetic and functional reasons.

10.2.1 Facial reconstruction with free flap

Malignancies of the ear and temporal bone are rare but in patients diagnosed with advanced carcinoma the only prospect of cure is radical temporal bone resection, subtotal petrosectomy or total petrosectomy. In cases where an aggressive approach is needed with regard to the resection, such a large surgical defect creates a major challenge for a need of reconstructive surgery. With the use of free tissue transfer as a reliable seal to the defect, the extent of tumour clearance and resection margins are inconsequential as the eventual size of the defect are irrelevant [99].

Transverse Rectus Abdominis Myocutaneous (TRAM) flap, Vertical Rectus Abdominis Myocutaneous (VRAM) flap (where the skin is oriented vertically compared to TRAM) and Pectoralis Major Myocutaneous flap are some of the more commonly used free flaps for head and neck reconstructive surgery as these flaps provide a large cutaneous island for coverage of large defects. Also, this type of flap is often preferred as it consists of three layers of, skin, subcutaneous fat and muscle, making the flap durable. Free flap reconstruction using rectus abdominis muscles can provide facial contour as well as movement of the muscle motor nerve of the donor site can be anastomosed to the proximal facial nerve, although this depends on the extent of resection. However cranial nerve resection which leads to facial paralysis is unavoidable in some cases [100].

As described in previous chapters, monitoring of free flaps and early identification of flap compromise is vital. In order to investigate the feasibility of using the developed PPG system and sensor in head and neck flaps, as a proof of concept study the system was evaluated on one patient undergoing reconstructive surgery of head and neck.

10.2.2 Preliminary in vivo evaluation on VRAM flap in head and neck

A 55 year old male undergoing total petrosectomy with VRAM flap reconstruction at Barts and The London Hospital was recruited into the pilot study. As this is a skin flap the same finger and flap PPG sensor and system were used from the previous study. Similarly with the other studies, ethics approval and signed consent were obtained.

10.2.2.1 Intra-operative PPG measurement protocol and result

Once the patient was anesthetised, the dissection of the ear was carried out followed by the ear, nose and throat (ENT) surgeon performing total petrosectomy and obliteration of the middle ear. Once the resection was completed suitable vessels were identified and prepared for anastomosis. Simultaneously the general surgeon performed the free flap dissection with the skin island which is elevated along with the rectus abdominis muscle. The main perforators were identified and dissected at an adequate length. Prior to the surgeons clamping the vessels the first PPG measurement was performed.

As the recording was carried out intra-operatively, the PPG sensor was covered with sterile film dressing (Tegaderm^{TM}) and the cable with EASI-DRAPE camera sleeve.

The PPG sensor was then taped onto the exposed skin of the flap using sterile surgical Op-Tape in order to record a measurement from the donor site while the main perforators remain attached. The finger PPG sensor was also clipped onto the patients' index finger.

Figure 10.7 shows good quality red, green and infrared ac PPG signals acquired from both the flap and the finger. As seen from the figure, the finger PPG signals are greater in amplitude comparing to the flap PPG signals, this is expected as the finger is a well perfused site and only one artery and one venous are supply blood flow through the flap.

Following the successful acquisition of signals from the flap, the recording was stopped, the PPG sensor was removed and the surgeon proceeded to clamp and cut the main perforators on the VRAM flap.

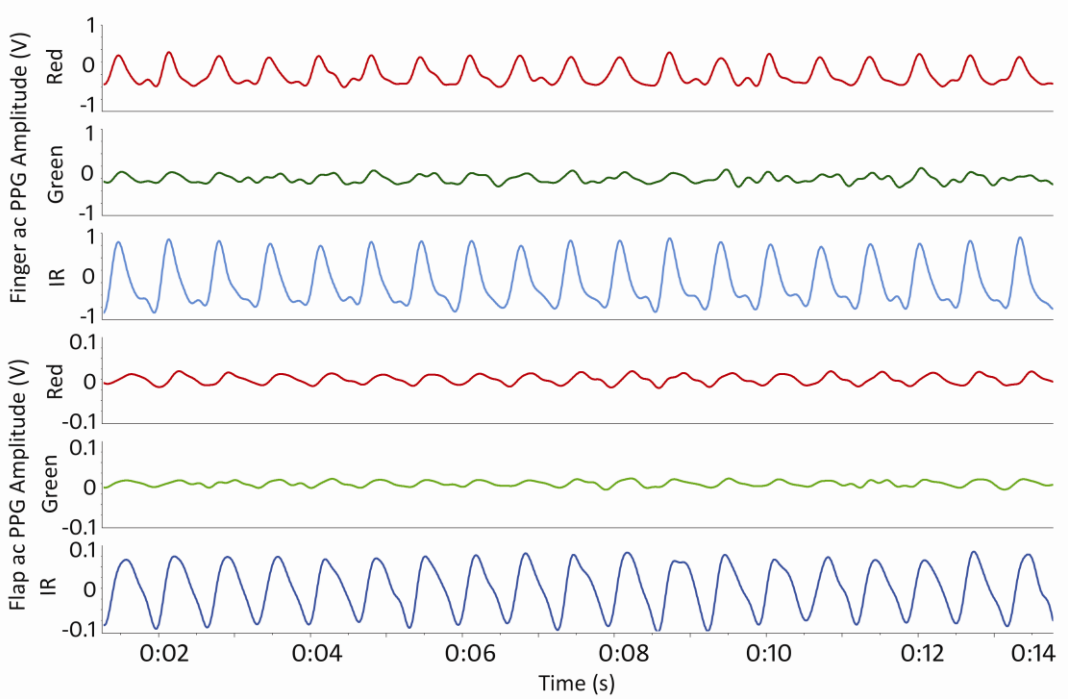

Figure 10.7: Measurement obtained from the flap intra-operatively with the main perforators attached.

The free flap was then transferred to the defect site where the plastic surgeon performed anastomosis on the flap and recipient site vessels. This procedure is approximately an hour long depending on the health of the vessels and skill of the surgeon. As soon as the vessels were anastomosed the PPG sensor was again taped on free flap and the recording began. In order to capture the reperfusion of the free flap a baseline measurement of 5 seconds was obtained followed by the removal of the venous and arterial vessels clamps.

The reperfusion of the free flap was confirmed by the surgeon by visually inspecting the pulsation of the anastomosed artery and re-established blood flow through the vein. Figure 10.8 shows infrared ac PPG signal capturing re-establishment of blood flow through the flap. A low amplitude noise is observed in the first 5 seconds of the recording, the vessel clamps were then removed where due to the motion of the removal of the clamps a high amplitude noise can be seen. An increase in the PPG amplitude is an indication of good arterial flow through the flap.

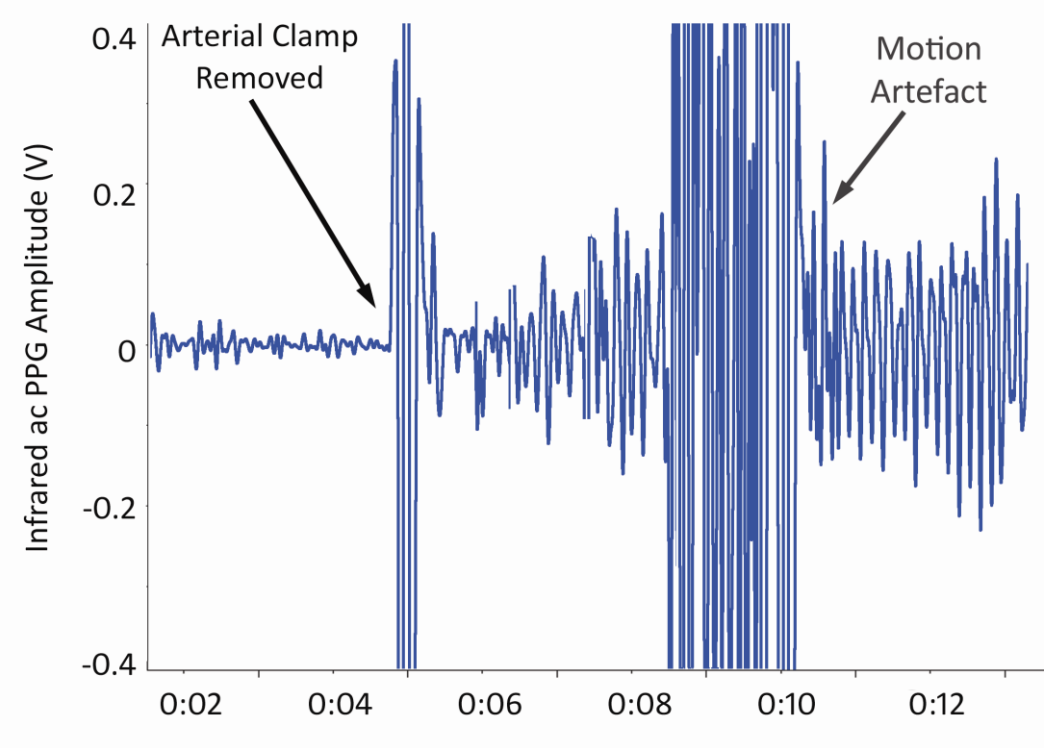

Figure 10.8: Reperfusion of the VRAM flap in head and neck reconstructive surgery.

Once the surgeons were satisfied with the perfusion of the free flap a second measurement was carried out 5 minutes following the removal of the clamps. A 10 second period of the intra-operative measurement is shown in Figure 10.9 where good quality infrared, green and red ac PPG signals with typical PPG waveform morphology can be observed both from the free flap and the patients' finger.

Following successful detection of PPG signals from all three wavelengths from the free flap the recording was stopped and the PPG sensor was removed. The free flap was then used to cover the defect and the facial wound and the donor site incisions were closed. The free flap wound was then loosely dressed with sterile gauze as the area would need to be observed intermittently overnight. The patient was then transferred to Intensive Therapy Unit (ITU) as the patient was to be kept ventilated. The PPG sensor was then re-covered using a new sterile adhesive dressing and the post-operative monitoring of the flap commenced in ITU.

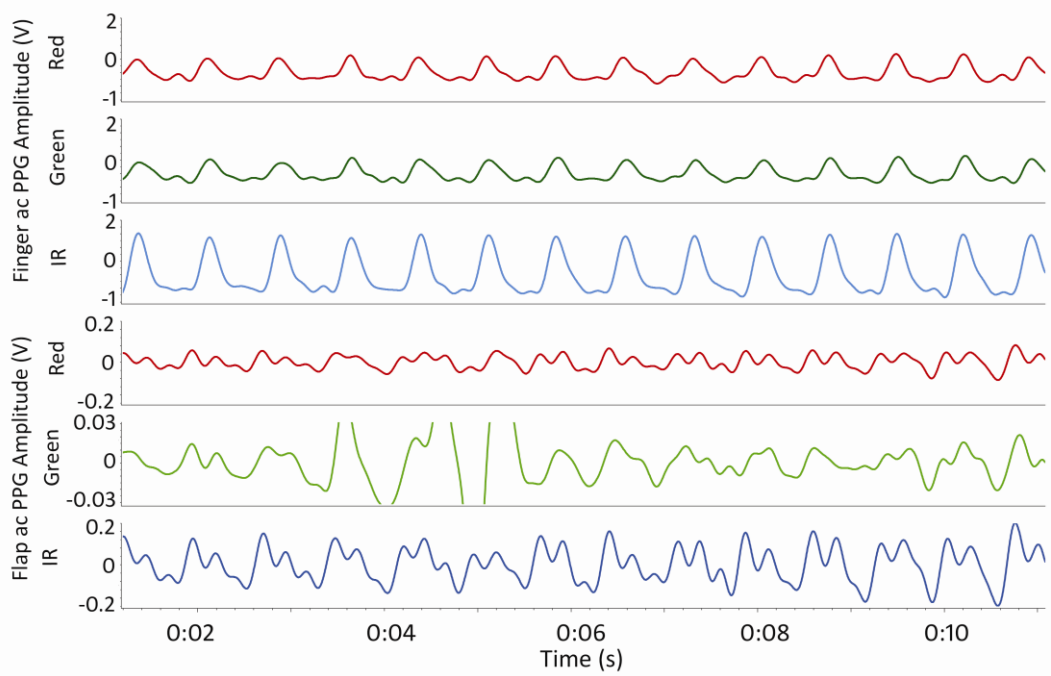

Figure 10.9: Typical infrared, green and red ac PPG signals obtained from flap and finger 5 minutes post clamp removal.

10.2.2.2 Post-operative PPG measurement protocol and results

The routine free flap post-operative monitoring performed at Barts and the London consisted of using a flap chart where the flap colour, capillary refill time and temperature are monitored at 15 minute intervals in the first 2 hours, every 30 minutes in the following 4 hours and hourly for the subsequent 24-48 hours following surgery. The PPG recordings were obtained at the same intervals as the clinical observations as well as a manual recording of the patient vital signs such as heart rate, SpO_2, blood pressure and temperature.

Figure 10.10 shows an approximately 10 second window of the ac PPG signals obtained from all three wavelengths of red, infrared and green from both finger and flap PPG sensors 3 hours following the reconstructive surgery. As observed the signals acquired are of typical PPG morphology with clear peaks and troughs.

As this was a lengthy surgical procedure it was only feasible to carry out the post-operative monitoring until the following morning, therefore half hourly recordings were performed for four hours in the post-operative period.

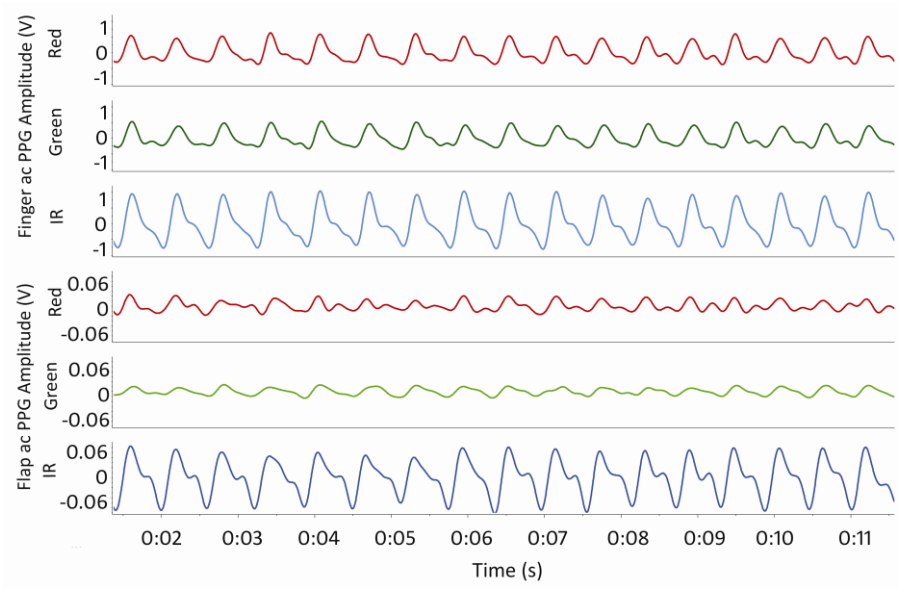

Figure 10.10: Typical PPG recordings from flap and finger 3 hours post surgery.

The amplitude of the red, green and infrared ac PPG signals detected from the free flap are presented as a histogram in Figure 10.11.

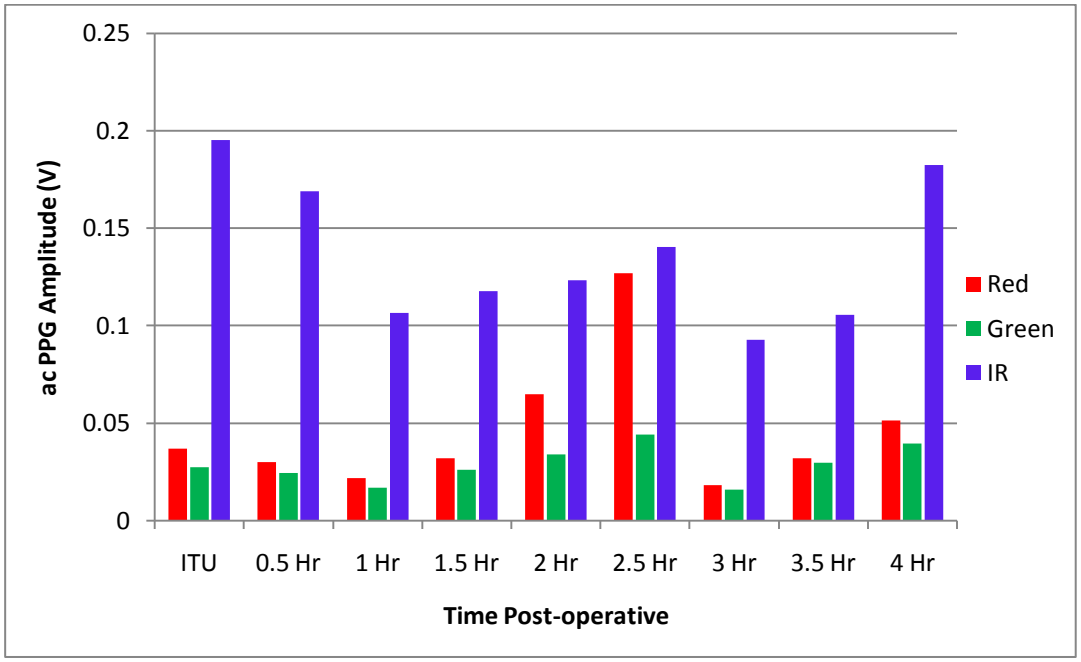

Figure 10.11: ac PPG amplitude of all three wavelengths obtained at all post-operative intervals.

10.2.2.3 Post-operative SpO_2 estimations

Following successfully acquiring signals from all three wavelengths at all post-operative intervals, the blood arterial oxygen saturation levels of the free flap and finger were estimated. The estimated SpO_2 values from the finger and flap from each post-operative interval as well as the SpO_2 values recorded from the commercial pulse oximeter used for routine ITU monitoring are presented as a histogram in Figure 10.12. It can be observed that the SpO_2 values estimated from the head and neck flap are on average 3% lower than those recorded from the commercial pulse oximeter whereas those values estimated using PPG signals from the finger PPG sensor are approximately 6% lower than the pulse oximeter values. It is suspected that the higher SpO_2 values from the flap are due to its position in the neck which has good perfusion levels. However as this is a pilot study, there are not enough samples in order to confirm this hypothesis.

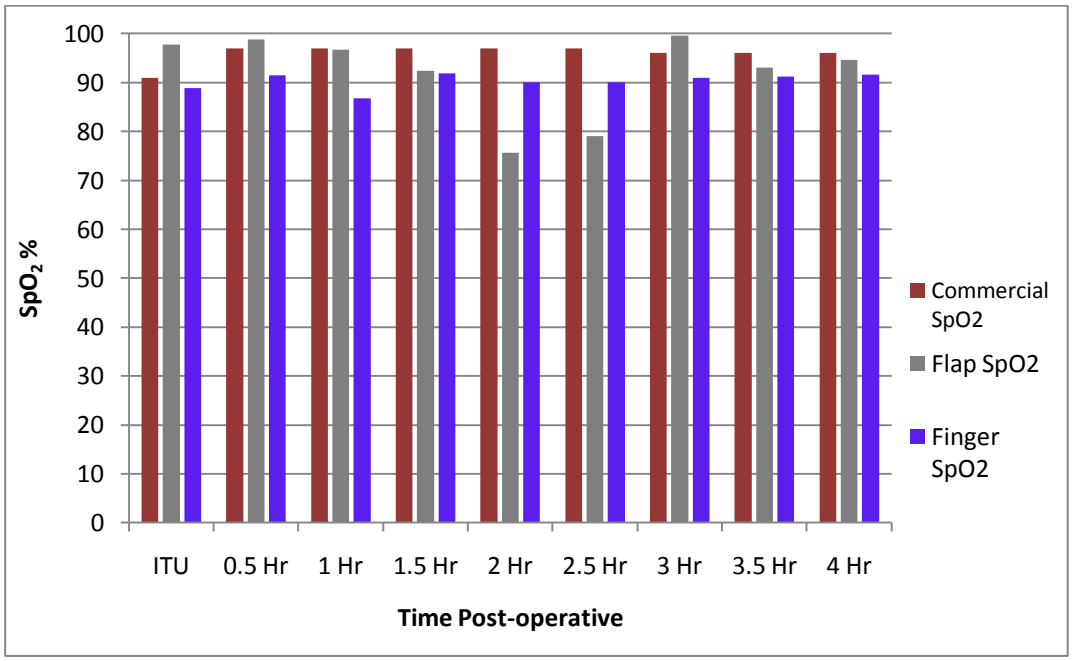

Figure 10.12: Estimated SpO2 values for flap and finger with the values from the commercial pulse oximeter.

10.3 Case Study 3: PPG and SpO2 measurements from jejunum free flap

Free jejunum flaps have been widely used as a reconstruction option after total laryngopharyngectomy. Monitoring of flap perfusion assists in early detection of flap failure, increasing the possibility of flap salvage. Considering the free jejunum flap is a hidden flap there is still no single reliable, non invasive perfusion monitoring technique to assist in recognizing flap failure. A dual-wavelength photoplethysmographic (PPG) sensor has been designed and developed and implemented to be used with the developed PPG processing system as described in Chapter 7. This chapter describes the design of the sensor as well as the *in vivo* evaluation of the system in two patients undergoing total laryngopharyngectomy followed by reconstructive surgery of the oesophagus using free jejunum flap. This is the first time such a minimally invasive monitoring technique has been used to monitor the jejunum free flap intra and post-operatively.

10.3.1 Reconstruction of the pharynx and oesophagus using jejunum free flap

Reconstruction of the pharynx and the cervical oesophagus is typically performed following trauma, benign strictures or cancer. In patients suffering from early carcinoma of the upper aero-digestive tract the procedure of Laryngopharyngectomy is performed which involves the removal of the larynx with partial or complete removal of the pharynx as shown in Figure 10.13. This leaves the patient with a permanent tracheotomy as well as the inability to breath, swallow and to speak [28].

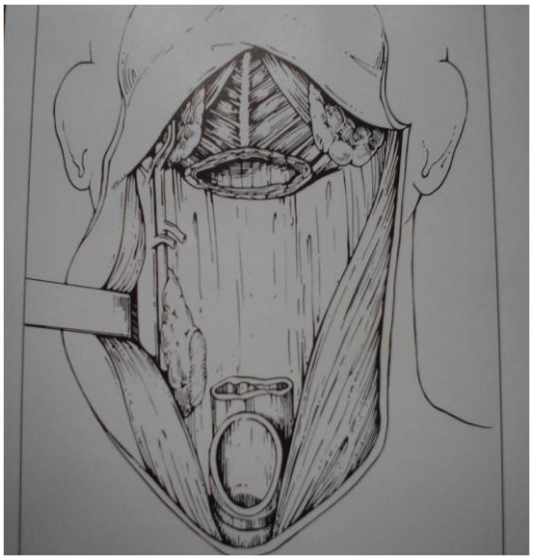

Figure 10.13: Excision of both the larynx and the pharynx.

Following a Laryngopharyngectomy, plastic reconstruction may be done with the primary goals to restore anatomy to allow normal breathing without the need for tracheotomy, preserve patients' ability to swallow without aspiration and to restore speech. The skin flap from the forearm or intestinal tissue, the jejunum, are two of the most common pharynx reconstructive options available[101]. The jejunum free flap is a standard technique commonly used in reconstructive surgery of the head and neck [102]. Figure 10.14 shows the reconstructed pharynx using a free flap.

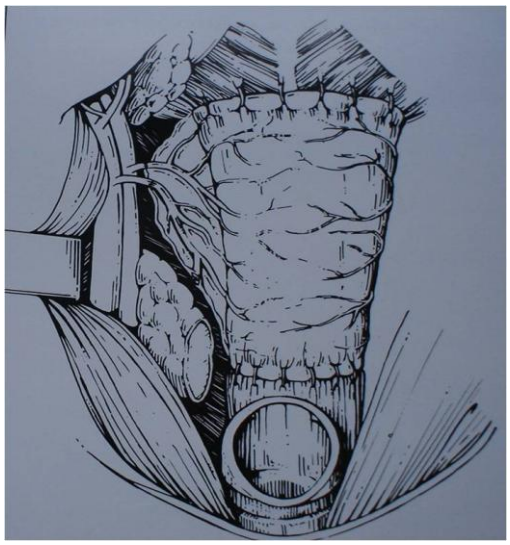

Figure 10.14: Plastic reconstruction of the pharynx using free flap.

Free jejunum flaps are preferable to skin flap from the patients' forearm as they can provide cover for large circumferential defects, secrete mucus, have intrinsic peristalsis, tolerate radiotherapy well and they do not cause strictures, these are important factors which are advantageous in selecting this flap for use in the upper pharynx and oesophagus [103]. Another factor which makes jejunum flaps favourable over other types of reconstructive options is that the diameter of the jejunum is approximately the same as the oesophagus, also the jejunum provides the flexibility of using different lengths of flaps depending on the size of the neck defect, in some centres where an exteriorized segment of the jejunum is used for monitoring of the health of the flap an additional 1 to 2 cm is required.

As mentioned in previous chapters, the most serious complication of free flap is anastomotic thrombosis which occurs post-operatively, resulting in graft necrosis [104]. The mortality rate of jejunum flap when used for reconstruction of the oesophageal defect is between 2.4% and 5% which usually occurs within the first 3 postoperative days [105]. In intestinal flaps the tolerance for low levels of oxygen in blood is 2 hours, after which the tissue becomes necrotic [28].

Therefore the success of such procedure strongly depends on the maintenance of adequate perfusion in the flap. It is imperative to detect any indication of ischaemia early as revision of microvascular anastomosis and restoring blood flow might salvage the flap to avoid further surgery and harvesting additional jejunum flap from the abdomen [104, 106]. Postoperative monitoring of the flap is necessary to identify vascular compromise as delayed diagnosis may result in flap failure.

Numerous techniques and monitoring devices have been used for assessing perfusion of jejunum flaps post operatively. Katsaros *et al* described one of the most popular methods of observing the viability of the flap post operatively by dividing the jejunum into two segments, one of which to be used for reconstructive purposes and the other segment used for monitoring; both of these parts are left on the same mesenteric blood supply [107]. The exteriorised section will be used for monitoring the flaps colour, temperature, peristalsis and bleeding during the postoperative period. Similar

methods of this monitoring technique with possible variation to its surgical procedure are “watch window” or sentinel [104-105, 108].

Laser Doppler flowmetry and microdialysis have also been used in monitoring the jejunum flap by securing the probe directly on the flap intra-operatively and leaving the probe in place for post operative monitoring [109-110].

However, there are disadvantages to these techniques such as; the requirement for technical skill or subjective interpretation from the medical staff, intermittent monitoring and invasive nature of the monitoring device. Therefore, there is still a need for a less invasive, accurate, easy to use, reproducible and inexpensive monitoring device.

In an attempt to overcome the limitations of the current techniques for assessing jejunum flap perfusion the technique of photoplethysmography was used. The concept of using photoplethysmography in monitoring free flaps has previously been discussed in Chapter 9 where PPG signals were successfully acquired from DIEP free flaps used in breast reconstructive surgery. However, as the jejunum and the oesophagus have a different dimension and shape to the area monitored in DIEP flaps, a new dual wavelength optical sensor based on the principle of reflectance photoplethysmography was designed and developed.

10.3.2 Development of Jejunum free flap Sensor

A new reflectance, dual-wavelength photoplethysmographic sensor was developed as shown in Figure 10.15 which consisted of one infrared (IR) and one red (R) ceramic chip surface mount LED (peak emission wavelengths at 940 nm and 660 nm respectively) and a photodiode (single photodiode with an active area of 7.5 mm^2 with spectral range sensitivity between 400-1100 nm).

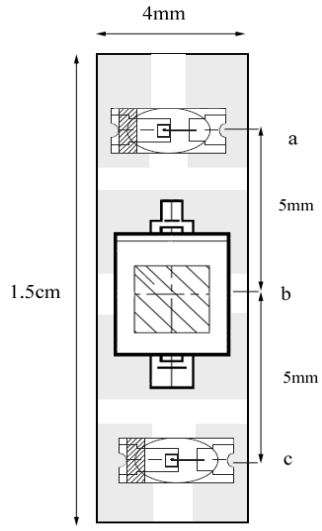

(i)

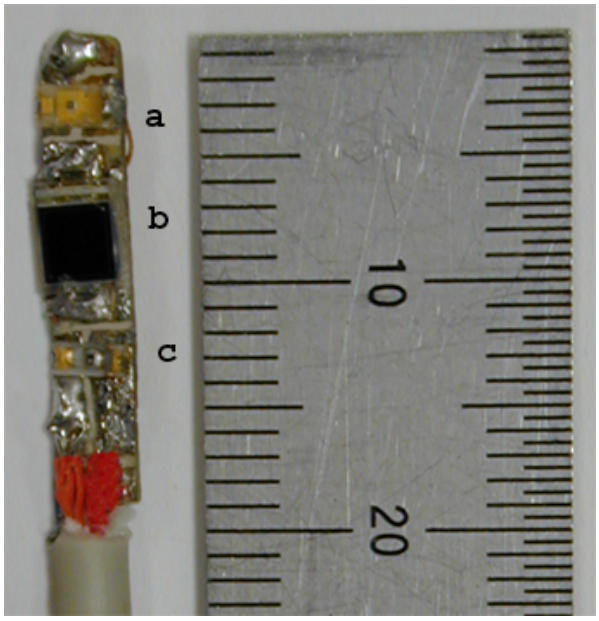

(ii)

Figure 10.15: Illustrated diagram (i) and photograph (ii) of the reflectance photoplethysmographic free jejunum flap sensor where (a): IR surface mount LED, (b): PIN photodiode in miniature flat plastic package and (c): Red surface mount LED.

The distance between the LEDs and the photodiode was 5 mm as such distance has been proven to provide good quality PPGs in reflectance pulse oximetry [94]. As shown in Figure 10.15 (i) the shape of the sensor was designed to be rectangular with dimensions of 150mm x 4mm which is adequately narrow in width in order to be accommodated into the jejunum flap which is 2.5 cm in internal diameter during and after the operation.

The optical components of the jejunum PPG sensor were designed to be compatible with the DIEP free flap PPG processing system. The PPG processing system was used to drive the optical components of the jejunal sensor and also to detect and pre-process the red and infrared ac and dc PPG signals as shown in a block diagram in Figure 10.16.

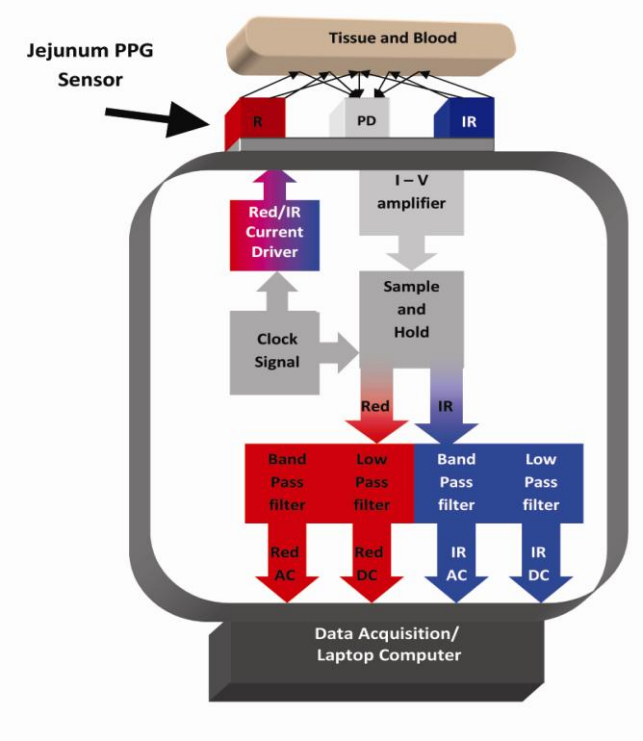

Figure 10.16: Block diagram of the Jejunum PPG sensor with the PPG processing system.

10.3.3 Preliminary *in vivo* evaluation of Free Flap Sensor

Prior to using the developed photoplethysmographic processing system and sensor for assessing perfusion of free flaps, the system was inspected and electrically safety tested by the Clinical Physics Department at The Royal London Hospital, UK where patients will be recruited for the study. As the developed PPG processing system was battery powered, the device was considered electrically safe for use on patients. Local research ethics committee approval and patient consent were also acquired prior to the study.

Two patients undergoing pharyngolaryngectomy with reconstructive surgery using jejunum flap were recruited into the study at The Royal London Hospital, UK. A pilot study on two free jejunum flaps surgical cases were carried out to test the functionality of the PPG sensor and its capability in detecting PPG signals at both wavelengths in the jejunum flap.

10.3.3.1 Intra-operative PPG measurement

Both of the recruited patients were monitored intra-operatively. As the first measurement was performed in the operating room, in order to maintain the sterility of the patient and the environment the PPG sensor was inserted inside a sterile disposable nasogastric transparent tube 20 CH (RT-2020, Pennine Healthcare, UK) which is used routinely in clinical practice, a silicon stopper was also used to prevent liquid damage to the sensor.

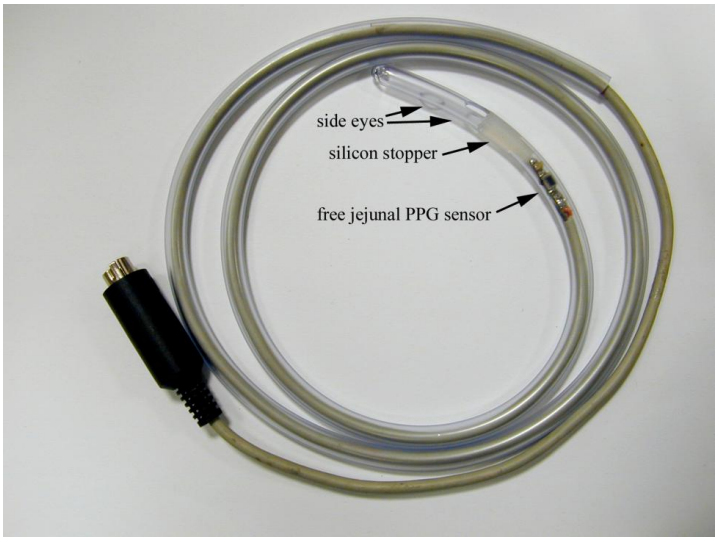

Figure 10.17: photograph of the PPG sensor inside the nasogastric tube with silicon stopper in place to prevent liquid damage to sensor.

Once the patient was anaesthetised and prepped the surgical procedure began by the ENT surgeons who carried out the tumour resection by performing a total pharyngolaryngectomy, the surgeons also isolate and prepared recipient vessels for anastomosis of the flap as shown in Figure 10.18.

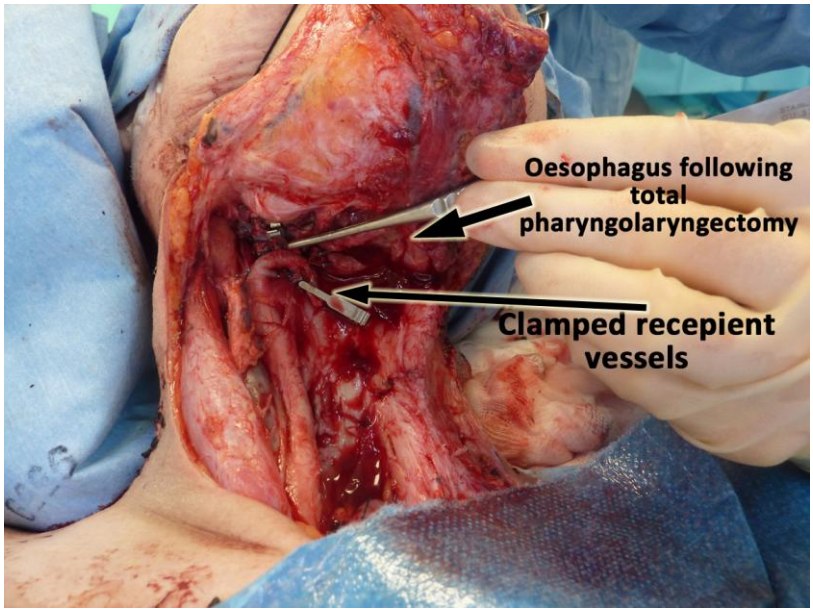

Figure 10.18: Photograph of the neck showing the distal end of the oesophagus following total pharyngolaryngectomy.

The general surgeon performed laparotomy followed by the plastic surgeon who harvested the flap. To harvest the flap, an upper abdominal incision was made. As shown in Figure 10.19, transilluminating the mesentery allows the visualization of the nutrient vessels where the arterial arcade was selected which is typically the vascular arcade of the proximal jejunum which has the most favourable anatomy.

Figure 10.19: Transillumination technique used to identify arterial arcade.

Once a chosen length of the jejunum (depending on the neck defect) was dissected with the main blood supply still attached in the donor site, the sensor in the sterile nasogastric tube was inserted in the jejunum free flap where the first measurement was obtained. The blood pressure, heart rate and SpO_2 values were recorded on the

Patient Log file on the personal laptop. Once the recording had stopped the blood vessels were then clamped and cut, the jejunum segment was then transferred to the recipient site and the vessels of the jejunum free flap and the prepared vessels in the recipient vessels in the neck were anastomosed. Prior to removal of the clamps, the sensor in the sterile nasogastric tube was inserted and hand held in the distal end of the jejunum free flap as shown in the photograph in Figure 10.20. As the patients' fingers could not be accessed in the intra-operative period, the finger PPG sensor was attached to the hallux (big toe) of the left leg. The recording was then started in order to capture the reperfusion of the flap. Once a baseline measurement was obtained the recording was continued as the plastic surgeon removed the venous followed by the arterial vessel clamps.

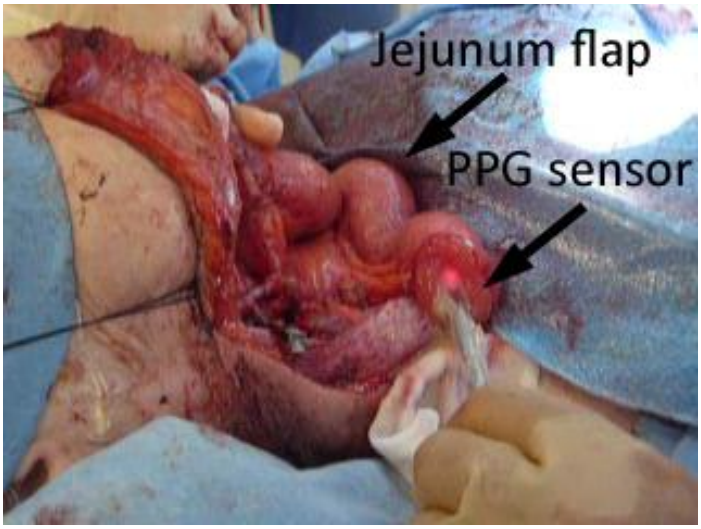

Figure 10.20: Photograph of the PPG sensor held in the distal end of the jejunum free flap to monitor its reperfusion following anastomosis of the vessels.

As the blood flow through the free flap was re-established and the surgeon was satisfied with the reperfusion of the flap, peristaltic movement and the mucous production of the flap was confirmed the recording was stopped and the PPG sensor was removed. The jejunum-oesophageal anastomosis was then performed.

The PPG sensor was then inserted through the nasal cavity and positioned in the mid segment of the flap where the final intra-operative PPG measurement took place in the operating room after the flap was re-perfused in its final position (in the recipient

site) as shown in Figure 10.21. The sensor was then secured in place to ensure the position of the sensor is not moved.

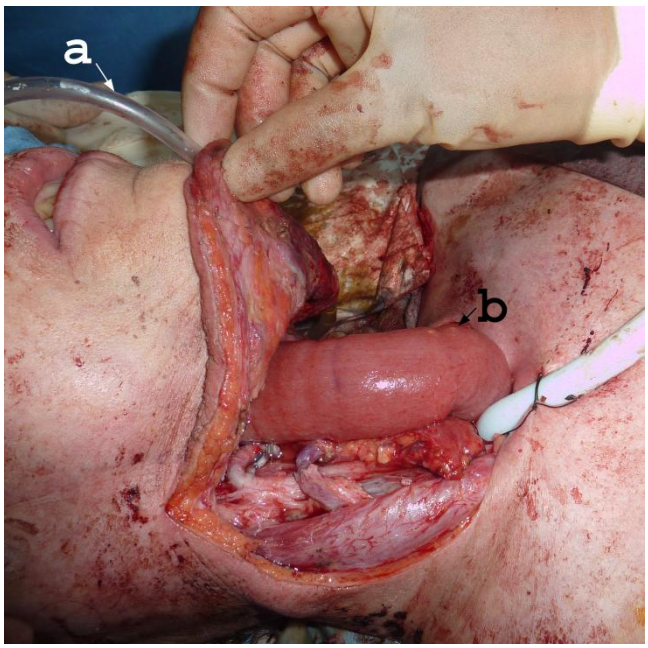

Figure 10.21: Jejunum flap sutured in recipient site; (a) jejunum PPG sensor in nasogastric tube fed through the nasal cavity; (b) the jejunum flap with PPG sensor.

Figure 10.21 shows a photograph taken intra-operatively after the upper and lower anastomosis of the jejunum and oesophagus were performed and prior to closing the surgical site with a chest drain in place.

Once the abdominal and the neck incisions were closed the patient was then transferred to the Intensive Therapy Unit (ITU) where the post-operative monitoring was performed on one of the two recruited patients. To ease transferring of the patient the PPG sensor was disconnected from the PPG processing system.

10.3.3.2 Post-operative PPG measurement

The patient was admitted to ITU as very close observations were needed due to the need for sedation overnight until the morning following the surgery. The post-operative monitoring commenced once the patient was stabilised and the ITU monitoring devices were attached for continued post surgery observations. The PPG sensor was then reconnected to the PPG processing system and the first post-operative measurement was acquired. At the Barts and The Royal London Hospital the

jejunum free flap was not monitored using any of the monitoring techniques mentioned previously. The general state of the patient was monitored continuously whilst the patients' vital signs and observations are recorded at 15 minute intervals for the first 2 hours, every 30 minutes for the following 4 hours and hourly for the subsequent 24 hours.

PPG measurements were obtained simultaneously with the routine observational checks overnight for up to 11 hours post-operatively. The patients' vital signs such as blood pressure, temperature, pulse rate and SpO_2 values from the commercial pulse oximeter were recorded.

10.3.4 Results from Case Study 3: Jejunum free flap

Intra-operative photoplethysmographic signals were successfully acquired intra-operatively in two patients undergoing reconstructive surgery of the oesophagus following pharyngolaryngectomy. Good quality PPG signals were acquired at all post-operative intervals in one patient. The results of these measurements are presented in this section.

10.3.4.1 Intra-operative results

Figure 10.22 shows typical good quality red and infrared ac and dc PPG signals obtained intra-operatively from the donor site. These signals were recorded from the jejunum prior to total dissection of the jejunum free flap with the main vessels still attached in the donor site.

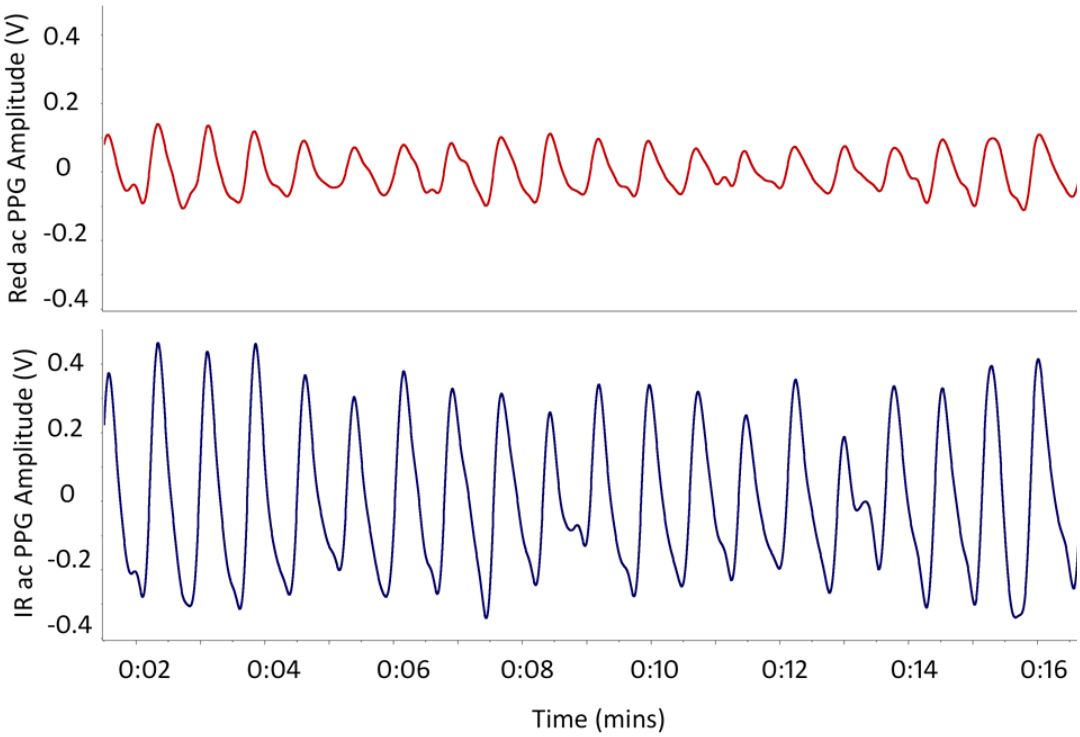

Figure 10.22: ac PPG signals obtained from the jejunum prior to flap harvesting.

As seen from the figure PPG signals with expected morphology of a typical PPG are detected from both wavelengths. This is an indication of pulsation of blood through the arterial blood supply in the tissue under observation.

The second intra-operative measurement was performed once the vessels of the jejunum free flap and the vessels in the recipient site had been anastomosed. To capture the reperfusion of the free flap as shown in Figure 10.23 the PPG processing system had been switched on as soon as it was positioned in the flap and the recording was continued as the vessel clamps were removed.

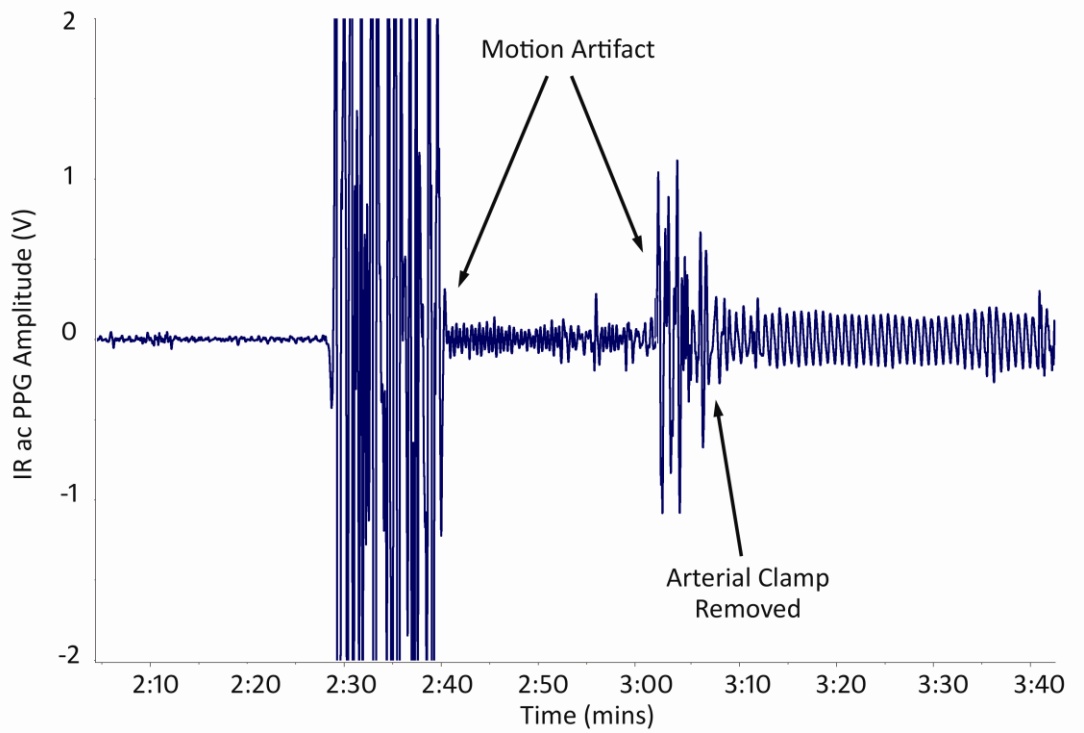

Figure 10.23: Free flap IR ac PPGs (arterial) after the arterial clamp was removed.

The infrared PPG signal detected from the jejunum free flap is shown in the figure where the arterial clamp was removed thus resulting in blood flow through the free flap. A low amplitude noise is observed in the first minute of the signal where no PPG was seen, the large amplitude signals detected at minute 2:30 and 3:00 are the result of motion artefacts caused by movement of the flap as the surgeons were preparing to remove the vessel clamps. The arterial clamp was removed at 3:05 where a sudden increase in PPG amplitude is noticed where the detected signal were in synchronous with the pulsation of the patients' heart as detected from the commercial pulse oximeter. The PPG signal detected is an indication of reperfusion of the free flap and successful flow of arterial blood through the jejunum flap.

Once the oesophageal and the jejunum free flap segment were anastomosed a final intra-operative PPG measurement was acquired. The PPG sensor in the sterile nasogastric tube was inserted through the patients' nasal cavity until positioned in the mid section of the flap. The finger PPG sensor was also attached to the patients' toe to monitor PPG signals from another site simultaneously for comparison purposes. Figure 10.24 shows a 15 second period of good quality red and infrared ac PPG signals

obtained intra-operatively from the jejunum free flap as well as infrared ac PPG signal detected from the patients' toe.

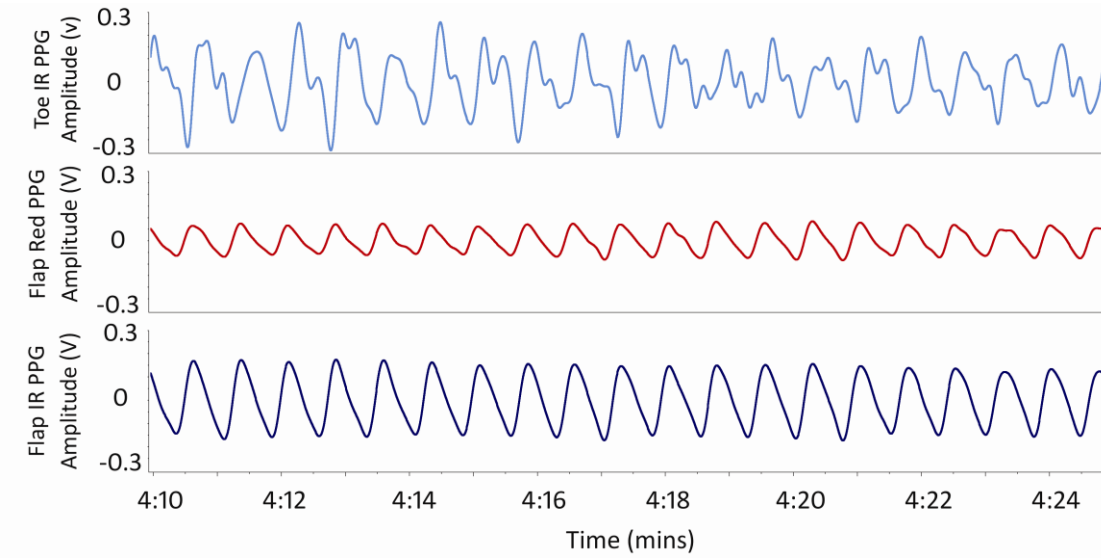

Figure 10.24: PPG signals obtained from the patients toe and free flap intra-operatively.

The PPG sensor on the toe had moved during the measurement and to continuously monitor the signal from the free flap it was not possible to adjust the sensor on the toe therefore noisy infrared and no red PPG signals could be detected.

Red and infrared ac PPG signals were successfully detected from two patients in the intra-operative period. The Table 10.1 presents the amplitude of the detected signals as well as calculations of the mean ± SD of the PPG signals from both patients.

Table 10.1: The red and infrared ac PPG amplitudes obtained from the jejunum free flap intra-operatively in two patients following the clamp removal.

	Red ac PPG Amplitude (mV)	IR ac PPG Amplitude (mV)
Patient 1	0.038	0.234
Patient 2	0.057	0.189
Mean	**0.048**	**0.212**
Standard Deviation	**0.013**	**0.032**

Post-operative monitoring of the jejunum free flap commenced upon transferring of the patient to ITU.

10.3.4.2 Post-operative results

In the first patient PPG monitoring in the post-operative period was not possible due to technical problems of the oesophageal sensor. Therefore, post-operative measurements were acquired only from one of the two patients. Figure 10.25 shows a 20 second period of typical PPG signals detected from jejunum free flap and the patients' finger one hour following surgery.

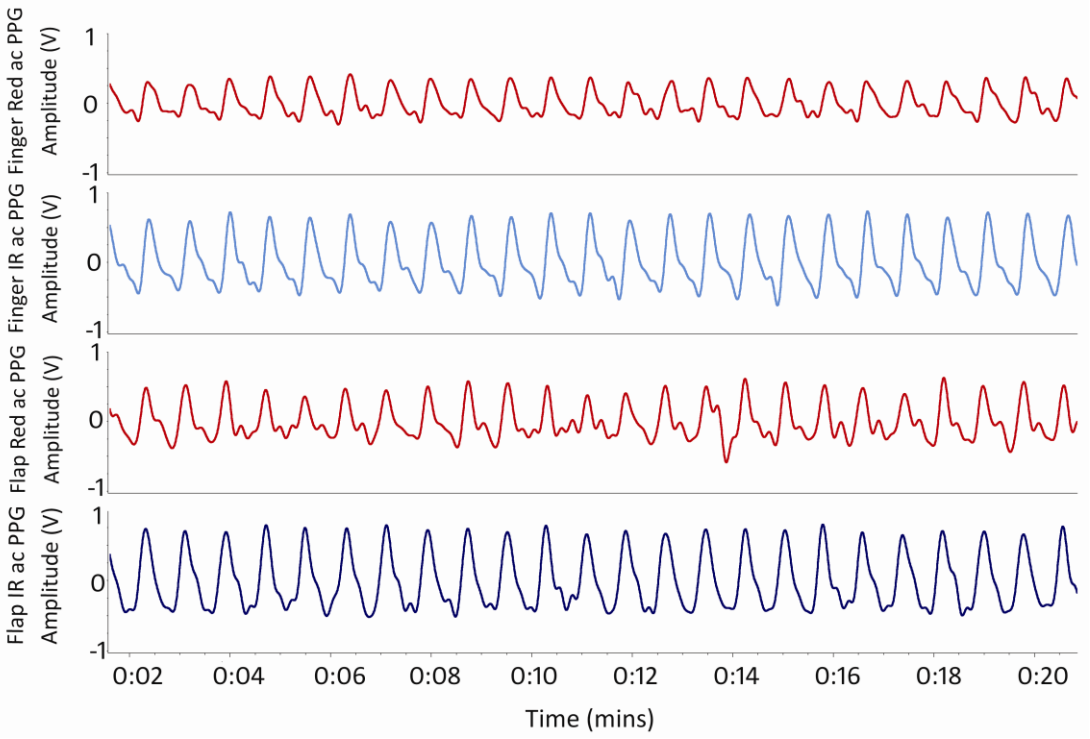

Figure 10.25: Typical red and infrared ac PPG signals detected from the free flap and finger one hour post surgery.

Red and infrared ac and dc PPG signals were successfully detected at all intervals in the post-operative period. The PPG amplitudes are plotted on a histogram as shown in Figure 10.26 in order to summarise the data.

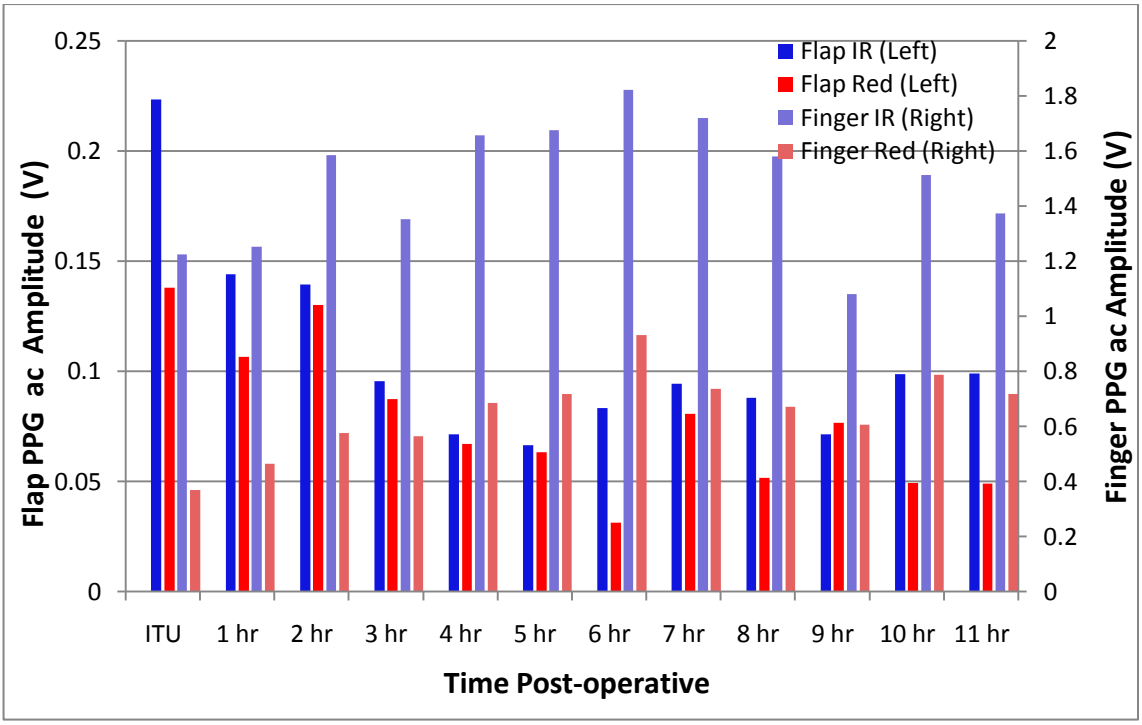

Figure 10.26: Histogram of red and infrared ac PPG signals obtained from the patients finger and free flap recorded at all post-operative intervals.

Initial observations show a gradual decrease in PPG amplitude in the first 5 hours during the post-operative period followed by a slight increase. It appears that the amplitude of the signal stabilizes from hour 7 of the post-operative period. At hour 6 the patient was diagnosed with hypovolaemia, this is a state of reduction in blood volume and plasma in blood; clinical symptoms of this condition include diminished blood pressure and absence of perfusion. From hour 6 until 9 in the post-operative period Geloplasma® (Fresenius Kabi, Germany) was administered intravenously. This could be a justification for the reduction of arterial blood volume detected which could be an indication of hypovolaemia, the slight increase in the PPG amplitude could also be due to administration of the medication which works as a plasma volume expander. However it can be observed from Figure 10.26 that the PPG signals from the patients' finger do not follow the same trend as the flap PPG signal which would confirm that the trend observed in the flap is a local trend. However, as this study was only performed on one patient there is a lack of data to draw any significant conclusions.

Simultaneous measurements of free flap and finger photoplethysmographic signals were also acquired at all post-operative periods. The mean (±SD) of the red and

infrared ac PPG signals acquired from both the flap and finger at all intervals are presented in Figure 10.27.

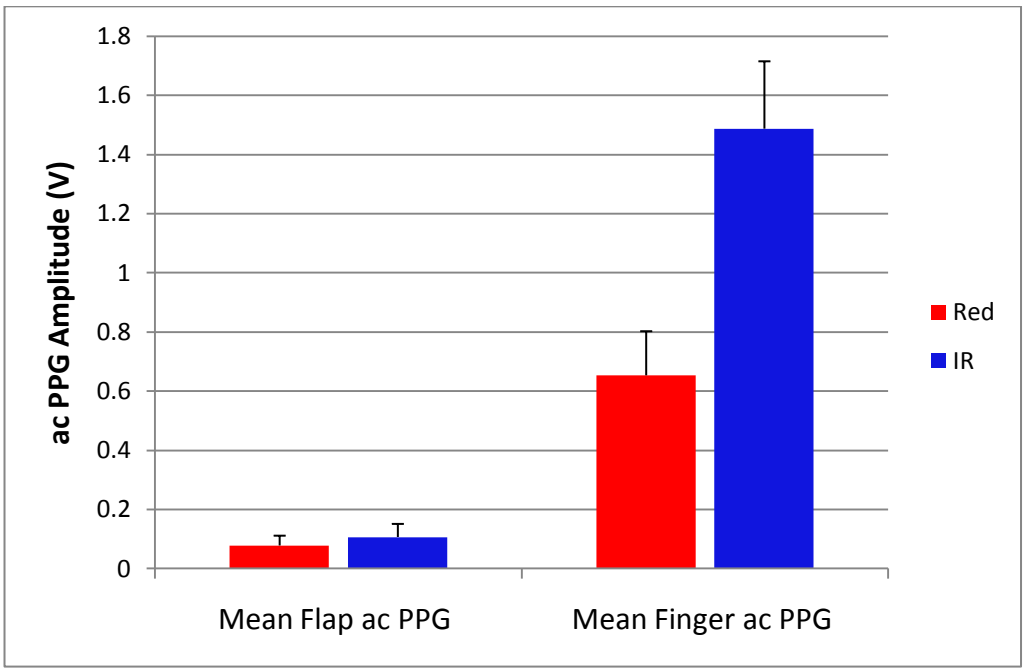

Figure 10.27: Mean (±SD) of red and infrared ac PPG signals at all intervals from finger and flap.

It can be seen that the average PPG amplitudes obtained from the finger are approximately ten times larger in amplitude than those acquired from the free flap. This is as expected since the finger is a well perfused site comparing to the jejunum free flap where the blood flow is newly re-established.

10.3.4.3 Post-operative SpO_2 estimations

Arterial oxygen saturation levels were estimated for both the finger and flap in all post-operative intervals. In addition SpO_2 values from the commercial pulse oximeter were also manually recorded at the same intervals in order to provide a comparison and confirm the accuracy of the estimation of the SpO_2 percentage of the free flap using the PPG processing system. Figure 10.28 illustrates the estimated arterial oxygen saturation values estimated at all post-operative intervals from the jejunum free flap and the finger as well as the recorded SpO_2 values from the commercial pulse oximeter used for routine observations.

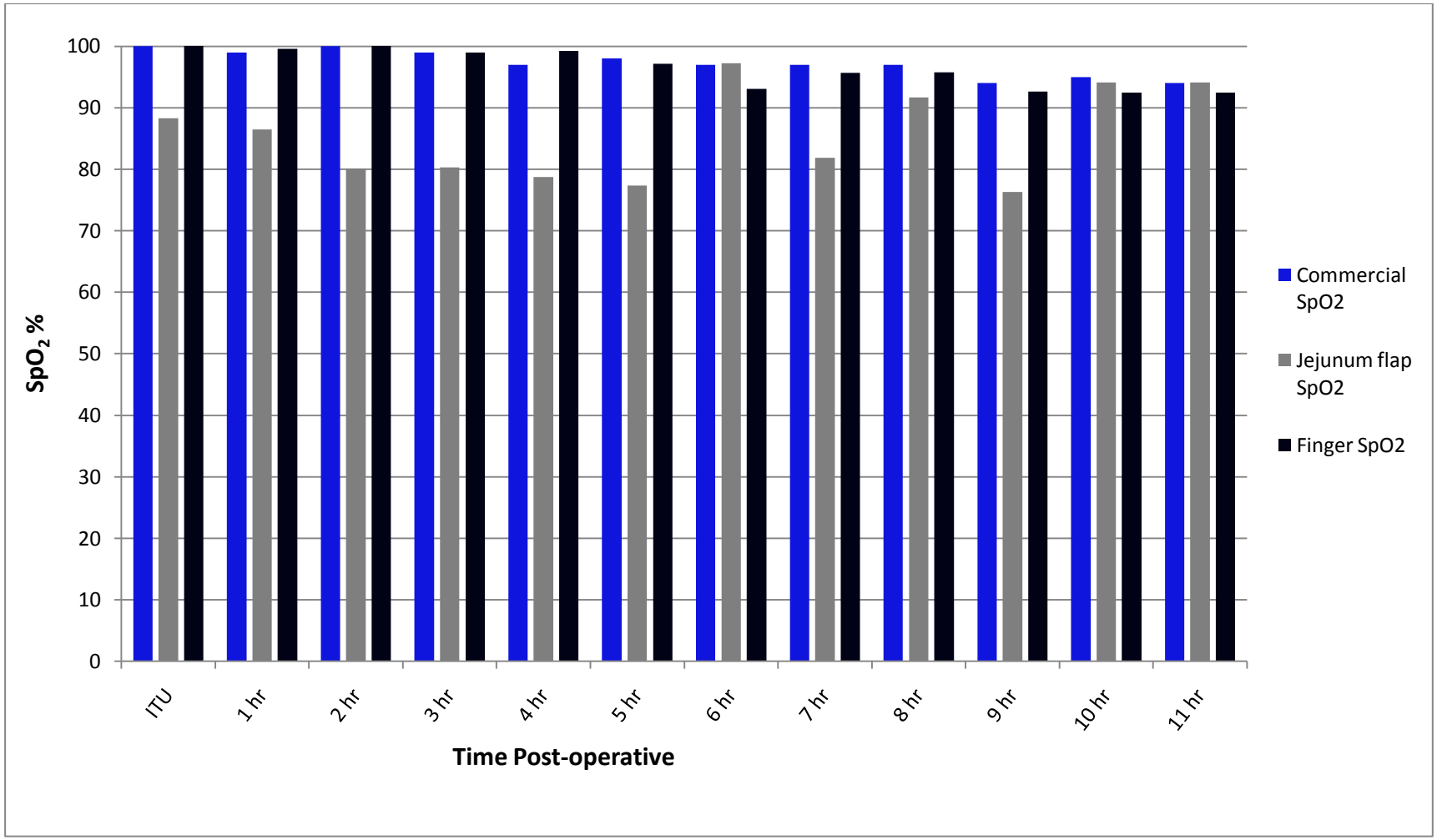

Figure 10.28: The estimated jejunum and finger SpO_2 % and the recorded SpO_2 values from the commercial pulse oximeter at all intervals during the post-operative period.

The mean (±SD) of the free flap, finger and commercial SpO_2 values were calculated in order to ease analysis of the data as shown in Figure 10.29.

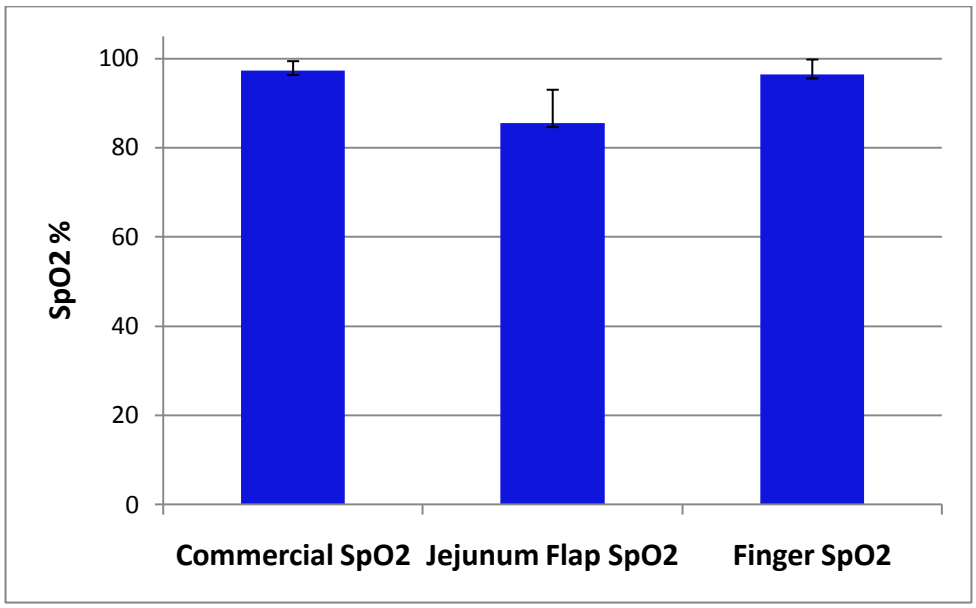

Figure 10.29: Mean (±SD) of the estimated free flap, finger and commercial SpO_2 values at all intervals.

It can be seen that the estimated finger SpO_2 values from the custom made PPG sensor and processing system are on average 0.7% lower than those recorded from the commercial pulse oximeter. It can be said that the estimated finger SpO_2 values are in broad agreement with the values recorded from the commercial pulse oximeter which is an indication of the capability of the PPG processing system accurately estimating arterial oxygen saturation levels. However, it can also be noted that the free flap values are predominantly lower than the SpO_2 values from the commercial pulse oximeter at most intervals. On average the SpO_2 values estimated from the jejunum flap were 11% lower than those from the commercial pulse oximeter.

In summery a dual-wavelength photoplethysmographic free jejunum flap perfusion sensor and processing system has been successfully designed and developed. The system was used in a pilot study for intra-operative measurements on two patients and post-operative measurements in one patient. Good quality photoplethysmographic signals, which act as an indicator of good perfusion, were acquired from the jejunum free flap during the operation and in the post-operative

period. Preliminary SpO_2 values from the jejunum sensor were calculated and were found to be lower than those from the commercial pulse oximeter, although those estimated using the finger PPG sensor were in broad agreement with the commercial finger pulse oximeter. This is the first time that a dual-wavelength (red and infrared) PPG system has been used for monitoring perfusion in free jejunum flaps as well as providing the advantage of estimating blood oxygen saturation in these flaps.

Chapter 11

Conclusions & Discussions

Following mastectomy for breast cancer a wide variety of techniques are currently available for post mastectomy breast reconstruction. One of the most common techniques used is Deep Inferior Epigastric Perforator (DIEP) free flap, which has proven to be a major advancement in transferring lower abdominal tissue for autologous breast reconstruction [1-2]. The DIEP flap is based on the deep inferior epigastric vessels, an artery and vein at the bottom of the rectus abdominis muscle. These vessels provide the primary blood supply to the skin and fat of the lower abdomen. However, due to its limited perforating vessels, there is reduced blood supply to and from the DIEP flap, so fat necrosis and partial flap loss are more common [1]. Postoperative ischaemia due to arterial occlusion, or more commonly, venous occlusion, is the most common cause of failure in microvascular free flaps.

The success of free flap reconstructive surgery depends strongly on the maintenance of adequate perfusion in the flap. Early diagnosis of ischaemia and surgical exploration to restore blood flow can often salvage the flap and may prevent graft failure. Therefore, a continuous method for monitoring perfusion of the flap would assist in early detection of inadequate blood supply. Currently in most centres the routine post operative free flap monitoring is performed by a member of the nursing staff where factors (observational) such as the flaps temperature, colour, texture and capillary refill time are monitored intermittently.

The effort of this research is to explore non-invasive optical techniques based on photoplethysmography (PPG) by developing an optical sensor and the accompanying instrumentation for investigating PPG signals from DIEP free flaps. The motivation is to create a technology which will have the capability of providing information in terms of DIEP flap monitoring more than what is currently available in hospitals today.

A prototype circular reflectance three wavelength PPG sensor with a diameter of 20 mm was designed and developed. The justification for the chosen shape and size of the sensor was the application site, which in this case is the DIEP free flap (see Chapter 6). The PPG sensor consisted of two infrared, two green and two red ceramic chip surface mount LEDs (peak emission wavelengths at 940 nm and 660 nm respectively) and a photodiode (single photodiode with an active area of 7.5 mm^2 with spectral range sensitivity between 400-1100 nm). A battery powered two channel (flap and finger) PPG processing system were constructed to drive the optical components on the sensor and to detect and pre-process photoplethysmographic signals. A virtual instrument was implemented in LabVIEW in order to display, acquire, analyse and store the PPG signals. Also, the research used the availability of the PPG signals in order to estimate blood oxygen saturation from the free flap and conduct some comparative studies with other body sites by using ac and dc, red and infrared PPG signals.

In order to verify the suitability of the developed system for clinical trials, *in vivo* experiments were performed in the laboratory. Initially a thermal test was conducted to identify if the heat radiated from the light emitting diodes used in the PPG sensor would result in undesirable thermal effect that would cause harm to the tissue under observation. It was found that the slight rise in temperature when all three LEDs were switched on would not cause thermal injury to the skin, therefore the sensor was deemed safe for use on skin. Functional test was then carried out on a healthy volunteer where by changing the intensity of the LEDs and the gain of the transimpedance amplifier PPG signals of high signal-to-noise ratio were observed from the red, green and infrared wavelengths. Following the successful acquisition of good quality red, infrared and green ac and dc PPG signals, it was concluded that the PPG processing system is safe for use on patients in clinical trials.

Approval from the Ethics Committee was obtained to study patients undergoing DIEP surgery. The preliminary clinical trials were carried out at St Andrews Centre for Burns and Plastic Surgery at Mid Essex Hospital which is one of the biggest regional specialist Plastic Surgery Units in the UK. Research & Development and individual surgeons'

approval was also acquired from the Centre. In addition, informed consent was obtained from each patient prior to the surgery.

Fifteen patients undergoing elective breast reconstructive surgery using Deep Inferior Epigastric Perforator flap were consented and recruited into the study. The PPG processing system was used to investigate changes in volume of arterial blood pulsating through the free flap and estimating the oxygen saturation of that blood. As most flap failures are due to vascular occlusion following anastomosis of free flap and recipient site vessels, the main focus of this research was to investigate the plausibility of using the developed system as a post-operative monitoring device. However, as a proof of concept to explore the reliability of the PPG processing system and sensor in detecting PPG signals and estimating SpO_2 values at all operative periods, the system was evaluated in the pre-operative and intra-operative stages of the DIEP flap reconstructive surgical procedure in six of the fifteen patients recruited.

Following successful acquisition of good quality red (n=5), green (n=4) and infrared (n=6) PPG signals with typical PPG morphology in the pre-operative period the system was evaluated intra-operatively where PPG signals were acquired using red (n=6), green (n=1) and infrared (n=6) wavelengths. The reperfusion of the free flap was also captured once the vessel clamps were removed after the anastomosis of the vessels using the infrared wavelength. This is the first time that photoplethysmographic signals from red, infrared and green wavelengths have been obtained from free flaps in the pre and intra-operative periods. Using the red and infrared PPG signals detected, the percentage of oxygen saturation (SpO_2) of the arterial blood in the free flap was also estimated. SpO_2 values from the commercial pulse oximeter attached to the patients' finger were also recorded at the time of measurement. It was found that SpO_2 values estimated from the free flap intra-operatively were on average 2% lower than the values estimated from the donor site pre-operatively. However, these investigations show that the SpO_2 values estimated from the PPG system are on average 10% lower than the values recorded from the pulse oximeter intra-operatively and 8% lower in the pre-operative period. One of the main reasons for this consistent underestimation of SpO_2 by the custom made system is the fact that is not calibrated as any other commercial pulse oximeter. Another explanation for the lower SpO_2 estimations could

be due to the excess adipose tissue in the abdomen for pre-operative measurements and the low perfusion state of the free flap following anastomosis. Lastly the low PPG pulsations at times might have also caused the inaccurate estimation of SpO_2.

The PPG processing system and sensor were also evaluated in fifteen patients post-operatively where the free flap was monitored simultaneously with the routine flap observations carried out at regular intervals over night for up to 12 hours. Investigation of the post-operative PPG measurements show that good quality PPG signals could be detected from all three wavelengths. Depending on the surgical time the length of post-operative monitoring period varied between patients as it was only possible to monitor the patient until approximately 5-6 am in the morning after the surgery. In patients where the surgery time was longer, the initial measurement was performed late in the evening following surgery. Therefore, in those cases, 12 hours of post-operative monitoring was not achieved which resulted in fewer patients monitored at 11 or 12 hours following surgery compared to the number of patients where PPG signals were obtained for in the recovery unit in the post-operative period.

Investigation of the PPG signals show that the amplitude of the green ac PPG signals are lower than those from red and infrared which is due to low penetration of green wavelength and its high absorption by blood therefore it is assumed that the PPG signal from the green wavelength is the reflected light from haemoglobin in the microcirculation or dermal capillaries [55, 111].

The use of photoplethysmography as a monitoring technique for free flaps has previously been explored by Futran *et a*l., Chubb *et al.* and Stack *et al.*; however these authors mainly investigated the use of green PPG signals in monitoring free flaps which would only provide information on the index of volume of blood in the capillaries in the post-operative period. This would only provide an indication of volume of blood in the arteries at a low penetration depth [55, 80, 112]. The developed system provides the capability of using red, green and infrared wavelengths simultaneous to monitoring changes in volume of blood flowing through the free flap at different depths of penetrations. Integration of the amplitude of PPG signals overtime will provide an index of perfusion of the flap which would in turn show how the vasculature of the flap

evolves in time. The mean of the obtained red, infrared and green ac PPG signals were plotted at each interval at all post-operative periods and initial observations show that there is a reduction in PPG amplitude after 6 hours following surgery. Many assumptions have been made regarding this change in blood volume in the flap. Pereira *et al.* explains that as free flap reconstructive surgery is typically 6-8 hours long with surgical procedures performed on the abdomen and the chest, this result in considerable blood, heat and fluid loss. If gone unnoticed this can bring about hypovolaemic vasoconstriction and hypothermia, which causes the blood flow through the flap to decrease by 50% in the first 6-12 hours following surgery [113]. However the clinical collaborators of the study have commented that hypovolaemia and hypothermia did not occur in these patients as they were looked after in specialised surgical HDU area with strict monitoring and quick intervention if physiological parameters deviated from a set value. Another explanation as suggested by our clinical collaborators was that during the ischemic period, metabolism in the flap occurs without oxygen (anaerobic metabolism) which leads to production of metabolites (or mediators) which causes dilatation of the vessels in the flap. This phenomenon occurs in the body in any anaerobic conditions to allow more blood to flow into the oxygen deprived tissues in order to get more oxygen. When the anastomosis is done and vessel clamps are removed oxygenated blood flows through the flap and starts the aerobic metabolism. Simultaneously the blood attempts to flush the metabolites accumulated in the flap. Once the metabolites are flushed out of the flap and oxygenated blood is perfusing the flap, it is unnecessary for the vessels in the flap to remain dilated. It must also be noted that there is no neural autoregulation of blood flow to the flap as the tissue is denervated. It must be considered that no study have yet been carried out on the time taken for the vasoconstriction of the vessels once the metabolites have been flushed out but it can be hypothesised that this could occur within 6-8 hours post-operatively which would explain the reduction in blood flow through the free flap.

As red and infrared ac and dc PPG signals were successfully obtained in the post-operative period, preliminary estimation of oxygen saturation levels of the blood in the tissue under observation was carried out. It was found that the SpO_2 values estimated

from the free flap were on average 11% lower than those recorded from the commercial pulse oximeter, which is 3% lower those values estimated from the donor site pre-operatively prior to dissecting and raising the flap. As was the case with pre and intra-operative period the estimated values from the free flap appear to be underestimating SpO_2 values when compared with a commercial pulse oximeter.

In order to confirm the reliability and accuracy of estimating SpO_2 values from the free flap using the custom made free flap PPG/SpO_2 sensor an identical custom made finger PPG/SpO_2 sensor was evaluated on five of the fifteen recruited patients where red, infrared and green PPG signals were successfully obtained at all post-operative intervals. It was found that the ac PPG signals detected from the patients' finger were considerably larger in amplitude in comparison with those obtained from the DIEP free flap which is due to the good blood supply in the finger in contrast with a free flap where the blood supply has newly been re-established. SpO_2 values were estimated using the ratio of ratios algorithm where initial observations show that the estimated SpO_2 values from the finger are on average approximately 7% lower than those from the pulse oximeter; these results also demonstrated that the SpO_2 values from the free flap were 17% lower than the average SpO_2 values recorded from the commercial device. This confirms that the SpO_2 values from the free flap were considerably lower which as expected due to poor perfusion of a free flap following surgery which confirms the capability of the system in estimating arterial oxygen saturation of the blood flowing through the DIEP free flap.

In this study it was not possible to compare our quantifying results with the inconclusive and qualifying results made by the clinical staff in the intensive care unit where a spreadsheet of clinical observation factors was used in order to assess the viability of the flap.

Lindsey *et al.* Menick *et al.* and Graham *et al.* used pulse oximetry for post-operative free flap monitoring, where all studies demonstrated the usefulness of pulse oximetry in monitoring free flaps. However these measurements were performed with "cannibalised" or modified commercial pulse oximeters. Lindsey used an ear probe

where the jaws were held apart using tape and Graham and colleagues also had difficulty in adapting the sensor for free flap monitoring. [86-88].

As a result of successful *in vivo* evaluation of the system on DIEP free flaps the custom made PPG processing system was further evaluated in a series of pilot studies carried out on different types of flaps. Initially the system was used in assessing the viability of flaps in 2 patients undergoing breast reconstructive surgery using Latissimus Dorsi flap at Barts and The Royal London Hospitals. Good quality PPG signals were obtained from all wavelengths intra-operatively and post-operatively as well as real-time estimation of SpO_2 values from the flap. The subsequent study was performed on a patient undergoing facial reconstruction using a free flap following cancer of the ear. In this patient the estimated SpO_2 values from the free flap were found to be in broad agreement with those from the custom made finger PPG system as well as the recorded SpO_2 values from the commercial pulse oximeter. This could be due to the proximity of the flap to the head as there is significantly better perfusion in that region.

Finally the system was used to monitor the viability of free jejunum flaps used in reconstruction of the oesophagus. However, as the jejunum and the oesophagus have a different dimension and shape to the area monitored in DIEP flaps, a new dual wavelength sensor was designed and developed. Two patients undergoing reconstruction using jejunum free flap at The Barts and The Royal London Hospital were recruited into the study, both patients were monitored intra-operatively where the re-perfusion of the flap following anastomosis of the vessels was successfully captured. The free flap was monitored for 12 hours post-operatively in one patient. Red and infrared PPG signals were successfully detected at all post-operative intervals; the patient was diagnosed with hypovolaemia after 5 hours in the post-operative period where a gradual reduction of ac PPG amplitudes was observed in the first 5 hours following surgery. An increase in PPG amplitude was noticed following intravenous administration of Geloplasma® which is used to replace the lost plasma in the blood. This is the first minimally invasive monitoring device developed for monitoring jejunum free flaps. To date there have been no reports on a technique

which would provide an indication of change in volume of blood as well as the oxygen saturation of that blood through the jejunum free flap.

These clinical studies suggest that the custom made PPG processing system is versatile and has the capability of monitoring different types of flaps where the PPG sensor can be easily modified to facilitate monitoring free flaps in various body sites.

The developed three wavelengths reflectance optical sensor used in the DIPE free flaps was unique as it has used three wavelengths within the visible and the NIRS spectrum to simultaneously investigate PPG signals obtained at all operative periods of the surgical procedure. The motivation for the chosen wavelengths is that it provides the capability of both estimating arterial blood oxygen saturation using the conventional pulse oximetry wavelengths but also using a wavelength that will allow us to monitor superficial vasculature in the flap as well as blood flow at different penetration depths where this had never been attempted previously.

This research contributes in new knowledge on the use of photoplethysmography in the understanding and monitoring of flap perfusion. PPGs and SpO_2s made possible by the developed system will enable the holistic haemodynamic mapping of flaps during the whole cycle of the surgical procedure to recovery. In conclusion the results from the *in vivo* study has demonstrated for the first time a custom made non invasive photoplethysmographic system which has the capability of monitoring and detecting changes in blood volume in the flap and accurately and reliably estimate arterial oxygen saturation of free flaps in patients undergoing breast reconstruction using DIEP flaps at all operative stages.

11.4 **Future work**

Following the investigations described in this thesis there are several lines of research arising from this project which should be pursued:

- Recruit more patients to confirm the reduction of PPG signals after 6 hours
- Monitor flap continuously
- Do mapping of flap at pre, intra and post op in order to investigate how PPG signals and SpO_2 values differ

- Measure metabolites from the vain draining the flap to note the time taken for concentration of metabolites to fall to normal in order to justify the 6 hours amplitude reduction

Appendix (i)

NHS

National Research Ethics Service

East London Research Ethics Committee 1

COPY FOR YOUR INFORMATION

Room 24, 2nd Floor Burdett House, Mile End Hospital, London E1 4DG
Telephone Number: 020 8 223 8602
Email Address: Sandra.Burke@thpct.nhs.uk

Professor Panicos Kyriacou
Professor of Biomedical Engineering
City University London
School of Engineering and Mathemati
Northampton Square
London EC1V 0HB

07 July 2010

Dear Professor Kyriacou

Study Title: **Non-invasive optical methods for monitoring free flap perfusion in plastic surgery**

REC reference number: **10/H0703/39**

Thank you for your letter of 24 June 2010, responding to the Committee's request for further information on the above research and submitting revised documentation.

The further information has been considered on behalf of the Committee by the Chair.

Confirmation of ethical opinion

On behalf of the Committee, I am pleased to confirm a favourable ethical opinion for the above research on the basis described in the application form, protocol and supporting documentation as revised, subject to the conditions specified below.

Ethical review of research sites

The favourable opinion applies to all NHS sites taking part in the study, subject to management permission being obtained from the NHS/HSC R&D office prior to the start of the study (see "Conditions of the favourable opinion" below).

The Committee has not yet been notified of the outcome of any site-specific assessment (SSA) for the non-NHS research site(s) taking part in this study. The favourable opinion does not therefore apply to any non-NHS site at present. I will write to you again as soon as one Research Ethics Committee has notified the outcome of a SSA. In the meantime no study procedures should be initiated at non-NHS sites.

Conditions of the favourable opinion

The favourable opinion is subject to the following conditions being met prior to the start of the study.

Management permission or approval must be obtained from each host organisation prior to the start of the study at the site concerned.

For NHS research sites only, management permission for research ("R&D approval") should be obtained from the relevant care organisation(s) in accordance with NHS research governance arrangements. Guidance on applying for NHS permission for research is available in the Integrated Research Application System or at http://www.rdforum.nhs.uk. *Where the only involvement of the NHS organisation is as a Participant Identification Centre, management permission for research is not required but the R&D office should be notified of*

the study. Guidance should be sought from the R&D office where necessary.

Sponsors are not required to notify the Committee of approvals from host organisations.

It is the responsibility of the sponsor to ensure that all the conditions are complied with before the start of the study or its initiation at a particular site (as applicable).

Approved documents

The final list of documents reviewed and approved by the Committee is as follows:

Document	*Version*	*Date*
Investigator CV		17 March 2010
Letter of Access - Mr N.S. Niranjan		
Confirmation of Indemnity - City University London		01 August 2009
REC application		17 February 2010
Covering Letter		17 March 2010
Response to Request for Further Information		24 June 2010
Participant Consent Form	1.3	11 February 2010
Amended Protocol	1.4	24 June 2010
Amended Patient Information Sheet	1.4	24 June 2010
Referees or other scientific critique report		19 January 2010

Statement of compliance

The Committee is constituted in accordance with the Governance Arrangements for Research Ethics Committees (July 2001) and complies fully with the Standard Operating Procedures for Research Ethics Committees in the UK.

After ethical review

Now that you have completed the application process please visit the National Research Ethics Service website > After Review

You are invited to give your view of the service that you have received from the National Research Ethics Service and the application procedure. If you wish to make your views known please use the feedback form available on the website.

The attached document *"After ethical review – guidance for researchers"* gives detailed guidance on reporting requirements for studies with a favourable opinion, including:

- Notifying substantial amendments
- Adding new sites and investigators
- Progress and safety reports
- Notifying the end of the study

The NRES website also provides guidance on these topics, which is updated in the light of changes in reporting requirements or procedures.

We would also like to inform you that we consult regularly with stakeholders to improve our service. If you would like to join our Reference Group please email referencegroup@nres.npsa.nhs.uk.

10/H0703/39	**Please quote this number on all correspondence**

Yours sincerely

P.P. Senior Research Ethics Administrator
A. T. Tucker BSc(Hons) PhD SRCS
Chairman
East London Research Ethics Committee 1
(Formerly known as East London and The City REC)

Enclosures: "After ethical review – guidance for researchers"
Copy to: *Dr Justin Phillips, City University London*

Mid Essex Hospital Services NHS
NHS Trust

Trust Approval Letter

Date 04/10/2010
Our Ref R&D 782
MEHT not Sponsor Version 2: 14 May 04

Research and Development
First Floor Broomfield Court
Broomfield Hospital
Chelmsford
Essex, CM1 7ET
Tel: 01245 514210
Fax: 01245 514678
neiljayasinghe@mehft.nhs.uk

Prof Sandip Pal
Consultant Anaesthetist
MEHT, Court Road
Chelmsford, CM1 7ET

RE: Non-invasive optical methods for measurement of free flap perfusion in plastic surgery

R&D: 782

Dear Prof Pal,

I am pleased to inform that the above project has been approved by Mid Essex Hospital Services NHS Trust (MEHT). Furthermore, MEHT has not agreed to act as Research Sponsor but City University has (see later for a description of the duties of Sponsor).

This approval is conditional on your agreement to accept and abide by:

- the Trust's Policies (including but not limited to the R&D Policy, given overleaf);
- the requirements of Research Governance (responsibilities of Principle Investigator and other researchers given): http://www.doh.gov.uk/research/rd3/nhsrandd/researchgovernance/govhome.htm
- the procedures issued by the Trust's R&D Department (available on request) and
- the requirement to notify the R&D Office if any significant developments[1] occur as the study progresses, whether in relation to the safety of individuals or to scientific direction
- obtaining an honorary contract for Mid Essex Hospital Services NHS Trust (if required) prior to starting the research and ensuring that this is kept up-to-date
- to ensure that any co-investigator who is not an employee of Mid Essex Hospital Services NHS Trust has an up-to-date honorary contract with the Trust
- Compliance with the Data Protection Act (1998) and Caldicott Principles

Please note if you are Principle Investigator (instead of Site PI) then you are responsible to ensure that the local responsibilities of Chief Investigator are met. A list of key references to guidance is given later in this letter. One aspect of this is that you must ensure that a research file is kept for possible future monitoring. Guidance on content is attached.

So that the R&D office can complete a number of governance requirements on your behalf, I should be most grateful if you could send the following to the R&D Office:

- A copy of each signed patient consent form within two weeks of obtaining it (if applicable).
- A copy of all correspondence to and from the Main Research Committee (to include any amendment to the protocol, notification of any adverse events etc).

[1] These include serious adverse events, serious adverse reactions and unexpected serious adverse reactions, as defined in the Medicines for Human Use (Clinical Trials) Regulations 2004.

- At the end of the financial year or when the project ends please complete and submit a project status form (attached).

As a condition of Trust and ethical approval (and to meet the requirements of the Serious Incident Policy), all of the following, occurring in Mid Essex Hospital Services NHS Trust patients are reported using the Datix System. The word '***research***' must be included in the synopsis. It is also a legal requirement to report any incidents which are covered under Health and Safety.

Adverse Drug Reaction (ADR)

In the pre-approval clinical experience with a new medicinal product or its new usages, particularly as the therapeutic dose(s) may not be established, all noxious and unintended responses to a medicinal product related to any dose should be considered adverse drug reactions. The phrase responses to a medicinal product means that a causal relationship between a medicinal product and an adverse event is at least a reasonable possibility, i.e. the relationship cannot be ruled out. Regarding marketed medicinal products: a response to a drug which is noxious and unintended and which occurs at doses normally used in man for prophylaxis, diagnosis, or therapy of diseases or for modification of physiological function.

Unexpected Serious Adverse Reaction

Any untoward medical occurrence that at any dose that:

- results in death
- is life-threatening
- requires inpatient hospitalization or prolongation of existing hospitalization,
- results in persistent or significant disability/incapacity or
- is a congenital anomaly/birth defect

Please remember to keep the R&D Office informed of presentations/posters/abstracts that arise from this research and send in copies of any papers, reports or theses. The building up a library of R&D at the Trust will help others.

I would like to take this opportunity to wish you every success with your project. The R&D Office is here to help you with all aspects of R&D, please contact the R&D Office in the first instance.

If you do not accept these terms and conditions then you should notify the R&D Department within 20 days of the issue of this letter.

Yours sincerely

.....

Dr David Blainey
Medical Director MEHT
Corporate Office
Broomfield Hospital
Court Road, Chelmsford
Essex, CM1-7ET

Professor Sandip Pal
Director of Research & Development

04 SEP 2010

Mid Essex Hospital Services NHS Trust
Broomfield Hospital
Broomfield Court, 1st Floor, Court Road
Chelmsford, CM1 7ET

Mid Essex Hospital Services NHS
NHS Trust

PATIENT INFORMATION SHEET

Ver 1.4 *Date – 24 June 2010*

Non-invasive optical sensor for the measurement of free flap perfusion in plastic surgery

1. Invitation

You are being invited to take part in a research study. Before you decide whether or not to take part, it is important for you to understand why the research is being done and what it will involve. Please take time to read the following information carefully, and discuss it with others if you wish.

Ask us if there is anything that is not clear, or if you would like more information. Take time to decide whether or not you wish to take part.

2. What is the purpose of the study?

A new type of optical sensor has been developed to measure the blood content and pulsation of blood in tissue. A potentially useful application of this technology has been identified whereby the blood supply to tissue transplanted in plastic surgery may be assessed. The health of the transplanted tissue depends on an adequate blood supply and it is hoped that using a probe similar to one we have developed may provide a simple and efficient 'early warning' of reduced blood supply, with greater accuracy and reliability than existing methods. The optical probe is roughly the size of a fifty-pence piece and is placed on the skin surface for several seconds whenever a measurement is required. Light passes into the tissue and the quantity of blood and the degree of pulsation is recorded from the intensity of the light returning to a light sensor in the probe.

3. Why have I been chosen?

The study aims to evaluate this measurement system in patients undergoing free flap plastic microsurgery.

4. Do I have to take part?

No. It is up to you to decide whether or not to take part. If you decide to take part you will be given this information sheet to keep and be asked to sign a consent form to confirm that you understand what is involved when taking part in this study. If you decide to take part you are free to leave the study at any time and without giving a reason. A decision to withdraw at any time, or a decision not to take part, will not affect the quality of care or planned treatment you receive.

5. What will happen to me if I take part?

During the operation the developed probe will be placed on the flap surface and measurements will be recorded. You will of course be asleep during this time. In the post operative period, when you will be awake, monitoring of the free flap will be done every 2 hours for the first 12 hours, then every 4 hours for the next 24 hours and this will be done every time the dressings

are removed for the site to be checked by a clinician and this should take no more than 5 minutes each time.

6. What are the side effects and risks of any treatment received when taking part?

No side effects are anticipated as the probe is non-invasive and uses red and near infrared light. Similar probes have been used routinely on the finger and earlobes of people in hospitals around the world for over twenty years with virtually no reported side effects.

7. What are the possible benefits of taking part?

There are no benefits or risks for you as a patient, but it is hoped that the results obtained from the proposed study will lead to the development of new techniques for monitoring transplanted tissue and provide information regarding the supply of blood to the tissue, leading to improved outcomes for this type of surgery in the future.

8. What if there is a problem?

If you have a concern about any aspect of this study, you should ask to speak with the researchers who will do their best to answer your question. If you remain unhappy and wish to complain formally, you can do this through the NHS Complaints Procedure. Details can be obtained from the hospital.

9. Will my taking part in this study be kept confidential?

Yes. All the information about your participation in this study will be kept confidential.
If you decide you would like to take part then please read and sign the consent form. You will be given a copy of this information sheet and the consent form to keep. A copy of the consent form will be filed in your patient notes, one will be filed with the study records and one may be sent to the Research Sponsor.

You can have more time to think this over if you are at all unsure.

Thank you for taking the time to read this information sheet and to consider this study.

Mid Essex Hospital Services NHS
NHS Trust

Research Participant Consent Form

Title of Project: **Non-invasive optical methods for measurement of free flap perfusion in plastic surgery**

Ver 1.3 *Date: 11 Feb 2010*

(Delete as appropriate)

➢ I confirm that I have read and understood the information sheet for the above study (version 1.4, date – 24 June 2010) and what my contribution will be.	Yes	No
➢ I have been given the opportunity to ask questions (face to face, via telephone or e-mail)	Yes	No
➢ I have read and understand all the proposed risks and benefits for the procedure.	Yes	No
➢ I understand that my participation is voluntary and that I can withdraw from the research at any time **without giving any reason**	Yes	No
➢ **I agree to take part in the above study**	Yes	No

Name of participant .....

Signature .....

Date .....

Name of researcher taking consent .....

Signature .....

The Faculty of Pharmaceutical Medicine has accredited this course for 9 Continuing Professional Development credits.

GCP web–based training course designed and developed by

INFONETICA

Ashford and St. Peter's Hospitals NHS
NHS Trust

Certificate Of Achievement

This is to certify that
Tina Zaman
of city university

has successfully passed a web–based examination covering all aspects of the International Conference on Harmonisation: Good Clinical Practice Guideline and EU GCP Directives – Good Clinical Practice Guideline Course

31 August 2010

(Recommended renewal date: 31 August 2012)

Certificate No: 12696–1–17047

Course Director
Dr Isaac John, Hon Lecturer
Royal Holloway, University of London
Assistant Director Research & Development
Ashford & St Peter's Hospitals NHS Trust

Royal Holloway
University of London

Endorsed by
Professor George Dickson
Head, School of Biological Sciences
Royal Holloway, University of London

Mid Essex Hospital Services NHS
NHS Trust

Miss Tina Zaman,
Biomedical Engineering,
City University,
Northampton Square,
London,
EC1V 0HB

Friday 28th September 2012

Dear Miss Zaman,

Honorary Research Contract – "Non-invasive optical monitoring of free flap perfusion" Study

I am pleased to offer you an honorary research contract in Mid Essex Hospital Services NHS Trust. I would be grateful if you would sign the attached three contracts, keep one yourself and return the other two to Paul Roberts at the address below. We will then send a copy of the signed contract to your substantive employer.

The contract if accepted by you begins on 28th September 2012 and ends on 30th June 2013 unless terminated earlier in accordance with the clauses in the contract. ***Please note that you cannot start the research until the Principal Investigator has received a letter from us giving permission to conduct the project.***

We will not reimburse any expenses you incur in the course of your research unless we have agreed to do so by prior arrangement. Similarly, we accept no responsibility for damage to or loss of personal property.

Your Research Passport Form may be subject to random checks carried out by us within the lifetime of the project. The information it contains must therefore remain up to date and accurate.

If your circumstances change in relation to your health, criminal record, ISA Registration status where applicable, professional registration or any other aspect that may impact on your suitability to conduct research, or your role in research changes, you must inform your employer through its normal procedures. You must also inform your nominated manager in this NHS organisation (Prof. Sandip Pal)

Where required by law, your HEI employer will initiate your Independent Safeguarding Authority (ISA) registration, and thereafter, will continue to monitor your ISA registration status via the on-line ISA service. Should you cease to be ISA-registered, this honorary research contract is immediately terminated. Your employer will immediately withdraw you from undertaking this or any other regulated activity. You MUST stop undertaking any regulated activity.

Once you have signed and returned two of the attached contracts, you should contact the R&D Department of this organisation, who will arrange for you to be issued with an ID badge.

Yours sincerely

Kay Rainsby,
Head of HR Operations,
Mid Essex Hospital Services NHS Trust

cc: **Paul Roberts**, Research Office, Building 2 Spencer Close, St Margaret's Hospital, The Plain, Epping, Essex CM16 6TN
C. Cremin, HR Advisor, City University, Northampton Square, London, EC1V 0HB

HONORARY RESEARCH CONTRACT BETWEEN

NHS organisation(s): Mid Essex Hospital NHS Trust

AND

Name: Miss Tina Zaman

Employer: City University, London
OR Place of Study:

Report To:
(Principal Investigator/Head of Department): Professor Sandip Pal

PERIOD of AGREEMENT

From: 28/09/2012 To: 30/06/2013

OR
Fixed term contract for: years months Effective Date:

SIGNATURES

Researcher: Date: 22/11/2012

Name: Miss Tina Zaman

On behalf of the NHS organisation(s): Kay Rainsby
Mid Essex Hospital Services NHS Trust
Date: 25.9.12

Name:

Whereas

A. The Researcher named in this Agreement ("the Researcher") is employed by the employing organisation named in this Agreement ("the Employer") to undertake research, during the course of which the Researcher requires access to the Trust(s) named in this Agreement ("the Trust(s)"), their premises, patients, their clinical samples, and clinical and personal information ("the Facilities"). Where independent contractors and their premises are involved with research activity, the Agreement is issued by the host PCT on behalf of the independent contractors.

B. The Trust(s) provide healthcare services to NHS patients, including patients who are protected by the criminal record disclosure arrangements.

C. The Trust(s) and Researcher have entered into this agreement whereby the Researcher can have access to the Facilities of the Trust(s) to conduct such research as confirmed in writing in the letter of permission for research from this NHS organisation, subject to the conditions below.

1. Status

The title and status of this Honorary Research Contract does not create an employment relationship and attracts no remuneration from the Trust(s). Its award will be subject to: a satisfactory criminal record disclosure if the research includes the categories of patients who are included in the criminal record disclosure arrangements; checks against the Independent Safeguarding Authority (ISA) barred lists, and on-going ISA registration, where this is a legal requirement; confirmation of registration with the GMC or other appropriate professional body if the Researcher is required to maintain such professional registration; and confirmation that the Researcher's health does not constitute a risk to patients of the Trust(s), employees of the Trust(s) or visitors to the Trust(s).

2. Reporting Arrangements

The Researcher shall report to the Principal Investigator/Head of Department named in this Agreement whilst conducting research under this Agreement.

3. Policies and Procedures

3.1. The terms and conditions of employment of the Researcher including applicable policies and procedures are determined by the Employer and the Researcher will be carrying out duties at the Trust(s) in accordance with the contract of employment with the Employer

3.2. In carrying out research under the terms of this Agreement, the Researcher agrees to act at all times in accordance with the policies and procedures of the Trust(s) including the Research Governance Framework, copies of which are available upon request.

3.3. The Researcher is required to co-operate with the Trust(s) in discharging relevant duties under the Health and Safety at Work etc Act 1974 and other health and safety legislation and to take reasonable care for the health and safety of himself/herself and others while on the premises of the Trust(s). The Researcher must observe the same standards of care and propriety in dealing with patients, staff, visitors, equipment and the premises as is expected of any other contract holder and must act appropriately, responsibly and professionally at all times.

3.4. The Researcher agrees to accept any variation to this Agreement necessitated by changes to research and development guidance issued by the Department of Health.

3.5. In the event of sickness or unavoidable absence, the Researcher must notify her/his line manager and/or the Trust(s) immediately. The Researcher must report any accident or injury, arising out of or in the course of her/his activities at the Trust(s) and make appropriate records and statements as required.

3.6. Adverse events or incidents arising from the research should be reported immediately in compliance with the policies of the Trust(s).

4. Confidentiality

Information concerning the Facilities is confidential and must not be disclosed under any circumstances. The Researcher must treat all material connected with her/his presence in the Trust(s) in accordance with the NHS Confidentiality Code of Practice and the Data Protection Act 1998 (which covers information concerning individuals stored in any systems belonging to the Trust(s)). Unauthorised disclosure could lead to prosecution under the terms of the Act.

5. Legal Claims

5.1. The Trust(s) agrees/agree to indemnify the Researcher for any claims in negligence in respect of those patients of the Trust(s) to whom the Researcher provides care and treatment when performing duties in accordance with this Agreement.

5.2. The Trust(s) takes/take no responsibility for any claims against the Researcher arising from her/his negligent acts or omissions in undertaking agreed programmes of research using the Facilities of the Trust(s) where these are covered by warranties or conditions of any third party contracts signed by the Employer/Place of Study.

5.3. The Researcher is therefore advised either to ensure that the Employer/Place of Study maintains adequate indemnity arrangements or, if not, maintains membership of her/his medical defence organisation or has other professional indemnity arrangements in place before starting to use the Facilities of the Trust(s).

5.4. The Trust(s) accepts/accept no responsibility for damage to or loss of the Researcher's personal property.

5.5. The Trust(s) accepts/accept no legal liability in respect of any decision it/they may take to terminate this contract pursuant to section 9 below.

6. Complaints and misconduct

6.1. The Researcher should raise any complaints against the Trust(s) with the Employer/Place of Study.

6.2. Complaints or allegations against the Researcher will be dealt with in accordance with the policies and procedures of the Employer/Place of Study. Partnership between the Trust(s) and the Employer/Place of Study will be assured.

6.3. The Researcher agrees to comply with any requests for data, information or documents from the Trust(s) or the Employer/Place of Study as part of any investigation of a complaint or of suspected misconduct.

9.7. It is the obligation of the Researcher to disclose any mitigating circumstances that may affect the Agreement such as a change in criminal record, registration, employment or occupational health status.

10. The Researcher warrants that she/he has the relevant skills and expertise to undertake the research for which she/he is permitted to use the Facilities of the Trust(s) and is supported through suitable professional development programmes or training by the Employer/Place of Study or research sponsor, to ensure that she/he is suitable to undertake research.

Mid Essex Hospital Services NHS

NHS Trust

Trust Approval for Amendment

Research and Development
First Floor Broomfield Court
Broomfield Hospital
Chelmsford
Essex, CM1 7ET
Tel: 01245 514210
Fax: 01245 516908
neil.jayasinghe@meht.nhs.uk

Date 28th July 2011
Our Ref R&D 782-Jul11

Prof Sandip Pal
Consultant Anaesthetist
MEHT, Court Road
Chelmsford, CM1 7ET

RE: Non-invasive optical methods for measurement of free flap perfusion in plastic surgery

R&D: 782-Jul11 **REC Reference No: 10/H0703/39**

Dear Prof Pal,

I am pleased to confirm that the following documents have been reviewed and approved by Mid Essex Hospital Services NHS Trust and as in the Trust Approval letter dated 04th October 2010 MEHT has NOT agreed to act as Sponsor;

Document	Version	Date
Participant Consent Form	1.6	31st January 2011
Participant Information Sheet	1.6	31st January 2011
Protocol	1.6	31st January 2011
Notice of Substantial Amendment (non-CTIMPs)	1	31st January 2011
Covering Letter		11th February 2011

The approval of amendments is subject to any conditions in the Trust Approval letter dated 04th October 2010.

Yours Sincerely

Dr Ronan Fenton
Medical Director MEHT
Corporate Office
Broomfield Hospital
Court Road, Chelmsford
Essex, CM1-7ET

Professor Sandip Pal
Director of Research & Development
15 AUG 2011
Mid Essex Hospital Services NHS Trust
Broomfield Hospital
Broomfield Court, 1st Floor, Court Road
Chelmsford, CM1 7ET

NHS
National Research Ethics Service

NRES Committee London - City & East
Room 24, 2nd Floor
Burdett House
Mile End Hospital
Bancroft Road
London
E1 4DG

Tel: 020 8223 8602

04 April 2011

Professor Panicos Kyriacou
Professor of Biomedical Engineering
City University London
School of Engineering and Mathematics
Northampton Square
London
EC1V 0HB

Dear Professor Kyriacou

Study title:	**Non-invasive optical methods for monitoring free flap perfusion in plastic surgery**
REC reference:	**10/H0703/39**
Amendment number:	**1**
Amendment date:	**31 January 2011**

The above amendment was reviewed at the meeting of the Sub-Committee held on 31st March 2011.

Ethical opinion

The members of the Committee taking part in the review gave a favourable ethical opinion of the amendment on the basis described in the notice of amendment form and supporting documentation.

Approved documents

The documents reviewed and approved at the meeting were:

Document	Version	Date
Participant Consent Form	1.6	31 January 2011
Participant Information Sheet	1.6	31 January 2011
Protocol	1.6	31 January 2011
Notice of Substantial Amendment (non CTIMPs)	1	31 January 2011
Covering Letter		11 February 2011

Membership of the Committee

The members of the Committee who took part in the review are listed on the attached sheet.

R&D approval

All investigators and research collaborators in the NHS should notify the R&D office for the relevant NHS care organisation of this amendment and check whether it affects R&D approval of the research.

Statement of compliance

The Committee is constituted in accordance with the Governance Arrangements for Research Ethics Committees (July 2001) and complies fully with the Standard Operating Procedures for Research Ethics Committees in the UK.

10/H0703/39:	Please quote this number on all correspondence

Yours sincerely

Dr Arthur T. Tucker
Chair

E-mail: sandra.burke@thpct.nhs.uk

Enclosures: *List of names and professions of members who took part in the review*

Copy to: *Dr Justin Phillips, School of Engineering and Mathematical Sciences*

NRES Committee London - City & East

Attendance at Sub-Committee of the REC meeting on 31st March 2011

Name	*Profession*	*Capacity*
Dr Louise Abrams	Pharmacology (Vice Chair)	Expert
Dr Arthur T. Tucker	Principal Clinical Scientist & Senior Lecturer (REC Chairman)	Expert

Barts and The London
School of Medicine and Dentistry

Barts and The London NHS
NHS Trust

FINAL R&D APPROVAL

Joint Research and Development Office
Queen Mary Innovation Centre
5 Walden Street
Whitechapel
London
E1 2EF

Tel: 0207 882 7250
Fax: 0207 882 7276

28th September 2011

Professor Richard Langford
Pain and Anaesthesia Research Centre
St Bartholomew's Hospital
Unit 11 Dominion House
West Smithfield
London
EC1A 7BE

Dear Professor Langford,

Protocol: **Non-invasive optical methods for measurement of reconstructive flap perfusion in plastic surgery**
ReDA Ref: **007921 BLT**
REC Ref: **10/H0703/39**

I am pleased to inform you that the Joint R&D Office for Barts and The London NHS Trust and Queen Mary, University of London, has approved the above referenced study and in so doing has ensured that there is appropriate indemnity cover against any negligence that may occur during the course of your project. Approved study documents are as follows:

Type	Version	Date
REC Approval		17 February 2011
REC Application		07 July 2011
Response to request for further information		24 June 2011
Notice of Substantial Amendment – Amendment 1, dated 31 January 2011	1	31 January 2011
REC Approval for Amendment 1, dated 31 January 2011		04 April 2011
Protocol	1.6	31 January 2011
Participant Information Sheet	1.6	31 January 2011
Participant Consent Form	1.6	31 January 2011
Confirmation of indemnity – City University London		01 August 2009
Letter of access – Ms Tina Zaman		09 September 2011

Please note that all research within the NHS is subject to the Research Governance Framework for Health and Social Care, 2005. If you are unfamiliar with the standards contained in this document, or the BLT and QMUL policies that reinforce them, you can obtain details from the Joint R&D Office or go to:
http://www.dh.gov.uk/en/Publicationsandstatistics/Publications/PublicationsPolicyAndGuidance/DH_4108962

You must stay in touch with the Joint R&D Office during the course of the research project, in particular:

- If there is a change of Principal Investigator
- When the project finishes
- If amendments are made, whether substantial or non-substantial

This is necessary to ensure that your R&D Approval and indemnity cover remain valid. Should any Serious Adverse Events (SAEs) or untoward events occur it is **essential** that you inform the Sponsor within 24 hours. If patients or staff are involved in an incident, you should also follow the Trust Adverse Incident reporting procedure or contact the Risk Management Unit on 0207 480 4718.

We wish you all the best with your research, and if you need any help or assistance during its course, please do not hesitate to contact the Office.

Yours sincerely

Gerry Leonard, Head of Research Resources

Copy to: Ms Tina Zaman, City University
Ms Anna Ramberg, CRIDO, City University, Northampton Square, London.

Barts and The London NHS
NHS Trust

Joint Research and Development Office
Lower Ground Floor
Queen Mary's Innovation Centre
5 Walden Street
London
E1 2EF

Tel: 020 7882 7274
Fax: 020 7882 7276
Email: nicholas.good@bartsandthelondon.nhs.uk

Our ref: LOA-UR

Ms Tina Zaman
City University
Northampton Square
London
EC1V 0HB

9th September 2011

Dear Ms Zaman

Letter of access for research

This letter confirms your right of access to conduct research through Barts and the London NHS Trust for the purpose and on the terms and conditions set out below. This right of access commences with immediate effect and ends on 1st October 2012 unless terminated earlier in accordance with the clauses below.

You have a right of access to conduct such research as confirmed in writing in the letter of permission for research from this NHS organisation. Please note that you cannot start the research until the Principal Investigator for the research project has received a letter from us giving permission to conduct the project.

The information supplied about your role in research at Barts and the London NHS Trust has been reviewed and you do not require an honorary research contract with this NHS organisation. We are satisfied that such pre-engagement checks as we consider necessary have been carried out.

You are considered to be a legal visitor to Barts and the London NHS Trust premises. You are not entitled to any form of payment or access to other benefits provided by this NHS organisation to employees and this letter does not give rise to any other relationship between you and this NHS organisation, in particular that of an employee.

While undertaking research through Barts and the London NHS Trust, you will remain accountable to City University but you are required to follow the reasonable instructions of Prof Richard Langford in this NHS organisation or those given on his behalf in relation to the terms of this right of access.

Where any third party claim is made, whether or not legal proceedings are issued, arising out of or in connection with your right of access, you are required to co-operate fully with any investigation by this NHS organisation in connection with any such claim and to give all such assistance as may reasonably be required regarding the conduct of any legal proceedings.

You must act in accordance with Barts and the London NHS Trust policies and procedures, which are available to you upon request, and the Research Governance Framework.

You are required to co-operate with Barts and the London NHS Trust in discharging its duties under the Health and Safety at Work etc Act 1974 and other health and safety

legislation and to take reasonable care for the health and safety of yourself and others while on Barts and the London NHS Trust premises. You must observe the same standards of care and propriety in dealing with patients, staff, visitors, equipment and premises as is expected of any other contract holder and you must act appropriately, responsibly and professionally at all times.

You are required to ensure that all information regarding patients or staff remains secure and *strictly confidential* at all times. You must ensure that you understand and comply with the requirements of the NHS Confidentiality Code of Practice (http://www.dh.gov.uk/assetRoot/04/06/92/54/04059254.pdf) and the Data Protection Act 1998. Furthermore you should be aware that under the Act, unauthorised disclosure of information is an offence and such disclosures may lead to prosecution.

You should ensure that, where you are issued with an identity or security card, a bleep number, email or library account, keys or protective clothing, these are returned upon termination of this arrangement. Please also ensure that while on the premises you wear your ID badge at all times, or are able to prove your identity if challenged. Please note that this NHS organisation accepts no responsibility for damage to or loss of personal property.

We may terminate your right to attend at any time either by giving seven days' written notice to you or immediately without any notice if you are in breach of any of the terms or conditions described in this letter or if you commit any act that we reasonably consider to amount to serious misconduct or to be disruptive and/or prejudicial to the interests and/or business of this NHS organisation or if you are convicted of any criminal offence. Your substantive employer is responsible for your conduct during this research project and may in the circumstances described above instigate disciplinary action against you.

Barts and the London NHS Trust will not indemnify you against any liability incurred as a result of any breach of confidentiality or breach of the Data Protection Act 1998. Any breach of the Data Protection Act 1998 may result in legal action against you and/or your substantive employer.

If your current role or involvement in research changes, or any of the information provided in your Research Passport changes, you must inform your employer through their normal procedures. You must also inform your nominated manager in this NHS organisation.

Yours sincerely

Nick Good
R&D Projects Manager

cc: Rowena Welsford, HR BLT
Prof Richard Langford

Barts and The London NHS
NHS Trust

Pain and Anaesthesia Research Centre
St Bartholomew's Hospital
West Smithfield
London, EC1A 7BE
Tel: 020 7601 7432
Fax: 020 7600 7748

PATIENT INFORMATION SHEET

Version 1.6

Non-invasive optical methods for the measurement of reconstructive flap perfusion in plastic surgery

1. Invitation

You are being invited to take part in a research study. Before you decide whether or not to take part, it is important for you to understand why the research is being done and what it will involve. Please take time to read the following information carefully, and discuss it with others if you wish.

Ask us if there is anything that is not clear, or if you would like more information. Take time to decide whether or not you wish to take part.

2. What is the purpose of the study?

A new type of optical sensor has been developed to measure the blood content and pulsation of blood in tissue. A potentially useful application of this technology has been identified whereby the blood supply to tissue transplanted in plastic surgery may be assessed. The health of the transplanted tissue depends on an adequate blood supply and it is hoped that using a probe similar to one we have developed may provide a simple and efficient 'early warning' of reduced blood supply, with greater accuracy and reliability than existing methods. The optical probe is roughly the size of a fifty-pence piece and is placed on the skin surface for several seconds whenever a measurement is required. Light passes into the tissue and the quantity of blood and the degree of pulsation is recorded from the intensity of the light returning to a light sensor in the probe.

3. Why have I been chosen?

The study aims to evaluate this measurement system in patients undergoing flap plastic microsurgery.

4. Do I have to take part?

No. It is up to you to decide whether or not to take part. If you decide to take part you will be given this information sheet to keep and be asked to sign a consent form to confirm that you understand what is involved when taking part in this study. If you decide to take part you are free to leave the study at any time and without giving a reason. A decision to withdraw at any time, or a decision not to take part, will not affect the quality of care or planned treatment you receive.

5. What will happen to me if I take part?

During the operation the developed probe will be placed on the flap surface and measurements will be recorded. You will of course be asleep during this time. In the post operative period, when you will be awake, monitoring of the free flap will be done every time the dressings are removed for the site to be checked by a clinician and there will be up to a maximum of 10 measurements in total over a period of no

longer than 24 hours after the end of the operation. Each monitoring event will take no more than 10 minutes.

6. What are the side effects and risks of any treatment received when taking part?

No side effects are anticipated as the probe is non-invasive and uses red and near infrared light. Similar probes have been used routinely on the finger and earlobes of people in hospitals around the world for over twenty years with virtually no reported side effects.

7. What are the possible benefits of taking part?

There are no benefits or risks for you as a patient, but it is hoped that the results obtained from the proposed study will lead to the development of new techniques for monitoring transplanted tissue and provide information regarding the supply of blood to the tissue, leading to improved outcomes for this type of surgery in the future.

8. What if there is a problem?

If you have a concern about any aspect of this study, you should ask to speak with the researchers who will do their best to answer your question. If you remain unhappy and wish to complain formally, you can do this through the NHS Complaints Procedure. Details can be obtained from the hospital.

9. Will my taking part in this study be kept confidential?

Yes. All the information about your participation in this study will be kept confidential.
If you decide you would like to take part then please read and sign the consent form. You will be given a copy of this information sheet and the consent form to keep. A copy of the consent form will be filed in your patient notes, one will be filed with the study records and one may be sent to the Research Sponsor.

You can have more time to think this over if you are at all unsure.

Thank you for taking the time to read this information sheet and to consider this study.

Barts and The London NHS
NHS Trust

Pain and Anaesthesia Research Centre
St Bartholomew's Hospital
West Smithfield
London, EC1A 7BE

Tel: 020 7601 7432
Fax: 020 7600 7748

CONSENT FORM Version 1.6

Title of Project: Non-invasive optical methods for measurement of reconstructive flap perfusion in plastic surgery

Principal Investigator: Professor Richard Langford
Study Number:

Please Initial Box to indicate Agreement

1.	I confirm that I have read and understand the information sheet. I have had the opportunity to consider the information, ask questions and have had these answered satisfactorily.	
2.	I understand that my participation is voluntary and that I am free to withdraw at anytime, without giving any reason, without my medical care or legal rights being affected.	
3.	I agree to take part in the above study.	

Name of Patient	Date	Signature
Name of Investigator	Date	Signature

BIOMEDICAL ENGINEERING RESEARCH GROUP
CITY UNIVERSITY LONDON

PROTOCOL

Version 1.6
31st January 2010

Non-invasive optical methods for monitoring free flap perfusion in plastic surgery

Short title/Acronym:

Funder: **Engineering and Physical Sciences Research Council (EPSRC)**

Sponsor: **City University**

Trust(s) where the research is taking place:

1. **Mid Essex Hospital / Broomfield Hospital**
2. **Barts and the London Trust**

INVESTIGATOR SIGNATURE _____ DATE _____

Key Contacts:

Chief Investigator:
Professor Panicos Kyriacou, School of Engineering and Mathematical Sciences, City University, Northampton Square, London, EC1V 0HB, Tel: 0207 040 8131, Email: p.kyriacou@city.ac.uk

Principle Investigators:
Ms Tina Zaman, School of Engineering and Mathematical Sciences, City University, Northampton Square, London, EC1V 0HB, Tel: 0207 040 3878, Email: tina.zaman.1@city.ac.uk

Broomfield Site:
Professor Sandip Pal, Anaesthetics, Theatres and Diagnostics Division, Broomfield Hospital, Chelmsford and Essex County Hospital, Court Road, Chelmsford, CM1 7ET, Tel: 01245 514080, Email: Sandip.Pal@meht.nhs.uk

Barts and the London Trust:
Professor Richard Langford, Consultant in Anaesthesia and Pain Medicine, Pain and Anaesthesia Research Centre, St Bartholomew's Hospital , West Smithfield, London, EC1A 7BE, Tel: +44 20 7601 7524, Email: r.m.langford@btconnect.com

Dr Alla Belhaj, Pain and Anaesthesia Research Centre, St Bartholomew's Hospital, West Smithfield, London, EC1A 7BE, Tel: +44 20 7601 432, Email: alaabelhaj@hotmail.com

Study Summary

Title	Non-invasive optical methods for measurement of reconstructive flap perfusion in plastic surgery
Short Title	Non-invasive optical measurement of reconstructive flap perfusion
Protocol Version Number and Date	Version 1.6 31 January 2011
Methodology	Type of study: Observational study
Study Duration	24 months
Study Centres	1. Mid Essex Hospital 2. Barts and the London Trust
Objectives	A pilot observational study to evaluate a novel non-invasive optical method for intra-operative and post-operative assessment of blood arterial pulsation and oxygen saturation in plastic surgery reconstructive flaps.
Number of Subjects/Patients	60
Main Inclusion Criteria	Patients undergoing flap reconstruction including both free flaps and pedicle flaps.
Statistical Methodology and Analysis	Regression analysis of signals compared to monitored data such as pulse oximetry

1. Introduction

1.1 Background

After some plastic surgery procedures, partial tissue necrosis can occur due to the insufficient blood supply to the transplanted tissue site. The causes of this insufficiency include arterial thrombosis, poorly attached blood vessels or vessel occlusion due to tissue swelling. Currently physicians assess the condition of the tissue by visual examination of the transplant site which is not standardised and unreliable, being dependent on many factors including ambient lighting and individual bias. There is therefore a medical need to develop a non-invasive, accurate, easy to use, reproducible and inexpensive monitoring device to assess tissue perfusion intra-operatively and postoperatively. Examples of monitoring devices and techniques used for assessing flap perfusion include Doppler ultrasonography, photoplethysmography, intravenous sodium fluorescein monitoring, temperature monitoring, tissue pH monitor, transcutaneous oxygen monitoring, laser Doppler flow meter, near infrared spectroscopy (NIRS), tissue oxygen tension, contrast-enhanced ultrasound (CEU) and laser-induced fluorescence of indocyanine green. All of these techniques share advantages and disadvantages, as well as have limitations that preclude their routine application for monitoring perfusion in skin flaps. Therefore, to date there is no widely accepted and readily available intraoperative or postoperative technique to reliably assess the viability of free flaps. The proposed research program includes development of new non-invasive optoelectronic measuring techniques and in vivo measurement in patients undergoing reconstructive flap microsurgery.

2 Study Aims and Objectives

The aim of this study is to develop new non-invasive optoelectronic measurement techniques based on pulse-oximetry technology. A measurement system has been developed, based on an optical probe which may be placed on the skin surface allowing the perfusion status and blood oxygen level of the transplanted tissue to be assessed. The study aims to evaluate this measurement system in patients undergoing free flap plastic microsurgery.
The work program will be carried out through experimental and clinical measurements in vivo encompassing the following objectives:

- To develop a flap reflectance photometric sensor with high time resolution used for the measurement of changes in oxygenated haemoglobin, deoxygenated haemoglobin and total haemoglobin concentration in the region of sensitivity of the probe. The sensor will also measure photoplethysmographic (optical signals that can be used to determine blood volume changes) signals and estimate flap arterial blood oxygen saturation. Also to develop instrumentation and software for the processing and analysis of the recorded physiological signals.
- To develop a flap temperature monitoring sensor incorporated in to the reflectance photometric sensor.

3 Study Design

3.1 Method

All patients undergoing flap reconstruction will be included in the study. Patients undergoing reconstructive flap surgery where tissue is buried under the skin e.g. a free muscle flap or where the flap is placed in areas difficult to access easily will be excluded from this clinical investigation. Patients under 18 years of ages and patients who cannot give consent (dementia, unconscious, etc) will also be excluded.

In vivo studies will be performed using a dedicated optical reflectance sensor. The clinical studies aim to evaluate a non-invasive optical method for monitoring flap perfusion. Potential participants will be provided with a patient information sheet. They will only be asked to complete and sign the consent form once they have had a chance to read the information sheet and ask any questions they may have.

The sensor will be placed on the flap after microvascular anastomosis (joining of the blood vessels) has taken place. Optical measurements will be made from the flap, if possible before and after removal of the arterial and venous clamps on the vessels supplying the flap. The duration of each measurement will be no more than 10 minutes. Simultaneous estimation of blood velocity will be made using a laser Doppler perfusion monitor. Sterility will be maintained by placing the sensors in sterile disposable transparent sheaths prior to use. With the surgeon's permission, a small mark will be made on the skin with a sterile marker to indicate the position of the sensor so that subsequent measurements may be made from the same position to maximize the reproducibility of the measurements.

In the post operative period monitoring of the perfusion in the flap will be performed whenever the flap is visually observed (immediately after visual observation) up to a maximum of 10 measurements in total over a period of no longer than 24 hours after the end of the operation. Again each monitoring event will take no more than 10 minutes. Data from observational charts will be recorded by the investigators for comparison with the optical measurements.

3.2 Study endpoints

- Confirmation or otherwise that photoplethysmographic signals are obtainable from plastic surgery free flaps.
- Successful acquisition of the photoplethysmograph (PPG) signal of suitable quality for identifying the oxygen saturation of the free flap.
- Correlation of the results obtained to the physicians findings about the perfusion of the transferred tissue.

4 Subject Selection and Withdrawal

4.1 Inclusion Criteria

- Adult patients aged (18-70) from whom full written informed consent will be sought.
- Patients undergoing flap reconstruction.

- Potential participants will only be approached if they have a good understanding of spoken and written English.

4.2 Exclusion Criteria

- Patients who decline consent.
- Patients undergoing flap reconstruction where tissue is buried under the skin as in using a free muscle flap or where the flap is placed in areas difficult to access easily.
- Patients under 18 years of ages and patients who cannot give consent due to mental incapacity.

4.3 Subject Recruitment and Screening

Potential participants will be identified from the plastic surgery operating lists. The patient's suitability will be assessed from consideration of the surgical procedure taking place. This assessment will be carried out by a researcher acting under arrangements with the responsible care organisation. This investigator will have medical qualifications (e.g. will be a clinical research fellow). Once identified potential participants will be approached on the evening of the day before their planned surgery, after admission to the hospital. If they agree they will be given a patient information sheet and will be asked to sign a consent form. The visit will take place on the night before their operation or in the morning on the day of their operation, before any pre-medication is given.

4.4 Withdrawal of Subjects

If the Consultant Anaesthetist/Surgeon responsible for the patient requests that we stop the study.

5 Statistical Plan

5.1 Sample Size Determination

This is a proof of concept study; the aim is to establish that reliable signals can be obtained. The present study is not intended to demonstrate the potential for medical decision support. We are however planning to obtain preliminary comparative data in a pilot to justify further studies. 60 patients is a realistic number of patients which we think we could recruit within the time frame of the study. Furthermore we feel that this number will provide enough data for meaningful inter-patient comparisons to be made.

5.2 Statistical Methods

The following will be measured post hoc from the data recording:
i) The percentage of time that data could be obtained that is useful for biosignal interpretation and processing.
ii) The percentage of total time with no signal
iii) The percentage of total time with artefacts– these will be visually inspected and classified (e.g. movement, mains interference etc).
iv) Regression analysis of signals compared to monitored data such as pulse oximetry.

5.3 Recording of Adverse Events

Documented in full as per GCP guidelines.

5.4 Study Stopping Rules

If the Consultant Anaesthetist, Surgeon or Intensivist in charge requests that we stop the trial. This will be documented with reasons explaining why.

6 Data Handling and Record Keeping

6.1 Confidentiality

The personal data and measurements recorded will be kept in a locked in the office of the Principal Investigator. All study data in electronic format (which identifies the patient only by initials and a study number), will be stored in a password protected computer. The computer will be kept in a locked office.

6.2 Study Documents

Patient information sheet
Consent form

6.3 Case Report Forms

A case report form has been devised.

6.4 Records Retention

Following the publication of the study results, the database will be stored on a CD–ROM and filed in a locked filing cabinet. The Research Group will act as custodians for this data.

7 Study Monitoring, Auditing, and Inspecting

7.1 Study Monitoring Plan

The study will be conducted according to ICH/GCP standards. The chief investigator and members of the study research group will be responsible for monitoring the conduct of the study.

8 Ethical Considerations

8.1 Local Regulations/Declaration of Helsinki

The local Investigator will ensure that this study is conducted in accordance with the Principles of the "Declaration of Helsinki" (as amended in Tokyo (1975), Venice (1983), Hong Kong (1989), South Africa (1996) and Edinburgh (2000)). http://www.wma.net/e/policy/b3.htm or with the laws of the country in which the research is conducted, whichever accords greater protection to the

individual. The study will fully adhere to the principles outlined in the Guidelines for Good Clinical Practice" ICH Tripartite Guideline (January 1997)

8.2 Informed Consent

The investigators will obtain written informed consent from each subject prior to participation in this study, following adequate explanation of the aims, methods, anticipated benefits and potential hazards of the study. Ample time will be given for consideration by the patient before taking part. The Investigator will explain to the subjects that they are completely free to refuse to enter the study or to withdraw at any time during the study, for any reason.

If new safety information results in significant changes in the risk/benefit assessment, the consent form will be reviewed and updated if necessary.

8.3 Independent Ethics Committee/Institutional Review Board

This protocol and the accompanying material given to a potential patient (Patient Information Sheet, Consent form) as well as any advertising material will be submitted by the Investigator to an Independent Ethics Committee in the UK. Full approval by the Committee will be obtained prior to starting the study and will be fully documented by letter to the Chief Investigator naming the study site, local PI (who may also be the Chief Investigator) and date the Committee deemed the study as permissible at that site.

9 Study Finances

9.1 Funding Source

The study will be financed by the Engineering and Physical Sciences Research Council (EPSRC).

9.2 Indemnity for the performance of the study

Indemnity will be provided by Broomfield Hospital NHS Trust and Barts and the London Trust

9.3 Subject Payments

None.

10 Publication Plan

The results of the study will be evaluated and publication of the results in a peer-reviewed journal is planned.

11 Attachments

This section should contain all pertinent documents associated with the management of the study. The following is a list of attachments, those with an asterisk* must be submitted to the Ethics Committee with the protocol.

- Consent Form*
- Information Sheet*
- Case Report Form

ST. ANDREWS CENTRE

FLAP CHART

NAME REGISTRATION No. CONSULTANT

Replant / Revasc / Flap (Delete as applicable) Affected part .....

Specific instructions .....

Date																							
Time																							
Sign/Initial																							
Colour																							
White = 0																							
Blue/white = 2																							
Paler = 4																							
Normal = 6																							
Darker = 8																							
Mauve/blue = 10																							
Purple/black = 12																							
Temperature	Touch/Temp probe (delete as applicable) (Use skin temp chart if using temp probe)																						
Touch Chart																							
Cold																							
Cooler																							
Warm																							
Hot																							
Texture																							
Spongy																							
Soft																							
Firm																							
Hard																							
Capillary Refill	Press firmly for count of 10 and release (venous return)																						
No blanch																							
>3 Secs																							
Slow																							
3 Secs																							
<3 Secs																							
No Refill																							

SUP 0644
(CSP LTD.) 7/08

ST. ANDREWS CENTRE

FLAP CHART

Nursing Checklist – Dressing bivalved Yes / No. Removed completely – Yes / No.

Light source																					
Natural																					
Ward lights																					
Lamps																					
Torch																					
Other =																					
Leeches applied																					
No																					
Yes																					
Result = Good																					
No difference																					
Poor																					
Heparin																					
Soak																					
Injected																					
Result = Good																					
No difference																					
Poor																					
Elevation																					
Above Heart																					
Heart level																					
Below Heart																					
Surgeon informed of deterioration																					
Yes (initials)																					
No (initials)																					
Divet Bleeding																					
Fast																					
Medium																					
Slow																					

References

1. Kroll, S.S., *Breast reconstruction with autologous tissue : art and artistry*. 2000, New York ; London: Springer. viii, 376 p.
2. Gill, P.S., et al., *A 10-year retrospective review of 758 DIEP flaps for breast reconstruction.* Plast Reconstr Surg, 2004. **113**(4): p. 1153-60.
3. Rogers, K., ed. *The Human Body: The Respiratory System*. 2010, Rosen Educational Publishing. 234.
4. Webster, J.G., *Design of pulse oximeters*. 1997, Bristol: Institute of Physics Pub. xvi,244p.
5. Longenbaker, S.N., S.S.U.h.a. Mader, and physiology, *Mader's understanding human anatomy & physiology*. 6th ed. ed. 2008, Boston, Mass. ; London: McGraw-Hill Higher Education. xvii, 478 p.
6. Tortora, G.J. and B. Derrickson, *Principles of anatomy and physiology*. 12th ed., international student / Gerard J. Tortora, Bryan Derrickson. ed. 2009, Hoboken, N.J.: Wiley ; [Chichester : John Wiley, distributor]. 2 v.
7. Scanlon, V.C. and T. Sanders, *Essentials of anatomy and physiology*. 2nd ed. ed. 1995, Philadelphia: F.A. Davis. xvii,606p.
8. Brandis, K.; Available from: http://www.anaesthesiamcq.com/downloads/odc.pdf.
9. Webster, J.G., *The measurement, instrumentation and sensors handbook*. 1999, Boca Raton: CRC Press.
10. Scanlon, V.C. and T. Sanders, *Essentials of anatomy and physiology*. 1991: F. A. Davis. xv,513,[46]p.
11. Steel, F.A.W. and B. Shaw, *The adventures of Akbar : [when a child]*. 1913, London: William Heinemann. vii, 204p, plates.
12. Aaronson, P.I. and J.P.T. Ward, *The cardiovascular system at a glance*. 3rd ed. ed. 2007, Oxford: Blackwell. 133 p.
13. Rosdahl, C.B. and M.T. Kowalski, *Textbook of basic nursing*. 9th ed. ed. 2007, Philadelphia, Pa. ; London: Lippincott Williams & Wilkins.
14. Beebe, R.W.O. and D.L. Funk, *Fundamentals of emergency care*. 2001, Albany, N.Y. ; Great Britain: Delmar.
15. Kumar, V. and S.L. Robbins, *Robbins basic pathology*. 8th ed. ed. 2007, Philadelphia, Pa. ; Edinburgh: Elsevier Saunders. xiv, 946 p.
16. Levinson, A.T., B.P. Casserly, and M.M. Levy, *Reducing mortality in severe sepsis and septic shock.* Semin Respir Crit Care Med, 2011. **32**(2): p. 195-205.
17. Sims, N.R. and H. Muyderman, *Mitochondria, oxidative metabolism and cell death in stroke.* Biochim Biophys Acta, 2010. **1802**(1): p. 80-91.
18. Evans, G.R.D., *Reconstructive surgery of the chest, abdomen, and pelvis*. 2004, New York, N.Y.

London: Marcel Dekker ;

Momenta, distributor. xii, 473 p.

19. McGregor, A.D. and I.A. McGregor, *Fundamental techniques of plastic surgery and their surgical applications*. 10th ed. / Alan D. McGregor, Ian A. McGregor / foreword by Sir Charles Illingworth / artwork by Ian Ramsden. ed. 2000, London: Churchill Livingstone.

20. *Mastectomy*. 2013 [cited 2013 May]; Available from: http://en.wikipedia.org/wiki/Mastectomy.
21. Querci della Rovere, G., J.R. Benson, and M. Nava, *Oncoplastic and reconstructive surgery of the breast*. Second Edition. ed. 2011, New York: Informa Healthcare. xv, 292 pages.
22. Rainsbury, D., *Breast Reconstruction: Your Choice*. 1st Edition ed. 2008: Class Publishing. 236 pages.
23. Development, B. *BreastReconstruction.org*. [cited 2013 May]; The comprehensive resource for breast reconstruction]. Available from: http://www.breastreconstruction.org/.
24. Rinzler, C.A., *The encyclopedia of cosmetic and plastic surgery*. 2009, New York: Facts On File ; London : Eurospan [distributor].
25. Kim, J.Y. *Latissimus Flap Breast Reconstruction* 2011 Jul 22, 2011 [cited 2013; Latissimus Flap Breast Reconstruction]. Available from: http://emedicine.medscape.com/article/1274087-overview.
26. Mendelson, B.C., *Latissimus dorsi breast reconstruction--refinement and results.* Br J Surg, 1983. **70**(3): p. 145-9.
27. Jatoi, I., M. Kaufmann, and J.Y. Petit, *Atlas of breast surgery*. 2006, Berlin: Springer. x, 133 p.
28. Thorne, C., W.C. Grabb, and J.W. Smith, *Grabb and Smith's plastic surgery*. 6th ed. / editor-in-chief, Charles H. Thorne ; editors, Robert W. Beasley ... [et al.]. ed. 2007, Philadelphia, Pa. ; London: Lippincott Williams & Wilkins.
29. Acland, R.D., *Microsurgery practice manual*. 1980, St. Louis ; London: Mosby.
30. Fitoussi, A. and Institut Curie., *Oncoplastic and reconstructive surgery for breast cancer : the Institut Curie experience*. 2009, Dordrecht ; New York: Springer. xi, 150 p.
31. Holzle, F., et al., *Free flap monitoring using simultaneous non-invasive laser Doppler flowmetry and tissue spectrophotometry.* J Craniomaxillofac Surg, 2006. **34**(1): p. 25-33.
32. Neligan, P.C., *Monitoring techniques for the detection of flow failure in the postoperative period.* Microsurgery, 1993. **14**(3): p. 162-4.
33. Devine, J.C., et al., *Flap monitoring after head and neck reconstruction: evaluating an observation protocol.* J Wound Care, 2001. **10**(1): p. 525-9.
34. Salgado, C.J., S.L. Moran, and S. Mardini, *Flap monitoring and patient management.* Plastic & Reconstructive Surgery, 2009. **124**(6 Suppl): p. e295-302.
35. Trust, A.U.H.N.F., *Guidelines on Micro-vascular Free Flap Monitoring. 1st Edition*. May 2010, Regional Maxillofacial Unit

Aintree University Hospitals NHS Foundation Trust: Aintree University Hospitals NHS Foundation Trust. p. 4.

36. Jallali, N., H. Ridha, and P.E. Butler, *Postoperative monitoring of free flaps in UK plastic surgery units.* Microsurgery, 2005. **25**(6): p. 469-72.
37. Samia Y. Sayed, H.M.G., Warda Y. Mohamed and Tarek A. El-Gamal, *Micro Vascular Free Tissue Transfer Surgeries : Impact of a Designed Teaching Protocol on Nurse's Performance for Reduction or Prevention of Post Operative Flap Failure* Life Science Journal, 2011. **8**: p. 158-170.

38. Machens, H.G., et al., *Techniques of postoperative blood flow monitoring after free tissue transfer: an overview.* Microsurgery, 1994. **15**(11): p. 778-86.
39. Stepnick, D.W. and R.E. Hayden, *Postoperative monitoring and salvage of microvascular free flaps.* Otolaryngol Clin North Am, 1994. **27**(6): p. 1201-17.
40. de Weerd, L., J.B. Mercer, and L.B. Setsa, *Intraoperative dynamic infrared thermography and free-flap surgery.* Ann Plast Surg, 2006. **57**(3): p. 279-84.
41. Salmi, A.M., E. Tukiainen, and S. Asko-Seljavaara, *Thermographic mapping of perforators and skin blood flow in the free transverse rectus abdominis musculocutaneous flap.* Annals of Plastic Surgery, 1995. **35**(2): p. 159-64.
42. de Weerd, L., S. Weum, and J.B. Mercer, *The value of dynamic infrared thermography (DIRT) in perforatorselection and planning of free DIEP flaps.* Ann Plast Surg, 2009. **63**(3): p. 274-9.
43. Carr, J.J. and J.M. Brown, *Introduction to biomedical equipment technology*. 4th ed. ed. 2001, Upper Saddle River, N.J.: Prentice Hall. xv, 743 p.
44. Kremkau, F.W., *Diagnostic ultrasound : principles and instruments*. 4th ed. ed. 1993, Philadelphia ; London: W.B. Saunders. xi, 411 p., [6] p. of plates.
45. Huntleigh. *Hand Held Dopplers / Desktop Doppler*. 15 September 2013]; Available from: http://www.huntleigh-diagnostics.com/diagnostics/uk/Products.asp?pagenumber=2527&ProductCategory_Id=215Hand.
46. Hirigoyen, M.B., M.L. Urken, and H. Weinberg, *Free flap monitoring: a review of current practice.* Microsurgery, 1995. **16**(11): p. 723-6; discussion 727.
47. Harrison, D.H., M. Girling, and G. Mott, *Experience in monitoring the circulation in free-flap transfers.* Plastic & Reconstructive Surgery, 1981. **68**(4): p. 543-55.
48. Stern, M.D., et al., *Continuous measurement of tissue blood flow by laser-Doppler spectroscopy.* Am J Physiol, 1977. **232**(4): p. H441-8.
49. Holloway, G.A., Jr. and D.W. Watkins, *Laser Doppler measurement of cutaneous blood flow.* J Invest Dermatol, 1977. **69**(3): p. 306-9.
50. Webster, J.G., *Encyclopedia of medical devices & instrumentation*. 2nd ed. ed. 2006, Hoboken, N.J.: Wiley-Interscience ; [Chichester : John Wiley, distributor]. 6 v.
51. Instruments, M., *moor instruments laser Dopple blood flow assessment*, M.i. Ltd, Editor: Devon.
52. Yuen, J.C. and Z. Feng, *Monitoring free flaps using the laser Doppler flowmeter: five-year experience.* Plastic & Reconstructive Surgery, 2000. **105**(1): p. 55-61.
53. Oberg, P.A., T. Tenland, and G.E. Nilsson, *Laser-Doppler flowmetry--a non-invasive and continuous method for blood flow evaluation in microvascular studies.* Acta Med Scand Suppl, 1984. **687**: p. 17-24.
54. Clinton, M.S., et al., *Establishment of normal ranges of laser Doppler blood flow in autologous tissue transplants.* Plastic & Reconstructive Surgery, 1991. **87**(2): p. 299-309.
55. Futran, N.D., et al., *Green light photoplethysmography monitoring of free flaps.* Arch Otolaryngol Head Neck Surg, 2000. **126**(5): p. 659-62.
56. Svensson, H., J. Holmberg, and P. Svedman, *Interpreting laser Doppler recordings from free flaps.* Scand J Plast Reconstr Surg Hand Surg, 1993. **27**(2): p. 81-7.

57. Yoshino, K., et al., *Intraoral free flap monitoring with a laser Doppler flowmeter.* Microsurgery, 1996. **17**(6): p. 337-40.
58. Tindholdt, T.T., S. Saidian, and K.A. Tonseth, *Microcirculatory evaluation of deep inferior epigastric artery perforator flaps with laser Doppler perfusion imaging in breast reconstruction.* J Plast Surg Hand Surg, 2011. **45**(3): p. 143-7.
59. Wardell, K., A. Jakobsson, and G.E. Nilsson, *Laser Doppler perfusion imaging by dynamic light scattering.* IEEE Trans Biomed Eng, 1993. **40**(4): p. 309-16.
60. Tindholdt, T.T., et al., *Monitoring microcirculatory changes in the deep inferior epigastric artery perforator flap with laser Doppler perfusion imaging.* Ann Plast Surg, 2011. **67**(2): p. 139-42.
61. Perimed, *PeriScan PIM 3 System Laser Doppler Blood Perfusion Imager*, in *Innovations in Microvascular Diagnosis*, Perimed, Editor, Perimed: Sweden.
62. Tonseth, K.A. and T.T. Tindholdt, *Microcirculation in single and multiple-based perforator flaps in an experimental model of rats.* Scand J Plast Reconstr Surg Hand Surg, 2007. **41**(2): p. 49-52.
63. Schlosser, S., et al., *Application of a new laser Doppler imaging system in planning and monitoring of surgical flaps.* J Biomed Opt, 2010. **15**(3): p. 036023.
64. van den Heuvel, M.G., et al., *Perfusion of the deep inferior epigastric perforator flap measured by laser Doppler imager.* Ann Plast Surg, 2011. **66**(6): p. 648-53.
65. Diakides, N.A. and J.D. Bronzino, *Medical infrared imaging*. 2007, Boca Raton, Fla.: CRC ; London : Taylor & Francis [distributor].
66. Humeau, A., et al., *Laser Doppler perfusion monitoring and imaging: novel approaches.* Med Biol Eng Comput, 2007. **45**(5): p. 421-35.
67. Colwell, A.S. and R.O. Craft, *Near-infrared spectroscopy in autologous breast reconstruction.* Clin Plast Surg, 2011. **38**(2): p. 301-7.
68. Repez, A., D. Oroszy, and Z.M. Arnez, *Continuous postoperative monitoring of cutaneous free flaps using near infrared spectroscopy.* J Plast Reconstr Aesthet Surg, 2008. **61**(1): p. 71-7.
69. Keller, A., *Noninvasive tissue oximetry for flap monitoring: an initial study.* J Reconstr Microsurg, 2007. **23**(4): p. 189-97.
70. Thorniley, M.S., et al., *The use of near-infrared spectroscopy for assessing flap viability during reconstructive surgery.* British Journal of Plastic Surgery, 1998. **51**(3): p. 218-26.
71. Irwin, M.S., et al., *Near infra-red spectroscopy: a non-invasive monitor of perfusion and oxygenation within the microcirculation of limbs and flaps.* Br J Plast Surg, 1995. **48**(1): p. 14-22.
72. Hayden, R.E., et al., *Oxygenation and blood volume changes in flaps according to near-infrared spectrophotometry.* Arch Otolaryngol Head Neck Surg, 1996. **122**(12): p. 1347-51.
73. Stranc, M.F., et al., *Assessment of tissue viability using near-infrared spectroscopy.* Br J Plast Surg, 1998. **51**(3): p. 210-7.
74. Scheufler, O., K. Exner, and R. Andresen, *Investigation of TRAM flap oxygenation and perfusion by near-infrared reflection spectroscopy and color-coded duplex sonography.* Plast Reconstr Surg, 2004. **113**(1): p. 141-52; discussion 153-5.
75. Challoner, A.V. and C.A. Ramsay, *A photoelectric plethysmograph for the measurement of cutaneous blood flow.* Phys Med Biol, 1974. **19**(3): p. 317-28.

76. Allen, J., *Photoplethysmography and its application in clinical physiological measurement.* Physiol Meas, 2007. **28**(3): p. R1-39.
77. Thorne, F.L., et al., *Photoplethysmography as an aid in determining the viability of pedicle flaps.* Plast Reconstr Surg, 1969. **44**(3): p. 279-84.
78. Bardach, J., et al., *The role of photoplethysmography in the prediction of the experimental flap survival.* Otolaryngology, 1978. **86**(3 Pt 1): p. ORL492-7.
79. Harrison, D.H., M. Girling, and G. Mott, *Experience in monitoring the circulation in free-flap transfers.* Plast Reconstr Surg, 1981. **68**(4): p. 543-55.
80. Stack, B.C., Jr., et al., *Spectral analysis of photoplethysmograms from radial forearm free flaps.* Laryngoscope, 1998. **108**(9): p. 1329-33.
81. Galla, T.J., D. Hellekes, and A.M. Feller, *Differentiation between arterial and venous vessel occlusion by simultaneous measurement with laser Doppler flowmetry and photoplethysmography.* J Reconstr Microsurg, 1999. **15**(1): p. 67-72.
82. Stack, B.C., Jr., et al., *Initial experience with personal digital assistant-based reflectance photoplethysmograph for free tissue transfer monitoring.* Ann Plast Surg, 2003. **51**(2): p. 136-40.
83. Kyriacou, P.A., *Pulse oximetry in the oesophagus.* Physiol Meas, 2006. **27**(1): p. R1-35.
84. Incorporated, N.P.B. 30/09/2011]; Available from: http://www.nellcor.com/prod/pulseoxtech.aspx.
85. Matviyenko, S., *Pulse Oximeter*, C.S. Corporation, Editor. 2005: WA, USA
86. Graham, B., D.A. Paulus, and H.H. Caffee, *Pulse oximetry for vascular monitoring in upper extremity replantation surgery.* J Hand Surg Am, 1986. **11**(5): p. 687-92.
87. Menick, F.J., *The pulse oximeter in free muscle flap surgery. "A microvascular surgeon's sleep aid".* J Reconstr Microsurg, 1988. **4**(4): p. 331-4.
88. Lindsey, L.A., J.D. Watson, and A.A. Quaba, *Pulse oximetry in postoperative monitoring of free muscle flaps.* Br J Plast Surg, 1991. **44**(1): p. 27-9.
89. Rosenberg, J.J., B.D. Fornage, and P.M. Chevray, *Monitoring buried free flaps: limitations of the implantable Doppler and use of color duplex sonography as a confirmatory test.* Plast Reconstr Surg, 2006. **118**(1): p. 109-13; discussion 114-5.
90. Hertzman, A., *Photoelectric Plethysmography of the Fingers and Toes in Man.* Proc Soc Exp Biol Med, 1937. **37**(3): p. 529-534.
91. Webster, J.G., *Design of pulse oximeters*. Medical science series. 1997, Bristol: Institute of Physics Pub. xvi,244p.
92. Moyle, J.T.B., *Pulse oximetry*. 2nd ed. ed. 2002, London: BMJ. viii, 182 p.
93. Aoyagi, T. and K. Miyasaka, *Pulse oximetry: its invention, contribution to medicine, and future tasks.* Anesth Analg, 2002. **94**(1 Suppl): p. S1-3.
94. Mendelson, Y. and B.D. Ochs, *Noninvasive pulse oximetry utilizing skin reflectance photoplethysmography.* IEEE Trans Biomed Eng, 1988. **35**(10): p. 798-805.
95. Limited, A. *Altium Designer*. 1985; Available from: www.altium.com.
96. Instruments, N.; Available from: http://www.ni.com/labview/.
97. Manual, L.U.

98. Bland, J.M. and D.G. Altman, *Statistical methods for assessing agreement between two methods of clinical measurement.* Lancet, 1986. **1**(8476): p. 307-10.
99. Malata, C.M., et al., *Petrosectomies for invasive tumours: surgery and reconstruction.* Br J Plast Surg, 1996. **49**(6): p. 370-8.
100. Edelstein, D.R., *Revision surgery in otolaryngology*. 2009, New York: Thieme.
101. http://reference.medscape.com/. *Jejunum Tissue Transfer*. Jun 25, 2010 07/03/2012]; Available from: http://emedicine.medscape.com/article/881905-overview.
102. Wei, F.-C. and S. Mardini, *Flaps and reconstructive surgery*. 2009, [Edinburgh]: Saunders.
103. Cocks, H.C., et al., *Free jejunal patch flaps in oral and oro-pharyngeal reconstruction.* J Laryngol Otol, 1999. **113**(7): p. 680-2.
104. Bradford, C.R., R.M. Esclamado, and W.R. Carroll, *Monitoring of revascularized jejunal autografts.* Arch Otolaryngol Head Neck Surg, 1992. **118**(10): p. 1042-4.
105. Li, Q., et al., *A "watch window" technique for monitoring buried free jejunum flaps during circumferential pharyngolaryngectomy reconstruction.* Eur Arch Otorhinolaryngol, 2011.
106. Zaman, T., P.A. Kyriacou, and S.K. Pal, *Development of a reflectance photoplethysmographic sensor used for the assessment of free flap perfusion.* Conf Proc IEEE Eng Med Biol Soc, 2011. **2011**: p. 4006-9.
107. Katsaros, J., et al., *Monitoring free vascularised jejunum grafts.* Br J Plast Surg, 1985. **38**(2): p. 220-2.
108. Dionyssopoulos, A., et al., *Monitoring buried jejunum free flaps with a sentinel: A retrospective study of 20 cases.* Laryngoscope, 2012. **122**(3): p. 519-22.
109. Hallock, G.G. and T.J. Koch, *External monitoring of vascularized jejunum transfers using laser Doppler flowmetry.* Ann Plast Surg, 1990. **24**(3): p. 213-5.
110. Sorensen, H.B., *Free jejunal flaps can be monitored by use of microdialysis.* J Reconstr Microsurg, 2008. **24**(6): p. 443-8.
111. Mateus, J. and A.R. Hargens, *Photoplethysmography for non-invasive in vivo measurement of bone hemodynamics.* Physiol Meas, 2012. **33**(6): p. 1027-42.
112. Chubb, D., W.M. Rozen, and M.W. Ashton, *Early survival of a compromised fasciocutaneous flap without pedicle revision: monitoring with photoplethysmography.* Microsurgery, 2010. **30**(6): p. 462-5.
113. Pereira, C.M., et al., *Anesthesia and surgical microvascular flaps.* Rev Bras Anestesiol, 2012. **62**(4): p. 563-79.